Sericin coated polymeric membrane for air and water purification

Thesis submitted in partial fulfilment

of the requirements for the degree

of

DOCTOR OF PHILOSOPHY

Submitted by

VISHAL KUMAR VERMA

(Reg. No. 146107021)

DEPARTMENT OF CHEMICAL ENGINEERING

INDIAN INSTITUTE OF TECHNOLOGY, GUWAHATI

GUWAHATI-781039, ASSAM, INDIA

February 2020

Dedicated to

my family and friends

for their

unconditional love, support, and encouragement

Indian Institute of Technology Guwahati, Guwahati, India

Guwahati-781039, Assam, India
Department of Chemical Engineering

Statement

This is to certify that I have carried out the research work presented in this thesis entitled **"Sericin coated polymeric membrane for air and water purification,"** at the Department of Chemical Engineering, Indian Institute of Technology Guwahati, under the supervision of **Dr. Senthilmurugan Subbiah**. The results documented in this thesis are achieved by me and have not been submitted to any other university or institute for the award of any degree or diploma.

In keeping with the general practice of reporting scientific observation, due acknowledgment has been made wherever the work described is based on the findings of other investigations.

(Vishal Kumar Verma)

Reg. No.: 146107021
Department of Chemical Engineering
Indian Institute of Technology
Guwahati-781039, Assam, India

Guwahati, February 2020

Indian Institute of Technology Guwahati, Guwahati, India

Guwahati-781039, Assam, India
Department of Chemical Engineering

Certificate

It is certified that the work contained in this thesis entitled **"Sericin coated polymeric membrane for air and water purification,"** being submitted by Mr. Vishal Kumar Verma (Reg. No. 146107021) for the award of Ph.D. degree, is a record of bona fide research carried out by him at the Department of Chemical Engineering, Indian Institute of Technology Guwahati, under my guidance and supervision. The work embodied in this thesis has not been submitted to any other university or institute for the award of any other degree or diploma.

(Dr. Senthilmurugan Subbiah)

Associate Professor
Department of Chemical Engineering
Indian Institute of Technology
Guwahati-781039, Assam, India

Guwahati, February 2020

Acknowledgments

You can go wherever you want to, see whatever you want to, but a place is only as good as people you know in it….

- Pittacus Lore

The journey of a doctoral thesis is always long, challenging, and difficult. Throughout this journey, there has been constant support and love from people I have in my life. I have always cherished their presence in my life for different reasons, and it is a great privilege to extend my sincere thanks to all these people. First and foremost, I would like to express my deep gratitude to my supervisor, Dr. Senthilmurugan Subbiah, for providing me with continuous support, inspiration, and guidance throughout the entire duration of Ph.D. work. I am indebted to him for his useful suggestions and constant encouragement throughout the period. He also provided me relentless mentorship, involved me in interesting and important discussions, and also gave me the freedom to carry out my Ph.D. work freely.

I want to express my sincere gratitude to all my doctoral committee members- Prof. G. Pugazhenthi, Prof. Ram Gopal V.S. Uppaluri of the Department of Chemical Engineering and Dr. Senthil Kumar of the Department of Bioscience and Engineering, for their valuable suggestion and contributions which further improved and enhanced the quality of my research work.

I also thank all the faculty members of the Department of Chemical Engineering for their kind co-operation and help during my stay. I am also thankful to all the staff members and scientific officers for their genuine help and assistance. I would also like to extend my thanks to the scientific officers at the Central Instruments Facility of IIT Guwahati for allowing me to carry out FESEM, EDX, and ITC analysis.

Life is partly what we make it, and partly what it is made by the friends we choose. I am very fortunate to have great friends and lab-mates without whom this journey would not have been possible. I especially like to acknowledge my love for all my dear friends- Ananya Bardhan, Anisha Akhtar, Balakumara V M, Bharat S. Rajput, Chayanika Das, Deepika Bishnoi, Deepti Nair, Dinesh Gautam, Habtom Teklu, Harjeet Nath, Kranti K Munubarthi, Munniraj Tippa, Mohan, Naveen Kumar Yarnal, Niveditha S, Neelam Dutta, Priyamjeet Deka, Puja Singh, Seema Bharati, Senthil S, Surender G, T. Venkatesh, Vigneshwaran K, and Viswanth R. I would also like to thank my lab assistants Banajeet Saloi and Bishnu Sarkar for their help, support and assistance.

In the end, I would like to give my due and sincere acknowledgment to my family, mom, dad, brother, and my lovely sisters for their love, care, support, and encouragement throughout life. Without all of you, nothing would have been possible.

Vishal Kumar Verma

Abstract

The environmental pollution has become a global issue catalyzed by the generation of multi-natured pollutants in the biosphere and demands immediate attention towards modification and advancement in existing abatement methods. The ongoing crisis and inevitable future shortage of access to fresh and pure water calls for efficient treatment and recycling of available water sources. In the last decade presence of emerging micropollutants (i.e., drugs and heavy metals) in drinking water has raised many questions towards the efficiency of available water treatment technology. These drug-based micropollutants present in water sources prove to be persistent, bioactive, and toxic even at low concentrations for human consumption. Therefore, the complete removal of the drugs from water is crucial to avoid long-term medical complications. Recent studies show an abrupt increase in air pollution and related health hazards in developing countries, particularly in India and China. The particulate matter and volatile organic compounds have emerged as a prime environmental concern with increasing air pollution in metropolitan cities leading to lung and heart-related issues. The available methods for air pollution remediation lack in targeting both particulate matter and volatile organic compounds using the same system, and usually, multiple systems are required. Hence, it demands a comprehensive approach to tackle the issue.

Membrane technology is one of the emerging and advanced processes that can provide a sustainable solution to water treatment. However, the membrane-based filtration system cannot achieve complete removal of the low molecular weight drugs, and most often, the membrane technology suffers massively from fouling-related issues. Hence, there is an apparent requirement for the existing membrane technology to be modified with smart materials that can render antifouling characteristics together with adsorptive properties to specifically capture the drug-based micropollutants from water.

The first stage of research focused on establishing the potency of Sericin as a bio-sorbent for the removal of drugs from water using Ibuprofen as a model drug. The removal of Ibuprofen from aqueous solution was studied using commercially available silk Sericin as an adsorbent in an integrated adsorbent-membrane process. The adsorption study was performed at a different physiological condition such as adsorbent concentration (1-10

g), Ibuprofen concentration (10-70 mg/L), temperatures (20, 30 and 40 °C) and pH (5, 6, 7, and 8). The occurrence of the Sericin-ibuprofen complex before membrane separation was confirmed by performing analysis of Sericin-ibuprofen interaction. Sericin-ibuprofen interaction was investigated using attenuated total reflection Fourier-transform infrared (FTIR), field-emission scanning electron microscope (FESEM), fluorescence spectroscopy, X-ray diffractometer (XRD), and isothermal titration calorimeter (ITC). Sericin and Ibuprofen interaction is spontaneous and endothermic in-nature, while the random coil transition of Sericin governed the adsorption system. ITC analysis exhibited a binding affinity (K_b) value of 2.51 x 10^4±1.4 and one binding sites (n≈1) per molecule at 27°C, revealing moderate binding of Ibuprofen to the Sericin protein. Complete removal of Ibuprofen (at 10 mg/L, pH 8) was achieved using 10 g of Sericin (pH 4) and at a temperature of 40°C in reverse osmosis membrane process. The results established in this work concludes that sericin may be used as an adsorbent for the removal of micropollutants, such as Ibuprofen from drinking water.

In the second stage of research, a novel and easy method was developed to coat sericin on polypropylene (PP) hollow fiber (HF) microfiltration (MF) membrane via surface coating. The sericin-coated adsorptive MF membrane was used for the removal of drug-based micropollutants. The sericin-coated membrane was tested for the removal of different classes of drugs from water. The membrane completely removed NSAIDs and antibiotics from water at 20 μg/L concentration. The adsorption mechanism was profoundly influenced by charge-based interaction (i.e., electrostatic interaction and hydrogen bonding), hence charged anionic drugs were more effectively removed than uncharged drugs. In multidrug mixtures, the removal efficiency was observed in the following sequence; ibuprofen > diclofenac > amoxicillin > ciprofloxacin > estrone > β-estradiol. The desorption of the drugs from the membrane surface can be effectively controlled by altering the pH of the membrane-cleaning solution. The presence of other inorganic salts in the aqueous drug solution did not interfere with the removal efficiency of the sericin-coated membrane. The performance of the sericin-coated membrane was studied using a continuous adsorptive membrane filtration approach. The dynamic adsorption behavior of a fixed-bed membrane column was predicted using the Bohart–Adams model. The model can predict the adsorption breakthrough curve with a minimum experimental error. This study reveals the unique application of sericin-coated MF

membrane for effective removal of drug-based micropollutants from water and demonstrates its easy regeneration and effectiveness for multiple cycles of filtration.

Sericin coated MF membrane hydrophilicity has improved significantly and exhibited high water content (64.87%) and low water contact angle (38°). In a comparative study with synthetic greywater treatment, the sericin coated membrane removed <90% turbidity and produced a higher volume of purified water with 15% less fouling compared to the uncoated membrane. The fouling experiment concludes that the sericin-coated membrane can reduce reversible and irreversible fouling by ≈30% and ≈83.00%, respectively, relative to the uncoated membrane using pure water backwash operation. In the second case, the sericin-coated membrane was able to provide consistent permeate quality with produced water: chemical oxygen demand <43 ppm, biological oxygen demand <6.8 ppm, suspended solids completely removed, total dissolved solids <112 ppm, turbidity <5 NTU and oil content <0.044 ppm, together with 10.5% less fouling than uncoated membrane. This study reveals that sericin coating enhanced membrane hydrophilicity and hence exhibited better antifouling properties. The sericin-coated MF membrane effectively treated greywater as well as produced water with less fouling and within limits of national standards for reusability.

In the final phase of research, a facile and novel method developed for the fabrication of polyester-based air filter via surface coating with Sericin for imparting effective removal of particulate matter and volatile organic compounds. A simple dip-coating method followed by thermal fixation has been adopted to coat Sericin on the polyester fiber. The developed changes in surface functionality and morphology of the polyester fiber were confirmed by Attenuated total reflection Fourier-transform infrared spectroscopy and Field emission scanning electron microscopy analysis. The fabricated air filter was tested for removal of particulate matter (generated burning incense stick) and volatile organic compounds (generated vaporizing gasoline), in an indoor chamber. The Sericin coated filter was able to remove the particulate matter, $PM_{2.5}$, and PM_{10} (from 1000 $\mu g/m^3$ level to 5 $\mu g/m^3$ in a 6.28 m^3 chamber) within 27 and 23 min of operation, respectively. The fabricated filter very effectively removed particulate matter for 2160 cycles with intermittent washing. The Sericin-coated air filter also proved very effective for the removal of volatile organic compounds (Benzene, Toluene, Ethylbenzene, and Xylene) from an indoor chamber at a varying initial concentration of 100–1000 $\mu g/m^3$. The

adsorption behavior was described by Langmuir-Freundlich (Sips) isotherm and pseudo-first-order kinetics with minimal error. The maximum adsorption capacity (mg/g) obtained with Sips Isotherm fitting followed the order Xylene (6.97)>Ethyl Benzene (5.68)> Toluene (5.35) >Benzene (4.78). This work provides a detailed insight into the use of sericin for membrane modification using a facile and novel modification method for air and water purification.

Table of Contents

List of Figures

List of Tables

Nomenclature

Abbreviations

AAQS	national ambient air quality standards
ACF	activated carbon fibers
APTS	aminopropyl-triethoxysilane
ATR-FTIR	attenuated total reflectance fourier transform infrared spectroscopy
ATSDR	agency for toxic substances and disease registry
BOD	biological oxygen demand
COD	chemical oxygen demand
EC	emerging contaminants
EDC	endocrine-disrupting compounds
EDX	energy-dispersive x-ray spectroscopy
EPA	united states environmental protection agency
FESEM	field emission scanning electron microscopy
HB	hydrogen bonding
HF	hollow fibre
HFMF	hollow fibre microfiltration
HPLC	high-performance liquid chromatography
IWMI	international water management institute
MC	methylcellulose
MD	membrane distillation
MF	microfiltration
MWCO	molecular weight cut-off
NOM	natural organic matters

NSAI	nonsteroidal anti-inflammatory agents
NSAID	nonsteroidal anti-inflammatory drug
NTU	nephelometric turbidity unit
PAC	powdered activated carbon
PCP	personal care products
PD	polydopamine
PEG	polyethylene glycol
PES	polyethersulfone
PET	polyethylene terephthalate
PPCP	personal care product
PP	polypropylene
PTFE	polytetrafluoroethylene
PW	produced water
RO	reverse osmosis
SD	standard deviation
TDS	total dissolved solid
UF	ultrafiltration
UNESCO	united nations educational, scientific and cultural organization
UV	ultra-violet
WHO	world health organization

Notations

mg/l	mille-gram per litre
µg/l	micro-gram per litre
µS	micro-siemens
g/l	gram per litre
H	hour
ng/l	nano-gram per litre
kDa	kilo-dalton
kPa	kilopascal
log D	distribution coefficient
log P	partition coefficient
pKa	dissociation constant
mS	millisiemens
mV	millivolt
nm	nanometer
Pa	pascal
ppm	parts per million

Chapter 1

Introduction

1.1. Background

Environmental pollution is one of the major challenges faced by humanity and other life forms on earth. Environmental pollution is the introduction of harmful, unwanted, poisonous, and detrimental substances into the natural habitats (i.e., air, water, and land), which has the potential to damage the health or well-being of humans, animals or plants [1]. The increasing population, rapid urbanization, and expansion of cities have led to the generation of more pollutants of different nature in the environment. These multi-nature pollutants affect different components of the environment and cause air, water, and land pollution [2]. In particular, water and air pollution have been the focus of concern for the last two decades. The United Nations Educational, Scientific and Cultural Organization (UNESCO) [3] reports that around 2 billion people may not have access to pure water, while around 4 billion people experience severe water crises for at least one month in a year [4]. According to the world health organization (WHO), the polluted environment is responsible for the death of around 1.7 million child deaths per year [5]. Around 5.9 million death among children under age five has been reported globally due to environment-related health issues [5].

Water is an essential commodity for every living being. The population growth, the industrial revolution, agricultural growth, developing economy, variation in consumption pattern, water-source mismanagement, and global warming have all led to water scarcity. This water scarcity has contributed to an increase in water demand at a rate of around 1% every year [3]. The major portion of this growing demand for water has been mostly reported in developing countries. The water stress globally stands at 13 percent which varies with countries and regions. The highest water stress is reported in the regions of Northern Africa and Central Asia (see *Figure 1.1*a-b). The International Water Management Institute (IWMI) 2003 report predicts that one person out of three in India will be deprived of access to pure water by 2025 [6]. The release of greywater from households, industrial effluents, produced water (PW) from oil and gas industries, pharmaceutical waste, agricultural waste, radioactive wastes, etc., are leading sources for water pollution [7–10]. The recycled water from these contaminated sources eventually becomes part of drinking water sources, and they are expected to residue from industrial chemicals, pharmaceuticals, and personal care products (PPCPs), pesticides, and hormones. These residual micropollutants cannot be removed by the conventional water treatment system.

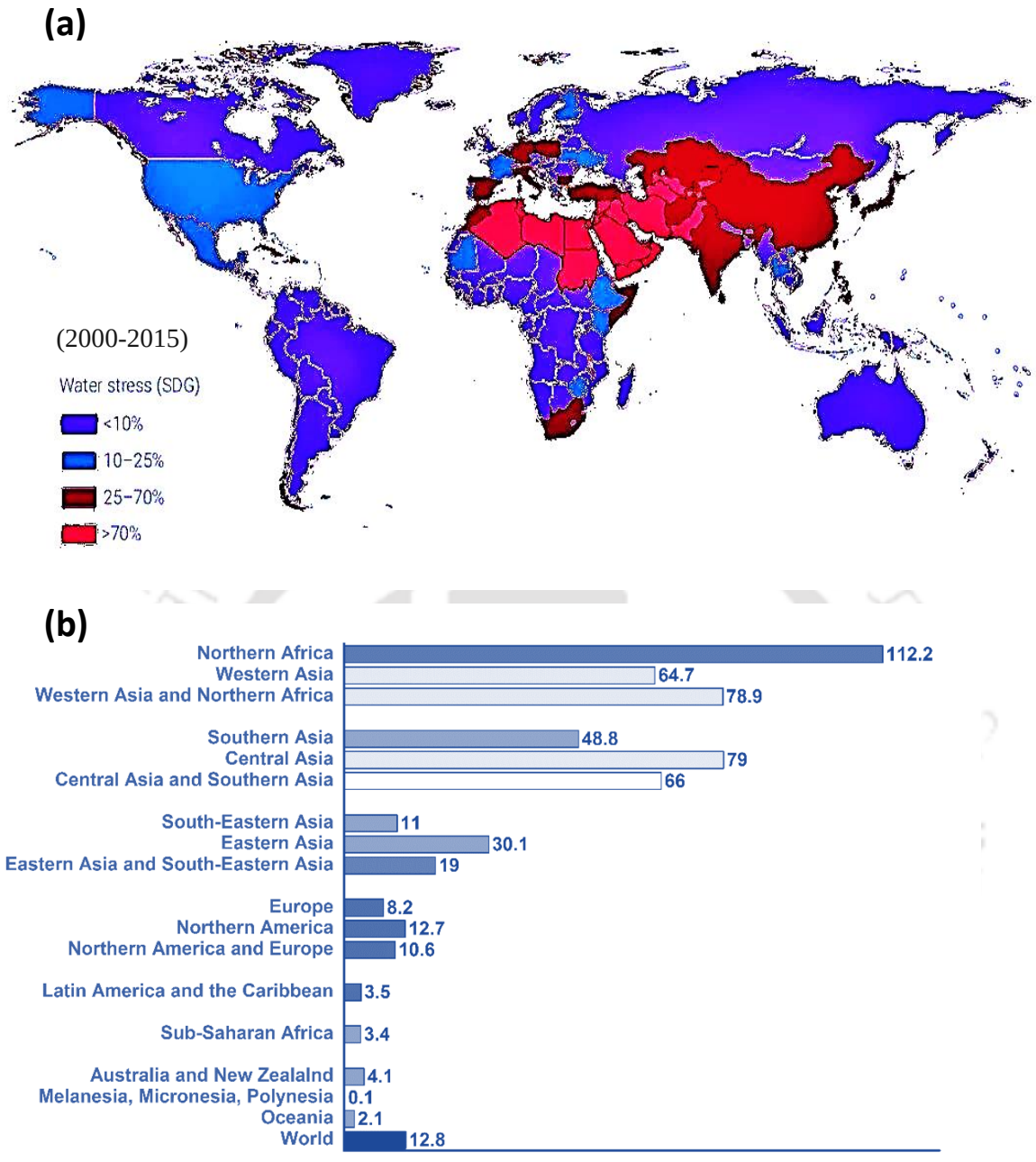

Figure 1.1 (a) Level of water stress (%) globally around different countries (b) Level of water stress (%) by region (source: FAO and UN-Water. 2018 [11]).

The contaminated trace synthetic or naturally occurring chemicals in water sources are known as emerging contaminants (ECs), which are not usually present in the freshwater sources but have the potential to enter the environment and capable of causing known or unknown adverse ecological and/or human health effects. The ECs have raised a lot of concern among people and responsible government bodies [12]. These ECs mainly involves pharmaceuticals (analgesics, antibiotics, hormones, etc.), pesticides, herbicides,

industrial chemicals, surfactants, endocrine-disrupting compounds (EDCs), and personal care products (PCP) which are consistently being found in all sources of water (i.e., groundwater, surface water, municipal wastewater, drinking water, and food sources) [13]. Among these contaminants presence of pharmaceutical drugs have grabbed attention due to threat of probable resistance development towards these drugs, particularly antibiotics, pain killers, and analgesic [14,15]. Hence, the removal of these pharmaceuticals is of prime importance to avoid any health-related issues.

1.2. Research Motivation

1.2.1. Importance of removal of Drug-based Micropollutants from drinking water

Micropollutants have emerged as one of the unresolved issues with water pollution. They are generated from many sources, which include emerging organic or mineral contaminants, which are toxic, persistent, and bio-accumulative even at low concentrations [16]. These contaminants are finally getting dissolved in wastewater streams from multiple sources [17]. The continuous discharges of micropollutants in wastewater stream are expected to cause long term hazards since the contaminants are bio-accumulating nature and even forming new mixtures in our water reuse cycle. Drug-based micropollutants like nonsteroidal anti-inflammatory agents (NSAI), antibiotics, and steroids/hormones have been detected in the ground, surface, and drinking water in the range of ng/l to µg/l in Indian [18,19] as well as global context [20,21].

The presence of these unwanted toxic micropollutants in water leads to an eco-toxicological effect on target as well as non-target organisms [22,23]. The exact impact on the ecological system by micropollutants are yet to be fully discovered. As per the recent lab analysis, the levels of drug pollutants measured in streams, lakes, and well water near pharmaceutical factories in India are 100,000 to 1,000,000 times higher in comparison to the levels measured in waters that receive sewage effluent in the US or China [24]. Many studies report the adverse effects of pharmaceuticals in aquatic organisms, chronic long term exposure to these drugs may have detrimental effects on the metabolism of non-target organisms, including microbes fish and other aquatic organisms [25–27]. Due to the profound use of diclofenac (a widely used Nonsteroidal anti-inflammatory drug, NSAID), an unusually high death rate among three different species of the vulture was reported in India and Pakistan [28]. The extent of the impact

of pharmaceutical waste on human beings is not as defined and well-studied. Still, it has been a topic of debate recently, and even in low dosages, long term exposure to pharmaceutical drug remnants may be hazardous to humans [23], particularly infants are at most vulnerable to the exposure of drugs. To date, no proper discharge guidelines, standards, and legal requirements have been framed for the release of these ubiquitous and biologically active substances into surface water. Over the last decade, the concentration in treated and untreated urban wastewater has been monitored periodically [29], but still, the presence of pharmaceuticals in the aquatic environment is largely an unregulated area. These pharmaceutical contaminations cannot be removed with conventional wastewater treatment technologies [30–33]. Therefore, the removal of these substances by conventional wastewater treatment plants has been found to be incomplete [34]. Hence, a holistic approach for the complete removal of these drug particles from drinking water is very much needed for avoiding the development of drug-resistance and other health-related complications in infants and adults.

1.2.2. Importance of removal of particulate matter and volatile organic compounds in ambient air

The current state of the menace caused by air pollution is unveiled by the fact that around 7 million death every year has been attributed to polluted air, in which 4.2 million deaths in 2016 was attributed to ambient air pollution [35,36]. WHO also reports that 91% of the world resides in places where air quality exceeds guidelines limits, and 9 out of 10 people breathe polluted air. The polluted air is continuously affecting our normal life whether indoors, outdoors, villages, or cities. The United States Environmental protection Agency (EPA) has listed particulate matter (PM) as one of the criteria pollutants (together with ozone, nitrogen oxides, sulfur oxide, carbon monoxide, and lead) in National Ambient Air Quality Standards (AAQS) under the Clean Air Act, 1970 [37]. Particulate matter is defined as suspended solid and liquid tiny gritty substances existing in the atmosphere. These airborne particles are classified based on aerodynamic diameter into total suspended particulate (<10 µm), respirable particles (PM_{10}, <10 µm), fine particles ($PM_{2.5}$, <2.5 µm), and ultrafine particles (<0.1 µm) [38,39]. The inherent filtration mechanism in the human body (cilia and mucus present in nostrils) can remove most of these PM generally $PM_{2.5,}$ which eventually gets retained in the lung (96% particles) and mostly observed in the alveolar and tracheobronchial regions [40]. The particle with a diameter between 0.003-0.5 µm penetrates with the lung's alveolar region passes through

the respiratory barrier and enters the circulatory system, and thus spread to another organ system [41]. These micro-particles can easily combine with other toxic agents, such as heavy metals and poly-aromatics, due to their specific surface.

The revised annual and daily standard for $PM_{2.5}$ is 40 µg/$m^{3,}$ and 60 µg/m^3 and PM_{10} are 60 and 100 µg/m^3, respectively, in India [42]. The current air quality index of cities in India shows that the PM_{10} and $PM_{2.5}$ are way above the prescribed national and International standard levels [43–45]. The severe impact of air pollution is mainly attributed to indoor air pollution (*Figure 1.2*) and is observed more in developing and economically backward countries (*Figure 1.3*) and. It has been reported that indoor air pollution affects human life more than outdoor air pollution [46,47]. Indoor air pollution mainly deals with the presence, amount, effects, and control of physical, chemical, and biological factors (PM, VOCs, CO, NO_X, SO_2, CO_2, and unburnt hydrocarbons, etc.) in homes, workplace, transportation media, etc. [46]. These multi-natured contaminants, when released into air and water, have severe implications on human health and other living organisms as well [22,23,41,48]. Therefore, purification systems that can render air and water devoid of harmful pollutants are crucial in present-day urban life.

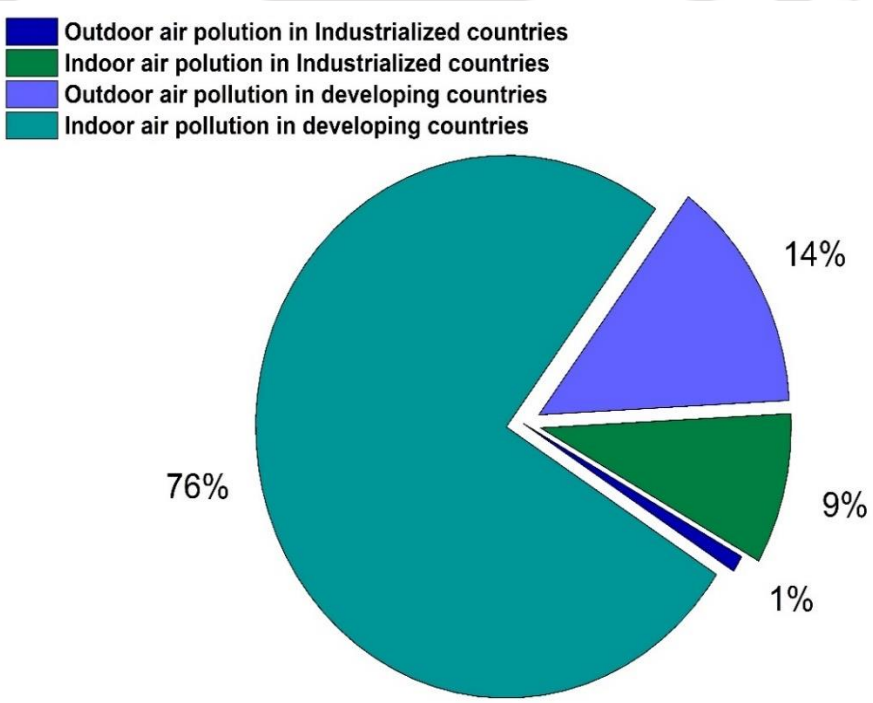

Figure 1.2. Pie chart showing total indoor and global outdoor exposure to particulate matter air pollution in developing and industrialized countries [49,50].

On the same reflection, the presence of volatile organic compounds is also a health issue. VOCs are gases emitted from certain organic liquids or solids with high vapor pressure and low boiling point. The concentration build-up for VOCs is higher indoors rather than outdoor [41]. Apart from petroleum products, VOCs are emitted by a wide variety of household products (paints, varnishes, wood preservatives, wax, organic solvents, cleansers, disinfectants, moth repellents, air freshener, cosmetic, degreasing, hobby products), building materials, furnishings, office equipment (copiers, printer, correction fluid), graphics, adhesive, permanent markers and photographic solution. VOCs presence in air leads to multiple health effects like sensory organs irritation (eye, nose, throat), headache, loss of coordination, nausea, vomiting, liver damage, central nervous system, and also compound to the long-term effect like cancer [48].

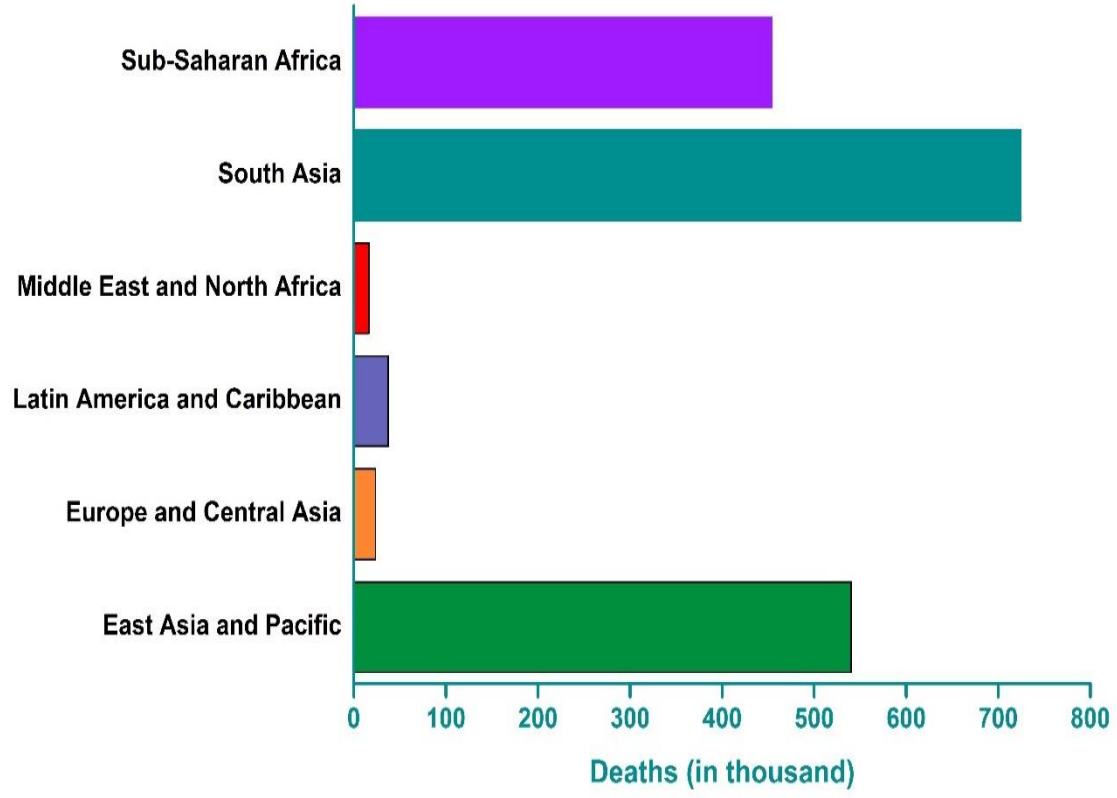

Figure 1.3. Deaths attributable to indoor air pollution exposure by regions [46,47].

Among all VOCs present in air benzene, toluene, ethylbenzene, xylene, and 1,2,4-trimethyl benzene accounts for around 60-90% [51]. Benzene, toluene, ethylbenzene, and xylene (generally known as BTEX) is listed as hazardous air pollutants in Agency for toxic substances and disease registry (ATSDR), and an extremely long term exposure causes neurological impairment, anemia, leukemia, critical neurotoxicity [52–56,56].

VOCs, together with other gaseous pollutants, i.e., nitrogen oxide and particulates form smog and creates environmental and health-related problems [57–59]. Therefore, the removal of these toxic pollutants from the air is essential to eliminate any health risks and hazardous effects in the long term.

1.3. Need for cost-effective membrane technology for water and air purification

1.3.1. Micropollutants removal from water

Membrane-assisted separation process has emerged as one of the technically feasible and cost-competitive methods to remove micropollutants from water sources [34,60]. The use of the membrane process provides a solution to the problems that can be persistent with conventional methods [61,62]. Low-pressure membrane processes such as microfiltration (MF), ultrafiltration (UF) are widely used as pre-treatment system in water and wastewater treatment application to remove macromolecules, colloids, organic/inorganic polymeric molecules and microbial biomass [63–66]. High-pressure membrane processes such as nanofiltration (NF) and reverse osmosis (RO) are used for brackish water desalination [67,68] to remove the dissolved solids [69,70]. Removal of drug-based micropollutants from water has been practiced with different kinds of membrane processes such as MF, UF, NF, RO, and membrane distillation (MD) [71,72]. Resent study concludes that RO and NF processes are capable of removing the micropollutants from drinking water sources, and they will also remove other minerals along with micropollutants from drinking water [73–75]. However, UF/MF membrane is not adequately efficient in removing drug-based micropollutants from water [71,76]. Though the high pressure-driven membrane processes like NF, RO, and MD are proven to show good efficiency with drug removal, still, a complete removal is not realizable in every case, and they are also an energy-intensive process in comparison to conventional water treatment process [71,72]. However, the use of RO water is not recommended as it devoid natural minerals from drinking water, and its use is suggested to be based on the total dissolved solids present in drinking water sources [77].

A better way to tackle this problem is to use hybrid technology where a combination of one or more treatment processes can be used for the effective removal of micropollutants. One such way is to use the specific interaction of adsorbents together with membrane-enhanced separation for the effective removal of drugs from the water. Hence low-

pressure driven systems like MF/UF, which can be operated at gravity-driven conditions. One such approach is the fabrication of adsorptive membranes, which can specifically remove target pollutants (like heavy metals, organic pollutants, sulfur, pharmaceuticals, etc.) energy efficiently [78–87] from water sources. The adsorptive membrane utilizes both membrane and adsorption processes together for water purification. The adsorptive membrane is characterized by the incorporation of specific membrane precursors with an affinity towards target compounds, where the membrane surface is modified with the addition or embedding of multi-functional groups containing adsorbents into membrane matrices via different methods (coating, blending, grafting, etc.) [88,89].

The use of coated membranes has been very promising for the removal of micropollutants from water [90–93]. Most industrial polymeric UF/MF membranes are made from polypropylene, cellulose, polysulfone, polyacrylonitrile, polyvinylidene fluoride, polyether ketone, and polyimide [94–96]. However, the hydrophobic nature of these polymeric UF/MF membranes makes them more susceptible to fouling related issues and results in the rapid decline of membrane flux due to deposition of micropollutants in the membrane pores during water filtration [97,98]. The accelerated fouling hinders the membrane performance and leads to frequent membrane replacement for achieving the desired production capacity. The economic feasibility of the membrane processes is limited by the cost of membrane cleaning and its replacement. Moreover, membrane cleaning and its replacement impose around 50% of the operational cost or 30% of the total MF/UF membrane system cost [94]. Hence, it becomes inexorable to choose a simple and economically viable method for membrane modification to rectify these performance issues. The membrane is generally modified using either of two methods [99]:

I. Modification of membrane matrix (involves blending and copolymerization)
II. Modification of membrane surface (hosting polar groups or embedding hydrophilic monomers)

Surface modification mainly involves altering the surface characteristics of the membrane, i.e., charge, energy, roughness, hydrophilicity, and functionality [100]. Membrane surface modification may involve (i) physical modification (i.e., heat treatment, solvent post-treatment, polymer blending, and coating or (ii) chemical modification (chemical post-treatment, chemical grafting, plasma treatment, ultraviolet

(UV) induced grafting, ozone-induced grafting, high energy irradiation, and enzymatic treatment) [100]. Since physical modification does not alter the chemical composition of the base membrane, it is preferred in cases where surface modification is desired, keeping base matrix integrity intact. The coating is a simple method where a suitable/desired material is coated on the membrane to form a thin layer non-covalently attached to the surface. The membrane coating methods are generally very facile, cost-effective, and appropriate for both flat and hollow fibre membranes.

The selection of suitable material that can provide micropollutants adsorptive property and fouling resistivity for the membrane is an important aspect. Sericin is reported to have both properties due to the presence of the carboxyl, hydroxyl, and amine groups. The strong polar side groups present in sericin make it suitable for coating, cross-linking, and immobilization on to the membrane surface. Recently the use of silk sericin, a globular protein waste from the silk degumming industry, has gained much attention in the field of biomedical, textile, cosmetics, and also in membrane research [101–106]. The multi-functional group containing sericin is non-toxic, hydrophilic, anti-oxidative, antimicrobial, hygroscopic [102,107–109], and can be easily blended or incorporated into other polymer matrices. With the realization of adsorptive membrane for specific adsorption of pollutants at the same time sericin being characterized and explored as a non-toxic biopolymer with multi-functional groups having inherent hydrophilic and antimicrobial properties, it seems to be the perfect opportunity to explore the potential synergy of sericin with the membrane by coating sericin on the membrane surface.

1.3.2. PM and VOC removal technology from air

Similarly, in the air purification application, the polymeric filters are found as an alternative for high-efficiency high-efficiency particulate air (HEPA) based PM filter because HEPA filter cannot be cleaned for reuse purposes, and they are not capable of adsorbing VOCs. However, the modified polymeric filter coated with novel adsorbent like sericin may be able to remove PM and VOC from the air, and it can be cleaned with the help of cleaning agents for filter reuse. At present industrial air filters are using HEPA and activated carbon filter to remove PM and VOCs, respectively.

Hence, this thesis focusses on the modification of polymeric filters using sericin for water and purification application. The modified polymeric filter will be tested for the following application: (i) MF hollow fiber membrane for removal capacity of drug-based

micropollutants from water, (ii) fouling resistance of sericin coated MF membrane by treating grey and produced water and (iii) polymeric air filter for removal of PM and VOC from air and reusability of filter after washing with cleaning agent.

1.4. Objective and Research Scope

The primary objective of this thesis is the evaluation and application of Sericin for membrane modification to provide antifouling properties, adsorptive removal of drug-based micropollutants from water, and fabrication of washable air-filter for air purification.

Based on identified gaps in the literature, the main objectives of the Ph.D. thesis are outlined below:

1) Evaluation of Sericin as an adsorbent for removal of Ibuprofen form aqueous solution.
2) Establish a sericin based coating method of polypropylene-based MF membrane for enhancing its hydrophilic and adsorptive properties.
3) Characterization of Sericin-coated MF-membrane
4) Assessment of fouling resistant properties of Sericin-coated MF-membrane using greywater and produced water.
5) Investigate the potential of sericin-coated MF-membrane for removal efficacy of drug-based micropollutants.
    a. Effect of operating conditions (concentration, flow rate, multiple-solutes, background salts), membrane regeneration
    b. Study kinetic modeling for adsorptive removal of drugs on Sericin-coated MF membrane
6) Fabricate sericin-coated air-filter for the indoor air filtration
7) Evaluation of sericin-coated air-filter for the separation of particulate matter and adsorptive removal of VOCs from a lab-scale indoor environment.
    a. Assessment of sericin-coated air-filter for removal of particulate matter
    b. Assessment of sericin-coated air-filter for removal of volatile organic compounds namely Benzene, Toluene, Ethylbenzene, and xylene (BTEX)
    c. Study adsorption isotherm and kinetics for the removal of BTEX from indoor air using sericin-coated air-filter

1.5. Thesis Organization

The thesis is being organized in the following eight chapters:

Chapter 1	Introduction
Chapter 2	Literature Review
Chapter 3	Experimental, analytical and modeling methods
Chapter 4	Prospects of Silk Sericin as an adsorbent for removal of Ibuprofen from aqueous solution
Chapter 5	Fabrication and characterization of sericin coated polymeric microfiltration membrane
Chapter 6	Application of sericin coated polymeric microfiltration membrane
Chapter 7	Sericin-coated polymeric filter for air purification
Chapter 8	Summary and recommendation for future research

Chapter 2

Review of Literature

This section provides a thorough overview of the contemporary research and development presented in various literature, their outcomes, and impact on the field and hence identifying the promising areas of research that need to be addressed in this thesis. State of the art has been presented for modification of polymeric microfiltration membrane for removal of micropollutants from water and air using sericin as a smart coating material.

2.1. Membranes for removal of micropollutants

The membrane separation process is highly effective in removing the unwanted substance from water, and the membrane removal efficacy will vary with respect to the pore size of the membrane and size of substance [110]. For example, MF and UF membranes are capable of removing particles with size above ~0.1 and ~0.01 micron, respectively. Therefore, conventional MF and UF membranes cannot stop micropollutants. However, it can be removed by modifying the membrane surface with adsorptive nature [111–115].

Jermann et al. (2009) [112] examined the fate of Ibuprofen and estradiol during a UF process in the presence of natural organic matter (NOM). In the absence of NOM, UF with hydrophilic membrane showed insignificant removal for Ibuprofen and estradiol, while hydrophobic membrane retained up to 80 % of estradiol and 25 % of Ibuprofen. While in the presence of NOM-substances of high molecular weight such as alginate and humic acid showed greater micropollutant removal, and this was mainly due to formation NOM cake/gel layer on the membrane surface.

Further to achieve better removal efficiency in UF process for drug-based micropollutants from water, Sheng et al. (2016) [113] used a hybrid process by combining ultra-filtration, powdered activated carbon, coagulation to remove target pharmaceuticals such as Acetaminophen, Bezafibrate, Caffeine, Carbamazepine, Cotinine, Diclofenac, Gemfibrozil, Ibuprofen, Metoprolol, Naproxen, Sulfadimethoxine, Sulfamethazine, Sulfamethoxazole, Sulfathiazole, Triclosan, and Trimethoprim. The standalone ultrafiltration, powdered activated carbon, and coagulation were able to remove 29%, 50%, and 7% of drugs, respectively, while the hybrid system was able to remove 90.3% of the drug.

Membrane properties enhanced with a coating of desired materials on the surface have been used for the removal of pollutants as well as enhance antifouling properties.

Capozzi et al. (2017) [116] fabricated polydopamine (PD) functionalized polysulfone-based UF membranes via two different methods. In the first method, the membrane was prepared by phase inversion followed by PD coating. In the other comparatively easy method, the phase inversion was done using PD containing solution facilitating polymer precipitation PD functionalization simultaneously. Positively charged methylene blue dye solution (0.5g/l) was filtered through these PD coated membranes of 100 μ thickness. The one step-coating method resulted in membrane with high removal efficiency for methylene blue via electrostatic interaction-based adsorption. The membrane was easily regenerated with pH alteration and could be reused for multiple cycles.

Nadour et al. (2019) [117] fabricated carbon-based polymeric ultrafiltration membranes using polysulfone as membrane matrix, methylcellulose (MC) as a pore-forming agent and commercial powdered activated carbon (PAC) as an adsorbent additive in an immersion-precipitation method. Diclofenac, Paracetamol, and Metronidazole were used as a model drug to analyze the removal efficiency of the membrane. Membrane permeability and rejection rate for drugs increased with the addition of MC and PAC. The membrane exhibited high removal for diclofenac, followed by paracetamol and Metronidazole.

Ouyang et al. (2019) [118] prepared a dually charged polyelectrolyte polyethersulfone (PES) UF membrane through the layer-by-layer technique using oppositely charged polyelectrolytes of polydopamine and quaternate chitosan. The modified membrane had a molecular weight cut-off (MWCO) of~935 Da and pure water permeability of 15.665$L \cdot m^{-2} \cdot h^{-1} \cdot MPa^{-1}$. The membrane showed a higher rejection of 76.22%, 87.29%, and 89.85% for atenolol, carbamazepine, and ibuprofen, respectively.

The removal of drug-based micropollutants NF membrane is mainly due to size exclusion effect and hydrophobic adsorption, but for UF membrane is mainly due to hydrophobic adsorption [111]. Therefore, at a steady-state, the removal efficiency of more polar compounds by the NF membrane was found to be more efficient than the UF membrane. For example, Yoon et al. (2006) [111] reported 44–93% of drug removal by NF membrane for selected drugs except for naproxen, and another hand the UF membrane was able to remove less than 40% of drug except for a few compounds (triclosan, 87%; oxybenzone, 77%; progesterone, 56%). Overall, the performance of the UF and NF

membrane is found to be adequate to remove less polar components such that EDC/PPCP concentrations were observed below the detection limit.

In another aspect, the pore size of the RO and NF membrane is smaller than the size of the micropollutants molecule so that both processes can remove micropollutants for water due to the sieve mechanism. Kimura et al. (2004) [119] investigated the removal efficiency of six pharmaceutical drug components by thin-film composites NF/RO membrane made of aromatic polyamide. The adsorption of the drug component on membrane surface resulted in dynamic variation of drug concentration in permeate till membrane saturated with drug components. The adsorption capacity of the membrane under high-pressure operation is found to be higher than static batch adsorption on the membrane surface. They concluded that the separation of drug component is achieved initially due to both adsorption and sieve mechanism, and later only sieve mechanism alone contributed to drug separation.

Nghiem et al. (2005) [120] inspected the retention mechanisms of three pharmaceuticals sulfamethoxazole, carbamazepine, and Ibuprofen by two different pore sizes NF membranes made of polyamide thin-film composite. Results show that the rejection of pharmaceuticals by the NF membrane is contributed to both steric (size) exclusion and electrostatic repulsion effects. The steric exclusion is more effective in the NF membrane with smaller pore size, and both effects are contributing to the retention of ionizable pharmaceuticals by a larger pore size NF membrane. Further speciation of pharmaceuticals will increase the molecule size, and that will improve the rejection of the NF membrane with small pore size for ionized, negatively charged pharmaceuticals. In the case of uncharged pharmaceutical species, intrinsic physicochemical properties substantially affected their retention. While at neutral condition, the Ibuprofen was found to adsorb considerably on the membrane surface because of its relatively high hydrophobicity.

Röhricht et al. (2009) [121] investigated two different types of NF flat membranes for the removal of pharmaceuticals from WWTP effluent. Naproxen and diclofenac (60%) were retained to a greater extent compared with carbamazepine. It was noticed that at pH 7 and 8, naproxen and diclofenac (with pKa values of 4.2 and 4.15, respectively) were deprotonated, while carbamazepine (pKa = 13.9) was not. Hence, naproxen and

diclofenac were efficiently rejected by the negatively charged membrane surface, whereas less removal was observed for carbamazepine.

Heberer (2011) [122] tested a mobile reverse osmosis purification system by purifying the water taken from the highly polluted *Tetlowkanal* canal (with municipal sewage effluents) in Germany. As expected, the dual-pass RO system was found to be very effective at removing pharmaceuticals (i.e., Caffeine, Carbamazepine, Clofibric acid, Diclofenac, Naproxen, Propyphenazone, Diurone, Mecoprop, etc.) by greater than 95%. The high removal was attributed to the pore size of the membrane that does not permit high molecular weight organic compounds through the RO membrane.

Yangali-Quintanilla et al. (2011) [123] compared the removal of various micropollutants (pharmaceuticals, pesticides, endocrine disruptors, and others) by NF and RO. The NF membrane rejection was very close to that achieved by RO membranes. The average rejection by tight NF was 82% for neutral contaminants and 97% for ionic contaminants, while RO was able to achieve 85% rejection for neutral contaminants and 99% rejection for ionic contaminants.

Summary and possible scope for further research

It is evident from the literature survey that a lot of work has been reported on the removal of drug-based micropollutants from water using the membrane process. The separation of drug particles can be categorized into two sections (1) size-based separation of drug particles using high-pressure membrane systems like NF and RO and (2) adsorption of drug particles on membrane surface based on charge-based interaction. The RO membrane is capable of removing drug-based micropollutants due to size exclusion, but the NF membrane removal is contributed by both size exclusion and surface adsorption phenomena. Due to high-pressure operation, both processes are observed to be expensive in comparison with conventional water treatment technology. Therefore, the modified low-pressure UF membrane with more adsorption capability may able to provide both water prefiltration and micropollutant removal solution at low cost for water treatment applications. However, most of the articles report limited removal of drug pollutants and presents fouling related issues. The lack of antifouling properties together with selective adsorption of drug particles, can be seen as a bottleneck in the research area. Therefore, this thesis focusses on the identification of smart material that can grant the dual property

of hydrophilicity as well as adsorptive properties to the membrane. Moreover, though high pressure-driven systems grant better removal capacity, the process becomes very costly eventually and removes most of the desired nutrients from the water. Hence this work has been targeted towards the use of the low-pressure processes, particularly gravity driven-systems using microfiltration membranes for adsorptive removal of drug-based micropollutants from water.

2.2. Membranes for air filtration

An air filter media may be defined as a semi-permeable barrier that can separate dispersed particles from the air passing through them. Textile based filter fabrics have long been used in the air-filter industry. The use of textile materials for air filters mainly includes either woven, knitted, or non-woven fabric [124]. Till the development of synthetic fiber and non-woven fabric technology, the use of textile fabric was limited to woven and knitted fabric materials [125]. The non-woven fabric has been widely used for air filters as it provides better filtration efficiency, air permeability, and less chance of yarn slippage [126,127].

The different types of woven-fiber are used in air filtration such as cotton filter cloth, nylon filter cloth, polyester filter cloth, polypropylene filter cloth. Cotton filter cloths use is less due to weak resistance against mildew fungus and instability of dimensions. Among the four different kinds of fabric, nylon has the greatest resistance to rubbing, has good elasticity, ideal for low temperature, and high tensile strength. The polypropylene filter is lightest among all, excellent gas permeability, free from mildew and oxidation, resistant to acid and alkali. The advantage of Polyester based fabric cloth for air purification over other includes high tensile strength [128], operable at elevated temperature, resistance to weak oxidizing agents, and easy to clean the filter cake [125].

Denny (1977) [129] fabricated air filters using polytetrafluoroethylene (PTFE) fibrils. To generate a multiplicity of fine fibrils interconnected weave, the woven PTFE fabric was heated substantially unrestrained to a temperature above the crystalline melting point of PTFE and stretched. The PTFE was also impregnated with fluorocarbon polymers and then thermally stretched. This fabric filter was found to be suitable for operation at high temperatures and in aggressive chemical environments.

Tamura (1984) [130] designed an air filter made of a non-woven fabric with an overlapped synthetic net which is intermittently point bonded together. The synthetic net raised bumps which generated the bonding points for the fabric. A fabric filter was structurally strong and also did not lose ventilating property or exhibited any huge air pressure loss. The fabricated filter was suitable to be used as an air filter for an air conditioner, cooler, heating apparatus, ventilation devices, air cleaners, etc.

Kothari et al. (2006) [125] studied the filtration behavior of woven and nonwoven fabrics at different physiological conditions (air flow rate, dust feed rate, dust loading, time intervals) and dust particles. The pressure drop increased with airflow rate in both woven and nonwoven filters. However, the pressure drop in the woven filter is found to be higher than the nonwoven filter. The long-term efficiency of woven fabric was found to be less compared to non-woven fabric. The cleaning efficiency of the woven filter with clay was lowest, followed by sand and Sipernat mixture. In the case of a nonwoven filter, the pressure drop was more with constant dust loading (i.e., the ratio of the amount of dust particle to the volume of air) than at constant dust feed rate.

Desai et al. (2009) [131] fabricated nanofibrous filter media by electrospinning of chitosan/ polyethylene oxide (90:10) solution on to spun-bonded non-woven polypropylene substrate. The airborne particulate filtration efficiency was analyzed based on the size of the nanofibers (pore size; 65-110 µm and diameter; 1.95-2.5 µm). The increasing fiber diameter resulted in diminished efficiency decreased because the maximum pore size and air permeability increased. Around 55% filtration efficiency was reported for 0.6 µm NaCl aerosol particles with a filter having an average pore size of 1.95-2.5µm and fibre diameter 65-110 nm.

Yuksekkaya et al. (2010) [132] fabricated needle-punched nonwoven filters using recycled polyester fibers, with different needling intensities with and without reinforcement fabrics. The acrylic fiber was used as a reinforcement fabric. The reinforcement fabric and high needling intensity increased the burst strength of the filters. The air permeability of filters decreased by using the woven reinforcement materials and increasing the needling intensity. The filters without reinforcing material were found to be suitable for a pre-filter application or in dry air filtration. However, filters with woven reinforcing having increased thickness can be used in the fields where high filtration is required.

Tanabe et al. (2011) [133] investigated the deposition of particles in three types of a synthetic fabric filter (acrylic, polypropylene, and polyester). They also analyzed the adhesive force of filter cakes in fabric filters. The fabrics were tested at superficial filtration velocity of 0.10 m/s and maximum pressure drop of 980 Pa across the filter for ten cycles of filtration. The filter was cleaned by backwashing with air at 0.12 m/s for 2 minutes to remove the cake layer. The particulate matter deposition was observed less in polypropylene filters than in the polyester and acrylic filters. However, the residual pressure drop was found to be high in polypropylene at the beginning due to the accumulation of particles. The adhesion force was higher for polypropylene-based filter and particles and hence causing irreversible cake formation.

Recently Gobi et al. (2019) [134] fabricated multi-layer non-woven fabrics using polyester, cotton, and viscose and binding fiber as polypropylene. Polyester, cotton, and viscose were sandwiched in three layers. Equal proportions of polyester, cotton, and viscose fibers were able to provide high air permeability while filtering the particles in the range of 2-3μm. The high amount of viscose fiber as the bottom layer leads to a reduction of air permeability with the particles of 0.3 to 1 μm.

Apart from woven and non-woven fibers, the most successfully used fibers in the air-filter industry include glass fibers, activated carbon fibers (ACF), nano-fibers, and superfine glass fibers. The use of glass fiber air filter goes way back to 1940 [135], and since then, its use in air-filter has gone up manifold with the efficiency of >99% for micron-size dust particles [136]. The high-efficiency particulate air (HEPA) filters first came in to picture with military requirements for protection against chemical, biological, radiological warfare agents and to nuclear exposure. The first HEPA filter was made of CC-6 paper consisted of a fine mixture of asbestos fibers and coarse cellulose fibers to give mechanical strength for use in gas masks [137]. HEPA filter made of glass fibers can remove more than 99% of dust, pollen, mold, bacteria, and any airborne particles with a size of 0.3 μm [138]. Zhang et al. (2018) [139] compared the dust loading capacity of the PTFE HEPA media with glass fiber HEPA media. Poly-disperse solid particles from potassium chloride particles generated through a nebulizer in the aerosol generator were used for the study. The velocities and aerosol concentrations had no effects on the dust loading performance for both glass fiber and PTFE HEPA media. The pressure drop in glass fiber media increases with the number of particles deposited during operation,

while for PTFE media, the pressure drop was comparatively very low, uniform and remained unchanged for whole operation. The results indicated that PTFE based HEPA is more energy-efficient than glass fiber except in circumstances of heavy loading or infrequent maintenance.

ULPA filters are closely related to HEPA filters but with more efficiency and specified to remove 99.999% of contaminants of 0.12 μm or larger in diameter. They are made up of countless randomly arranged fiber together with a dense mat. Typically these filters are composed of a fibrous filter media like fiberglass bound by an acrylic resin arranged in a pleated structure within a frame [140]. The filter fiber collects particulate matters through interception, inertial impaction, and diffusion [141]. The particulate matters which are smaller than 0.1 μm are trapped easily by diffusion, while PM with size more than 0.4 μm are collected due to inertial compaction. The PM with size in the range of 0.1-0.4 μm is too large to trapped by effective diffusion and too small for inertial compaction, and the filter efficiency is low in this range [142].

With the birth of nanotechnology in the late 1980s, the use of nano-fiber for air-filtration has been studied extensively. The larger specific surface area, surface energy, and surface tension increases the deposition of airborne particulates on the fibre surface and consequently improve filtration efficiency and longer service life [143]. The high surface-to-volume ratio, low flow resistance with high filtration performance make nanofibers an attractive material for applications in air filtration.

Podgorski et al. (2006) [144] developed a modified melt-blown technology to produce filters composed of a micrometer as well as nanometer-sized fibers. The filters were tested with aerosol particles in the range of diameters 10–500 nm. The removal efficiency of bilayer systems composed of micro-fibrous support and a nano-fibrous facial layer was considerably higher than for a micro-fibrous filter alone. Also, the utilization of many-layer nano-fibrous filters combined with a single micro-fibrous backing layer was found to be more profitable from the quality factor standpoint.

Leung et al., (2010) [145] proposed multi-layering to fabricate nanofiber filters with a greatly reduced pressure drop. The used a non-woven microfiber medium made of electro-spun polyethylene oxide nanofibers (diameter 208 nm) with negligible filtration efficiency and pressure drop compared to the nanofiber layer. The media was tested with

aerosol is sodium chloride with size ranging from 50 to 480 nm. The results showed that when nanofiber packing density increases from 3.9 to $36\times10^{-3,}$ the most penetrating particle size decrease from 140 to 90 nm. While when nanofiber packing density was maintained at 8.7×10^{-2} with triple the nanofiber layer thickness, the most penetrating particle size decreases slightly from 140 to 120 nm. They are suggesting that nanofiber packing density has a more prominent effect on most penetrating particle size than nanofiber layer thickness. However, when the face velocity is increased from 5 to 10 cm/s, the filtration efficiency decreases.

Daehwan et al. (2013) [146] evaluated the efficiency of a nano-fibrous filter media made of polyacrylonitrile (PAN) nanofibers with and without TiO_2 nanoparticles. The hybrid nano-fibrous filter media had larger pore size and broader pore size distribution than pure PAN-based nano-fibrous filter media. The pressure drop of PAN/TiO_2 hybrid nanofibers filters media was four times less than that of the counterpart filter media at an air velocity of 80 cm/s. Despite lower fiber coverage density and reduced pressure drop, the filtration efficiency of the nano-fibrous filter media made with PAN/TiO_2 hybrid fibers was found to be much higher than pure PAN fibers.

Zhang et al. (2016) [147] fabricated high-efficiency polyimide-nanofiber air filters for removal of particulate matter at elevated temperatures (25-370 °C). The filters exhibited high flux low-pressure drop and very high efficiency (>99.5%). The nano-fiber filter continuously worked for more than 120 h for $PM_{2.5}$ index >300.

Gao et al. (2018) [148] fabricated a nanofiber air filter using silk fibroin and polyethylene oxide via the electrospinning process. The silk fibroin rich in functional group exhibited a high filtration efficiency of 99.99% with a relatively low air resistance of only 75 Pascal. The membrane was biodegradable hence can be disposed of easily after sufficient use.

Activated carbon fibers use for air filtration goes way back to 1959 with the industrialization of carbon fibers [149]. The ACF provides fast intra-particle adsorption kinetics compared to granular and pelletized carbon. The ACF possesses around 70% of micropores, which results in high surface area in the order of >2000 m^2/g making it suitable for higher adsorption. Navarri et al. (2001) [150] used ACF for the removal of gases like xylene, ethyl acetate, perchloroethylene. The used ACF exhibited around 54%

adsorption capacity for perchloroethylene at 10% breakthrough for 300 mg/Nm^3 concentration. Ao and Lee (2003) [151] immobilized TiO_2 on activated carbon filter for removal of nitrogen oxide, benzene, toluene, ethylbenzene, and o-xylene (BTEX). The combination of TiO_2 and activated carbon significantly increased removal at short residence time with high humidity levels. As a further extension of their work in 2005 [152], they used a similar setup in an indoor air cleaner. The modified filter was able to remove NO by 97% and generated 1.6% NO_2. Sidheswaran et al. (2012)[153] used the ACF media for removal of VOCs that included toluene, benzene, o-xylene, 1-butanol, limonene, undecane and formaldehyde in heating, ventilating, and air conditioning (HVAC) system. The pollutants upstream were in the range of 20-30 ppb and flow velocity at 0.5 m/s. The adsorption capacity of the media was found to be 90 mg VOC per gram of ACF. The results indicated that the combination of ACF and a 50% reduction in ventilation would decrease indoor concentrations of VOCs by 60%-80%. The ACF also reduced formaldehyde concentrations by 12%-40%.

Summary and possible scope for further research

From the above-discussed literature, it may be found that a range of materials has been used for the fabrication of filters for air purification, which includes woven/non-woven fibers, glass fibers, activated carbon fibers, nano-fibers, and superfine glass fibers. Among these the commercially successful filters like HEPA, ULPA, etc. usually employs glass fibers and activated carbon-based fibres. Though these reported filters are very efficient in the removal of particulate matter, these units are usually fitted with an additional unit of activated carbon and other class of adsorbents for removal of VOCs and other pollutants. It was observed that most of the research had been focused on targeting either PM or VOC removal from air, and very limited study has been reported where PM and VOCs have been targeted simultaneously. Therefore, this research has been designed to target efficient separation of PM as well as the removal of VOCs from indoor air.

Moreover, the advanced filters like HEPA and ULPA are not washable and hence can be used for single operational cycles. Hence, one of the objectives of this research is to fabricate an air filter that can be used for separation of PM as well as adsorptive removal of VOCs from indoor air. Also, in the present study, one of the prime focus is to impart washable property to the air filter for easy cleaning and longer operational cycle.

2.3. Silk Sericin

Silk consists of two major components, fibroin, and sericin, in which fibroin fibres are structural center glued together by sericin to form robust cocoons [154]. Sericin is an amphoteric globular protein comprised of 17-18 amino acids [155], among which serine, aspartic acid, glycine, threonine, and glutamic acid are the most abundant [156]. *Table 2-1* shows the amino acid composition of sericin reported in the literature. The presence of multiple hydrophobic and hydrophilic amino acids gives sericin different functional groups for diverse applications. For a long time, sericin existed as a waste product during the silk degumming process. It is only during the last decade that sericin has found its application in biomedical science, regenerative medicine, textile-industry, and membrane fabrication [101–106].

Table 2-1. Silk sericin amino Acid composition (mole %)

References	**Gamo et al. (1977)** [157]			**Aramwit et al. (2009)** [158]		
Amino Acid	Highest yield	Average	SD	Highest yield	Average	SD
Alanine	7.2	6.14	1.16	4.98	4.51	0.44
Arginine	4	3.6	0.39	3.09	2.97	0.11
Aspartic Acid	13.9	12.8	0.82	15.97	15.74	0.19
Cystine	4.7	0.94	0.90	0.44	0.38	0.09
Glutamic acid	10.7	7.54	2.72	4.86	4.74	0.12
Glycine	18	14.72	2.94	15.14	15.09	0.05
Histidine	3.1	1.78	0.84	1.37	1.22	0.13
Isoleucine	2.2	1.46	0.67	1.46	0.65	0.04
Leucine	2.8	1.94	0.91	1.15	1.09	0.07
Lysine	6.3	4.16	1.85	2.78	2.55	0.21
Methionine	Trace	-	-	3.39	1.38	1.75
Phenylalanine	3.4	1.44	1.17	0.39	0.34	0.05
Proline	3.4	2.23	1.60	0.71	0.62	0.08

Serine	38.1	29.26	7.98	34.5	33.99	0.45
Threonine	11.1	7.14	3.05	8.43	8.31	0.13
Tyrosine	9.0	4.8	2.96	3.64	3.52	0.10
Valine	3.8	2.32	1.59	3.04	2.95	0.08

2.3.1. Sericin functionality for application in the field of water and air purification

Sericin consists of polar side chains made of hydroxyl, carboxyl, and amino groups that enable easy cross-linking, co-polymerization, and blending with another polymer [102,107]. Hence, these functional groups assist the incorporation of sericin into the polymeric membrane surface. Apart from these sericin inherent characteristics such as hydrophilic nature, excellent moisture absorption and release properties (hygroscopic), UV resistance, anticoagulant, antioxidant activities may also provide antimicrobial and antifouling properties to membrane surface [102,107–109]. The incorporation of sericin can also provide structural strength and selectivity to the membrane as bio-sorbent. Its high solubility with increasing temperature limits sericin use as an adsorbent; thus, the molecular transition of sericin becomes necessary [159], and hence, it is usually immobilized incorporated or combined with a suitable substrate. The amphoteric nature (act as both acid and base) of sericin makes it a suitable candidate for adsorption of various micropollutants (like antibiotics and NSAIDs, EDCs, and heavy metals) [160,161]. Sericin, with slight modification, have been used in its various form of a hydrogel, encapsulated beads, micelle and polymer film for drug delivery and adsorption of micropollutants and textile dyes [161–164].

Sericin antioxidant nature has also been harnessed in the production of sericin-coated PET (Polyethylene terephthalate) and Nylon indoor air filtration membranes [165]. Purwar, Sai Goutham, and Srivastava (2016) [166] fabricated sericin/PVA/clay-based nanofibrous mats via electrospinning technique for air filter masks. The fibre diameter varied in-between 300-400 nm. The filter was able to collect PM of size 2.5 µm in the concentration of 1.407 mg/m^3 and PM of size 10 µm in the concentration of 4.175 mg/m^3. Wang et al. (2016) [167] fabricated a lightweight silk nanofibre based air filter for filtration of $PM_{2.5}$ and submicron particles. The air-filter exhibited high filtration efficiency for $PM_{2.5}$ (98.8%) and submicron; 300 nm particles (96.2%) with low-pressure

drop. Two years later, Min, Kim, and Kim 2018 [168] generated silk protein nanofibers on a window screen via electrospinning to fabricate air filters. The filters were capable of removing 90% of $PM_{2.5}$ and 97% PM_{10} particles from the air and were naturally degradable hence safe to dispose of in the environment. These findings suggest that sericin has a promising application in membrane modification to enhance its antifouling properties as well as for the adsorption of micropollutants from water and air.

2.3.2. Sericin application for membrane modification

Chen et al. (2011) [169] reported adsorption of acidic dyes acid yellow and copper (II) Phthalocyanine-3,4′4″4‴ tetrasulfonic acid by electrostatic interaction between the negatively charged sulfonate group of the dye molecule and the positive protonated amino groups on sericin. Structural similarity of these acidic dyes to many acidic pharmaceutical active compounds suggests that sericin could have potential applications for the removal of these micropollutants.

Kwak et al. (2013) [170] fabricated Silk sericin (SS) into beads and utilized as a heavy metal adsorbent. SS beads were investigated for their Cr(VI) adsorption ability and found that adsorption depended on the coagulant used for the fabrication of the SS beads. When methanol was used as a coagulant, the beads had a better adsorption capacity than when ethanol was used except at pH 1. The adsorption behavior of Cr(VI) on the SS beads followed the BET isotherm. The maximum adsorption capacity was 33.76 mg/g at pH 2, while desorption was carried out using NaOH solution, and it was found that 73.19% of the adsorbed Cr(VI) could be detached.

Da Silva et al. (2015) [171] evaluated sericin-alginate blended particles for biosorption of zinc and copper metals. The gelation technique, dripping blends in aqueous and alcoholic solutions of $CaCl_2$, was applied to produce particles with 1%, 2% and 3% w/v of alginate in sericin solution (2.5% w/v) with the thermal cross-linking process at 40, 100, 125 and 150 °C. It was observed that water solubility of particles decreases when produced in an alcoholic solution, and it was related to the formation of the β-sheet structure. The thermal cross-linking process increased the adsorption capacity until 100 °C, with values around 75% and 65% of the reduction of Cu^{2+} and Zn^{2+}, respectively.

Silva et al. (2015) [172] studied biosorption of Bordeaux S dye onto sericin powder derived from silkworm cocoons in a batch adsorption system. The adsorption occurred

favorably at pH below 3.2. The kinetic and equilibrium studies showed fast adsorption and interaction were limited to the monolayer surface, with pseudo-second-order and Langmuir models providing the best fits. Thermodynamic studies indicated that the system is spontaneous and exothermic and that physical interactions govern the adsorption process. The obtained results established sericin powder potential as a bio-sorbent for the treatment of wastewater containing the dye.

Koley et al. (2016) [173] fabricated complex hybrid flowers with hierarchical porosity through a green and facile co-precipitation method by using industrial waste natural silk protein sericin. The large surface areas and porosity of the micro-size hybrid flowers facilitated the adsorption of different heavy metal ions. The high adsorption capacity depends on their morphology, which was controlled by sericin concentration during their fabrication. Superior adsorption and greater selectivity for Pb(II) ions were confirmed with excellent thermal stability.

2.3.3. Sericin use as an antifouling agent

It is known from the literature that foulants can adsorb to the membrane surface through a physical or chemical interface like hydrophobic interaction, hydrogen bonding, van der walls attraction, Lewis acid-base interaction, and electrostatic interaction [174,175]. Surface characteristics of most of the UF/NF/RO membranes, such as hydrophobicity, roughness, and surface charge, contribute to fouling [176,177]. Sericin inherent characteristics such as excellent moisture absorption (hydrophilicity) and release properties [178], UV resistance [179], anticoagulant, antioxidant activities provide improved antifouling properties.

Yu et al. (2013) [105] deposited the sericin layer on the RO membrane through dip-coating, which showed improved surface hydrophilicity, enhanced surface negative charge, smoothed surface morphology, and decreased salt permeability coefficient.

Voicu et al. (2016) [103] reported studies on the covalent immobilization of sericin to green cellulose membrane. The surface of the cellulose acetate membrane was immobilized with the aminopropyl-triethoxysilane (APTS) functional group, while the protein was immobilized through glutaraldehyde that was used as a linker between aminopropyl-triethoxysilane and sericin. Subsequently, the performance of the

membranes was characterized, and the retention was found to be more than 90% after 90 min of process.

2.3.4. Sericin use as an antimicrobial agent

Many kinds of literature show the antibacterial activity of silk sericin over a broad spectrum of gram-positive and gram-negative bacteria. Sarovart et al. (2003) [165] found antibacterial and antifungal activity in silk sericin of Thai cocoon varieties coated on nylon and polyester fabrics. In this study, they coated PET and Nylon based filters with sericin to impart antimicrobial properties for indoor air filters. The antioxidant properties of sericin inhibit the oxidation reaction of free radicals and hence the growth of microorganisms. The sericin powder from Bombyx mori (Mulberry silk) obtained using deionized water had antibacterial activity when coated on bleached wool fabric using bacterial strain at pH 3.8 [180]. Sericin extracted from Eri silk using alkali was shown to have high antibacterial activity [181]. Sericin from Mulberry silk extracted using base was coated on cotton fabric showed antibacterial activity. Also, Mulberry silk cocoon extracts in Tris–HCl buffer pH 7.5 was found to be antibacterial [182] (tested for *Escherichia coli, Bacillus cereus, Staphylococcus aureus, Pseudomonas aeruginosa, and Klebsiella pneumonia*).

Sericin has been used as a capping agent for the preparation of silver nanoparticles (AgNPs) in the range of 48-117 nm diameter for enhanced antimicrobial activities. The carboxylate groups obtained from alkaline degradation of sericin works as a reducing agent for the generation of AgNPs while COO^- and $NH2^+$ groups stabilized the AgNPs and prevent their precipitation or aggregation [183,184].

Zhao et al. (2014) [185] fabricated chitosan/sericin composite nanofibers by electrospinning for wound dressing application, the composite nanofibers showed good bactericidal activity against both Gram-positive and Gram-negative bacteria. Joshi et al. (2015) [186] showed metal complexed sericin film to have a good antimicrobial property and very good oil barrier property with and without alum. These scientific studies elucidate that sericin can have potential application as an antimicrobial agent in membrane synthesis.

Summary and possible scope for further research

The above-discussed literature signifies the potential of sericin as a smart material for membrane modification. The multi-functional group like amide, hydroxyl, and carboxyl part of amino acid cluster present in sericin provides its desired properties for blending with other materials. The hydrophilic nature of sericin can be harnessed for imparting antifouling properties to the membrane and easy washing for the air filter. The inherent antioxidant, antimicrobial properties also makes it a very suitable candidate as a coating material for air filter since it can resist the growth of microbes once fouled with pollutants. However, the use of sericin has been limited to imparting hydrophilicity to the membrane, for removal of heavy metals and for facilitating antimicrobial properties to the membrane and air filter. Whereas the charged multi-functional groups can be hypothetically used for adsorption of organic compounds. Hence this thesis focusses on utilizing sericin for membrane modification for removal of drug-based micropollutants from water and VOCs from the air.

2.4. Research Gap

Based on the extensive literature survey, the following gaps in research have been identified.

- To meet the requirements of safe drinking water, proposed new methods need to be stable, economical, and more effective as compared with the already existing techniques. For this, existing treatment technologies have to be modernized, that is, updated or modified or replaced by developing materials and methods which are efficient, cost-effective, and reliable.
- The available physiochemical methods involved in the removal of pharmaceuticals from drinking water are effective but are limited in some way such as toxic transformation products, incomplete removal, very high capital, and operation costs, and sophisticated maintenance and skilled personnel requirements have become hurdles to the implementation of these technologies.
- Since pharmaceuticals are mostly synthetic and designed in a way to be biologically stable and are intentionally polar structured, both properties, persistent against biochemical degradation and polar structure, however, may be

responsible for the incomplete removal during conventional biological sewage treatment.

- Although activated carbon is used as adsorbents for removal pharmaceuticals, it can not be easily and cost-effectively regenerated.
- The membrane filtration processes like nano-filtration and reverse osmosis are very effective in the removal of these drugs. However, trace quantities of some target compounds have been reported of breaching NF/RO membranes while the adsorptive MF/UF membranes suffer from fouling related issues as well as performance inadequacy.
- The membrane cleaning and its replacement impose around 50% of the operational cost or 30% of the total membrane system cost. Hence a simple and economically viable method for membrane modification is very much needed.
- Hydrophilicity has been related to imparting the antifouling characteristics to the membrane, and hence a variety of polymers using different techniques has been used to enhance the antifouling properties in membranes. However, most of the methods adopted for membrane modification using hydrophilic polymers were either very tedious or not cost-effective.
- One of the important phenomena governing the performance of an air filter is its reusability for a longer time, which very much depends on membrane cleaning. The most successful HEPA, ULPA filter is not washable and works for single use. While the cleaning process with other fabric-based filter does not regain its initial properties, since the complete removal of particles is not possible during cleaning. The study based on modified fabric for air filtration is very scarce, and there is too much scope for modified air-filter with washing capabilities, for which a comprehensive study on the hydrophilic coating of filter membranes is needed.
- The use of sericin as a coating material for air-filter membranes has been limited, and its potency for removal of particulate matters and VOCs together has not been studied.
- The use of a sericin biopolymer for membrane modification about water purification has been limited. Though there have been few recent studies on the use of sericin for removal of micropollutants like heavy metals and textile dyes, there has been no report of any study involving sericin modified membrane for adsorptive removal of pharmaceuticals from drinking water.

Chapter 3

Experimental, Analytical and Modelling Methods

Parts of this Chapter are published as research articles:

- V.K. Verma, S. Subbiah, Prospects of Silk sericin as an Adsorbent for Removal of Ibuprofen from Aqueous Solution, Ind. Eng. Chem. Res. 56 (2017) 10142–10154. doi:10.1021/acs.iecr.7b01827.
- V.K. Verma, S. Subbiah, Fouling resistant sericin coated polymeric microfiltration membrane, J. Chem. Technol. Biotechnol. (2019) jctb.6169. doi:10.1002/jctb.6169.
- V.K. Verma, S. Subbiah, Sericin coated polymeric microfiltration membrane for removal of drug-based micropollutants, J. Chem. Technol. Biotechnol. (2019) jctb.6168. doi:10.1002/jctb.6168.
- V.K. Verma, S. Subbiah, S.H. Kota, Sericin-coated polyester-based air-filter for removal of particulate matter and volatile organic compounds (BTEX) from indoor air, Chemosphere. 237 (2019). doi:10.1016/j.chemosphere.2019.124462.

3.1. Material

The materials used for membrane surface modification and characterization are summarised in this section.

3.1.1. Sericin as biopolymer and adsorbent

Commercially available pharmaceutical-grade sericin with molecular weight ≈50-250 kDa procured from Swapnaroop Drugs and Pharmaceuticals, Aurangabad, Maharashtra, India, was used in this study. The obtained sericin was stored in an amber bottle in a moisture-free place until used. The change in pH of sericin solution with varying concentrations is shown in Figure 3.1.

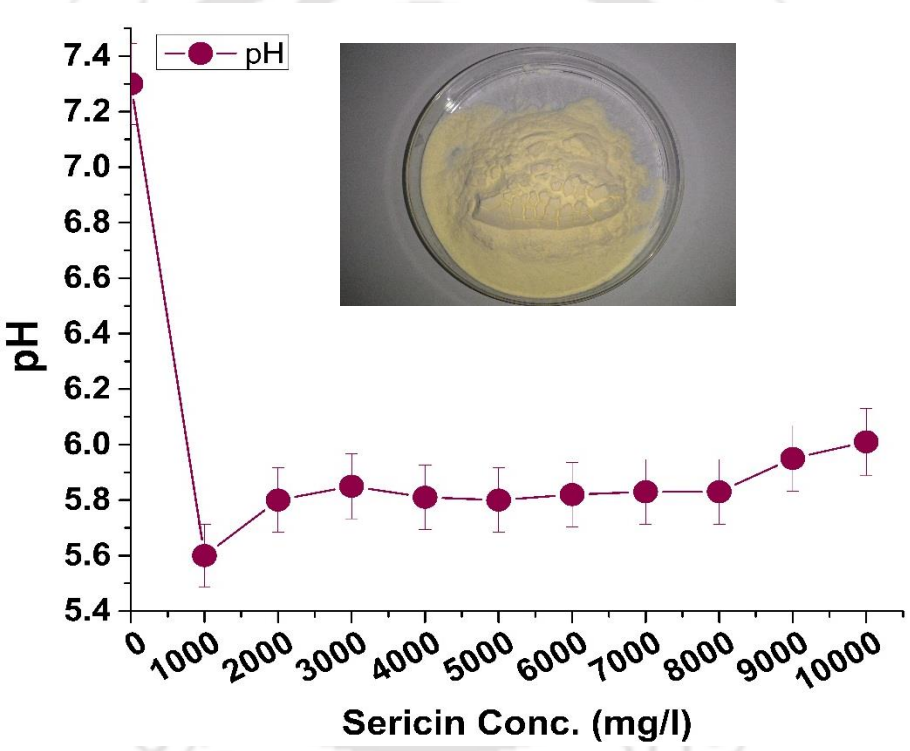

Figure 3.1. Change in pH of sericin solution with varying concentration.

3.1.2. Pharmaceutical Drugs for Removal Study

Drugs from a different class of applications have been used to study the performance of sericin coated membranes. Categorically Nonsteroidal anti-inflammatory (Ibuprofen, Diclofenac), Antibiotics (Amoxicillin, Ciprofloxacin), and Steroids/hormonal drugs (Estrone, β-estradiol) were used. The selection of drugs for the current study is based on their wide therapeutic application, high consumption rate, reported persistent occurrence in water, eco-toxicity, physicochemical properties, and validated analytical methods

[187,188]. The target pharmaceutical compound Ibuprofen, Diclofenac, Amoxicillin, Ciprofloxacin, Estrone, and β-Estradiol was obtained from Sigma-Aldrich Chemicals Pvt. Limited. The stock solutions for all drugs were prepared in Millipore water. The physicochemical properties of all the drugs used are given in *Table 3-1*. The stock solutions were used to obtain the calibration curves and for other experimental studies. All dilutions were done in Millipore water. The calibration curve for High-performance Liquid Chromatography (HPLC) analysis was prepared (see Appendix A1) and was found linear in the used range of concentrations with the R^2 value of 0.99. M/s. Merck Ltd, India supplied the eluent for HPLC analysis such as Acetonitrile and Buffer solution. The literature reported the concentration of these drugs in water sources is summarized in *Table 3-2*, and sericin coated membrane is tested with a similar concentration level.

Table 3-1. Physiochemical properties of selected drugs [189]; HSDB (https://toxnet.nlm.nih.gov/cgi-bin/sis/htmlgen?HSDB)

Property	**Ibuprofen**	**Diclofenac**	**Amoxicillin**	**Ciprofloxacin**	**Estrone**	**β-estradiol**
Molecular Formula	$C_{13}H_{18}O_2$	$C_{14}H_{11}Cl_2NO_2$	$C_{16}H_{19}N30_5S$	$C_{17}H_{18}FN_3O_3$	$C_{18}H_{22}O_2$	$C_{18}H_{24}O_2$
Molar Weight ($g.mol^{-1}$)	206.28	296.15	365.40	331.34	270.37	272.38
CAS Number	15687-27-1	15307-86-5	26787-78-0	85721-33-1	53-16-7	50-28-2
Solubility (mg/L); (at 25°C)	21	2.37	$3.43X10^3$	$3.00X10^3$	30	3.90
Melting point (°C)	76	283-285	194	225-257	260.2	178.5
Vapour pressure (mm Hg) at 25°C	$4.74X10^{-5}$	$6.14X10^{-8}$	$4.69X10^{-17}$	$2.85X10^{-13}$	$2.49X10^{-10}$	$6.38X10^{-9}$
Octanol-Water partitioning log K_{ow}	3.97	4.51	0.87	0.28	3.13	4.01
Soil organic- carbon partition coefficient K_{oc}	3,400	245	100	61,000	457-18,000	30,000
Henry Coefficient Air/Water	1.5	$4.73X10^{-12}$	$2.49X10^{-21}$	$5.09X10^{-19}$	$3.8X10^{-10}$	$3.64X10^{-11}$
pKa at 25°C	4.91	4.15	pKa1=2.63 pKa2=7.16 pKa3=9.55	pKa 1=6.09 pKa=8.74	10.40	10.71

IBU= Ibuprofen, DIC=Diclofenac,AMX=Amoxicillin, CPF-Ciprofloxacin, EST=Estrone, β-ESD=β-estradiol

Table 3-2. Reported maximum concentration of drugs in water sources in India and International context

Indian context				
Class of drugs	**Drug**	**Concentration**	**Place**	**References**
Antibiotics	Ampicillin	23.5-263.3 µg/L	Yamuna River, New Delhi	[190]
	Ciprofloxacin	9.7-45.4 µg/L	Yamuna River, New Delhi	[190]
	Ofloxacin	7.5 µg/L	Ujjain, Madhya Pradesh	[191]
	Ciprofloxacin	236.6 µg/L	Ujjain, Madhya Pradesh	[191]
	Norfloxacin	22.8 µg/L	Ujjain, Madhya Pradesh	[191]
	Levofloxacin	8.8 µg/L	Ujjain, Madhya Pradesh	[191]
	Ciprofloxacin	28,000-31,000 µg/L	Patancheru, Hyderabad	[21]
	Losarton,	2400-2500 µg/L	Patancheru, Hyderabad	[21]
	Enoxacin	150-300 µg/L	Patancheru, Hyderabad	[21]
	Ciprofloxacin	14000 µg/L	Patancheru, Hyderabad	[24]

	Norfloxacin	520 µg/L	Patancheru, Hyderabad	[24]
	Enoxacin	160 µg/L	Patancheru, Hyderabad	[24]
Analgesic	Ibuprofen Acetaminophen Ibuprofen Diclofenac	1.90 µg/L 9-11.5 µg/L 1.4-2.3 µg/L 0.31-.5 µg/L	Coimbatore, TamilNadu Karnataka and Nagpur Ghaziabad and Lucknow New Delhi and Lucknow	[192] [193] [194] [195] [19]
Stimulant Hormones	Caffeine Testosterone	61-102 µg/L 0.1-.0.5 µg/L	Karnataka and Nagpur Chennai, India	[193], [194] [196]
International Context				
Class of drugs	**Conc.**	**Place**	**References**	
Antibiotics **Analgesic** **Stimulant**	6-11 µg/L 13-134 µg/L 32 µg/L	USA	[197]	
Antibiotics **Analgesic** **Stimulant**	0.53-1.6 µg/L 0.1-27 µg/L 0.091 µg/L	UK	[198]	
Antibiotics **Analgesic** **Stimulant**	0.06-7.35 µg/L 0.81-58.7 µg/L 61-102 µg/L	South Africa	[199]	
Antibiotics **Analgesic** **Stimulant**	0.46-1.1 µg/L 2-3.4 µg/L 6-82 µg/L	Germany	[200]	

3.1.3. Chemicals and reagents

All the chemicals, like, Glutaraldehyde, Sulfuric acid, Hydrochloric acid, Sodium Hydroxide, Calcium Chloride used in the study were of analytical grade and were procured from M/s. Merck Ltd, India. A complete list of the chemicals used in this research work is given in *Table 3-3*. For sample filtration, Whatman (0.45µm) and syringe-filters (0.22µm) were procured from M/s. Merck Ltd. India. All the plastic-ware and glassware were procured from M/s. Tarson Products Pvt. Ltd. India and M/s. Borosil Glassworks Ltd.

Table 3-3. List of chemical and reagents used in the research

Sl. No.	Reagent/Chemicals	Grade	Purity (%)	Manufacturer
1.	Hydrochloric Acid	AR	36	M/s. Merck Ltd. (India)
2.	Phosphoric Acid	AR	85	
2.	Sulfuric Acid	AR	98	
3.	Sodium Hydroxide	AR	97	
4.	Calcium Chloride	AR	99	
5.	Glutardialdehyde	AR	25	
6.	Isopropanol	AR	99.9	
7.	Acetonitrile	HPLC	99.9	
8.	Methanol	HPLC	99.9	

3.1.4. RO-membrane for Removal of Ibuprofen

Flat Sheet RO-membrane from DOW FILMTEC™ of dimension 7.007 X 3.293 cm with an effective area of 22.935cm^2 was used for filtration of aqueous sericin ibuprofen solution (*Figure 3.2*). Pure water flux for the RO-sheet membrane (ΔP; 10-90 psi) was obtained (see Appendix Figure A2).

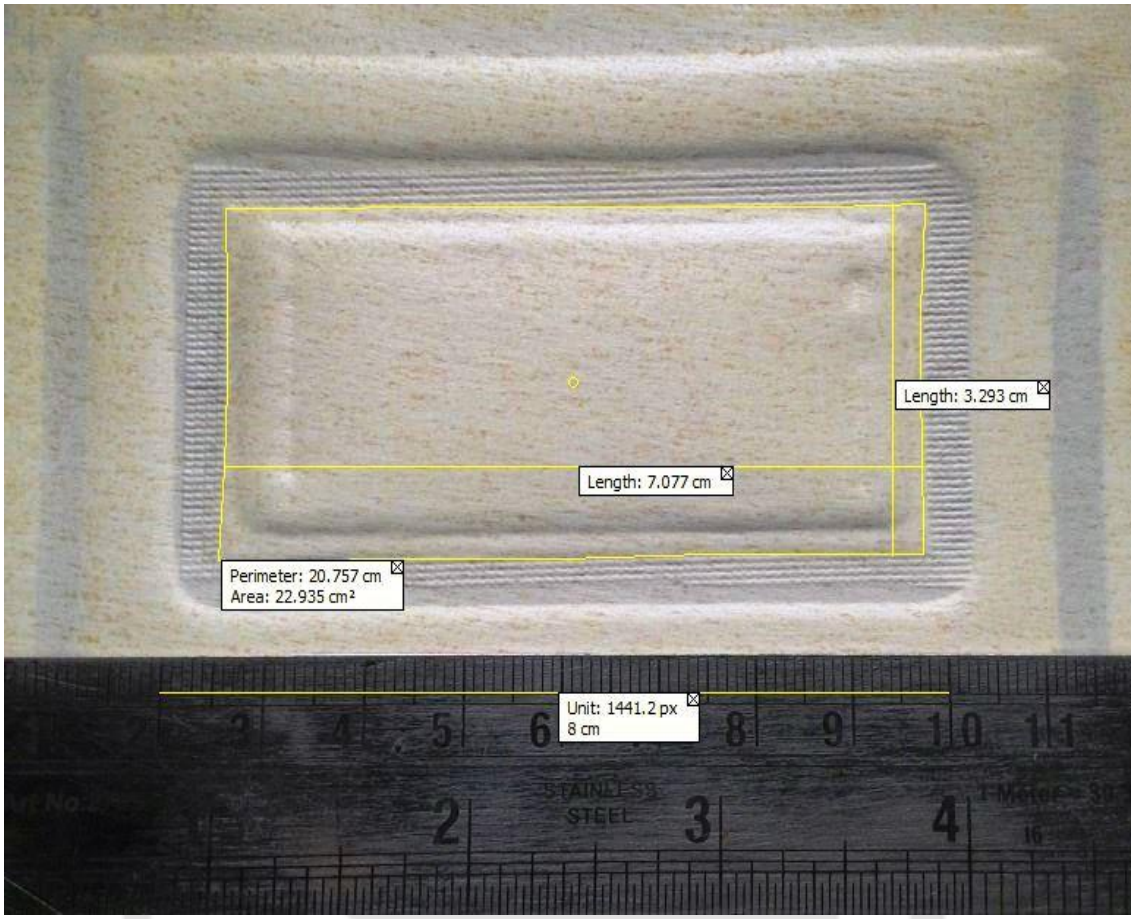

Figure 3.2. Flat Sheet RO-membrane dimension used in the test cell and effective area measured using Digimizer 4.6.1 software.

3.1.5. MF-membrane for Sericin Coating

For membrane modification, Polypropylene based hollow fibre microfiltration (MF) membranes with a surface area of 1.27 m^2 were used for the fabrication of sericin coated MF filters. It was supplied by HI-TECH Sweet Water Technologies Pvt. Ltd., Bangalore, India. The outer diameter of the MF hollow fibre was 0.5 mm, and the length of the fibre was 0.38 m. The total number of fibre was 2100.

3.1.6. Polyester fabric for Air-filter

In this study, a bi-component polyester fabric sheet has been used as a base material for fabricating sericin coated air-filter. Hornwood Incorporation, USA, provided the bi-component polyester hybrid sheet. The bi-component polyester hybrid fabric weighed 81.37 gm for per meter square of cloth used, mesh-count-40, and thickness of 200 µm.

3.1.7. Particulate Matters for Air Purification

In the air purification study, the particulate matter (PM) was generated by burning incense stick (locally purchased) in the closed chamber until a concentration of 1000 µg/m^3 is reached. The PM concentration used in this study is higher than the maximum reported concentration (≈350 µg/m^3) in major cities in India [43,45] (See Appendix Table A1). The concentration of particulate matters was monitored using a PM sensor, VR-SMART-126 portable four in one air quality monitor.

3.1.8. Volatile organic compounds (BTEX) for Air Purification

The use of petroleum products is one of the main sources of generated VOCs in the environment. Gasoline generates a range of VOCs, and the most prevalent compounds are benzene, toluene, heptane, ethylbenzene, cyclohexane, and xylene, accounting for almost 50% of the total fraction. Hence, in this study, we have focussed on the removal of VOCs, namely Benzene, Toluene, Ethylbenzene, and Xylene, together known as BTEX. For the BTEX removal study, VOCs were generated by evaporating the required amount of gasoline in the closed chamber. The concentration used in this study lies inbetween100 to1000 µg/m^3. The reported concentration of selected VOCs in India is listed in Appendix Table A1. A VOC analyzer (PhO Check TIGER, ION Science limited, United Kingdom) was used to detect the concentration of required VOCs throughout the experiment. The physicochemical properties of all the selected target VOCs are listed in Appendix Table A1.

3.1.9. Synthetic Greywater for fouling study

To study the fouling behavior of sericin coated MF membrane, the synthetic greywater solution was formulated using 15 g of Ariel (Procter and Gamble Company, India) detergent dissolved in 50 L of freshwater together with $CaCl_2$ [201]. An increasing amount (1, 2, 3, 4, 5, 6, 7, 8, 9, 10 mL) of $CaCl_2$ solution (at 10,000 ppm) was dissolved in the detergent solution (200mL), and solution turbidity was measured for precipitation. Active precipitation was observed when 6 mL of $CaCl_2$ was mixed in 200mL of detergent solution. Hence, a lower $CaCl_2$ concentration (≈250 ppm) was used maintained to formulate a synthetic greywater solution for further fouling studies. The characteristics of synthetic greywater used in this study are given in *Table 3-4* (the values correspond to the average of analysis performed in triplicate).

Table 3-4. Characteristics of Synthetic greywater

Sl. No.	Parameters	Value
1.	Conductivity	1084 µS/cm
2.	TDS	706 ppm
3.	Turbidity	57.1 NTU
4.	COD	234 ppm
5.	BOD	14 ppm
6.	pH	9.6

3.1.10. Produced water for fouling study

The produced water is used to test sericin coated UF membrane fouling resistivity. Produced water was received from the drilling site of Oil and Natural Gas Corporation Limited (ONGC), Geleki, Shivsagar Assam. The characteristic of the obtained produced water is shown in *Table 3-5* (the values corresponds to the average of analysis performed in triplicate).

Table 3-5. Characteristics of Produced water

Sl. No.	Parameters	Value
1.	Conductivity	2.12 mS/cm
2.	TDS	1092 ppm
3.	Turbidity	91 NTU
4.	COD	190 ppm
5.	BOD	16.2 ppm
6.	pH	7.3
7.	Oil content (HEM*)	18.7 mg/l

*n-hexane extractable material

3.2. Methodology

Identification of sericin as a potent adsorbent and smart material for membrane surface modification has been investigated in this research. This section presents different methodologies adopted for studying the interaction of sericin with selected drugs to ascertain its applicability for the removal of drugs generally reported in the water. Different methods and characterization techniques adopted for the coating of polymeric microfiltration membrane and air filter have been presented. The post-modification process adopted for the assessment of modified polymeric membrane and air-filter has been discussed.

3.2.1. The method used to study Sericin and drug interaction

3.2.1.1. *Integrated adsorption-cum-RO process*

An integrated adsorption-cum-RO process was designed to evaluate the efficacy of sericin to bind with Ibuprofen, and hence size-based separation can be facilitated for the complex in the integrated system. In this method, initially batch adsorption studies were carried out on a magnetic stirrer operated at a constant speed of 350 rpm, coupled with a digital temperature controller for temperature regulation. In each test, two-liter of ibuprofen solution (of required concentration) was placed in a 5-liter beaker, and the required concentration of sericin was added from a stock solution (1000 ppt). Ibuprofen has a pKa value of ≈4.9 and hence, exists in anionic form when released into the environment [202]. While sericin has an isoelectric point (pI) close to pH≈5-6, where it has zero overall charge and the smallest intermolecular repulsive force [203]. Since, proteins have net negative charge above their pI values (pH > pI) and net positive charge below their pI values (pH < pI), sericin was buffered at pH 4 (to keep it in the protonated state) while Ibuprofen pH was changed from 5 to 8 to facilitate charged based interaction. The solution was stirred continuously for the required time, and the temperature was monitored using a temperature controller. Sericin-ibuprofen solution was passed as feed through an RO-flat sheet membrane at regulated flowrate using bypass valve and dampener (see *Figure 3.3*). The setup was run in cross-flow filtration mode and recirculation mode, i.e., permeate and reject recirculated back to the feed tank. As per the membrane manufacture's guideline, a feed flow rate of 100 L/Hr and transmembrane pressure of 75 psi was maintained throughout the process. Permeate samples were taken at regular intervals of time to measure permeate flux and Ibuprofen concentration. The

feed and permeate samples were analyzed using HPLC analyzer. The change in physiological condition triggers conformational changes in protein and hence can affect how a protein interacts with a ligand (i.e., drug) [204]. Hence, experiments were conducted at different operating conditions (a) sericin concentration (b) ibuprofen concentration (c) solution pH (d) solution temperature, to evaluate the effect of parameters on binding interaction between ibuprofen and sericin and hence removal efficiency.

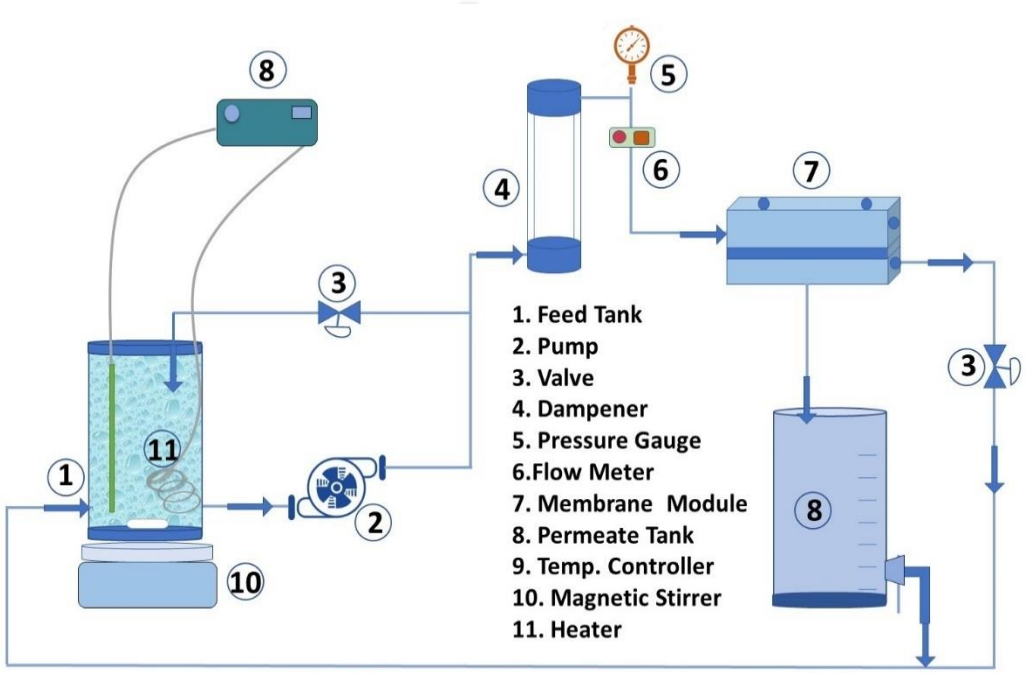

Figure 3.3. Integrated adsorption-cum-RO-membrane filtration setup.

3.2.1.2. *Characterization techniques used for Sericin-drug analysis*

ATR- Fourier transform infrared spectroscopy

The absorption of IR-radiation causes a vibrational transition in polypeptide units of protein (sericin), and this phenomenon gives nine characteristics bands named as amide-A, Amide-B, and amide I to VII. Among these, the Amide-I (1600 to 1700 cm^{-1}) is most sensitive to the composition of protein secondary structure. The variation in corresponding IR vibrational frequencies can provide information related to the structural conformation of sericin due to sericin and Ibuprofen interaction [205]. Hence ATR-FTIR spectra (4000-400 cm^{-1}) were acquired using ATR spectrophotometer (Model: Spectrum TWO from Perkin Elmer) to confirm structural conformation of sericin after complex

formation with ibuprofen. Experiments were conducted at room temperature with 32 scans per second, at a resolution of $4cm^{-1,}$ and obtained data were analyzed using OMNIC software.

Fluorescence Spectroscopy

The protein folding and unfolding is expected while interacting with the ligand. This phenomenon leads to exposure of tyrosine and tryptophan present in the protein from the core to the solvent phase, and a similar phenomenon is expected to happen while sericin and Ibuprofen interaction. The fluorescence intensity of both tyrosine and tryptophan can be measured by the fluorescence quenching mechanism [205]. Therefore, the drug-mediated sericin conformational changes were monitored by tyrosine intrinsic fluorescence. Drug (Ibuprofen)-induced tyrosine intrinsic fluorescence quenching studies were carried out on spectrofluorometer (model: Fluoromax-4) at room temperature. 1 µM of sericin protein was incubated with a diverse range of ibuprofen drug starting from 0.1mM to 1mM while maintaining pH 7.5 using 10 mM of phosphate buffer at room temperature. Samples were excited at 280nm (2nm slit width) and collect emissions between 300 and 450nm and averaging three scans.

Isothermal Titration Calorimeter (ITC)

ITC measures the changes in the power needed to maintain the isothermal conditions between the reference and sample cell, which gives the measures of heat absorbed or generated when molecules interact [206]. These heat changes are very low level (sub-millionths of a degree) but can be detected using high sensitivity thermocouple. The binding of ibuprofen drug with sericin protein is expected to be endothermic/exothermic in nature. The heat of adsorption during complex formation was measured by isothermal titration calorimetry using MicroCal ITC-200 (MicroCal, Northampton, MA, USA). Sericin protein and drug samples were prepared with 10 mM phosphate buffer (pH 7.5) and they were degassed through thermovac vacuum pump prior to use in ITC. In this experiment, 50 µM of sericin protein was filled in the sample cell and titrated with 4.5 mM of Ibuprofen drug at 27°C. Typically, 25 consecutive injections of 1.5 µl in two min intervals were injected into the sample cell with adequate mixing. The heat of mixing due to the buffer solution is measured in a separate experiment and was subtracted from the total heat of adsorption.

Field emission scanning electroscopic microscopy

Sericin used in this study had a molecular weight of ≈250 kDa. The structural morphology of the sericin powder used was visually analyzed using (FE-SEM) field emission scanning electron microscopy (Make: Zeiss, Model: Sigma) instrument. Powder sample was fixed on top of the stub using carbon tape and layered with gold using an auto fine coating instrument (JEOL JFC-1300) before morphology analysis.

FE-SEM images for powder samples of ibuprofen, sericin, and ibuprofen-sericin complex were acquired and analyzed for structural changes. The sericin-ibuprofen complex aqueous solution was prepared by mixing them in distilled water, then using open pan dry method (40 °C) the aqueous solution containing sericin-ibuprofen complex was dried to remove the water molecules. Adsorption of Ibuprofen on sericin was visually confirmed using FE-SEM. All the samples used for FE-SEM analysis were stored in a desiccator prior to analysis.

Surface area analysis

The surface area and pore size for sericin powder were analyzed using the Brunauer-Emmett-Teller (BET) method in the Quantachrome surface area and pore size analyzer ((Model: Autosorb-IQ MP, Make: Quantachrome, USA). Before analysis, the powder sample of sericin was dried in a hot-air oven at 80 °C for four hours, followed by degassing at the same temperature for five hours. N_2 sorption experiments were carried out at –196 °C (77 K) and by varying the partial pressure of nitrogen above the sample in a P/P0 range of 3.4 × 10-4 to 0.99.

X-ray diffractometer

The amorphous and crystalline structure of sericin, ibuprofen, and complex were examined using XRD and analyzed for any change noticed after complex formation. X-ray diffraction pattern for native sericin, ibuprofen, and sericin-ibuprofen complex was obtained at ambient temperature using an X-ray diffractometer (XRD; make: Bruker; model: D8 Advance) using a step size of 0.05°/sec in the range of 2θ = 5 to 80° under the acceleration voltage of 40 kV and 40 mA.

High-Performance Liquid Chromatography

The feed and permeate samples were analyzed using a High-performance liquid chromatography (HPLC) analyzer (Shimadzu, model UFLC SPD-20A) equipped with a Merck Chromolith® HighResolution reverse-phase C-18 end-capped column (1.5 μm, 4.6 mm ×100 mm) and UV-Detector (SPD-20A/20AV).

Table 3-6. HPLC assay used for quantitative estimation of different drugs

Sl. No.	**Drug**	**Mobile phase ratio (Acetonitrile: phosphate buffer)**	**λ_{max}- wavelength (nm)**	**Reference**
1.	Ibuprofen	65:35	220	[207]
2.	Diclofenac	35:65	262	[208]
3.	Amoxicillin	5:95	230	[209]
4.	Ciprofloxacin	77:23	278	[210]
5.	Estrone	45:55	277	[211]
6.	β-estradiol	45:55	275	[211]

Acetonitrile and phosphate buffer were used as mobile phase, and the intensity was checked at the respective wavelength (Ibuprofen, 220 nm; Diclofenac, 262 nm; Amoxicillin, 230 nm; Ciprofloxacin 278 nm; Estrone, 277.5nm; β-estradiol 275nm) in isocratic mode to quantify the concentration of selected drugs. The HPLC assay used for the quantitative estimation of different drugs is shown in *Table 3-6*, and the calibration plot for each drug is shown in Appendix Figure A1. All the experimental analysis was done in triplicates.

3.2.2. Membrane Modification

3.2.2.1.Flow-through Coating method for hollow fibre MF membrane modification

A facile novel method was developed for sericin coating on polypropylene hollow fibre microfiltration (PP-HFMF) membrane to modify its permeation and adsorptive

properties. Modification of the PP-HFMF membrane involves four steps (i) pre-conditioning, (ii) flow-through deposition of sericin, (iii) crosslinking and (iv) heat curing. *Figure 3.4* shows the flow chart for the modification procedure of the PP-HFMF membrane module via the sericin coating. Before modification, the PP-HFMF membrane is first soaked in de-ionized water for around 4 hours, replacing the water every hour, then rinsed thoroughly to remove any preservative agent if present. The pure water flux of the uncoated HFMF membrane was determined. In the pre-conditioning step, the PP-HFMF membrane is subjected to chemical pre-treatment for generating functional groups on the membrane surface. The PP-HFMF membrane is pre-treated using H_2SO_4 and H_2O_2 solution at a volume ratio of 3:1 and 65°C temperature for 90 minutes to generate hydroxyl groups on the membrane surface [212,213]. The proposed reaction involved in the hydroxylation of the PP-HFMF fibre surface is shown in Appendix Figure A3. After the surface hydroxylation step, the PP-HFMF membrane was thoroughly washed with de-ionized water to remove any residual chemicals if present.

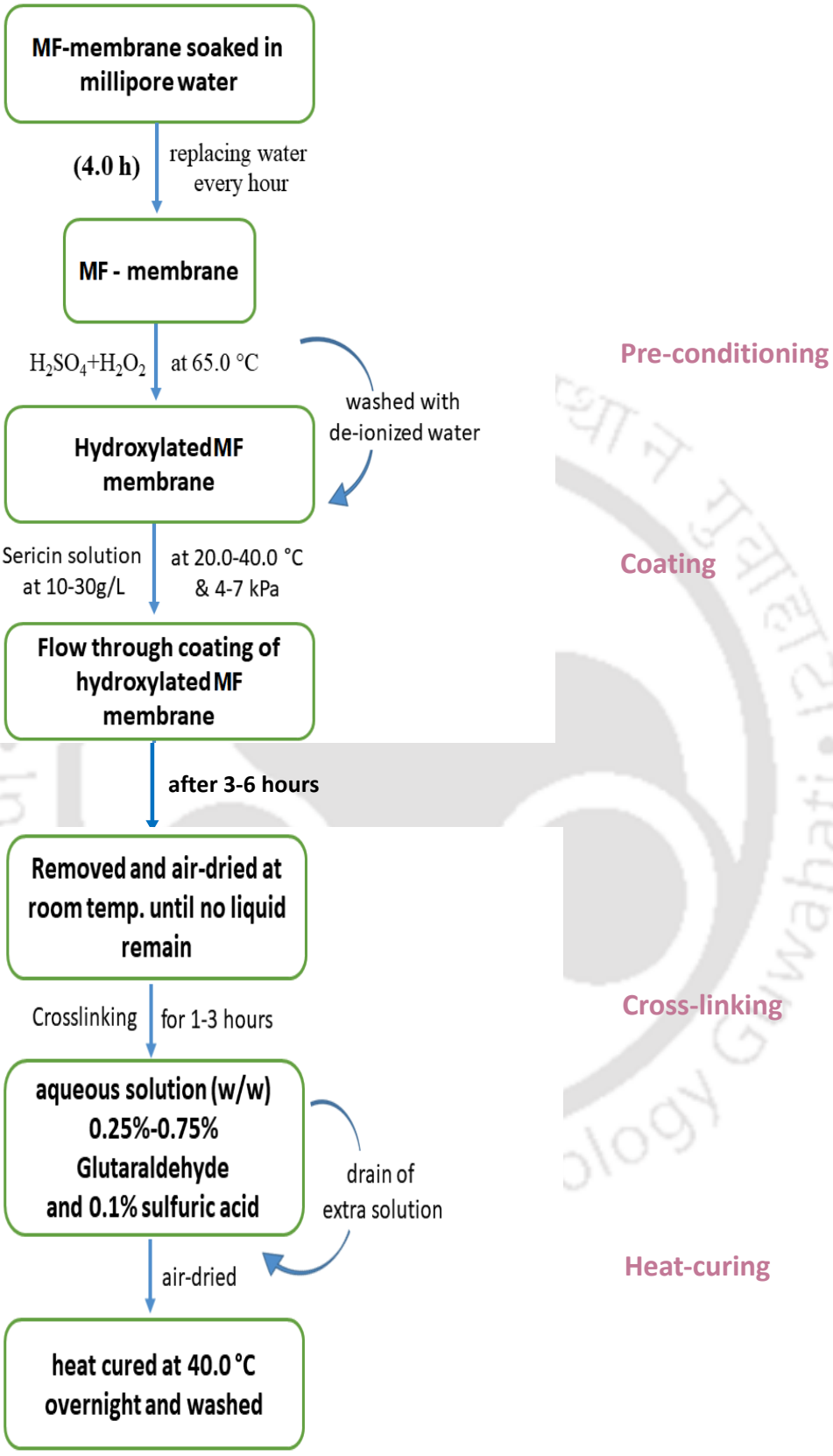

Figure 3.4. Flowchart of the fabrication process for the sericin coated HFMF-membrane.

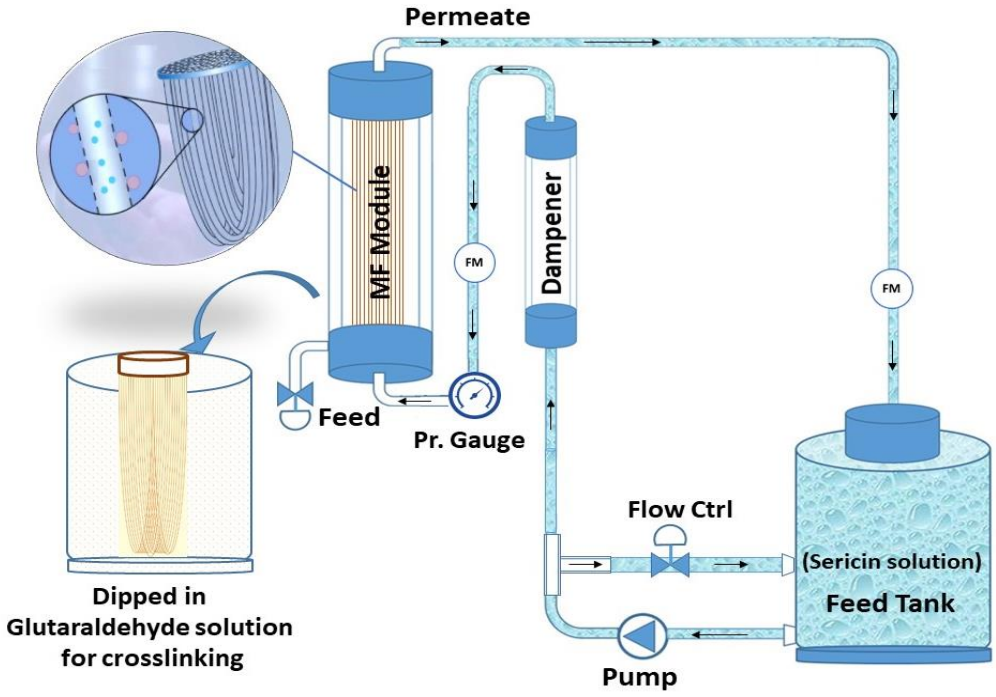

Figure 3.5. Schematic diagram of the flow-through method used for sericin deposition on MF membrane.

Membrane coating was then carried out in a clean assembly room using the pre-determined content of sericin solution (10-30 g/l) at 25°C. Sericin solution was passed through the PP-HFMF membrane (in a flow-through method) at low pressure (4kPa) in full circulation mode for a required time, i.e., 3-6 hrs (see *Figure 3.5*) A submersible centrifugal pump (VND-380-SP1, 38217, 24VDC), was used for membrane coating. Sericin adheres to the polypropylene membrane surface via hydrogen bonding (see Appendix Figure A4). After sericin-coating, the PP-HFMF membrane was air-dried at room temperature until no liquid remains in the membrane. Then in the cross-linking stage, an aqueous solution with 0.75% Glutaraldehyde (w/w) and 0.1% Sulfuric acid was prepared for cross-linking, and the sericin coated HFMF membrane was dipped in the prepared solution for 3 hours (Appendix A5). Detail mechanism for the cross-linking reaction of sericin by glutaraldehyde via hemiacetal and Schiff base formation is elaborated in Appendix Figure A6 and Figure A7. The self-cross-linking of deposited sericin via glutaraldehyde provides robustness to the modified surface and prevents leaching of bonded sericin, thus inhibiting further solubilization. In the last step, the cross-linked membrane is heat cured at 40°C overnight in a hot air oven, resulting in thermal fixation of cross-linked sericin network on to the membrane. The finished

membrane is then washed multiple times with de-ionized water and stored in de-ionized water until used. Leachability of the coated sericin and Glutaraldehyde was verified by washing the modified membrane with distilled water and analyzing feed/permeate water through a spectrophotometer. Since the protein particles have a tendency to agglomerate under a wide variety of conditions such as protein concentration, temperature, pH, mechanical stress, etc. [204]. The amount of sericin coated on the PP-HFMF membrane may vary with these process conditions and hence experiments were conducted at different (a) sericin concentration; 10-30 g/l (b) temperature; 10-40 °C and (c) pH; 4, to evaluate its effect on sericin coating.

3.2.2.2.*Methods used for membrane characterization*

Field emission Scanning electron microscope

The surface and cross-sectional morphology of the uncoated and sericin coated membrane was characterized by a field-emission scanning electron microscope (FESEM, Make: Zeiss, Model: Sigma**).** The single hollow fibre sample was cut into a small piece of 1 cm and was then fixed to a microscope slide using double-sided tape. Then the hollow fibre membrane was cut at an inclined angle, which was used for FESEM analysis. Before analysis, vacuum-dried membrane samples were sputter-coated with a thin gold layer and images were obtained at an acceleration voltage of 3kV and 15kV at different magnification.

ATR- Fourier transform infrared spectroscopy

The ATR-FTIR spectra (4000-400 cm^{-1}) for uncoated PP membrane, sericin-coated PP membrane, and acid-treated membrane were acquired using the ATR spectrophotometer (Model: Spectrum TWO from Perkin Elmer) to confirm the change in functional groups and deposition of sericin layer on to the modified membrane. Experiments were conducted at room temperature with 32 scans per second, at a resolution of $4cm^{-1,}$ and obtained data were analyzed using OMNIC software. The membrane samples were dried overnight at 40°C under vacuum before ATR-FTIR analysis.

Contact angle measurement

Overall, the hydrophilicity of a membrane can be measured by evaluating the contact angle between the membrane and a droplet of aqueous phase (i.e., water); lower the angle more the hydrophilicity. Hence, the water contact angle was measured to compare the

improvised surface hydrophilicity of the sericin coated and uncoated HFMF membrane. One µL of Millipore water was dropped on to dry membrane surface with a micro-syringe, and a series of images of the water droplet on the membrane surface was acquired using a contact angle goniometer (Make: HOLMARC, Model No: HO-IAD-CAM-01B) equipped with video/image capture at room temperature. Then, the measured contact angle of uncoated and sericin coated membrane were compared to analyze the enhanced hydrophilicity.

Swelling (Water content) and porosity tests

The swelling property of the membrane provides information about bulk hydrophilicity and porosity. Water content was evaluated using the difference between the weight of the wet and dry membrane for both sericin coated and uncoated membrane,

$$Water\ content\ (\%) = \frac{w_w - w_d}{w_w} X\,100 \tag{3.1}$$

Where W_w is the weight of wet membrane (g), W_d is the weight of dry membrane (g).

The porosity of the membrane was determined by using the gravimetric method, wherein dried sericin coated and the uncoated HFMF membrane was weighed (W_d) and then immersed in isopropanol for 24 Hr. Then, the membrane was separated from the solution and drained off until no visible solution remained on the outer surface, and the membrane was weighed again (W_w). The porosity was calculated using the following relation:

$$Porosity\ (\%) = \frac{\frac{\left(w_w - w_d\right)}{\rho_w}}{\frac{w_w - w_d}{\rho_w} + \frac{w_d}{\rho_m}} X\,100 \tag{3.2}$$

Where W_w is the weight of wet membrane (g), W_d is the weight of dry membrane (g). ρ_w is the density of isopropanol (786 g/litre), and ρ_m is the density of membrane ($\rho_{m(uncoated)}$ = 166.487g/l and $\rho_{m(Sericin\ coated)}$) = 170.909 g/l). Pore size distribution before and after sericin coating was analyzed using Capillary flow porometry Air/Liquid porosimeter (Make: TECHPoro Capillary Flow Porometer; Model No: TECH Poro-AL-500).

Zeta potential and particle size Measurement

Zeta potential of the membrane surface, detergent, greywater foulants as well as sericin particle size was determined using electrophoretic light scattering method with DelsaNano (Model No.: Delsa Nano C; Make: M/s Beckman Coulter, Switzerland) apparatus.

Spectrophotometer

The leaching of sericin from the coted MF membrane was analyzed using a spectrophotometer (Model No.: UV-2600, Make: Shimadzu, Singapore). A calibration plot for the sericin solution at different concentrations was obtained. The sericin-coated membrane was washed multiple times with distilled water after sericin coating to ascertain any sign of leaching post-coating. Afterward, the membrane was washed with different pH (5, 7, and 9) solution to see the effect on leachability. pH was maintained using 1M NaOH and 1N HCl solution and measured using a pH meter (Cyberscan pH 510, Eutech Instrument Pvt. Ltd., Thermo Fisher Scientific).

3.2.3. The method used for fabrication of sericin coated air-filter

The method used for the coating of Sericin on the polyester mesh is a modification of the sericin-coating method developed by Gupta et al., 2015 [106]. *Figure 3.6* shows the schematics of the procedure followed for sericin coating on the polyester-based bi-component filter. The sericin coating on the Polyester mesh involves four steps (i) pre-conditioning, (ii) dip-coating for sericin deposition, (iii) crosslinking, and (iv) heat curing. Before coating, the polyester fabric is first soaked in de-ionized water for around two hours, and then rinsed thoroughly to remove any dust and preservative agent. In the pre-conditioning step, polyester fabric mesh is subjected to chemical pre-treatment for generating functional groups on the membrane surface. The PP-UF-membrane is pre-treated using a solution of sodium hydroxide (at 2M). The polyester fabric is dipped in the solution for one hour at a temperature of 90 °C [106]. In the second stage, the polyester fabric is dipped in the pre-determined content of sericin solution (10-30 g/L) at 40 °C for six hours. Then in the cross-linking stage, the coated polyester fabric was dipped in the aqueous solution with 0.75% Glutaraldehyde (w/w) for three hours. In the last step, the cross-linked sericin coated polyester fabric was heat cured at 40 °C overnight in a hot air oven, resulting in thermal fixation of cross-linked sericin network on to the

membrane. The heat cured polyester mesh is washed with de-ionized water and stored in de-ionized water until used.

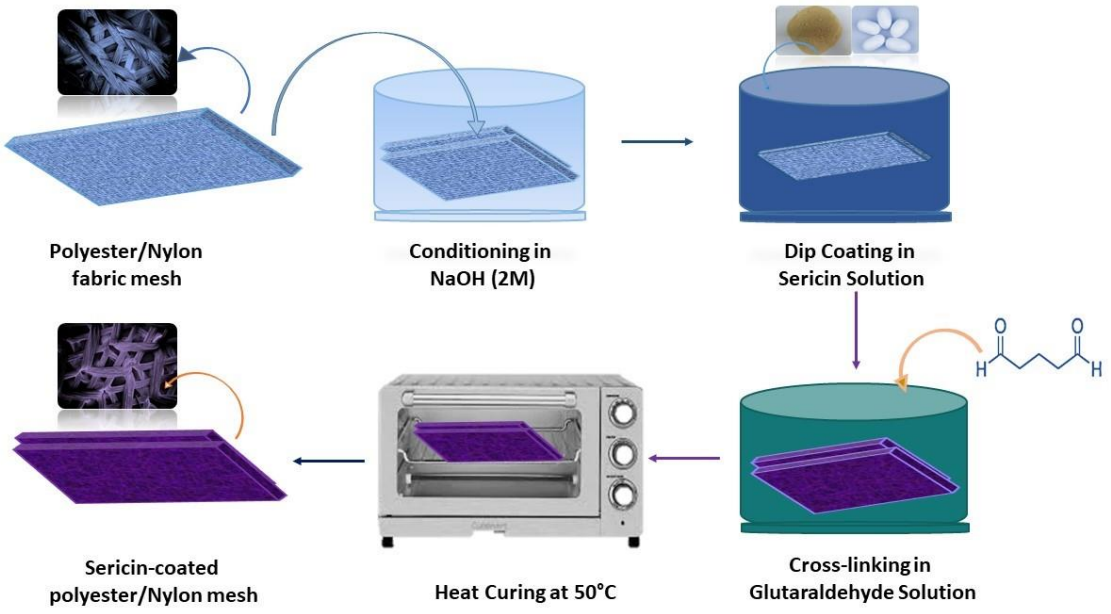

Figure 3.6. Process flow diagram for sericin coating on the polyester/nylon mesh.

3.2.3.1.*Methods used for air-filter characterization*

FESEM

A field-emission scanning electron microscope was used to characterize the surface morphology of the uncoated and coated polyester fabric (FESEM, Make: Zeiss, Model: Sigma)**.** The fabric samples were cut into a small piece of 1 cm and was then fixed to a microscope slide using double-sided carbon tape and used for FESEM analysis. Before analysis, vacuum-dried membrane samples were sputter-coated with a thin gold layer, and images were obtained at an acceleration voltage of 3 kV and 15 kV at different magnification.

ATR- Fourier transform infrared spectroscopy

ATR-FTIR spectra (4000-400 cm^{-1}) were acquired using the ATR spectrophotometer (Model: Spectrum TWO from Perkin Elmer) to confirm the deposition of the sericin layer on to the polyester mesh and to confirm adsorption/desorption of VOCs on the filter surface. Experiments were conducted at room temperature with 32 scans per second, at a

resolution of 4 $cm^{-1,}$ and obtained data were analyzed using OMNIC software. The fabric samples were dried overnight at 40°C under vacuum before ATR-FTIR analysis.

X-ray Diffractometer

The amorphous and crystalline structure of polyester sheet before sericin coating and post sericin coating were analysed. X-ray diffraction pattern for uncoated polyester sheet and sericin–coated polyester was obtained at ambient temperature using an X-ray diffractometer (XRD; make, Bruker; model, D8 Advance) using a step size of 0.05 degree in the range of 2θ = 5–50° with the acceleration voltage of 40 kV at 40 mA.

3.2.4. The method used for air filtration Experiments

A closed chamber with facilities to generate the required amount of PM and VOCs was designed for evaluating sericin-coated air-filter performance. *Figure 3.7* shows the experimental set-up used for the air-filtration experiment. The set-up consists of a leak-proof sealed chamber (6.28 m^3) to simulate a closed indoor environment. The closed chamber includes (a) air filter system (b) hot-plate (c) fan (d) PM sensor and (e) VOC analyzer.

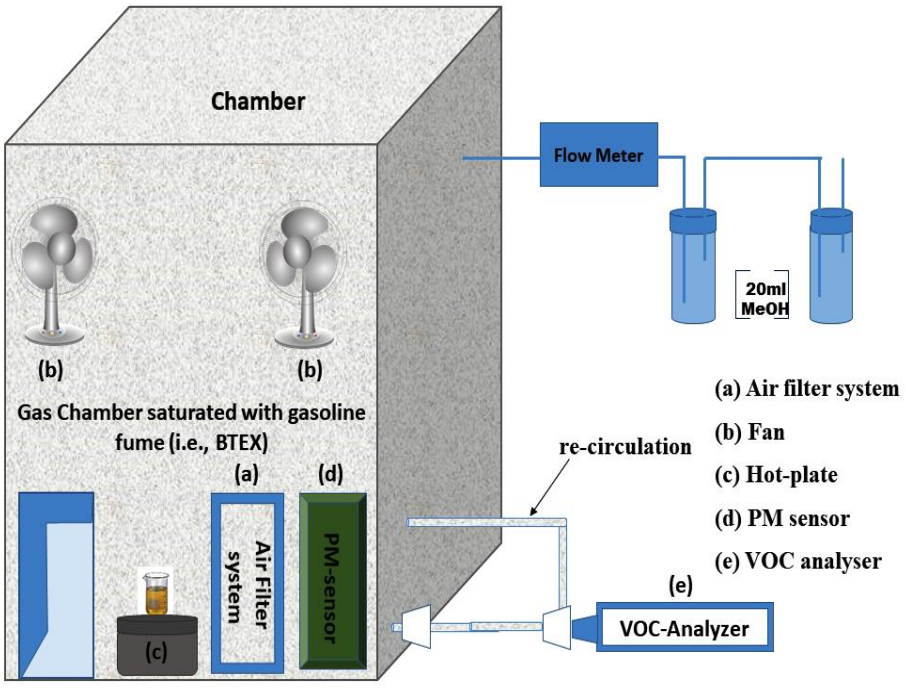

Figure 3.7. Air-purification experimental setup.

The Air filter system with the sericin-coated membrane is pre-fitted in the system. The incense stick was burned inside the chamber to generate particulate matters (≈1000 $\mu g/m^3$). While the hot-plate was used to generate the VOC fumes from gasoline. In a small beaker, Gasoline was heated up, and the resultant gases were distributed to the whole cubical using a fan. The air filter system is controlled from outside the cubicle using a remote. The fan was used to circulate the generated PM and VOCs throughout the whole cubicle and not concentrated at some fixed location. All the sensors were calibrated before the start of every set-up of experiments.

3.2.5. The method used for fouling resistance study

The setup used for fouling based study is shown in *Figure 3.8*. A flow rate of 50 L/Hr at 18 psi transmembrane pressure was used during normal operation. The sericin coated HFMF membrane is backwashed for 2 minutes after every 50 L filtration cycle of greywater. In pure water backwash mode, the pure water was passed through the permeate channel of the HFMF membrane (≈35L/Hr), and backwashed water is collected at the retentate side in the same condition (see *Figure 3.8*). The filtration and backwash operation was performed for both sericin coated and uncoated HFMF membrane and results were analyzed to study the improvement in fouling resistance. The turbidity of the synthetic grey/produced water was measured at a fixed interval of time and results were evaluated. After each 50-liter filtration cycle, the membrane was backwashed with pure water for 2 minutes to clean the fouled membrane. At the end of the fouling experiment, the membrane was chemically cleaned by using 0.01M NaOH solution at 25°C, and pure water flux was measured to assess the efficiency of the chemical cleaning. The turbidity of the synthetic feed solution is expressed in the nephelometric turbidity unit (NTU) and measured using the turbidity meter (Eutech Instruments, model number TN100). Diaphragm booster pump (Hi-Tech Pvt. Ltd., India, Model number E-B300), with maximum pressure 140 psi, was used during fouling studies. Feed and permeate flow-rates were measured using a flow meter (MICRO-FLO purchased from OMEGA Engineering, USA) and the temperature was maintained by using a circulating water bath (model: WB 2000V, Rated Supply: 230V, 50Hz, Sr. No.: WB 201508002) purchased from ANM Industries. De-ionized water was used for the backwashing of the fouled membrane.

Permeate water flux of the membrane was determined by measuring the permeate water volume collected over a certain period in terms of a liter per square meter per second and using the following equation.

$$J = \frac{V}{AX\ \Delta t} \tag{3.3}$$

Where J is the volumetric permeate water flux ($m^3/m^2.s$), A is the membrane area (m^2) of the membrane for permeation, and V is the volume of permeate (m^3) over a time interval Δt (sec).

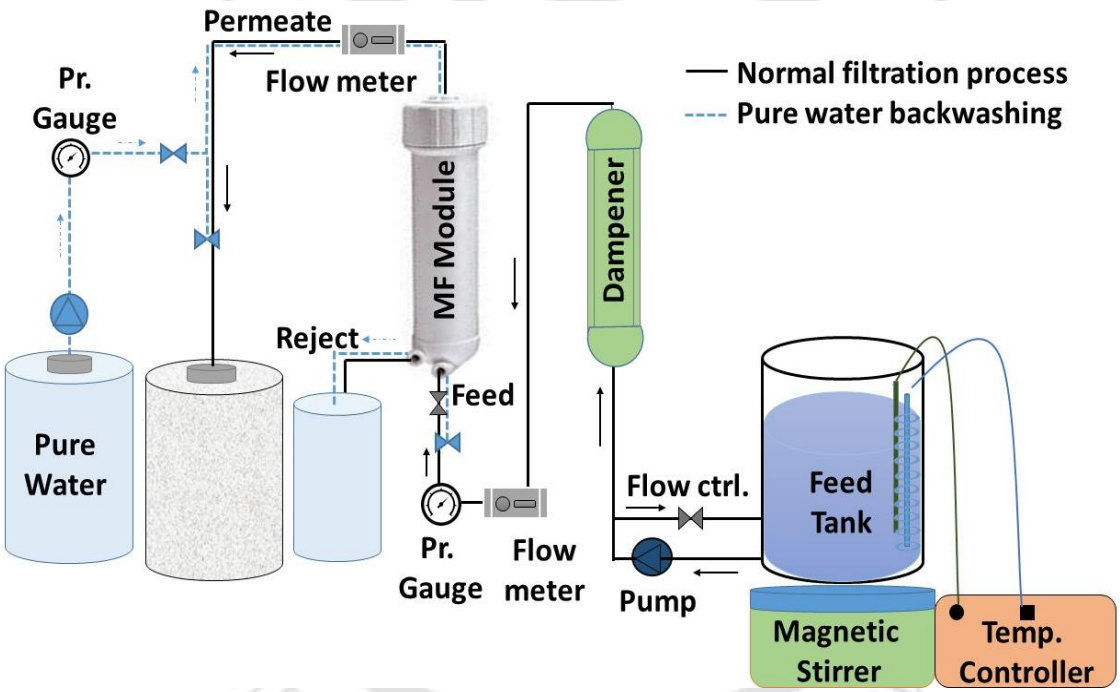

Figure 3.8. Process flow diagram of the membrane filtration unit used for fouling based study (solid lines) and backwash unit (dotted lines) for membrane cleaning.

The measured pure water flux (J_w) under transmembrane pressure (ΔP_{tm}) was then used to calculate the membrane pure water permeability (P_m). Flux recovery after backwashing and chemical cleaning were calculated using the following relation.

$$Flux\ recovery = \frac{J_c}{J_0} X\ 100 \tag{3.4}$$

Where Jc is a pure water flux of cleaned membrane ($m^3/m^2.s$), and J_0 is the pure water flux of new membrane ($m^3/m^2.s$).

3.2.6. The method used for drug removal study using sericin coated membrane

Performance of the sericin-coated HFMF membrane for removal of drug-based micropollutants present in the water at low concentration is evaluated using the synthetic water solution spiked with selected model drugs. A laboratory-scale filtration setup (see *Figure 3.9*) was employed to conduct dead-end filtration experiments. The set-up mainly consists of a feed tank equipped with a stirrer, a temperature controller, flow control valves, and a sericin coated HFMF membrane with housing. The one side open porous HFMF membrane bundle is fitted in the membrane housing. In the HFMF membrane, the feed is transported from the shell side to the fiber lumen side, and the filtrate is collected from the fiber lumen side, i.e., the open end of the HFMF membrane bundle. Samples were collected at a regular interval of time from the permeate outlet to record the drug removal efficiency of the process.

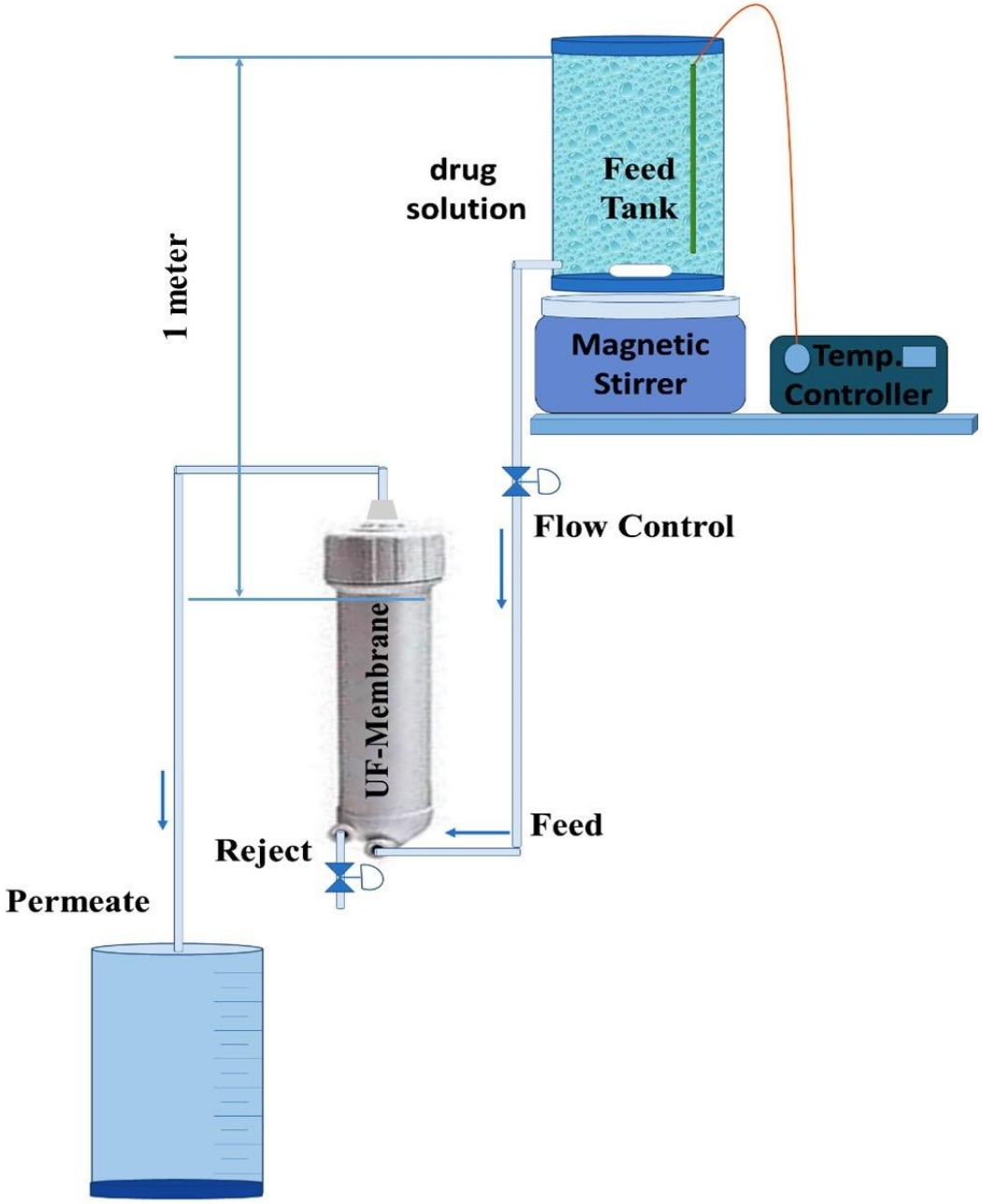

Figure 3.9. Filtration set-up used for dead-end filtration of drug-based micropollutants from the water solution.

3.2.7. The design of experiment for drug removal study using sericin coated membrane

Experiments were designed to evaluate the removal efficiency of the sericin-coated membrane at different operating conditions (feed concentration, flow rate) using Ibuprofen as a model drug. Initial experiments were conducted at a different flow rate and concentration to ascertain adsorption as a primary removal mechanism.

Subsequently, the removal efficiency of the sericin-coated membrane was tested with a different class of selected drugs to establish its vast and real-time applicability. Also, the effect of background salt and mixed drug conditions on the removal efficiency of the membrane were analyzed. *Table 3-7* shows the list of experiments conducted at different conditions to evaluate sericin coated HFMF membrane performance. Diaphragm booster pump (Hi-Tech Pvt. Ltd., India, Model number E-B300; maximum pressure 140 psi) was used to pump drug solution at a different flow rate (5 l/h, 10 l/h, 15 l/h, 20 l/h) for initial experiments with Ibuprofen. The continuous filtration process (i.e. 5 cycles of 3 litre) for different class of drugs was operated under gravity-based flow (permeate flux = 2.75 $lh^{-1}m^{-2}$, head = 1meter). The membrane was regenerated using alkaline solution (0.01M NaOH) wash after each filtration cycle. In gravity-based flow, the feed tank is kept at a higher point, and flow is mediated to membrane module kept at the lower point under normal gravity without any external pump mimicking gravity-based commercial filters (i.e., HUL pureit, Tata Swatch, Eureka Forbes aqua sure).

Table 3-7. Design of Experiment for drug removal using sericin-coated HFMF membrane

Removal at different operating condition (for Ibuprofen)	
Effect of feed flow rate (500 µg/L, pH 7, 30°C)	Flow rate 5 l/h, 10 l/h, 15 l/h, 20 l/h
Effect of feed Concentration (pH 7, 30°C, flow rate 5 l/h)	Feed concentration 100 µg/l, 500 µg/l, 1000 µg/l, 1500 µg/l
Removal with a different class of drugs	
NSAIDs	
Ibuprofen Diclofenac	500 µg/l, pH 7, 30°C, flow under gravity (Operated for 5 consecutive cycles of 3l)

Antibiotics	
Amoxicillin Ciprofloxacin	500 µg/l, pH 7, 30°C, flow under gravity (Operated for 5 consecutive cycles of 3l)
Steroids	
Estrone β-estradiol	500 µg/l, pH 7, 30°C, flow under gravity (Operated for 5 consecutive cycles of 3l)
Effect of background salt on removal with drugs	
Ibuprofen Amoxicillin Estrone	Salt (100 mg): NaCl, $CaCl_2$, $MgSO_4$, and Mixture of NaCl, $CaCl_2$, $MgSO_4$
Removal with a mixture of drugs	
Ibuprofen, Diclofenac, Amoxicillin, Ciprofloxacin, Estrone, β-estradiol at 100 µg/l (each drug)	pH 7, 30°C, flow under gravity
Ibuprofen, Diclofenac, Amoxicillin, Ciprofloxacin, Estrone, β-estradiol at 20 µg/l (each drug)	pH 7, 30°C, flow under gravity

3.2.8. Modeling methods

This section presents the different modeling methods adopted for evaluating the performance of sericin-coated membrane for the removal of drug-based micropollutants from water as well as VOC removal from the air.

3.2.8.1. *Kinetics modeling for adsorption of drugs on sericin coated membrane*

Experiments were conducted to evaluate the adsorption capacity of the sericin-coated membrane for selected drugs (Ibuprofen, Diclofenac, Amoxicillin, ciprofloxacin, Estrone, β-estradiol) from the aqueous solution. The six liters of aqueous drug solution (initial conc. 500 µg/l) was passed through the sericin-coated membrane (with 3.14 g/m^2 coated sericin) in a dead-end filtration mode mimicking a fixed-bed column adsorption experiments at temperature 30°C and pH=7 and permeate flux = 2.75 lh^{-1}m^{-2}. Permeate concentration was measured at a regular interval of time. The experimental results were analyzed to calculate adsorption capacity (see equation 5), and the breakthrough curve was drawn (i.e., drug concentration versus time profile). The quantity of the drug adsorbed in the HFMF membrane is calculated by integrating the breakthrough curve. The effect of flow rate and concentration on adsorption capacity was evaluated for Ibuprofen as a model drug.

Adsorption capacity at equilibrium (q_e) is calculated from the total amount adsorbed (q_{total}) per dry weight of adsorbent in the column (w_a) at the end of each experiment using equation 3.5.

$$q_e = \frac{q_{total}}{w_a} \tag{3.5}$$

The drug % removal with respect to the time/volume of the solution filtered can be calculated using equation 3.6.

$$\%\, removal(t) = \left(1 - \frac{C_p(t)}{C_f}\right) X 100 \tag{3.6}$$

Where, C_p = permeate concentration; C_f = inlet feed concentration

Bohart-Adams, Thomas, Yoon–Nelson, and Clark fixed bed models were applied to experimental breakthrough curve data using nonlinear regression to determine the adsorption parameters. The Thomas model used for breakthrough modeling assumes plug flow behavior, no axial dispersion, and uses Langmuir isotherm second-order kinetics for

adsorption-desorption [214]. The Thomas model for adsorption in a fixed bed is described by equation 3.7.

$$\frac{c_t}{c_0} = \frac{1}{1+\exp\left[\left(\frac{k_{TH} q_e w_a}{Q}\right) - k_{TH} c_0 t\right]} \tag{3.7}$$

Where k_{TH} = Thomas model constant (mL/min.mg); q_e = adsorption capacity (mg/g); w_a = mass of adsorbent (g); Q = influent flow rate (ml/min)

The Yoon-Nelson model assumes that the rate of decrease in adsorption for each adsorbate particle is proportional to the adsorbate adsorption and the breakthrough [215]. The model is expressed by equation 3.8.

$$\frac{c_t}{c_0 - c_t} = \exp\left(k_{YN} t - \tau k_{YN}\right) \tag{3.8}$$

Where k_{YN} = rate constant (1/min); τ = time required for 50% adsorbate breakthrough

The Clark model utilizes the mass-transfer concept together with the Freundlich isotherm to explain the breakthrough curve [216] and can be presented by equation 3.9.

$$\frac{c_t}{c_0} = \left(\frac{a}{1+Ae^{-rt}}\right)^{1/(n-1)} \tag{3.9}$$

Where $A = \left(\frac{c_0^{n-1}}{c_b^{n-1}} - 1\right) e^{rt}$ and $r = (n-1)\frac{K_T}{F}\frac{dz}{dt}$

C_b = breakthrough concentration; F = flow rate per unit cross-section area; z = total bed depth; n= Freundlich parameter

The Bohart-Adams model describes the dynamic behavior of a fixed bed column in terms of effluent concentration versus time profile (i.e., breakthrough curve). The model derived by Bohart and Adams [217,218] assumes a negligible axial dispersion (i.e., D_L=0) and presented as

$$\frac{c(t)}{c_f} = \frac{\exp(\alpha)}{\exp(\alpha)+\exp(\beta)-1} \tag{3.10}$$

$$\alpha = k_{BA}\, C_o\, (t - \tfrac{z}{v}); \quad \beta = \tfrac{k_{BA}\, \rho_m\, q_e Z}{v} (\tfrac{(1-\varepsilon)}{\varepsilon})$$

Where C(t) is a concentration of drug in permeate with time, Z is the total bed depth, ν is superficial flow velocity across HFMF bundle, t is time, ε is HFMF membrane module void fraction, and ρ_m is adsorbent density.

The above equation was fitted using nonlinear-regression analysis to obtain the parameter k_{BA} (Bohart-Adams rate constant) for binary aqueous drug-solution adsorption studies. The parameter of the Bohart-Adams Model for the HFMF membrane column used for the adsorption experiment is given in *Table 3-8*.

Table 3-8. Bohart-Adams model parameters for HFMF membrane packed module.

Properties	**Value**
Column internal Diameter(d)	8.036 cm
Column Height (l)	30 cm
Column volume (v)	1520 cm^3
Effective Flow Area (A)	46.57 cm^2
Superficial flow velocity (υ)	0.0130 cm/s (Q =5 l/h)
Membrane density (ρ)	0.17 g/cm^3
Column void fraction (ε)	0.89702
Initial Feed Concentration (C_f)	0.5 mg/l, 1 mg/l, 1.5 mg/l
Sericin adsorbent in MF membrane	4 g

3.2.8.2.*Adsorption Isotherm and kinetics for VOC gases adsorption*

The batch adsorption experiments were conducted to evaluate the adsorption capacity of the sericin-coated air-filter for BTEX compounds generated using gasoline. To study the adsorption isotherm and kinetics, different concentration of BTEX (from 1 to 10 mg m^{-3}) was passed through sericin-coated air filter at temperature 30°C, humidity 85%, and flow rate 145 m^3/h. Chamber initial concentration (C_0) and concentration with time (C_t) for BTEX were measured at a regular interval of time until equilibrium was achieved. The amount adsorbed (Q_t; mg/g) was estimated and plotted against time (t; min) for kinetic studies. The adsorption process was fitted by the pseudo-first-order kinetic, pseudo-second-order kinetic, and the model with a higher correlation coefficient (R^2) was chosen. The pseudo-first-order rate equation is given by equation (3.11):

$$\log\left(Q_e - Q_t\right) = \log Q_e - \left(\frac{k_1}{2.303}\right)t \tag{3.11}$$

Where, Q_t is the amount adsorbed (mg/g) at time t (sec), Q_e (mg/g) is the amount adsorbed at equilibrium condition, k_1 is the pseudo-first-order rate constant (s^{-1}) and calculated by linear regression of log (Q_e - Q_t) versus t plot.

The pseudo-second-order rate constant is given by equation (3.12):

$$\frac{t}{Q_t} = \frac{1}{k_2 Q_e^2} + \left(\frac{1}{Q_e}\right)t \tag{3.12}$$

Where k_2 is the pseudo-second-order rate constant ($gmg^{-1}s^{-1}$) and can be calculated by linear regression of t/Q_t versus t plot. The amount adsorbed at equilibrium (Q_e) and at time t, can be calculated using equation (3.13) and (3.14):

$$Q_e = \left(\frac{c_0 - c_e}{M}\right)V \tag{3.13}$$

$$Q_t = \left(\frac{c_0 - c_t}{M} \right) V \tag{3.14}$$

Where, C_0 is the initial concentration of BTEX in the chamber (mg/m^3); C_t is the concentration of volatile compounds (BTEX) at time t (mg/m^3), C_e is the concentration at equilibrium (mg/m^3). V is the total volume (m^3), and M is the amount of sericin (g) coated on the air filter.

Various isotherm equations, such as the Langmuir, Freundlich, and Langmuir-Freundlich models, have been used to describe the equilibrium characteristics of adsorption. If the adsorption follows the Langmuir model [219], the adsorption process can be expressed as:

$$Q_e = \frac{K_L . Q_m . C_e}{1 + K_L . C_e} \tag{3.15}$$

Where Q_e is the amount adsorbed at the equilibrium state (mg/g), Q_m is the maximum adsorption capacity (mg/g), and K_L is the Langmuir equilibrium constant (m^3/mg), and C_e is adsorbate concentration at equilibrium (mg/m^3).

If the adsorption follows the Freundlich model [220], then the isotherm can be described as follows:

$$Q_e = K_f . (C_e)^{1/n_f} \tag{3.16}$$

Where, K_F (mg/g(m^3/mg)$^{1/n}$) and n_f are the Freundlich physical constants related to the adsorption capacity and adsorption intensity of the adsorbent, respectively.

Langmuir-Freundlich model (equation 3.17) proposed by Sips 1948 [221], is a combined form of Langmuir and Freundlich models and has three parameters: Q_m is the maximum adsorption capacity of the monolayer (mg/g); K_S is the equilibrium constant (m^3/g), and n is the Sips coefficient which indicates the presence or absence of cooperativity.

$$Q_e = \frac{Q_m K_s (C_e)^n}{1 + K_s (C_e)^n} \tag{3.17}$$

The Freundlich, Langmuir, and Sips models are applied using a non-linear regression method to fit the experimental equilibrium data. The chi-square and the coefficient of determination (R^2) value were used to analyze the fit of each model.

Chapter 4

Prospects of Silk Sericin as an adsorbent for the removal of drug pollutants from aqueous solution

Parts of this Chapter are published as research articles:

- V.K. Verma, S. Subbiah, Prospects of Silk sericin as an Adsorbent for Removal of Ibuprofen from Aqueous Solution, Ind. Eng. Chem. Res. 56 (2017) 10142–10154. doi:10.1021/acs.iecr.7b01827.

4.1. Theoretical consideration

Pressure-driven membrane filtration processes such as NF, and RO is widely used for drinking water treatment application to improve the taste of the water by removing dissolved salts [222]. The complete removal of salt from drinking water is also not desirable because that leads to a mineral deficit issue. Both RO and NF process highly effective alternative methods for the removal of organic micropollutants [110,111]. However, selective and complete removal of micropollutants is not possible, and it is limited by membrane separation efficiency [111,123,223–225]. Adsorption process has earned preference as a sustainable solution for the complete removal of micropollutants from polluted drinking water [226]. Besides, the adsorption process enables safe disposal without producing toxic by-products. PAC (powdered activated carbon) and GAC (granular activated carbon) have been reported to have high removal of pharmaceutical compounds, especially hydrophobic compounds [227,228]. However, the selective removal and isolation of micropollutants may be an expensive step to achieve with PAC and GAC. Therefore different materials have been investigated for their characteristics and adsorption capability for pharmaceutical drugs; some of the reported adsorbents include soil minerals, metal oxide, siliceous material, zeolites, agricultural waste, industrial waste, and other materials [202,229–231]. Still, the identification of adsorbents with following properties are very important in the field of drinking water treatment: (i) nontoxic, (ii) low-cost, and (iii) selective removal capacity of pharmaceutical micro pollutants. In this study, we have evaluated the feasibility of sericin uses as an adsorbent for removal of drug from water.

4.2. Hypothesis

Even though NF and RO are regarded as highly effective in the removal of pharmaceuticals with varying degrees of rejection (from 45-90%) [223,224], trace quantities of target pharmaceutical compounds have been found to breach membrane barrier. In this study, the model drug ibuprofen is mixed with sericin at different concentrations and expecting that the ibuprofen to form a complex with sericin based on functional groups present in them. The interaction will result in high molecular weight complex formation, which can be easily filtered with the RO membrane. Moreover, due to the higher molecular weight of the sericin molecule, any unbounded sericin particle will be removed entirely by the RO membrane while passing aqueous sericin-drug

solution [232]. Therefore, the integrated sericin based adsorption with the RO process can enable dual activity, i.e. (i) selective adsorption of micropollutants with sericin molecule and (ii) removal of combined molecule in the RO membrane. This novel approach will enable complete removal of Ibuprofen from aqueous solution. This work aims at establishing adsorbing properties of sericin for capturing drug particles from aqueous solution. The knowledge gained from this work will assist in the synthesis of adsorptive membrane filtration units with desired qualities targeting the removal of drug-based pollutants form from drinking water.

4.3. Experimental

The removal of Ibuprofen was assessed in an integrated adsorption-cum-RO process. The MWCO value of the DOW Filmtec^{TM} RO membrane used in this study lies in the range of ~200-400 Da. While, Ibuprofen has a molecular weight of 206 daltons [189], and hence RO membrane is not supposed to retain it efficiently. On the other hand, the MWCO for sericin is found to be 10-400 kDa. Therefore, sericin is expected to be retained entirely by the RO membrane. Fabiani et al. (1996) [233] used UF/RO filtration method for filtration of wastewater from silk degumming processes, and the overall rejection of sericin was found to be more than 97 %. Li et al. (2015) [234] performed the sericin separation experiment using both silk degumming wastewater and commercial grade purified sericin in the NF hollow fibre membrane to study the effect of sericin molecular weight. They observed complete removal with commercial-grade pure sericin and partial removal achieved for silk degumming wastewater, and the same was confirmed by Capar et al. (2012) [203].

Further, to achieve complete removal of sericin by the RO membrane, the purified higher molecular weight sericin has to be used. Based on these facts, we have designed an integrated method where sericin specific affinity towards ibuprofen has been coupled with membrane filtration for its removal from aqueous solution. Schematics of size-based separation of Ibuprofen using sericin adsorbent together with RO-membrane shown in *Figure 4.1*. The drug molecules are supposed to adsorb on sericin, and that resulted in complete rejection of sericin and drug molecules by the RO membrane due to a size-based steric exclusion mechanism. Different analytical techniques were adopted to assess the interaction between sericin and Ibuprofen (a) ATR- Fourier-transform infrared

spectroscopy (b) Fluorescence Spectroscopy (c) Isothermal Titration Calorimeter (d) Field Emission-Scanning Electron Microscopy and (e) X-ray diffractometer.

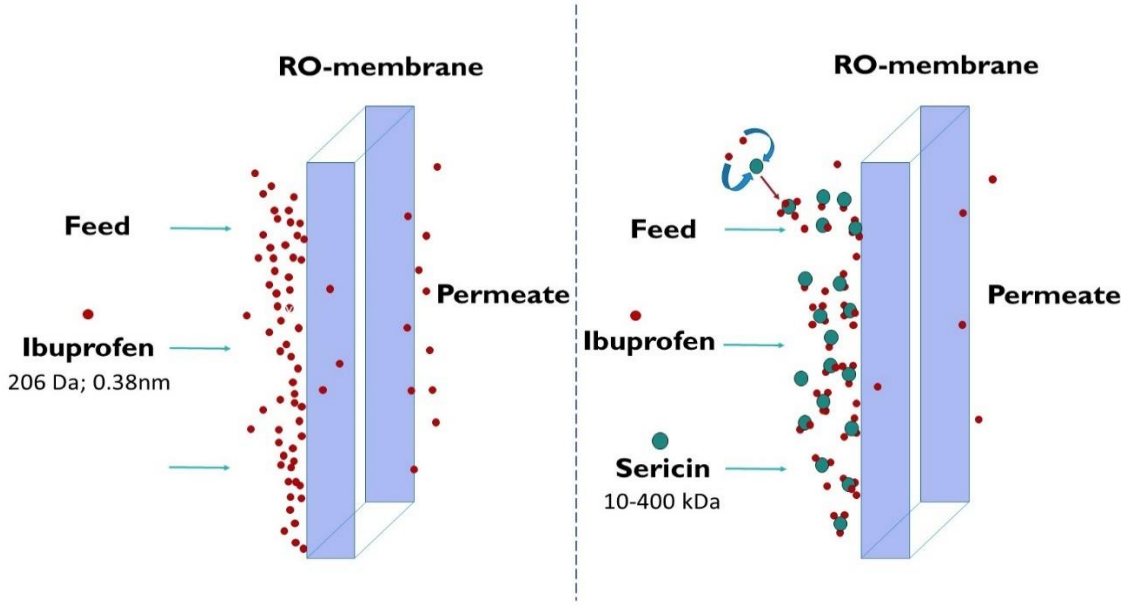

Figure 4.1. Schematic of size-based separation of Ibuprofen using sericin adsorbent and RO- membrane.

4.4. Result and Discussion

4.4.1. Sericin Characterisation

The results obtained from BET analysis of sericin (*Table 4-1*) showed the surface area of 5.47 m^2g^{-1} with an average pore diameter of 4.05 nm and a pore volume of $5.550x10^{-3}$ cc/g, indicating a non-porous morphology. In a study involving removal of dye, Chen et al. (2012) [235] reported a surface area of 1.5 m^2g^{-1} for sericin powder obtained from a commercial source.

4.4.2. Experimental studies in integrated adsorption-cum-RO process

4.4.2.1. Flux through the RO membrane

Pure water flux (see Appendix A2) curve was obtained for the RO- membrane sheet, and the estimated membrane permeability is 0.281017 x 10^{-12} m^3/m^2.s.Pa. The membrane was preconditioned by operating for one hour at 50 Psig with distilled water before conducting the experiments with the sericin-ibuprofen solution. Permeate flux with respect to time for Ibuprofen (10 mg/L), sericin (10g/L), and sericin-ibuprofen complex (1000:1) is

shown in *Figure 4.2*. The flux study shows a constant decline in water flux with time for sericin and sericin-ibuprofen complex, which may be attributed to the deposition of sericin/complex on to the membrane surface.

Table 4-1. BET analysis of sericin

Sample	Silk Sericin	
Multi-Point BET	Surface Area	5.473 m^2/g
	pore volume	0.005 cc/g
	pore Diameter	4.055 nm
BJH adsorption	Surface Area	2.939 m^2/g
	Pore Volume	0.006 cc/g
	Pore Diameter	7.111 nm
BJH desorption	Surface Area	4.542 m^2/g
	Pore Volume	0.007 cc/g
	Pore Diameter	1.872

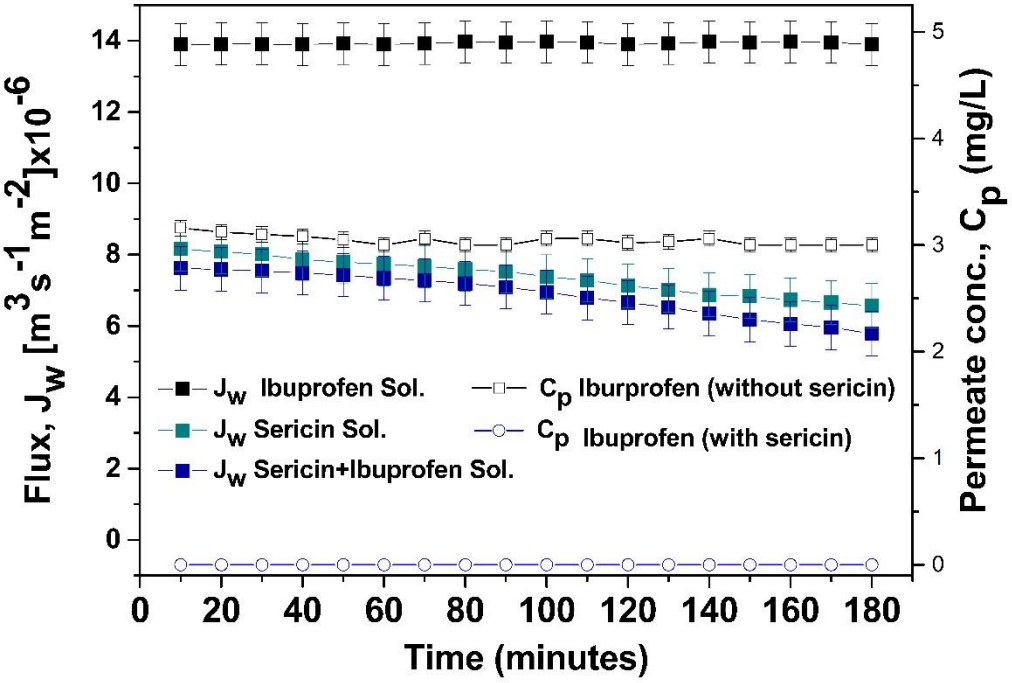

Figure 4.2. Water and solute flux through RO membrane for sericin (10g/l), ibuprofen (10 mg/L) and sericin-ibuprofen complex (1000:1 mg/l) at 517 kPa, pH 6 and 30°C, (sericin was removed completely in permeate in all cases; C_p Ibuprofen error = ±2.33%).

4.4.2.2. Effect of sericin concentration

The effect of sericin concentration was evaluated by adding different concentrations of sericin (1 to 10 g/L) with a fixed initial concentration of Ibuprofen (at 10 ppm) solution. The solution was stirred for 3 hours on a magnetic stirrer. The experiment was conducted at 25 °C and without altering ambient pH. After 3 hours, the solution was filtered through the RO membrane in complete re-circulation mode, and obtained results were evaluated. *Figure 4.3*a shows variation observed in permeate concentration of ibuprofen with a gradual increase of sericin concentration in the feed. It was noticed that the removal of ibuprofen increases with the increasing amount of sericin, and around 10g/L of sericin was needed for complete removal of Ibuprofen at 10 ppm. Since commercial ibuprofen is a racemic mixture and contains equal quantities of R(-)ibuprofen and S(+)ibuprofen enantiomer and a larger amount of sericin is expected to be used for non-specific binding and complete removal of Ibuprofen. In another aspect, protein conformation also plays a vital role, and binding is supposed to be site-specific, which was later found in FTIR, ITC, and fluorescence studies that single binding sites (n~1) are responsible for the sericin-ibuprofen complex formation. More than 99% of rejection was noticed with 10g/L of sericin for Ibuprofen. The observed rejection of ibuprofen drug demonstrates the competence of sericin as an adsorbent to remove ibuprofen from aqueous solution.

4.4.2.3. Effect of Ibuprofen concentration

Ibuprofen solution at different concentrations was first filtered through the RO membrane, and its inherent removal capacity was evaluated. Since it was found that around 10 gm/L of sericin was required for complete removal of Ibuprofen from feed solution from 10 ppm. Solution initial concentration of sericin is fixed at 10 gm/L, and corresponding ibuprofen rejection efficiency was assessed at different concentrations of Ibuprofen (from 10 to 70 ppm). RO experiments were conducted at room temperature and with Ibuprofen solution at pH 8. *Figure 4.3*b shows the Ibuprofen concentration in the RO permeates while varying RO feed concentration. Permeate Ibuprofen concentration is always found to be higher when the feed solution is without sericin. On the other hand, sericin complex formation with Ibuprofen has increased the Ibuprofen rejection by the RO membrane in comparison to standalone Ibuprofen molecule rejection.

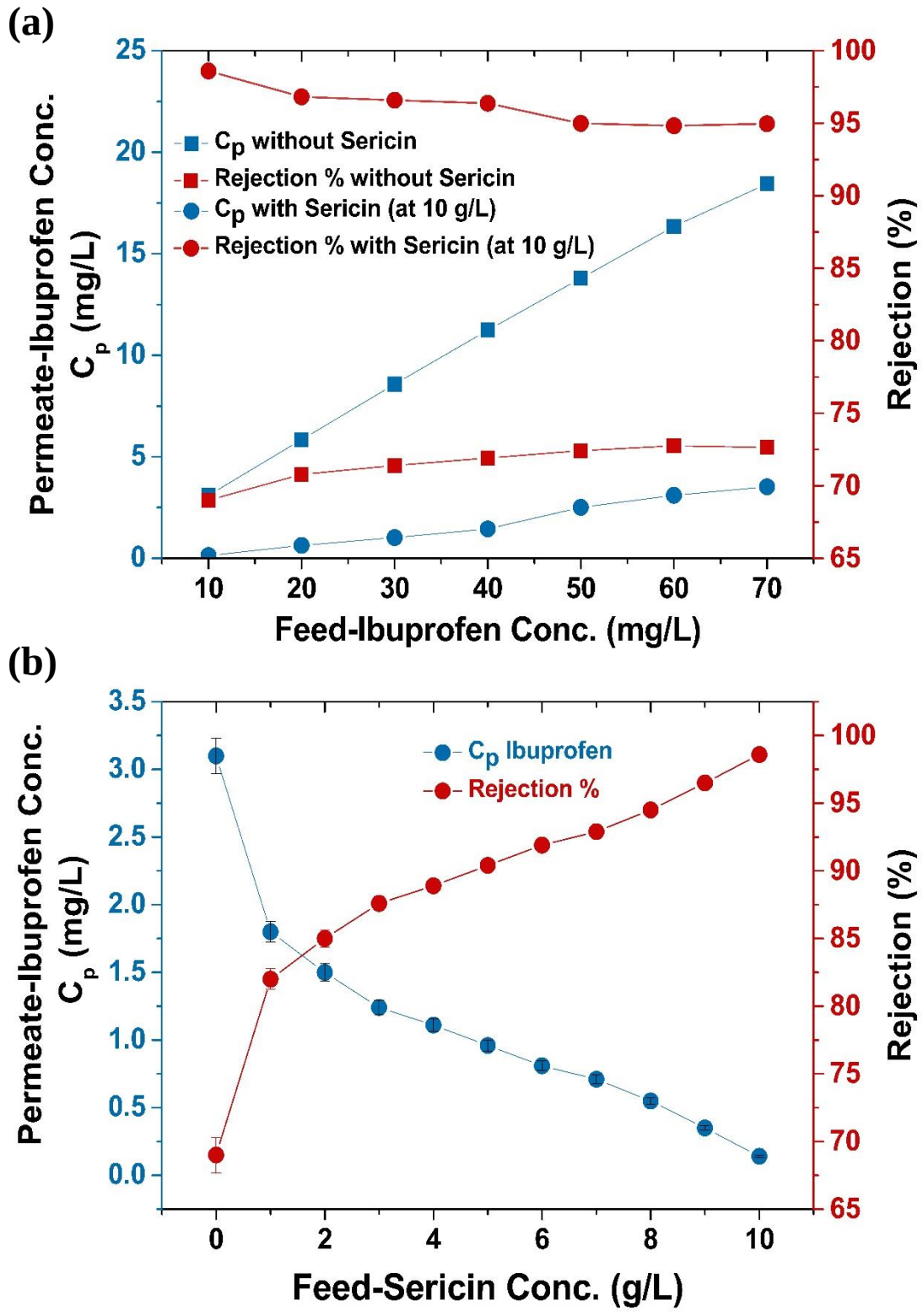

Figure 4.3. Ibuprofen concentration in permeate (a) with increasing feed sericin concentration; at 10 ppm of initial Ibuprofen concentration (b) with increasing feed Ibuprofen concentration; at 10mg/L of sericin initial concentration (C_p Ibuprofen error =3.25 %).

4.4.2.4. Effect of Ibuprofen solution pH

Solution pH is supposed to affect the surface charge on solute particles and hence play an important role in adsorption. The effect of pH on Ibuprofen removal was assessed from a range of 5 to 8, to assess its effect on the interaction of Ibuprofen with sericin particles. Experiments were performed at 10g/L of sericin (at pH 4) and room temperature, while the required pH of Ibuprofen solution was adjusted using 1M NaOH and 1M HCl. *Figure 4.4*a shows the effect of pH on the adsorption of Ibuprofen, and it was found that higher pH shows better removal capacity. Because Ibuprofen has a Pka value of 4.9 and hence exists as neutral species below this value and above this value, Ibuprofen attains a negative charge and hence exists in anionic form. Sericin solubility has been found to decrease with increasing acidity of water. Moreover, it has been reported that sericin solubility in water is least at low pH, slowly escalate at a pH 5-8, and it has high solubility from 8 onwards [236]. Hence, higher pH must have escalated charged based interaction and non-specific binding of negatively charged ibuprofen enantiomers with protonated sericin particles, resulting in better removal capacity.

4.4.2.5. Effect of solution Temperature

The separation efficiency for Ibuprofen with respect to temperature for fixed sericin concentration (at 10g/L) is shown in *Figure 4.4*b. Since the temperature is one of the important factors that affect the heat of mixing and heat of adsorption. The experiments were performed at three different temperatures (20, 30, and 40°C) to assess the effect on seasonal removal capacity. It was observed that the adsorption of ibuprofen on sericin was a fast process and spontaneous, almost 80 % of the drug was adsorbed within 5 minutes of contact time. However, after 5 minutes, the adsorption rate decreases over time until saturation was achieved in around 25 minutes (see *Figure 4.5*).

The filtration process exhibited better removal capacity with an increase in temperature. Since sericin solubility also increases with temperature due to destabilization of the protein conformation, random coil structure becomes more dominant with temperature, which may have contributed to better binding capability. Moreover, since the binding of Ibuprofen with sericin was found to be endothermic (as found in ITC analysis), so an increase in temperature must have assisted in improved binding capacity. The adsorption process at 40°C shows the best performance with almost complete removal of Ibuprofen from solution after 25 minutes of contact time for a period of 15 minutes of filtration. For

20°C and 30°C a maximum of 91 % and 96 % Ibuprofen separation efficiency were achieved, respectively.

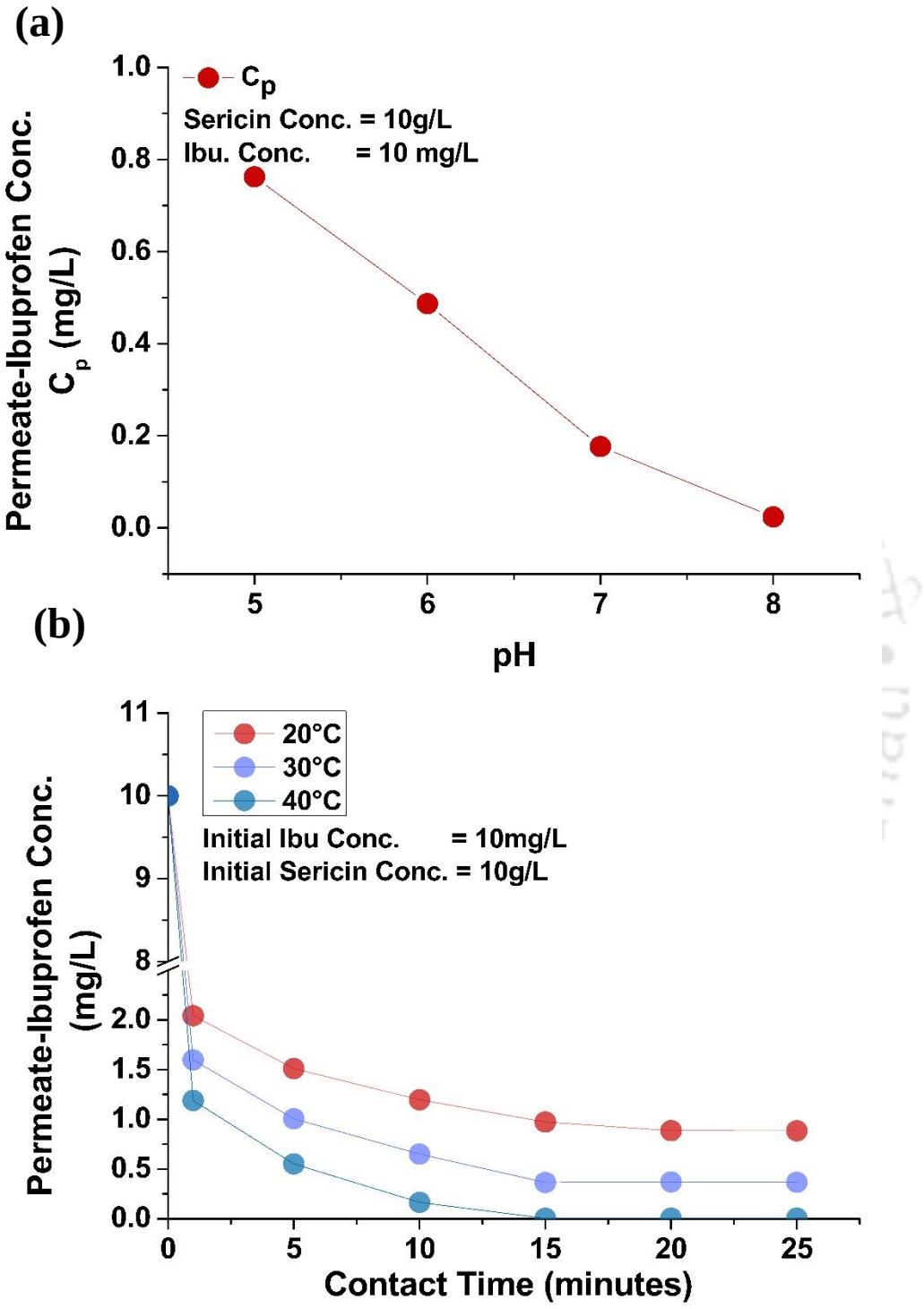

Figure 4.4. Ibuprofen concentration in permeate (a) with increasing pH of Ibuprofen feed solution (b) at different temperature (20, 30 and 40 °C) with increasing time of contact ($C_{p\ Ibuprofen}$ error =3.25 %).

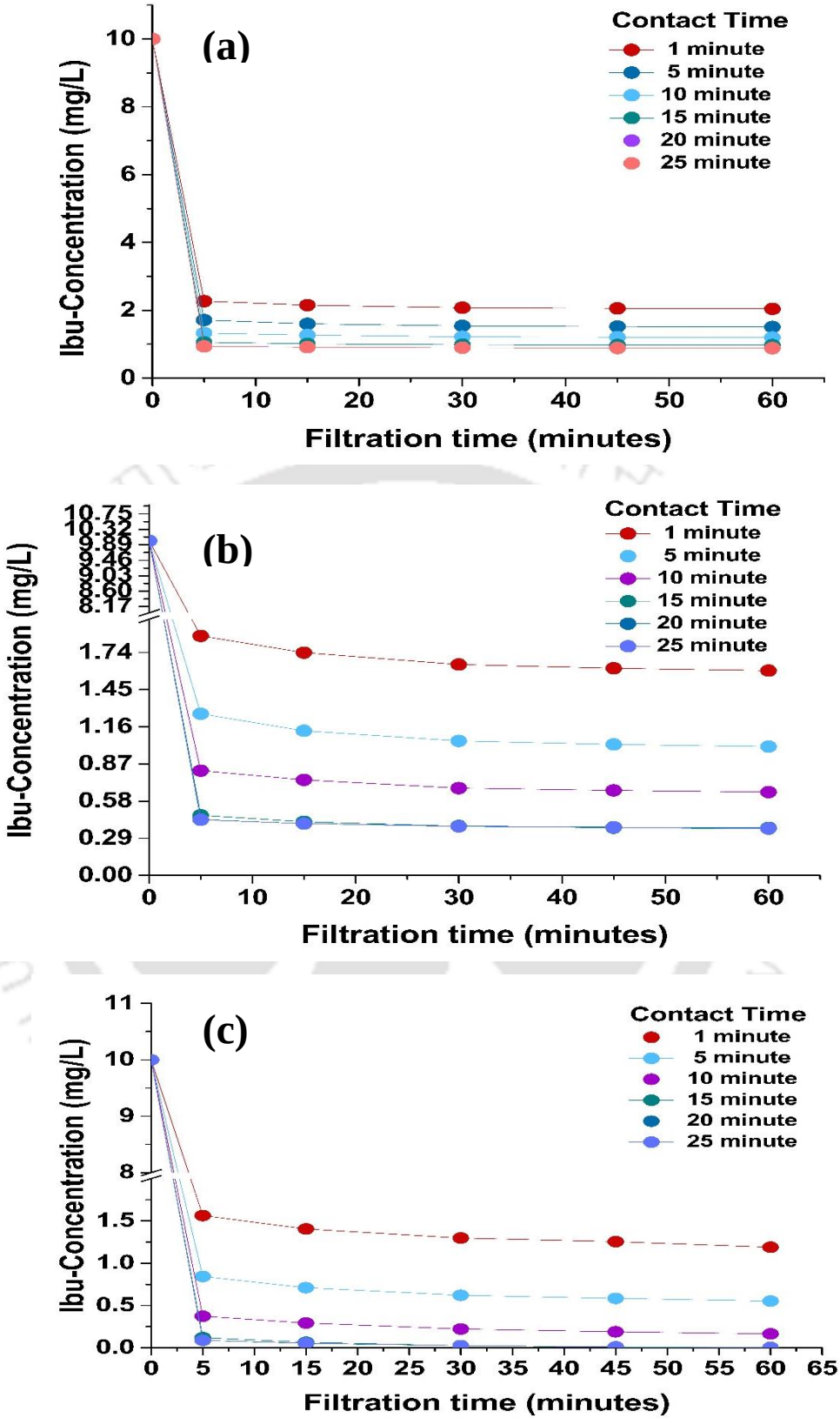

Figure 4.5. Ibuprofen (10mg/L) removal with sericin (10g/L) at different temperature with increasing time of contact and filtration time at (a) 20 °C, (b) 30 °C, (c) 40 °C; ($C_{p\text{-}Ibuprofen}$ error =3.25 %).

Based on results obtained from current study applicability of sericin for membrane modification and the specific removal of micropollutants has been compared with existing adsorbents in *Table 4-2*. Sericin shows very spontaneous binding and fast removal compare to other adsorbents, highly specific, suitable for membrane modification owing to its functional groups, antifouling, and antibacterial properties.

Table 4-2: Comparison of different adsorbents performance for removal of drug-based micropollutants

Sl. No.	Adsorbents	Efficiency	Remarks	References
1.	Granular Activated Carbon	80-98%	not specific towards drugs, quick breakthrough, regeneration issue, not suitable for polymeric membrane modification, prone to fouling	[115,228,237,238]
2.	Powdered Activated Carbon	>90%-99%	not specific towards drugs, high doses, long contact time, not suitable for polymeric membrane modification, prone to fouling	[173,228,239]
3.	Carbon nanotubes	>90%	not specific towards drugs, not suitable for polymeric membrane modification	[240]

4.	Chitosan	>90%	Specific towards some drug, high reusability, suitable for polymeric membrane application, antifouling properties	[241]
5.	Cyclodextrin	>80%	Specific towards the drug, high reusability, suitable for polymeric membrane application	[242]
6.	Zeolites	99%	Nonspecific, Highly pH-dependent, not suitable for polymeric membrane modification	[243]
7.	Clay	88-90%	Long contact time, strongly affected by temp. and pH	[244,245]
8.	Silica	>95%	Drug specific, Long contact time, suitable for membrane grafting	[246]
9.	Sericin	Complete removal	Highly specific, very spontaneous fast removal, applicable at neutral pH, suitable for membrane application, antifouling, and antibacterial properties	*current study

4.4.3. *RO-membrane sheet characterization*

FE-SEM images were obtained to study the morphological structure of the top surface of the RO sheet (*Figure 4.6*). The FE-SEM images before filtration (see *Figure 4.6*a, b) shows a densely packed, interconnected, sponge-like structure with mesoporous voids in between the structure. While, the FE-SEM images of RO-sheet after filtration (see *Figure 4.6*c, d) clearly shows the deposition of the sericin-ibuprofen complex on to the membrane.

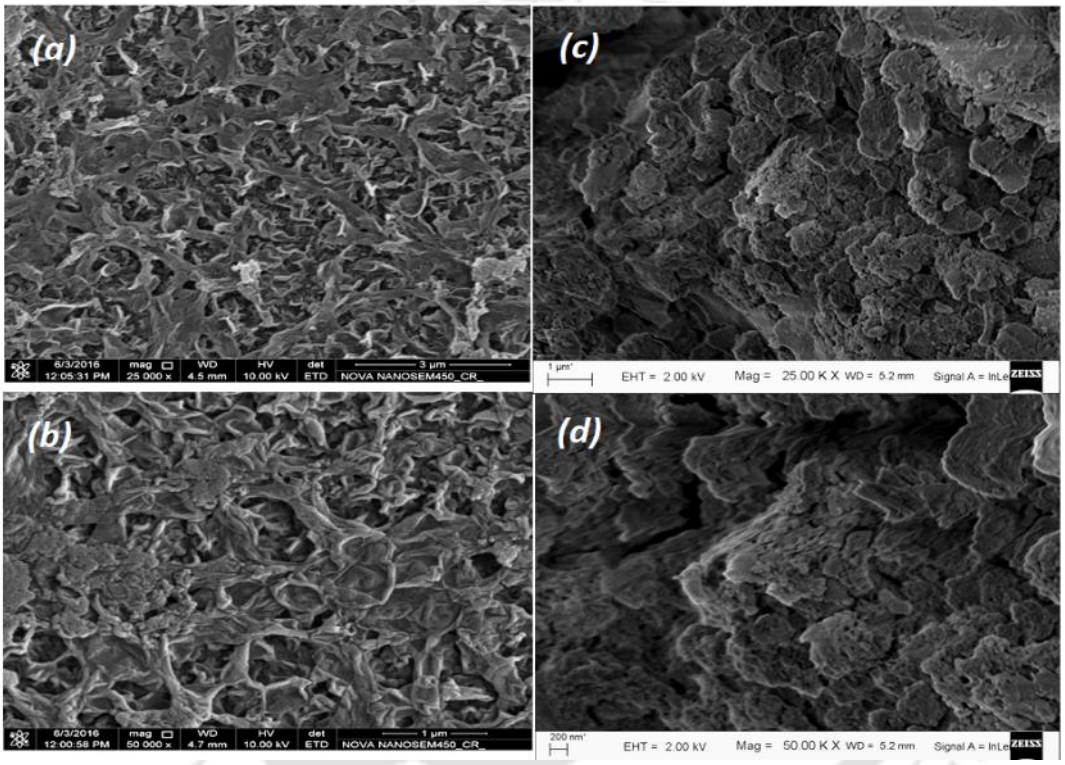

Figure 4.6. FE-SEM images for RO membrane before filtration at (a); 25KX, (b); 50KX and after filtration (c) at 25KX, (d) 50KX.

4.4.4. Sericin and Ibuprofen interaction study

4.4.4.1. ATR-FTIR

The ATR-FTIR Spectra of sericin, ibuprofen, and sericin-ibuprofen complex was analyzed for binding confirmation and to study molecular interaction between Ibuprofen and sericin (see *Figure 4.7*a-c). Ibuprofen spectra show characteristic peaks at 1700 cm^{-1} for C=O (carbonyl stretching), 3345 cm^{-1} for O-H stretching of the COOH group, 2800-3100 cm^{-1} for alkyl stretching (3052 and 3026 cm^{-1} for C-H symmetric and antisymmetric stretching; 2960 cm^{-1} for C-H stretching; 2950 cm^{-1} for CH_2 antisymmetric stretching;

2926 cm^{-1} for CH_3 in-phase symmetric stretching; 2905 and 2842 cm^{-1} for CH stretching, 1500-1600 cm^{-1} for C-C stretching, 1400-1500 for CH_2 deformation, 1300-1400 cm^{-1} for C-H bend, 1100-1200 cm^{-1} for C-H and C-O-H in-plane bending and 1000-400 cm^{-1} for aromatic and alkene bends [247,248]. Ibuprofen characteristic peak at 1700 for C=O (carbonyl stretch) and at 3345 cm^{-1} for OH-stretch of carboxyl group was found to be missing from the sericin-ibuprofen complex spectra, which validates the interaction between the carboxyl group of Ibuprofen and amide groups present in the sericin. The OH-stretch peak of sericin at 3260 cm^{-1} shifted to 3280 $cm^{-1,}$ while Ibuprofen peaks at 3052 cm^{-1}, 2950 cm^{-1}, 2926 $cm^{-1,}$ and 2868 cm^{-1} re-appeared together with peaks for aromatic and alkene bends (500-1000 cm^{-1}) in sericin-ibuprofen complex and hence confirms Ibuprofen adsorption on sericin.

Further, to calculate the variation in corresponding IR vibrational frequencies in Amide -1 region, the following analysis is presented. The Amide-I band has been widely used to identify the changes in protein secondary structure [249–251]. Considering the complexity involved in the analysis of other types of amide bands, they are generally not used for protein structure conformational analysis. Native protein generally consists of more than one secondary structure, and hence, absorbance usually overlaps for the amide I region and provides rise to the merged featureless band [252]. Hence, quantitative information about secondary structure modification was obtained by linear curve-fitting analysis of the component bands. Fourier self-deconvolution and second derivative procedure were used to characterize individual overlapping absorption [252,253] for native sericin as well as sericin–ibuprofen complex. The broad amide I curve was resolved into five distinct bands using the second derivative spectrum peak position, which is attributable to different secondary structure folding. To determine the proportion of resolved components Gaussian curves were iteratively fitted to deconvolved spectra.

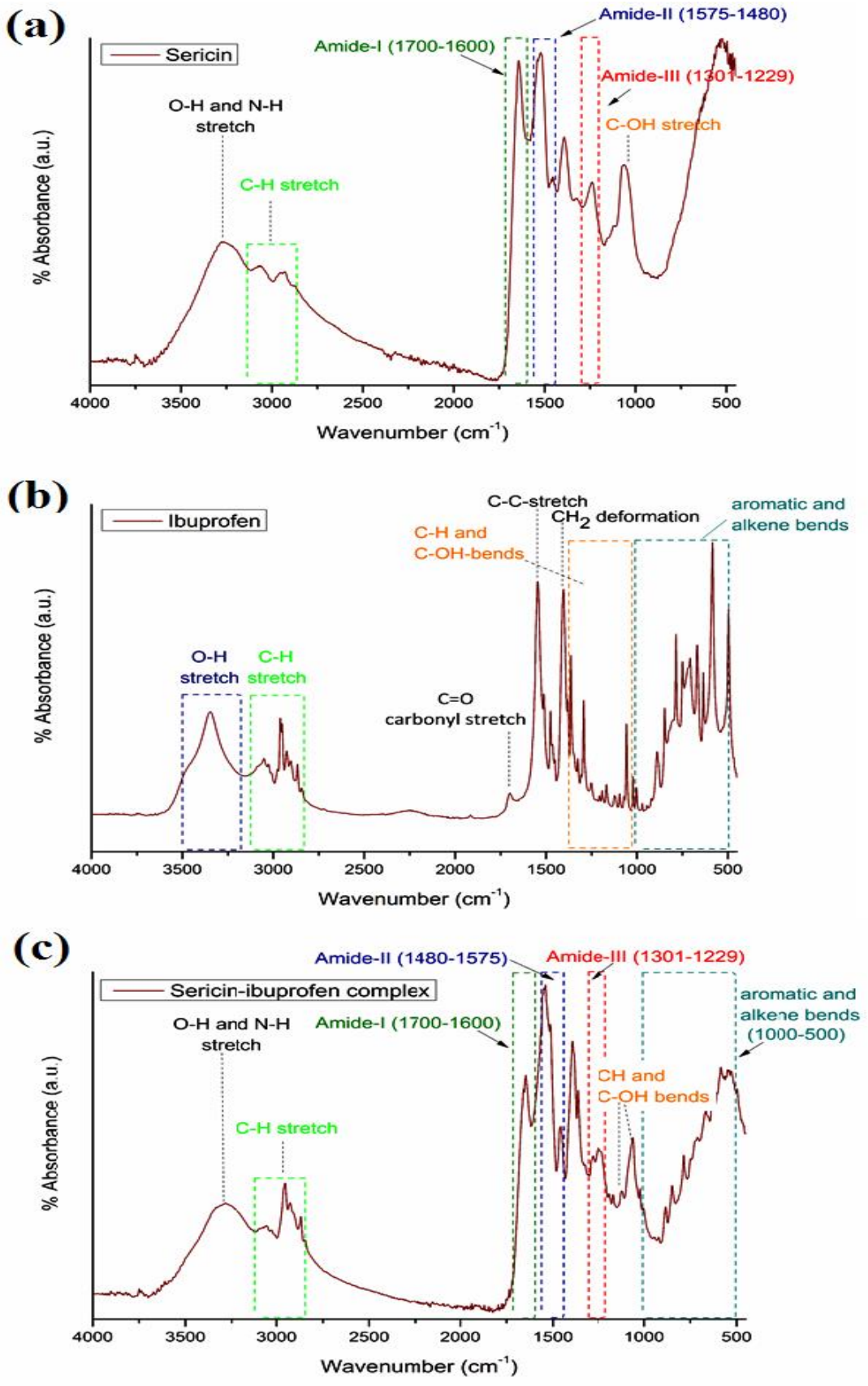

Figure 4.7. ATR-FTIR spectra of sericin-ibuprofen complex, sericin, and ibuprofen.

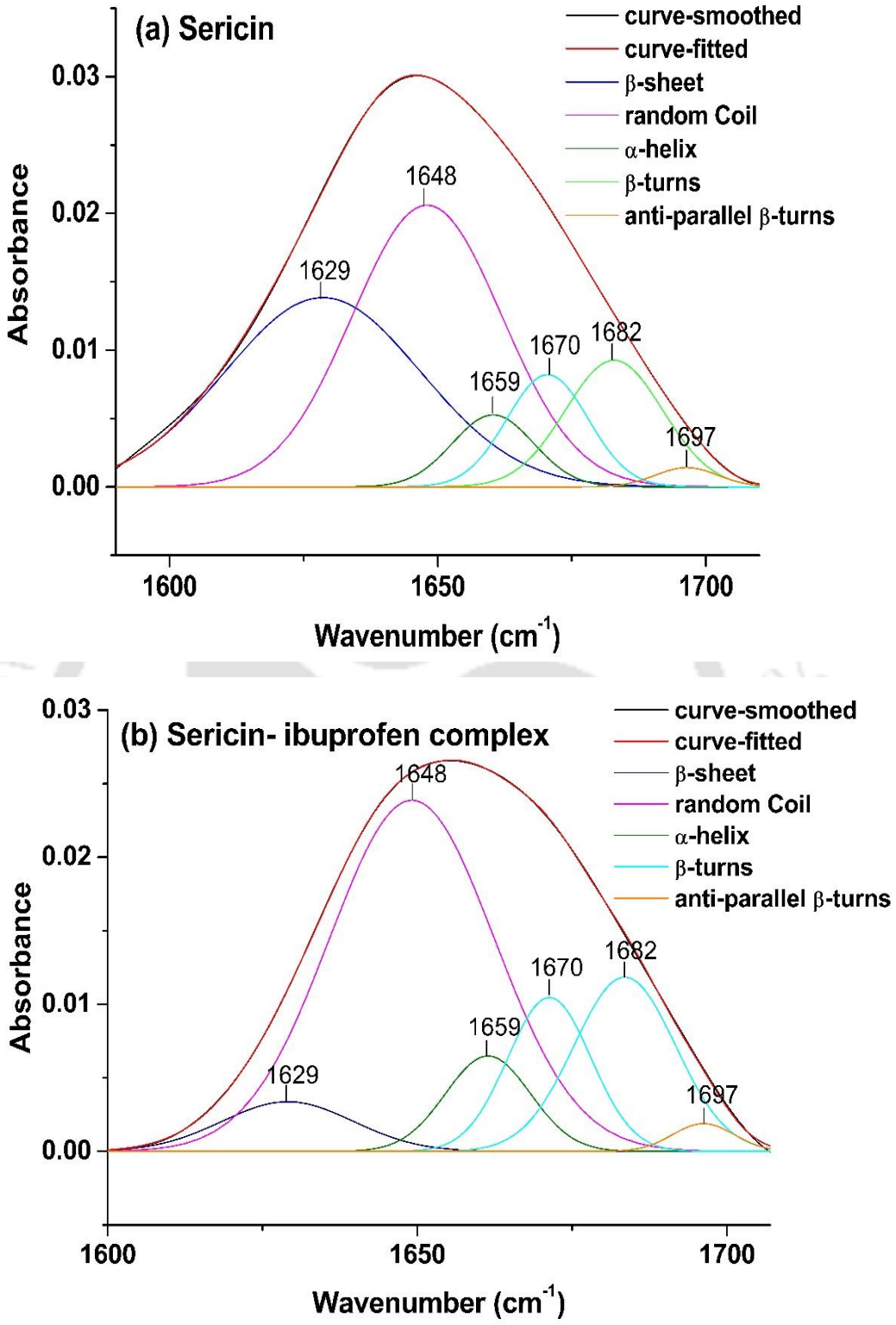

Figure 4.8. The spectrum of the protein amide I region. (a) Pure sericin (b) sericin-ibuprofen complex (five Gaussian curves were fitted iteratively to the deconvolved curve using the peak position obtained from the second derivative spectrum as initial parameters).

Prior to curve fitting, baseline correction and seven-point Savaitzky-Golay smoothing were used for the amide I region curve. Excellent agreement was noticed for band positions of the fitted curves with those obtained by the second derivative spectrum. Secondary structure conformation to overlapped five single bands was assigned as follows and according to the previous studies [249,251]: band at 1629 cm^{-1} as β-sheet, 1648 cm^{-1} as random coil, 1659 cm^{-1} as α-helices, 1668 cm^{-1} and 1680cm^{-1} as β-turns, and 1697 cm^{-1} as antiparallel β-sheet.

Table 4-3. Assignment of Individual Amide I components (Sericin native protein)

Assignment	**Frequency (cm^{-1})**	**Peak area (%)**
β-sheet	1629	34.35506
Random coil	1648	39.17869
α-Helix	1659	5.43163
β-turn	1670, 1682	8.478, 11.43774
Antiparallel β-sheet	1697	1.11887

Table 4-4. Assignment of Individual Amide I components (sericin-Ibuprofen complex after adsorption)

Assignment	**Frequency (cm^{-1})**	**Peak area (%)**
β-sheet	1629	6.20341
Random coil	1648	55.24681
α-Helix	1659	7.73929
β-turn	1670, 1682	12.25749, 16.92279
Antiparallel β-sheet	1697	1.63021

The percent content of individual secondary structure components in sericin and sericin-ibuprofen complex were calculated (see *Table 4-3* and *Table 4-4*), and their distribution

is shown in *Figure 4.8*a-b. It was found that in the native state, sericin has a higher content of random coil (39.17%) and β-sheet (34.35%); a similar trend was reported in earlier literature [156,254,255]. In the sericin-ibuprofen complex, random coil conformation (55.24%) increased in content while β-sheet (6.20%) was noticed to decrease subsequently. These indicate that Ibuprofen can bind to the exposed unfolded polypeptide chain of sericin. Hence, disordered random coil structure became a dominant characteristic of the complex after the adsorption of Ibuprofen on to sericin.

4.4.4.2. Steady-state fluorescence spectroscopy

Although the specific content of the tyrosine and phenylalanine vary somewhat across reported literature [156,205], their presence in sericin can be identified by measuring the fluorescence level. Quenching studies employing tyrosine intrinsic fluorescence of sericin is an indispensable approach to analyze the interior location of the fluorophore and subsequent structural alteration after Ibuprofen binding.

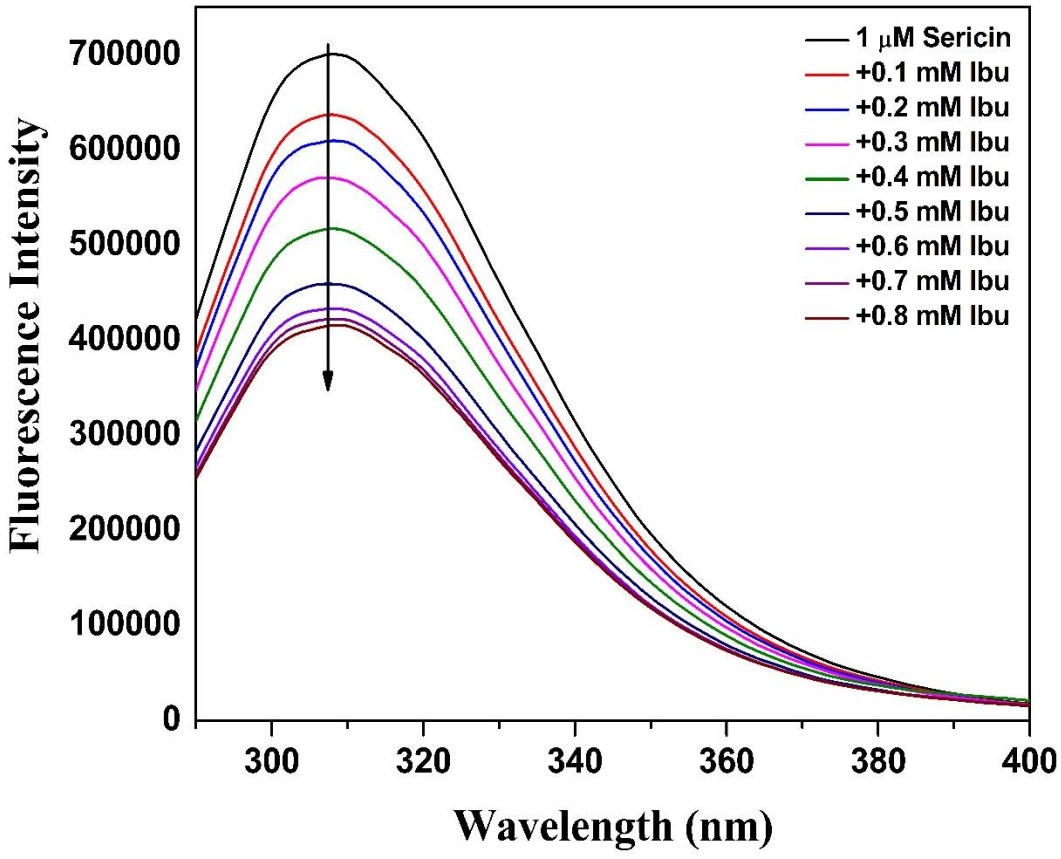

Figure 4.9.The quenching effect of Ibuprofen on sericin fluorescence intensity, λmax=308±2.

Sericin exhibited intrinsic fluorescence when excited at 280 nm to show emission spectra in the 290–400 nm range with the highest intensity peak at 308±1 nm (see *Figure 4.9*). As shown in *Figure 4.9*, the fluorescence intensity is found to be decreasing while adding Ibuprofen.

$$\frac{F}{F_0} = 1 + K_{SV}[Q] \tag{4.1}$$

This phenomenon confirms that fluorophores (i.e., tyrosine) buried inside protein structure are coming out in the solvent phase, and that leads to a decrease in fluorescence intensity [256]. Fluorescence quenching can be dynamic, which results from the collision of fluorophore and quencher, or static when ground state complex forms between the fluorophore and quencher. Fluorescence quenching is explained by most studied Stern-Volmer equation [256]; Where F_0 and F represent the fluorescence intensity in the absence and presence of quencher (Ibuprofen), respectively, K_{sv} is the Stern-Volmer quenching constant [Q] is the concentration of quencher. The Stern–Volmer plot (see *Figure 4.10*a) of the quenching of sericin fluorescence with Ibuprofen shows a good linear relationship between Q & (F/F_0) (R^2= 0.9937) and estimated slope (K_{sv}) is 9.196 x 10^4 ± 0.02581 $Lmol^{-1}$.

The observed fluorescence quenching intensity data can also be used to obtain the binding constant (Ka) and the number of binding sites (n). When drug molecules bind independently to a set of equivalent sites on a protein macro-molecule, the equilibrium between free and bound molecules is given by below-given relationship [257,258];

$$\log\frac{F_0 - F}{F} = \log K_a + n\log[Q] \tag{4.2}$$

The value of K_a and n were obtained from the intercept and slope of the double-logarithm curve (log [(F_0 − F)/F] vs. log [ibu]), as shown in *Figure 4.10b*. The calculated number of binding sites (n) is ~0.98, indicating that there was one sericin binding site for Ibuprofen, and K_a was found to be 9.09 x 10^4 ± 0.01654 $Lmol^{-1}$. Protein can be unfolded by disturbing the weak interactions that maintain the folded structure (i.e., hydrogen bonding, electrostatic interactions, and hydrophobic interactions). Ibuprofen binding must have modified the polypeptide conformation in an unfolded structure, and the same was confirmed in FTIR, using the amide I spectrum, where β-sheet conformation decreased and random coil conformation was found to be increased after sericin-

ibuprofen complex formation. The binding thermodynamics of ibuprofen-sericin was further investigated through ITC.

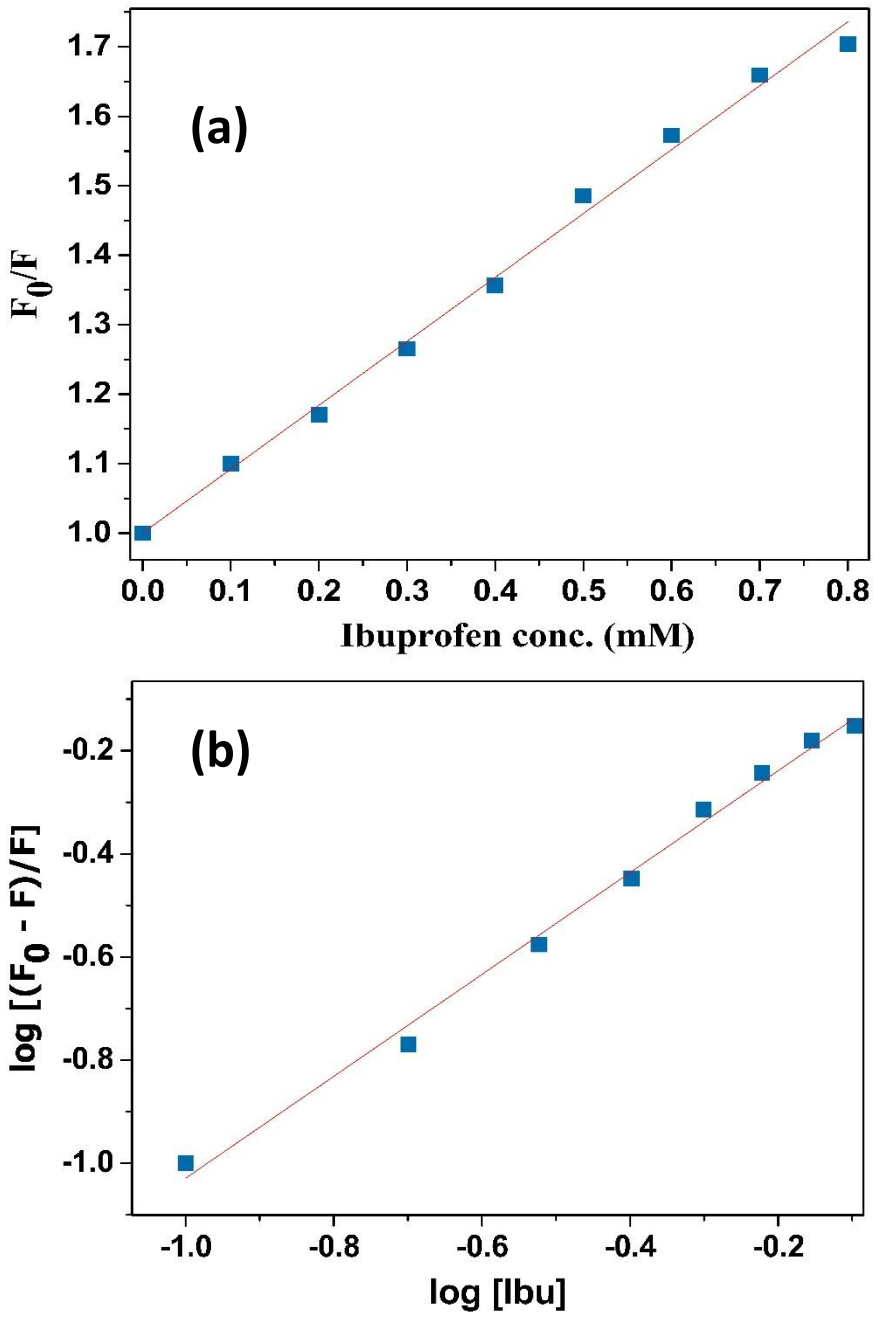

Figure 4.10. (a) Stern-Volmer plot (b) double logarithmic plot; for quenching of sericin by ibuprofen.

4.4.4.3. Isothermal Titration Calorimetry

ITC is an efficient method to study the binding affinity between protein and drug molecules and provide binding constant (K_b), binding stoichiometry (n), total enthalpy

change (ΔH) as well as total entropy change (ΔS) involved during the binding reaction [206]. The ITC thermogram of Ibuprofen titration with Sericin has shown best fitting in one set of the binding model after subtraction of buffer and highlighted the presence of the single binding site in Sericin for Ibuprofen with endothermic pattern in thermogram (*Figure 4.11a,b*).

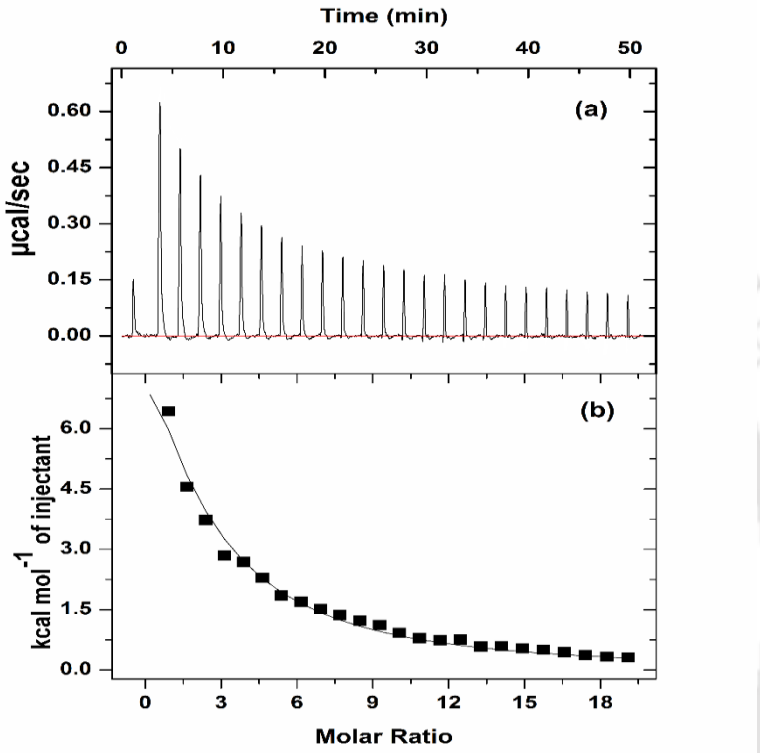

Figure 4.11. ITC thermogram for the binding of Ibuprofen to sericin at 27 °C in 10mM phosphate buffer (a) primary raw data (b) binding curve derived from the raw data.

ITC analysis also revealed the binding affinity (K_b) value $2.51x10^4$ at 27°C that concludes the moderate binding of Ibuprofen to the Sericin protein. Diverse potential interaction forces such as hydrophobic, electrostatic, hydrogen bonds, and van der Waal's are usually involved in such interaction. Therefore, ITC analysis also can reveal the driving force of corresponding interaction based on binding thermodynamics. If $\Delta H<0$, $\Delta S<0$, driving force is van der Waal's and hydrogen; if $\Delta H>0$, $\Delta S>0$, hydrophobic interaction is dominant while $\Delta H<0$, $\Delta S>0$ signify the dominancy of electrostatic force [206]. Therefore, positive values of ΔH and ΔS also has revealed that hydrophobic interactions are the predominant driven force in present binding. Thermodynamic parameters of drug binding with sericin protein have been listed in *Table 4-5*. The values of -TΔS were

determined by $\Delta G_{app} = \Delta H - T\Delta S$, while ΔH and ΔS values were obtained directly from the multi-injection mode ITC experiment.

Table 4-5. Thermodynamic parameters of the sericin and Ibuprofen interaction obtained by ITC at 27°C temperature.

	Stoichiometry (n)	**K_b ($mole^{-1}$)**	**ΔH (Kcal/mol)**	**ΔS (Kcal/mol.K)**	**ΔG_{app} (Kcal/mol)**
Sericin-Ibuprofen interaction	1.15±0.021	2.51E4	4.62±0.36	36.18	-31.9

The binding of Ibuprofen to sericin protein was found to be overall endothermic from the upward peak indicating the heat intake while adding ibuprofen into the sericin solution. ΔH provides information about the total energy of the process and includes the contribution from solute as well as solvent, and it is barely plausible to form favorable interaction without affecting each other. Indeed the ΔH of sericin-ibuprofen binding involves formation and disruption of individual interactions, which includes (i) the loss of hydrogen bonds and Van der Walls interaction (between sericin and solvent and between Ibuprofen and solvent), (ii) the formation of non-covalent interaction (between sericin and Ibuprofen) and (iii) solvent restructuring near the complex surface [259]. These phenomena lead to net enthalpy change. Similarly, binding entropy ΔS is contributed by following three phenomenon such as (i) solvent entropy change (solvent release upon binding), (ii) conformational entropy change (conformational freedom of both sericin and Ibuprofen upon binding), and (iii) change in rotational and translational entropy (reduction in degrees of freedom upon complex formation) [259]. These three entropic terms represent the net entropy change, with a negative or positive contribution to binding free energy. A negative binding free energy (ΔGapp = -31.9Kcal/mol) shows spontaneous binding mediated by enthalpy-entropy compensation for sericin-ibuprofen complex formation. Ibuprofen adsorption on sericin can be considered to be an analog of protein unfolding since Ibuprofen adsorption, and protein denaturation has coalesced with each other. As revealed in FTIR, the protein unfolds from beta-sheet to unordered random coil structure, which may be related to the endothermic effect. Hydrophobic

interactions play the main role in the binding interaction, and the presence of polar group may be related to the positive values of ΔH° and ΔS°. Hence it was assumed that sericin protein unfolding to random coil conformation was the dominant factor for sericin-ibuprofen complex formation, i.e., adsorption process.

4.4.4.4. FESEM

FE-SEM images of sericin, Ibuprofen, and sericin-ibuprofen complex revealed the adsorption of Ibuprofen on sericin protein (see *Figure 4.12*). Pure sericin without Ibuprofen, as a control, is shown in *Figure 4.12a,d.* Surface texture and morphology of Ibuprofen crystals are visualized in *Figure 4.12b,e*, which can be seen very clearly to be deposited on the sericin protein surface (in *Figure 4.12c,f*). The complex particles were found to have dotted chiseled Ibuprofen structure adsorbed on the native sericin protein surface.

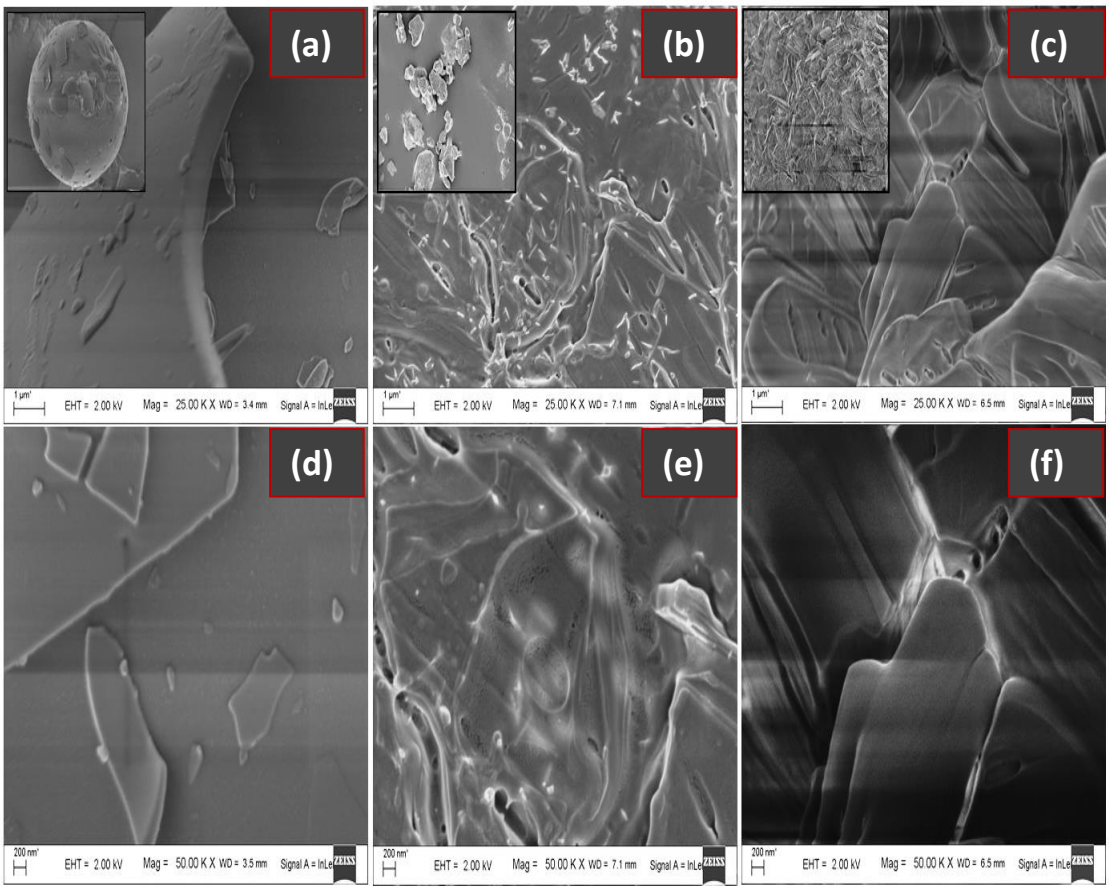

Figure 4.12. FE-SEM of sericin, Ibuprofen and sericin-ibuprofen complex at 25 KX (a, b and c), at 50 KX (e, f, and g), respectively.

4.4.4.5. XRD

The XRD results for sericin exhibited a large diffraction peak at around 2θ=21.15°, and the broad curve indicates amorphous nature (see *Figure 4.13*). A similar XRD profile with a peak at 2θ=19.2º has been reported [172]. This peak is characteristic of the β-sheet structure due to intermolecular hydrogen bonding between the hydroxyl groups of the amino acid present in sericin. Similar results have been reported in earlier studies with sericin obtained from different sources [109,255]. Ibuprofen XRD peaks showed its characteristic crystallinity and were found to be in good agreement with previously reported literature [260]. The sericin-ibuprofen complex XRD plot was crystalline and retained most of the ibuprofen characteristic peaks hence depicting adsorption of Ibuprofen on sericin.

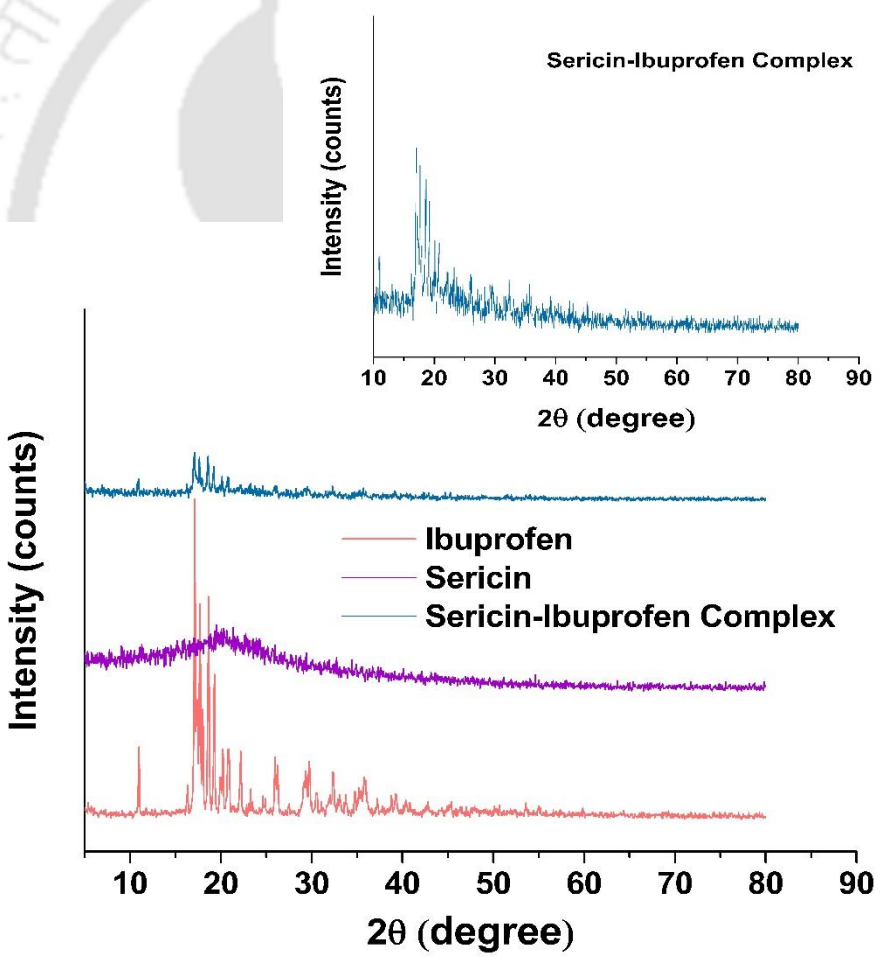

Figure 4.13. XRD profile for Ibuprofen, sericin, and sericin-ibuprofen complex.

4.5. Conclusion

This work deals with the evaluation of silk sericin as an adsorbent for the removal of Ibuprofen from aqueous solution using an integrated adsorption-cum-membrane filtration setup. The preliminary studies on sericin characterization were done to assess its physicochemical properties relative to adsorption. The non-porous sericin was found to have a low surface area, and conformational change was noticed with exposure to increasing temperature. The adsorption ability of sericin was analysed at different operating conditions (concentration, temperature, and pH). High pH and increasing temperature were found to assist in better adsorption of Ibuprofen. Complete removal for Ibuprofen was achieved at pH 8, 40ºC, and using 10g/L of sericin concentration. Ibuprofen interaction with sericin was investigated, and the endothermic peaks in ITC, together with the FTIR study, provided information about protein unfolding playing a dominant role in adsorption. Ibuprofen binding was related to the sericin transition to a random coil structure. Sericin- ibuprofen binding and complex formation were established using FTIR, ITC, Fluorescence spectroscopy, and XRD analysis. The use of sericin with the membrane process seems to enhance and achieve expected removal capacity. This study will help in the modification of existing filtration processes and provide a better solution for the removal of drug-based micropollutants from aqueous solution.

Chapter 5

Fabrication and Characterization of sericin-coated polymeric microfiltration membrane

Parts of this Chapter are published as research articles:

- V.K. Verma, S. Subbiah, Fouling resistant sericin coated polymeric microfiltration membrane, J. Chem. Technol. Biotechnol. (2019) jctb.6169. doi:10.1002/jctb.6169.

5.1. Theoretical consideration

Membranes are used for water purification to remove the pollutants. Removal efficiency is observed to be a function of membrane characteristics [261], such as physicochemical properties of the membrane, the morphology of porous layer, and surface properties of the active layer [262]. The surface properties of polymeric membranes can be enhanced by coating the membrane surface with materials having desired properties. The membrane can be coated with desired adsorbents for target-specific removal of pollutants [79]. The use of such adsorptive membranes has been limited to the removal of heavy metals and other micropollutants [78–87] but has not been explored considerably for the removal of drug-based micropollutants. Moreover, most of the existing adsorbents are packed in the adsorption column and integrated with the membrane system to achieve efficient removal. The regeneration ability of adsorbent used for micropollutant removal is not explored yet.

The polymeric membranes such as polyvinylidene fluoride, polysulfone, polypropylene (PP), polyethylene, polyacrylonitrile, and polyimide are expected to have hydrophobic surface, and these membranes are used in water treatment application [263,264]. For example, the PP membrane is used extensively in water treatment applications for its high mechanical strength, chemical-thermal stability and low price [265,266]. In another aspect, the hydrophobic membrane is not recommended when the feed contains fouling causing content, and also, these membranes provide low water permeability than hydrophilic membranes [264]. Therefore, the surface modification of hydrophobic PP membrane becomes very much desirable which can guarantee antifouling characteristics while the presence of fouling causing content in the feed. The hydrophobic surface of the PP membrane restricts the hydrogen bond interaction with water molecules, while the natural hydrophobic interaction between solute and surface increases the entropy and makes it favorable for the foulants to adsorb on the membrane surface [99]. The hydrophobic components present in water are known to cause more irreversible fouling than the hydrophilic and transphilic (i.e., polarity in between hydrophobic and hydrophilic) fractions [267,268]. Hydrophilicity is known to create a hydration layer on the membrane surface [269], which resists the deposition of foulants present in the aqueous phase [212]. The induced hydrophilicity on the membrane surface provides antifouling characteristics to the membrane by keeping foulants at bay [270–272]. Therefore, imparting hydrophilic functionality on the PP membrane surface must provide

antifouling properties, thereby increasing its performance and service life. The presence of charged functional groups with hydrogen bonding capacity can also assist in the adsorption of charged polar pollutants (like heavy metals and drug particles) [273–279].

However, the surface modification of the PP membrane requires pre-treatment before physical modification. Various techniques are available for surface modification of PP membrane depending upon requirement and suitability. Ahsani and Yegani, 2015 [213] generated hydroxyl group on inert PP membrane surface via acid treatment [212], which can be further used for bonding with other functional groups. A similar approach has been used in this work for pre-treatment of PP membrane for enhancing its adsorptive and antifouling properties via sericin coating on the membrane surface. The prior knowledge of sericin inherent ability to impart hydrophilicity together with the presence of multi-functional groups has been harnessed here to modify the PP based MF membrane.

5.2. Hypothesis

The multi-functional groups (i.e., carboxylic, hydroxyl, and amine) present in sericin can form complex (via hydrogen bonding and electrostatic interaction) with hydroxylated PP membrane surface. This complex formation can be stabilized via cross-linking and fixed through heat curing. Once sericin is coated on the membrane surface, the inherent property of sericin as a hydrophilic material is supposed to enhance the hydrophilicity of PP membrane while the presence of multiple functional groups will enable charged based interaction between drug particles and coated protein surface for adsorption. This will, in turn, facilitate dual property of antifouling and adsorptive nature for the removal of drug particles from the water and better performance cycle.

5.3. Experimental

As described in section 2.2.2, a commercially available PP based hollow fibre microfiltration (HFMF) membrane has been modified using sericin to enhance its surface properties by inducing hydrophilic properties on to the membrane surface. The outer and inner surface of the PP-HFMF membrane is coated in a flow-through process where the sericin solution at different physiological conditions is passed through the membrane at low pressure and flow rate for sufficient time. The deposited sericin on the membrane surface is then cross-linked using a cross-linking agent to provide the additional strength to the structure. The cross-linked membrane unit is then heat cured to fix the bonded

structure to make it insolubilized and resist leaching henceforth. The finished membrane unit is then tested for leachability. The membrane is washed with pure water, and wash water is checked for any sign of leaching. The optimal process parameters for sericin coating is derived by coating the membrane at different conditions such as sericin pH, temperature, and concentration; the optimal set of the parameter that resulted in the high amount of sericin coating on the PP membrane were adopted for final membrane fabrication. The sericin coated membrane performance was analyzed using membrane characterization methods such as sericin leachability test, pure water permeability, FE-SEM, ATR-FTIR, contact angle measurement, swelling analysis, and porosity analysis.

5.4. Result and Discussion

5.4.1. Study on MF PP membrane coating process condition

5.4.1.1. *Effect of initial hydroxylation*

The initial hydroxylation of the PP-HFMF membrane with sulphuric acid and hydrogen peroxide (see section 3.2.3) generates hydroxyl groups on to the membrane surface to which the coating material (i.e., sericin) adhere via hydrogen bonding (see appendix A3).

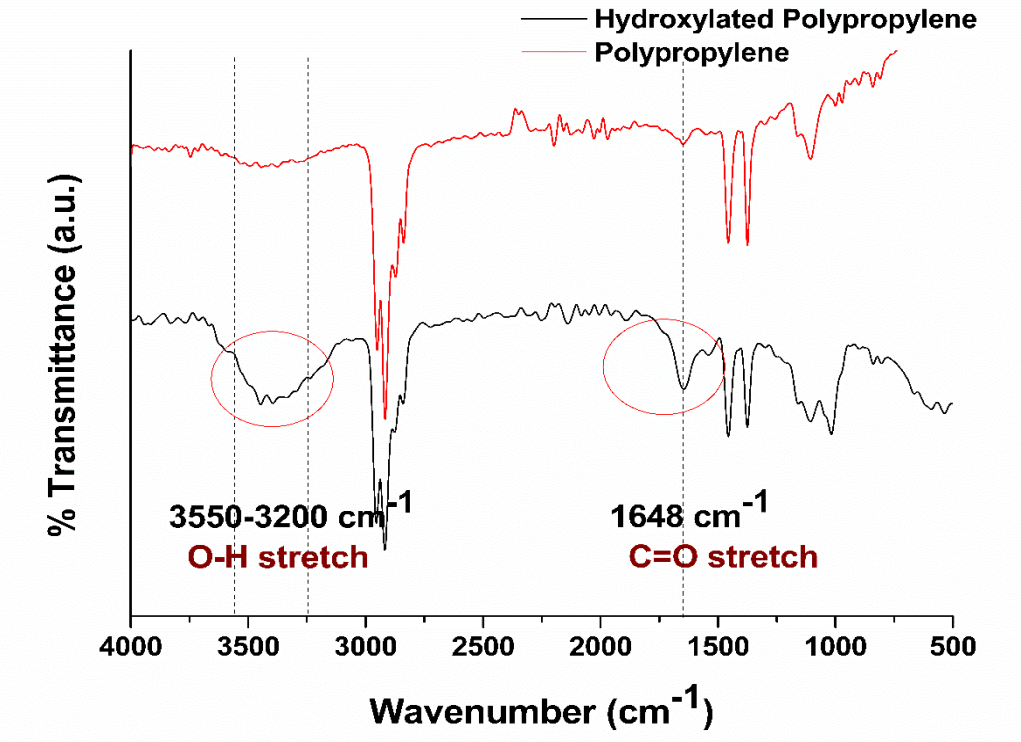

Figure 5.1 ATR-FTIR spectra for hydroxylated PP-HFMF fibre after chemical pre-treatment with H_2SO_4 and H_2O_2 solution (3:1).

The FTIR analysis of pristine and acid-treated PP membrane fibre is shown in *Figure 5.1*, where the broad peak for hydroxyl group (3200-3550cm-1) and carboxyl C=O stretch can be seen on PP-fibre after hydroxylation.

Effect of Sericin Concentration

PP-HFMF membrane coating was performed at three different sericin concentrations of 10, 20, and 30 g/l at 40°C and pH 6. Sericin deposition rate on the membrane surface can be measured by analyzing feed solution sericin concentration during operation. *Figure 5.2* shows time-dependent normalized flux (J/J_0), and the amount of sericin deposited on the membrane surface during the coating of the HFMF membrane.

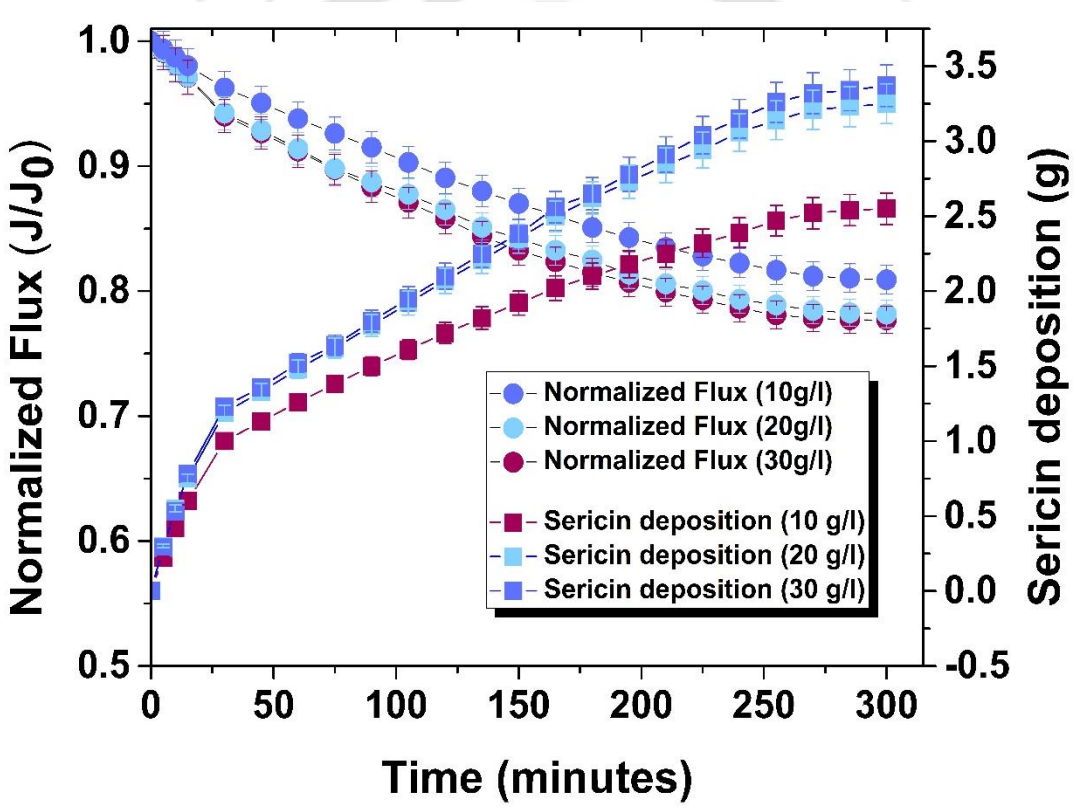

Figure 5.2. Normalized permeate flux (J/J_0) and amount of sericin deposited on membrane surface as a function of time during coating with different initial sericin feed concentrations (10, 20, and 30g/l) at a fixed temperature of 40 °C and pH 6.

The deposition profile of sericin confirms that maximum sericin deposition on the membrane surface was achieved at 20 g/l of initial feed concentration. The particle size analysis of sericin solution using the electrophoretic light scattering method also revealed agglomeration of sericin particles with increasing concentration (see Table 5-*1*).

Table 5-1. Average sericin particle size at different solution parameters conditions

Sl. No.	Parameters	Particle Size (nm)	Standard deviation
	Sericin Concentration (g/l)		
1	10	218	22
2	20	406	36.67
3	30	712	26.53
	Temperature (℃)		
4	10	1830	33.29
5	20	1201	20.51
6	30	1092	27.45
7	40	406	36.67
	pH (-)		
8	4	512	24.24
9	6	406	36.67
10	8	312	21.38

Sericin particles agglomerate at a higher concentration with intra-particle bonding, and hence, more rejection was noticed at higher concentrations (see Appendix Figure A8). However, the amount of sericin deposited was less at both low (10 g/l) and high (30 g/l) initial feed concentration. The membrane pore size distribution in the further analysis also revealed that the majority of pores pre-coating lies between 0.1-0.6 microns, and hence, the maximum coating was observed at the initial feed concentration of 20 g/l. At a low concentration of 10 g/l, the smaller sericin particle might have passed through the larger pores, while the agglomeration of sericin particles at very high concentrations may have blocked access to hydrogen bonding sites. Spectrophotometric analysis of feed sericin concentration revealed that the maximum amount of sericin is coated at 20 g/l of initial sericin feed concentration. Hence, the feed sericin concentration of 20 g/l was selected for further sericin deposition.

5.4.1.2. *Effect of Temperature*

During membrane coating, the sericin solution was circulated at a different temperature of 10, 20, 30, and 40° C to evaluate the effect of temperature on the coating of sericin to PP membrane surface (see *Figure 5.3*). It was found that an increase in temperature

assisted in a better deposition, and hence, more surface coating is achieved. The particle size analysis of sericin solution at different temperatures shows increasing agglomeration with decreasing temperature (see Table 5-*1*). As particle size increases, the HFMF membrane is expected to provide more rejection at low temperature and cake layer formation at the surface, which leads to less sericin deposition on membrane pores. Also, more sericin deposition may have been assisted at higher temperature operation by the fact that sericin exists primarily in random coil structure at high temperature and hence are more exposed to hydrogen bonding with other groups on the membrane [280]. While at a lower temperature, the random coil structure starts converting into the β-sheet structure and forms a gel-like appearance [281] and hence restricts access to the hydroxyl group [282]. Thus, the moderate temperature of 40°C was picked for further modification process.

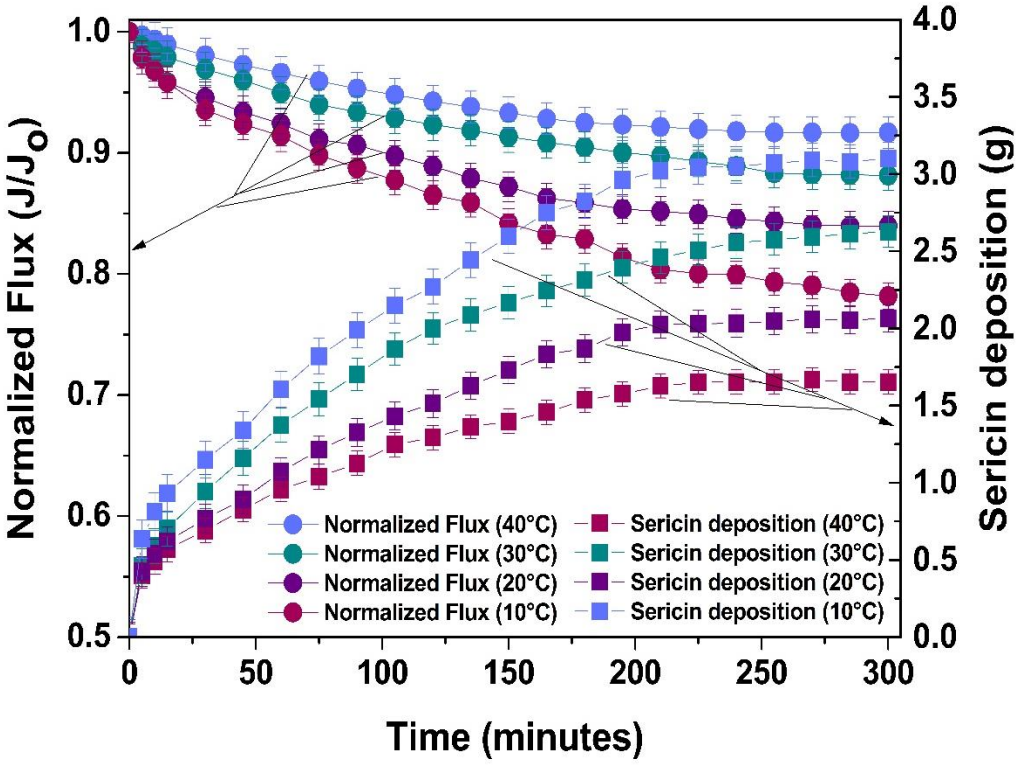

Figure 5.3. Time-dependent normalized flux (J/J_0) and the decrease in feed sericin concentration during coating of HFMF membrane at different temperatures (10, 20, 30, and 40 °C) with fixed initial sericin feed concentration (20 g/l) and pH 6.

5.4.1.3. *Effect of pH*

The HFMF membrane was coated at different pH (4, 6, and 8) using 20 g/l of sericin feed concentration at 40 °C temperature and analyzed for sericin deposition and flux behavior. *Figure 5.4* shows a change in time-dependent normalized flux (J/J_0) and sericin deposition during coating of HFMF membrane at different pH, obtained for 300 minutes. At lower pH (4), flux decline was more. Particle size analysis of sericin solution at different pH revealed agglomeration at low pH (see Table 5-*1*). Approximately 2.7, 3.25 and 3.5 gram of sericin was coated on to the PP membrane at pH 8, 6 and 4 respectively. Sericin molecules near the isoelectric point (pH 3.9) [283] have the same charge, and hence they aggregate due to decreased electrostatic repulsion [284].

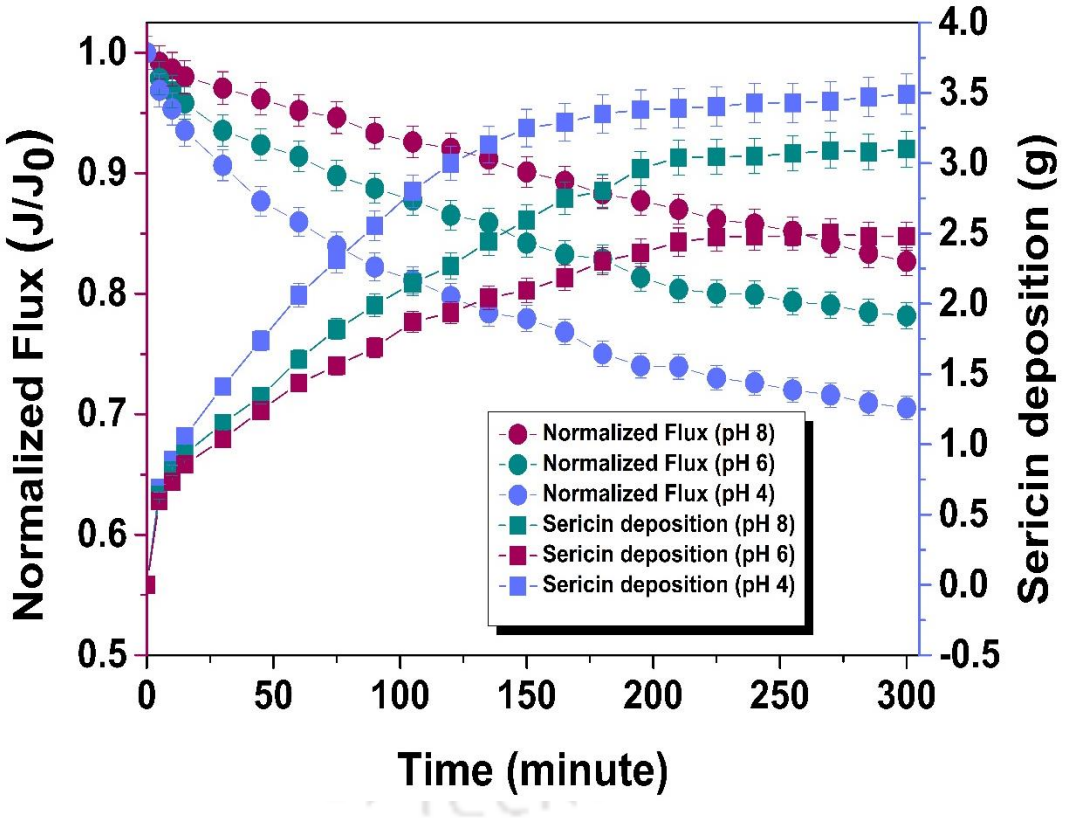

Figure 5.4. Normalized permeate flux (J/J_0) and feed sericin concentration with respect to coating time at different pH (4, 6, and 8) with fixed initial feed concentration (20 g/l) and temperature 40 °C.

While as pH is increased, sericin cohesion gets inhibited due to inter-particle repulsion. However, at lower pH, more entities of the protonated hydroxyl group of sericin are available to form hydrogen bonding with hydroxyl groups on the PP membrane surface

[104] and hence sericin adhesion to the membrane surface, and its pores are found to be more at pH 4. Therefore, more sericin deposition was observed on the membrane surface (see *Figure 5.4*) at pH 4. Hence, a lower pH of 4 was selected for further coating, and modification of the HFMF membrane.

5.4.2. Membrane characterization

5.4.2.1. *Leachability test for Sericin coated membrane*

Sericin coated HFMF membrane was washed 3-4 times with double distilled after coating and then tested for leachability of coated sericin at different pH (5, 7, and 9). The leachability profile for regular washing and washing at different pH is shown in Figure *5.5*. At first washing, the unbonded sericin solution and glutaraldehyde adhered to the membrane can be seen to come out in the wash solution, which eventually vanished with subsequent washing. Once appropriately washed, no further leaching was noticed with sericin coated membrane even when washed at different pH.

5.4.2.2. *Pure Water Permeability Test*

Permeation attribution regarding pure water flux was measured for the uncoated and sericin coated PP-HFMF membrane. Membranes were tested with de-ionized water for the determination of pure water flux (J_w) at the applied transmembrane pressure. Membrane pure water permeability was estimated for coated and uncoated membranes. As shown in *Figure 5.6*, the uncoated membrane has a relatively high pure water permeability of about 2.2132 x 10^{-9} m^3/m^2.s.Pa. The HFMF membranes coated at pH 8, 6, and 4 exhibit comparatively low pure water permeability by 5.34%, 14.80% and 19.10%, respectively (pH 8 = 2.1033 x $10^{-9}$$m^3/m^2$.s.Pa, pH 6 = 1.9575 x $10^{-9}$$m^3/m^2$.s.Pa and pH 4 = 1.8582 x 10^{-9} m^3/m^2.s.Pa) with respect to pristine membrane. A similar decrease in water flow has been reported [105] in earlier cases of membrane modification with sericin. The pure water permeability was found to decrease with the amount of sericin deposited on the membrane surface. The uniform deposition of sericin on membrane surface/pores resulted in narrowing the pore size of the sericin coated membrane, which facilitated an additional hydraulic-resistance to water flow and hence exhibited low water permeability.

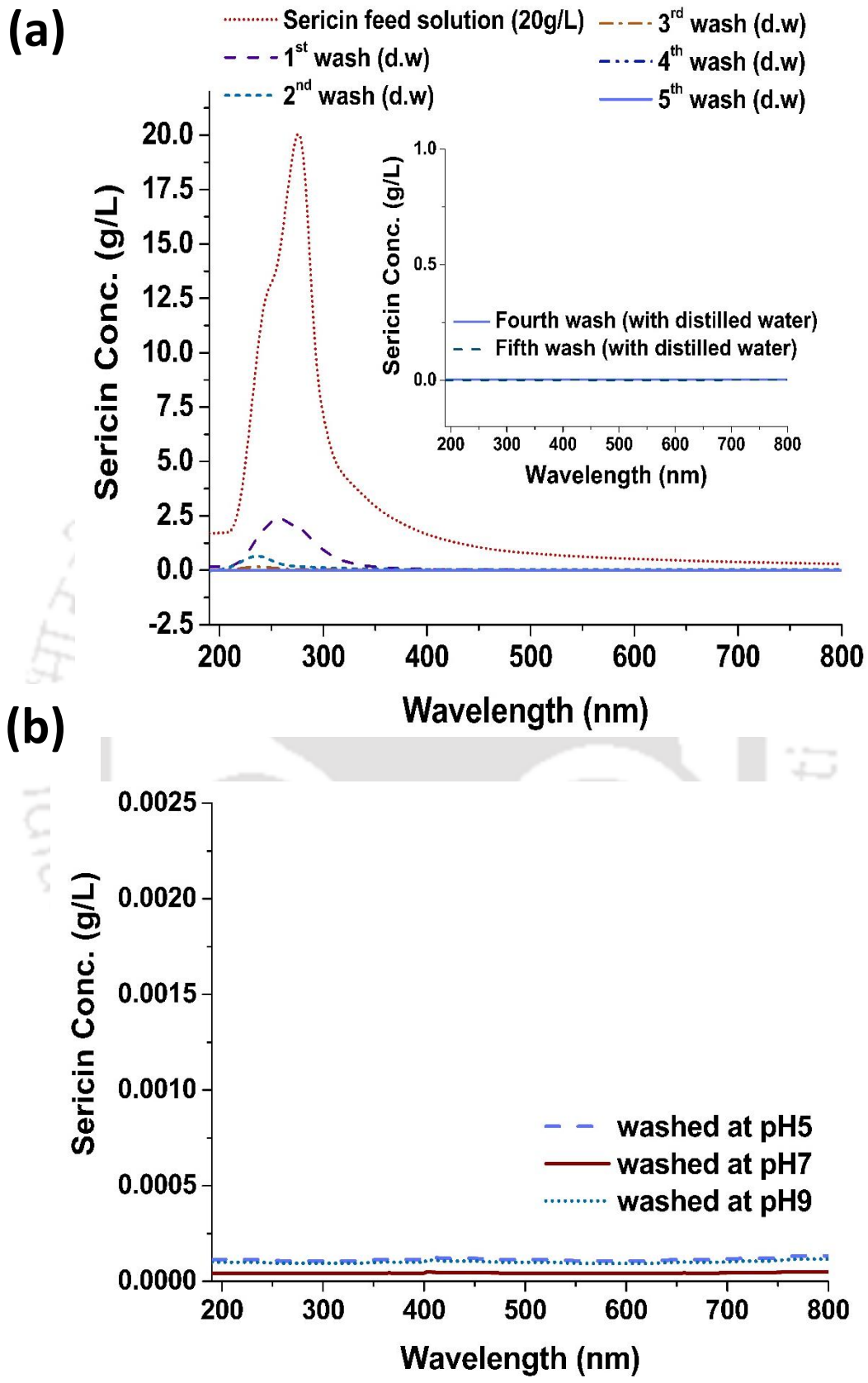

Figure 5.5. Spectrophotometric profile for sericin presence during the membrane leachability test (a) multiple washes with distilled water (b) washing at different pH.

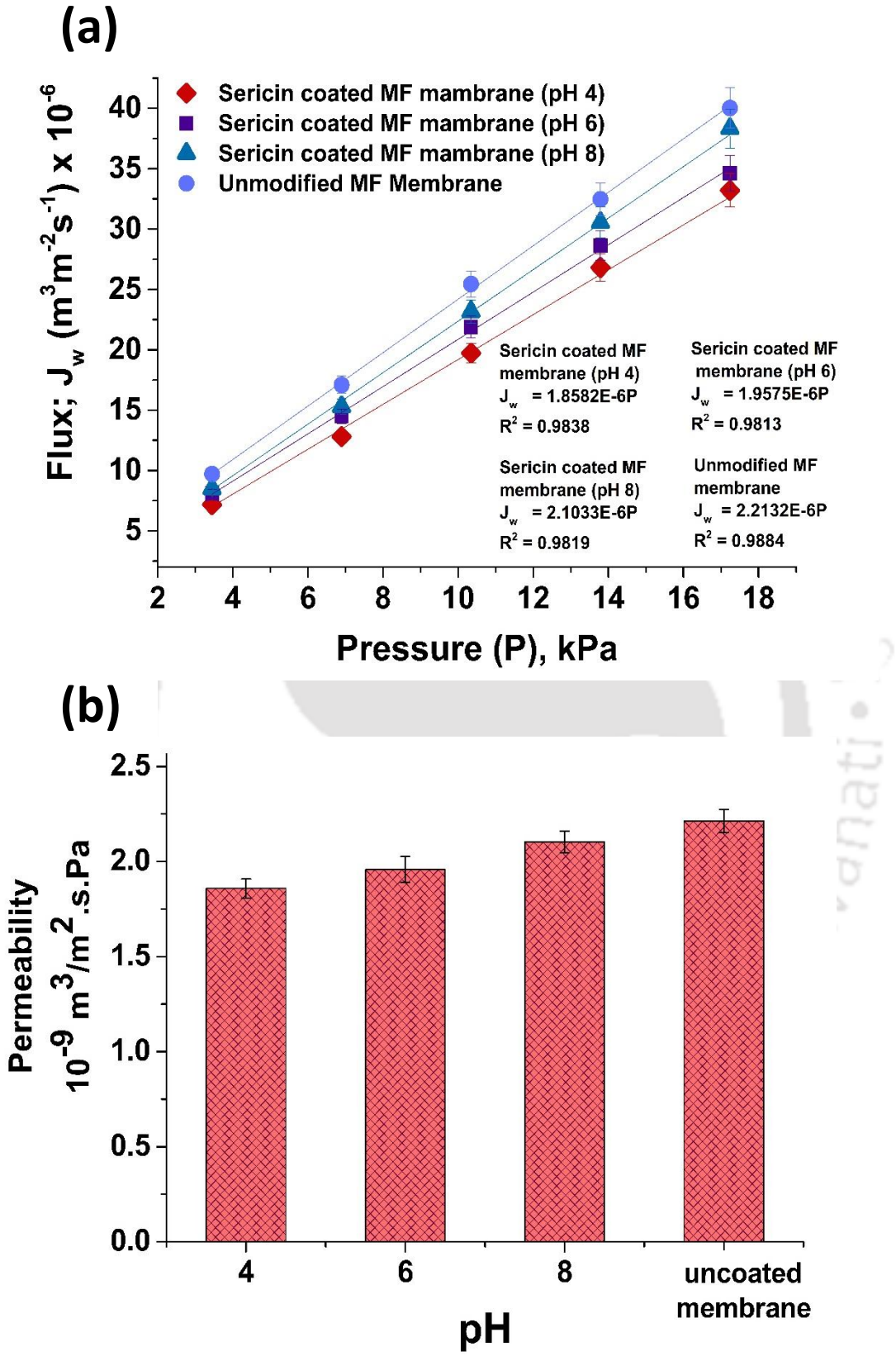

Figure 5.6. (a) Pure water flux with respect to differential pressure for uncoated and sericin coated HFMF membrane at different pH (4, 6, and 8) (b) Permeability at different pH.

5.4.2.3. *FE-SEM and EDX*

The surface morphological structure of the uncoated HFMF membrane and sericin coated HFMF membrane was evaluated by FE-SEM, and the representative images are presented in *Figure 5.7*. We noticed changes in surface texture and reduction in pore diameter with deposition of sericin on to the membrane (see *Figure 5.7*a-d). The cross-sectional view of the sericin coated membrane shows the deposition of sericin on to the inner surface as well as pores of the membrane (see *Figure 5.7*e-j). The surface and cross-sectional FE-SEM analysis confirm the deposition of sericin throughout the membrane surface.

Energy dispersive spectra of uncoated and sericin coated HFMF fibre on the outer surface, inner surface, and cross-section were obtained to ascertain the binding of sericin on the membrane surface (see *Figure 5.8*a-f). Acid hydrolysis generated more hydroxyl groups on the membrane surface, and hence carbon percentage decreased while oxygen percentage increased. Moreover, earlier, there was no nitrogen on HFMF fibre while sericin coating presence of nitrogen (5.9-7.2%) was detected on outer and inner membrane surface as well as pores, which indicates deposition of sericin.

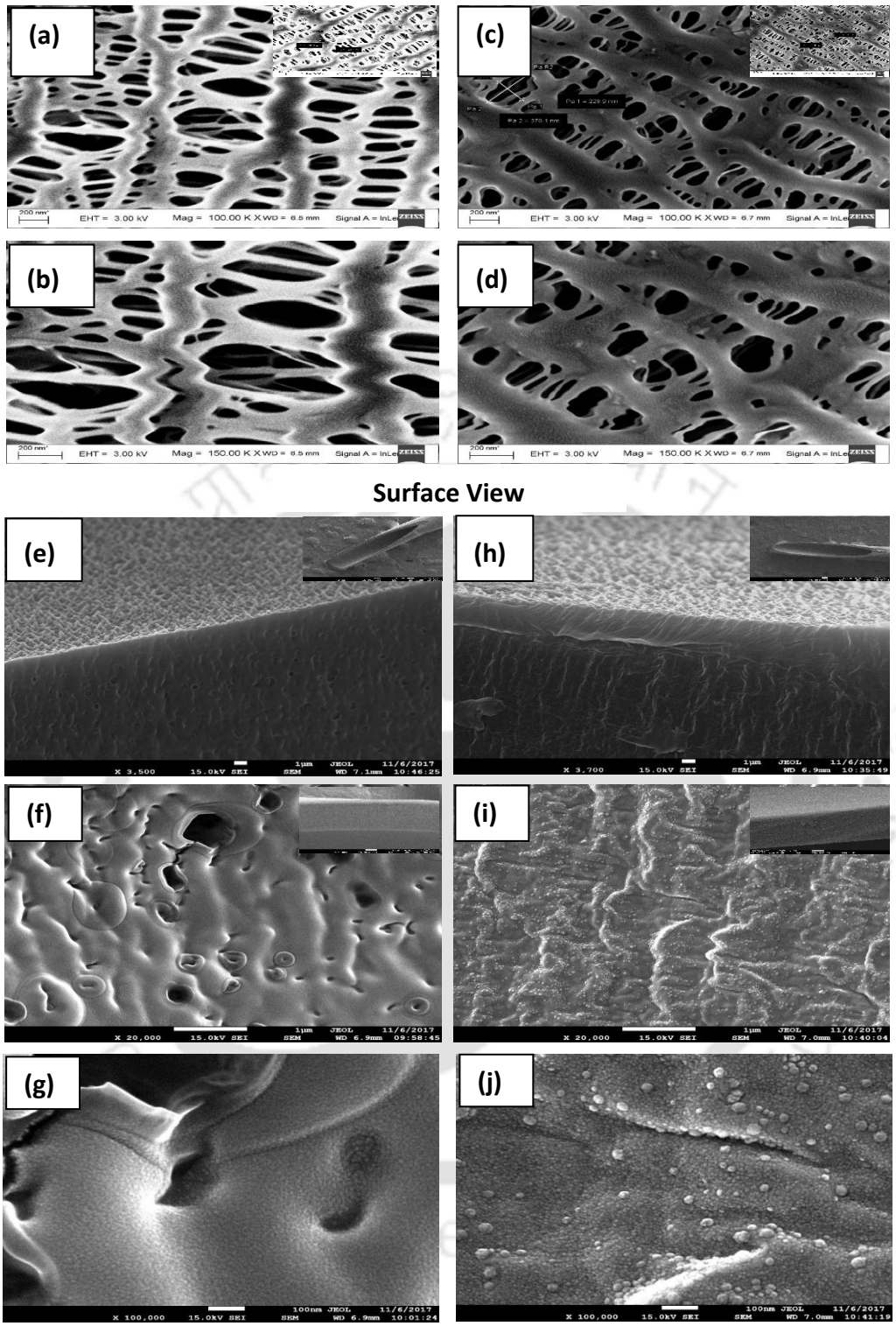

Figure 5.7. FESEM analysis of PP MF-membrane: before sericin coating; surface morphology at 100KX (a), 150KX (b) with a cross-sectional view at 3.5KX (e), 20KX (f), and 100 KX (g), after sericin coating; surface morphology at 100KX (c), 150KX (d) with a cross-sectional view at 3.5KX (h), 20KX (i), and 100 KX (j).

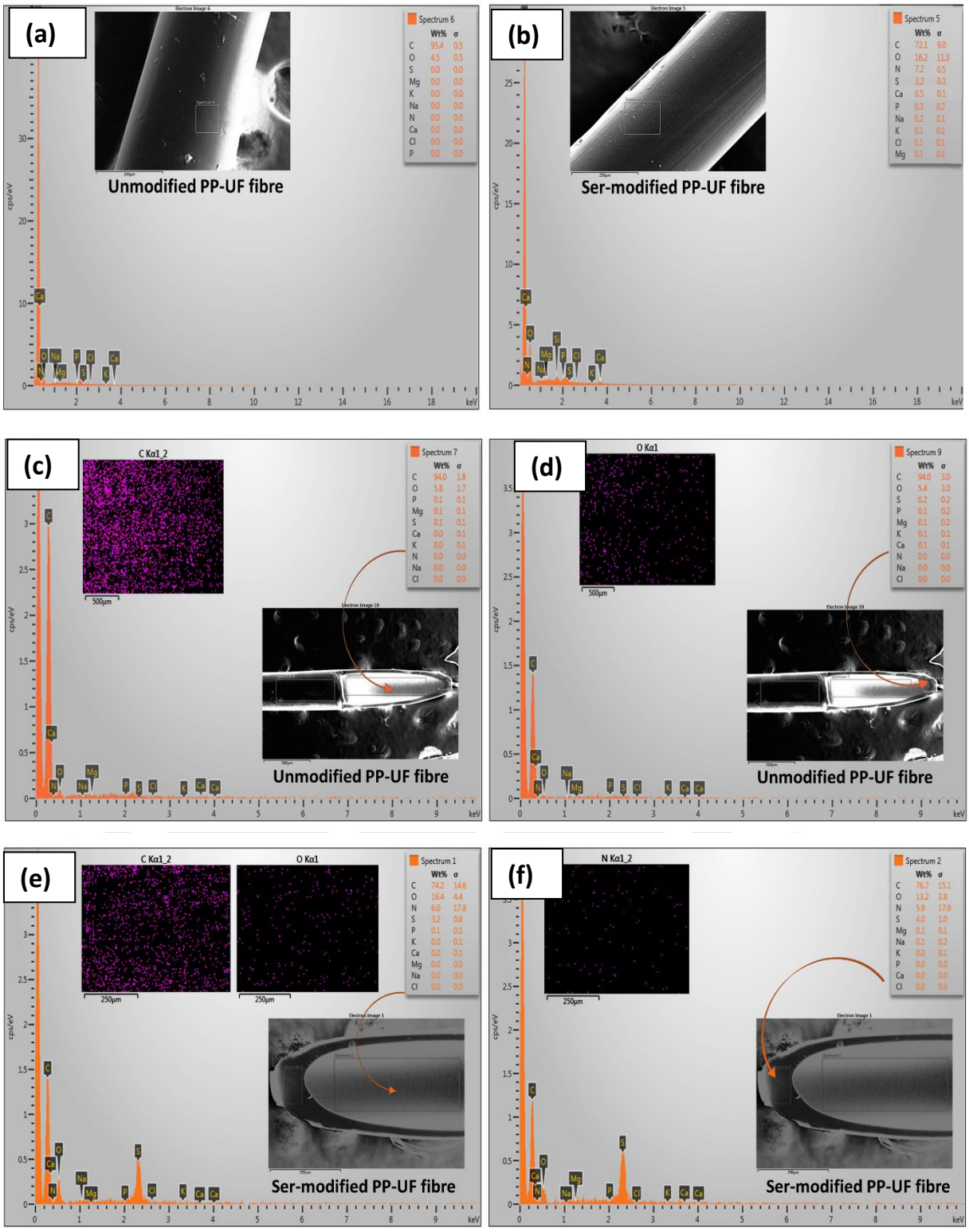

Figure 5.8. EDX pattern on (a) outer surface of unmodified PP-HFMF fibre (b) outer surface of sericin-modified PP-MF fibre (c) inner surface of unmodified PP-HFMF fibre (d) cross-section of unmodified PP-HFMF fibre (e) inner surface of sericin coated PP-HFMF fibre (f) cross-section sericin coated PP-HFMF fibre.

5.4.2.4. *ATR-Fourier transform infrared spectroscopy*

The ATR-FTIR Spectra of PP-HF, sericin, sericin coated PP-HF was analysed for binding confirmation and to study molecular interaction between PP-membrane surface and sericin (see *Figure 5.10*). Polypropylene spectra show characteristic peaks at 2951 cm^{-1} for CH_3 (asymmetric stretching), 2916 cm^{-1} for CH_3 (symmetric stretching), 2872 and 2836 cm^{-1} for CH_2 (symmetric stretching). At lower wavenumber peaks were observed at 1455 cm^{-1} for CH_3 (asymmetric stretching) and CH_2 (symmetric deformation), 1375 cm^{-1} for CH_3 (symmetric), CH_2 (wagging), CH (bending) and CC (backbone). 1107 cm^{-1} for CH_3 (stretching), CH_2 (wagging), CH (twisting and bending) and CC (backbone) [285–287]. After chemical pre-treatment with (H_2SO_4: H_2O_2), the PP-fibres exhibited broad hydroxyl peak (3350-3200 cm^{-1}) and carbonyl stretch at 1648 cm^{-1} indicating generation of the hydroxyl group on the membrane surface (see *Figure 5.9*).

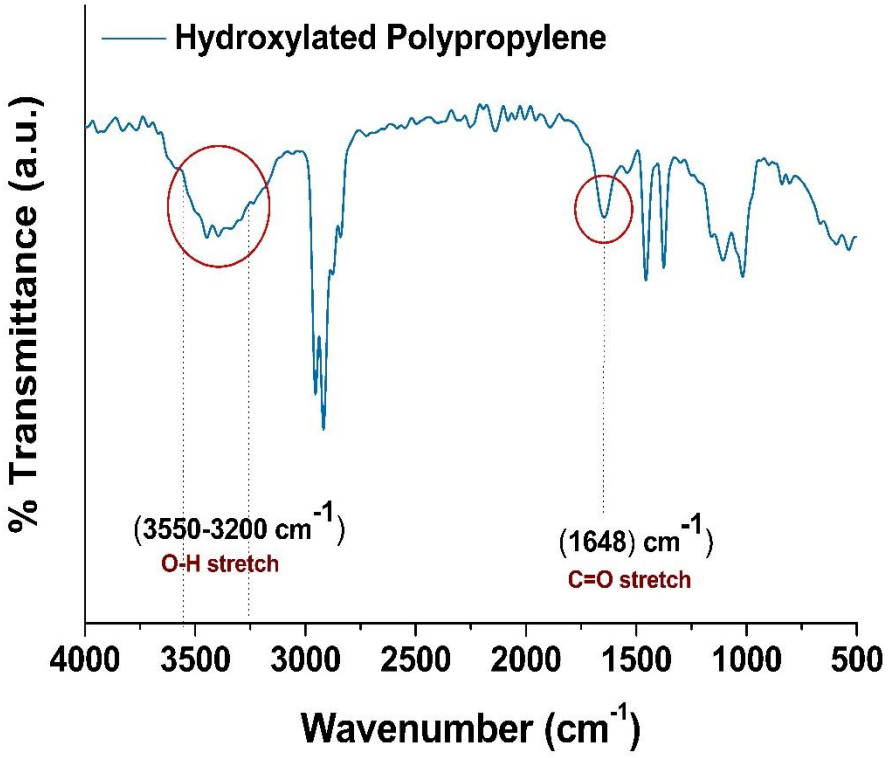

Figure 5.9. ATR-FTIR spectra for hydroxylated PP-HFMF fibre after chemical pre-treatment with H_2SO_4 and H_2O_2 solution (3:1).

Sericin spectra exhibit broad amide A peak at 3270 cm^{-1}, amide I and amide II bands at 1650 and 1530 cm^{-1}, signature peak at 1400 for CH, OH bending and 1068 cm^{-1} for C-OH stretching vibration [109]. Sericin coated PP fibre shows characteristic polypropylene

peaks at 2950, 2920, 2875, 2840 cm^{-1}. However, new NH and OH stretch peak for sericin appeared at 3320 cm^{-1}, while amide I, II, and III peaks for sericin appeared at 1695, 1580, and 1295 cm^{-1}. The CH_3 stretch, CN bending, C-OH stretching, which relates to the bonding of sericin with PP fibre appeared at 1450 and 1160 cm^{-1}. The disappearance of broad hydroxyl and primary amine peak at 3270 cm^{-1} shows the bonding of sericin with polypropylene via hydrogen bonding involving hydroxyl groups. The crosslinking of the amine group with glutaraldehyde is observed from the appearance of secondary amine peak in sericin coated hollow fibre at 3320 cm^{-1}. These changes in characteristic band suggest incorporation of sericin on to the PP-HFMF membrane surface, and ATR-FTIR provides evidence of the presence of cross-linked sericin on to the membrane surface.

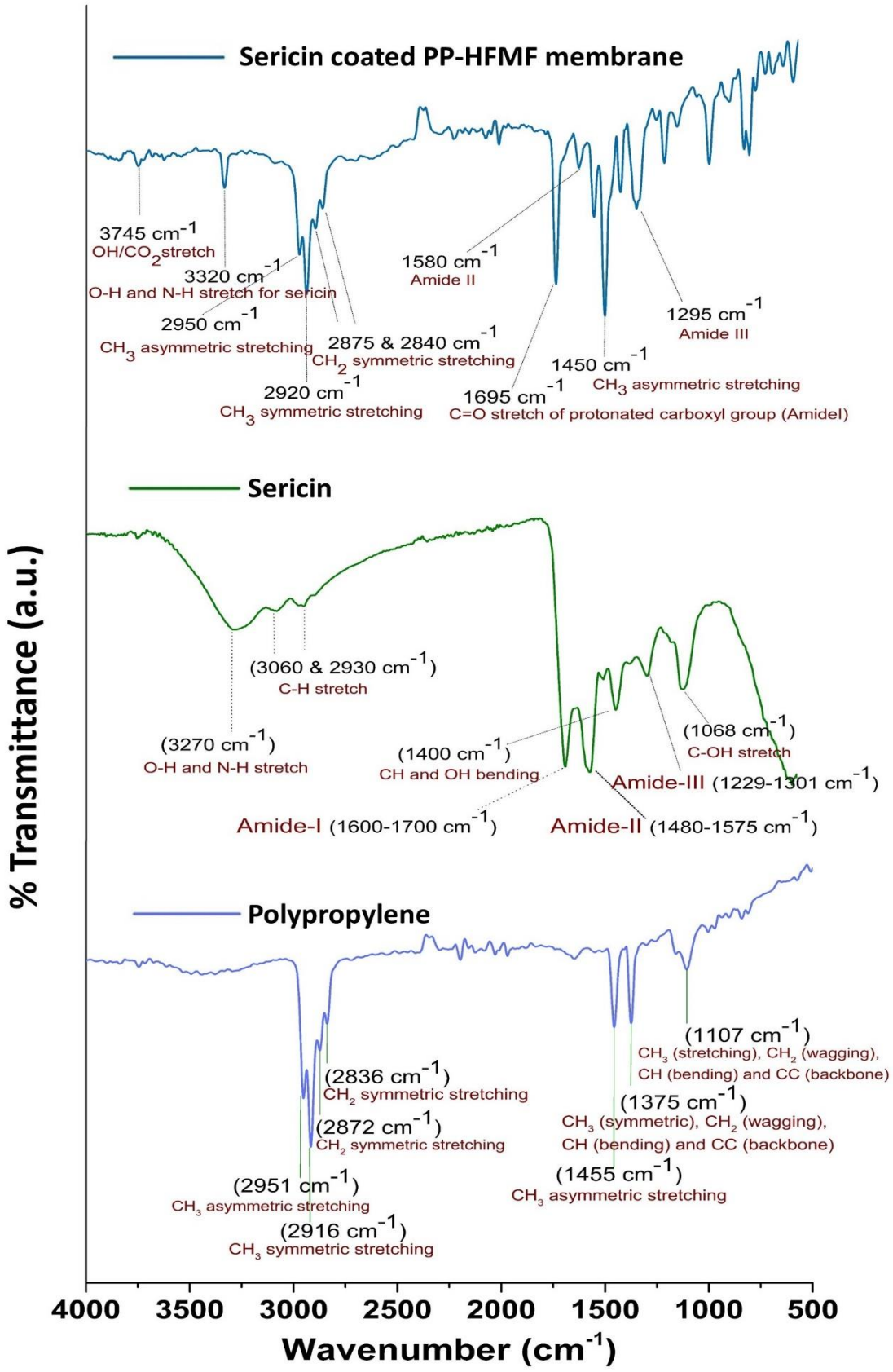

Figure 5.10. ATR-FTIR spectra of (a) Sericin coated PP-HFMF membrane, (b) Sericin, and (c) PP- HFMF membrane.

5.4.2.5. *Contact angle measurement*

The contact angle results of uncoated, acid hydrolyzed, and sericin coated PP-HFMF membrane is shown in *Figure 5.11*. The contact angle of 81.5° is indicating that low hydrophilicity is observed for the uncoated membrane. After acid hydrolysis of the PP-HFMF membrane, the contact angle decreased from 81.5° to 73° due to the generation of hydroxyl groups on the membrane surface. Sericin coating on to the membrane surface further enhanced the hydrophilicity by enriching the surface with hydrophilic groups present in the sericin. The Sericin coated PP-HFMF membrane exhibited a low contact angle of 38°, showing high hydrophilicity.

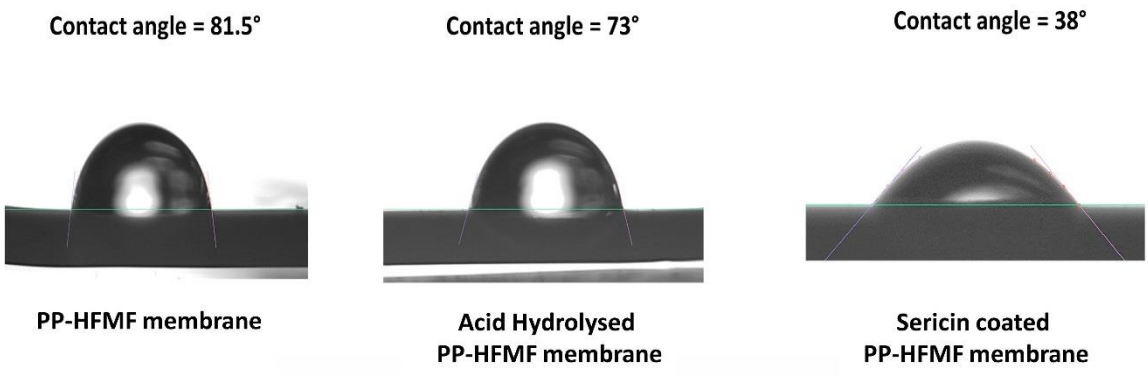

Figure 5.11. The contact angle of uncoated, acid hydrolysed and sericin coated PP-HFMF membrane (error±2.5).

5.4.2.6. *Swelling and porosity test*

Swelling property can be directly related to the membrane hydrophilicity. Table 4.2 shows the water content percentage of uncoated and sericin coated membranes. The water content for uncoated PP-HFMF membrane was found to be 50.29%, while for sericin coated PP-HFMF membrane, it increased to 64.87%. This improvement must have happened because of the incorporation of sericin on to the surface of the membrane. Membrane porosity determined by the gravimetric method shows around 18.47 % decrease in porosity of the coated membrane (see *Table 5-2*). This was evident from FESEM analysis, also where deposition of the sericin layer was apparent, and membrane pores size was found to be reduced. The mean pore size of membrane before the coating was found to be 0.41 microns and after coating pore size reduced to 0.20 microns (coated at pH 4, Temp 40 °C, and concentration 20g/l). The pore size distribution of the

membrane before and after sericin coating is shown in *Figure 5.12*. In the uncoated membrane, around 84% of the pores exist above 0.3 µm before coating. It was found that pore diameters larger than average sericin particle size at pH 4 (~ 0.5 microns) were blocked, and the pore size is reduced after coating and most of the pores (~74%) lie in-between 0.15 to 0.35 microns. However, larger pores are not reduced because smaller sericin particles might have passed through the larger pores. Therefore, the narrow membrane pore size distribution may be achieved by selecting an appropriate temperature and pH for given sericin concentration and can be taken as a future study.

Table 5-2. Water content and porosity of PP-HFMF membrane and sericin coated PP-HFMF membrane

Membrane	Water Content (%)	Porosity
Uncoated PP-HFMF	50.29	53.63%
Sericin-coated PP-HFMF	64.87	35.16%

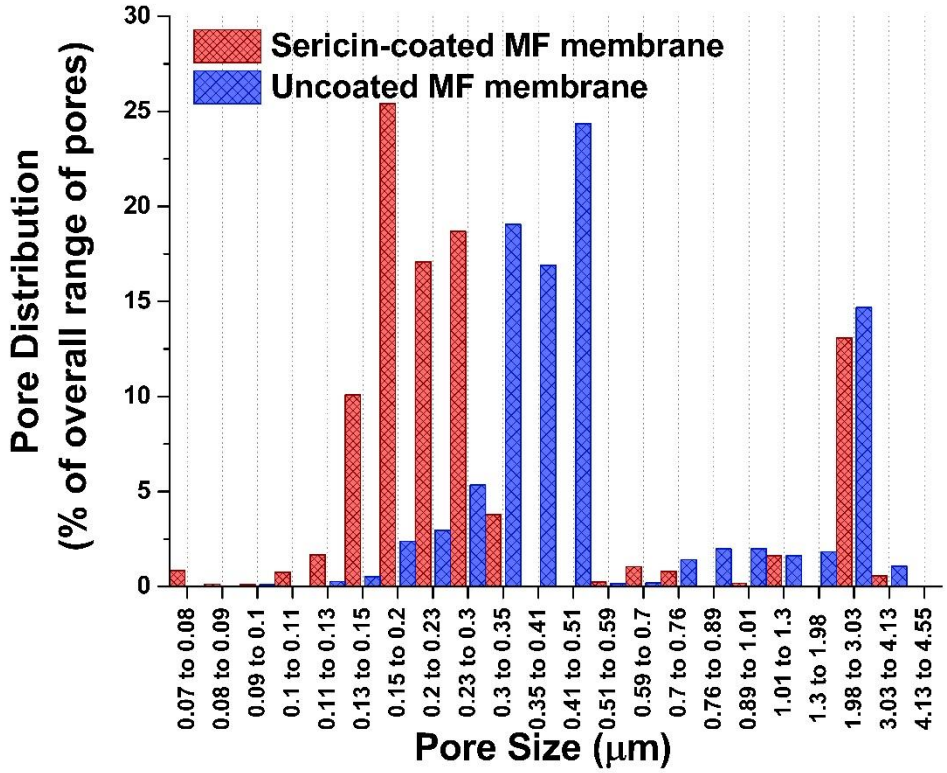

Figure 5.12. Pore size distribution for uncoated and sericin coated MF membrane at pH 4, temperature 40° C and concentration 20 g/l.

5.5. Conclusion

In this work, a Polypropylene based hollow fibre MF membrane was modified using sericin as a hydrophilic polymer in a flow-through coating method. The morphology, hydrophilicity, permeation, and fouling properties were investigated before and after sericin coating, and the results were analysed. The obtained results from FESEM, EDX, and ATR-FTIR shows conclusive evidence for the uniform deposition of sericin on the modified membrane surface. It was found that the reduced pore size after sericin coating resulted in decreased pure water permeability by 19.10% compared to that of the pristine membrane. The sericin coated PP-HFMF membrane exhibited increased hydrophilicity, which is further established by a reduced contact angle (38°) and high water content (64.87%) analysis. The sericin-coated membrane exhibited enhanced hydrophilicity in the presence of sericin functional groups on the membrane surface. The sericin enhanced hydrophilic membranes can be used as an adsorptive membrane for charge-based separation of pollutants from water.

Chapter 6

Application of sericin-coated polymeric microfiltration membrane

Parts of this Chapter are published as research articles:

- V.K. Verma, S. Subbiah, Fouling resistant sericin coated polymeric microfiltration membrane, J. Chem. Technol. Biotechnol. (2019) jctb.6169. doi:10.1002/jctb.6169.
- V.K. Verma, S. Subbiah, Sericin coated polymeric microfiltration membrane for removal of drug-based micropollutants, J. Chem. Technol. Biotechnol. (2019) jctb.6168. doi:10.1002/jctb.6168.

6.1. Theoretical Consideration

The modified sericin-coated adsorptive membrane is expected to provide selective adsorption of charge based molecule and fouling resistivity. In the first part, the modified sericin-coated adsorptive membrane has been tested for the removal of drugs from a different class of applications like analgesic/painkillers NSAID drugs (Ibuprofen, Diclofenac), Antibiotics (Amoxicillin, Ciprofloxacin), and Steroids/Hormones (Estrone, β-estradiol). Among the selected drugs Ibuprofen, Diclofenac, Amoxicillin, and Ciprofloxacin are supposed to exist in anionic form, while estrone and β-estradiol are uncharged at neutral pH (see Appendix A9). Molecular speciation (Charged and uncharged abundance of different species at particular pH) of selected drugs in this study (see *Figure 6.1*) is calculated using the formula shown below [288]

$$\%\,ionization = \frac{100}{1+10^{X\,(pH-pKa)}} \tag{6.1}$$

Where X= -1 if the acid drug or +1 if the basic drug

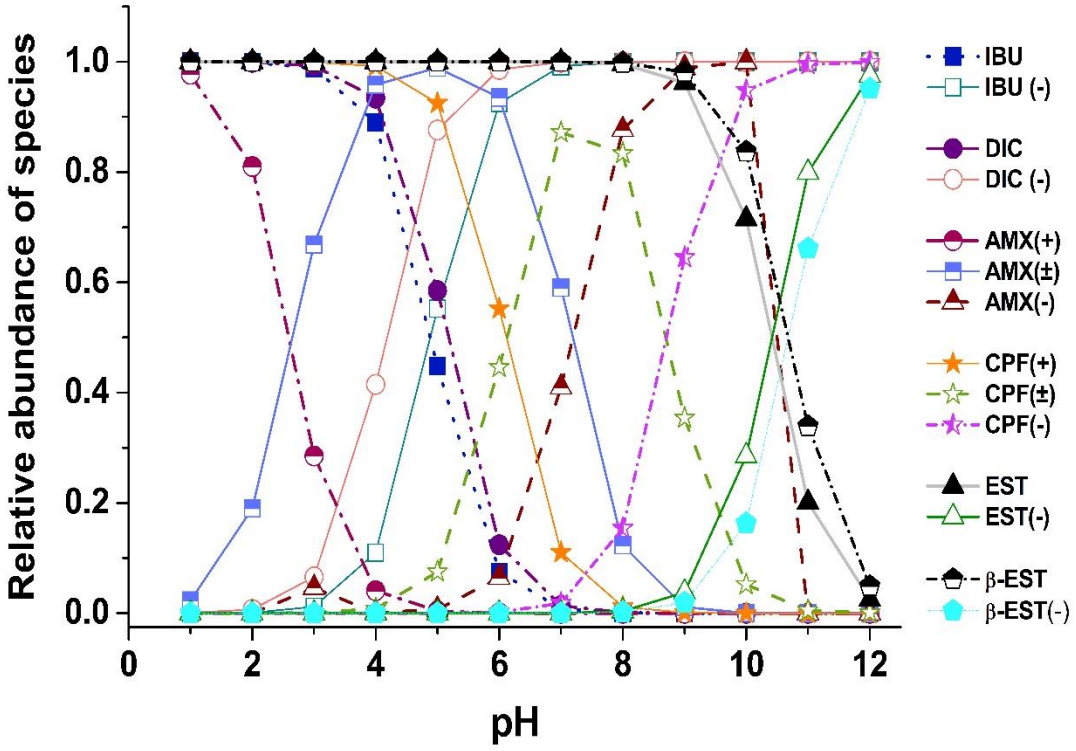

Figure 6.1. Molecular speciation diagram of selected drugs in this study (Charged and uncharged abundance of different species at neutral pH (≈7); IBU-Ibuprofen, DIC-Diclofenac, AMX-Amoxicillin, CPF-Ciprofloxacin, EST-Estrone, β-EST-β-estradiol.

The sericin-coated MF-membrane have amine functional groups present on the membrane surface, which can act as a hydrogen bond (HB) donor as well as acceptor. The selected drugs have functional groups such as carboxyl, ketone, and hydroxyl, which can form hydrogen bonding with amine functional groups present on the membrane surface depending on their affinity towards drug structure. Ibuprofen (pKa 4.91) [289] and diclofenac (pKa 4.15) [290] exist in anionic phase (≈99%), the negatively charged carboxylate group of the drug (act as HB acceptor) forms HB with amine present on the sericin coated membrane (act as HB donor). Whereas in the case of Amoxicillin and Ciprofloxacin, both exist in the zwitterionic phase at neutral pH (≈7), and hence the ionized carboxyl group of the drug interacts with the amino group present on the membrane surface.

Ciprofloxacin (pKa1 = 6.09, pKa2 = 8.74) exist in zwitterionic (87.2%) form while around 11% species exist in cationic form and 1.8% as anion at neutral pH [22]. In the case of amoxicillin (pKa1 = 2.63, pKa2 = 7.16 and pKa3 = 9.55), almost 60% species exists in zwitterionic phase while 40% species exist in anionic phase at neutral pH [291]. However, the carboxyl group in both drugs is deprotonated at neutral pH. Hence, amoxicillin and ciprofloxacin carboxylate group may form HB with an amine group present on the membrane surface. In the case of steroid drugs, Estrone (pKa 10.40) and β-estradiol (10.71) [292] exist in an uncharged state at neutral pH. Though these drugs are uncharged, the presence of hydroxyl and ketone groups may assist in weak hydrogen bonding with amine groups of the membrane surface.

6.2. Hypothesis

Based on results obtained from the previous work, the sericin coated membrane is established to have adsorbing properties for drugs as well as the sericin-coated membrane exhibited good antifouling properties. The presence of positively charged amine groups on the surface of the sericin-coated membrane is supposed to attract and involve in hydrogen bonding/electrostatic interaction with the negatively charged (at neutral pH) drug particles present in water. The removal is supposed to be highly dependent on the charge-based interaction of drug particles with the amide groups present on the membrane surface. Since particles are supposed to be weakly adsorbed to the membrane surface, the separation and regeneration of bonded drug particles can be achieved by altering the pH of the stripping solution used for membrane cleaning.

The hydrophilic and hygroscopic properties of sericin must have enhanced the hydrophilicity of the PPMF membrane, which in turn will impart antifouling properties. The presence of sericin on the membrane surface leads to the formation of the hydration layer, which will resist the deposition of foulants on the membrane surface. In this sense, the presence of the sericin protein facilitated hydration layer will reduce the fouling propensity, and membrane flux recovery can be enhanced for better performance and life cycle.

6.3. Experimental

The sericin-coated adsorptive membrane was tested for the removal of different drug particles from an aqueous solution. Different experiments were performed to analyze the removal and adsorption capacity of the membrane. The adsorption kinetics and breakthrough curves were modeled using Bohart-Adams, Thomas, Yoon–Nelson, and Clark fixed bed models. The effect of multi-solute and multi-drug mixture on the removal capacity of the sericin-coated membrane was studied. Later, the antifouling properties of the sericin coated membrane were also evaluated by purifying greywater and produced water.

6.4. Result and Discussion

6.4.1. Sericin coated MF membrane for removal of drug-based micropollutants

6.4.1.1. Effect of feed flow rate

Experiments were conducted with Ibuprofen as a model drug to evaluate the effect of flow rate on removal efficiency of sericin-coated HFMF membrane with respect to volume filtered (*Figure 6.2*a). Operated in a dead-end filtration mode at a different feed flow rate (5, 10, 15, 20 l/h) with fixed feed concentration (500 µg/l), pH 7 and temperature 30°C. The complete removal was noted for up to 1750 ml, 750 ml of volume filtered at 5l/h, 10 l/h of flow rate. As the flow rate was increased, further removal of ibuprofen decreased significantly at 15 l/h and 20 l/h, respectively. At a higher flow rate, there is a decrease in residence time, so drug particles had a shorter time to interact with the membrane surface, hence leaving the column early, and appearing in the permeate [293,294]. A gradual decrease in removal efficiency with an increase in flow rate concludes the role of adsorption in the removal of Ibuprofen.

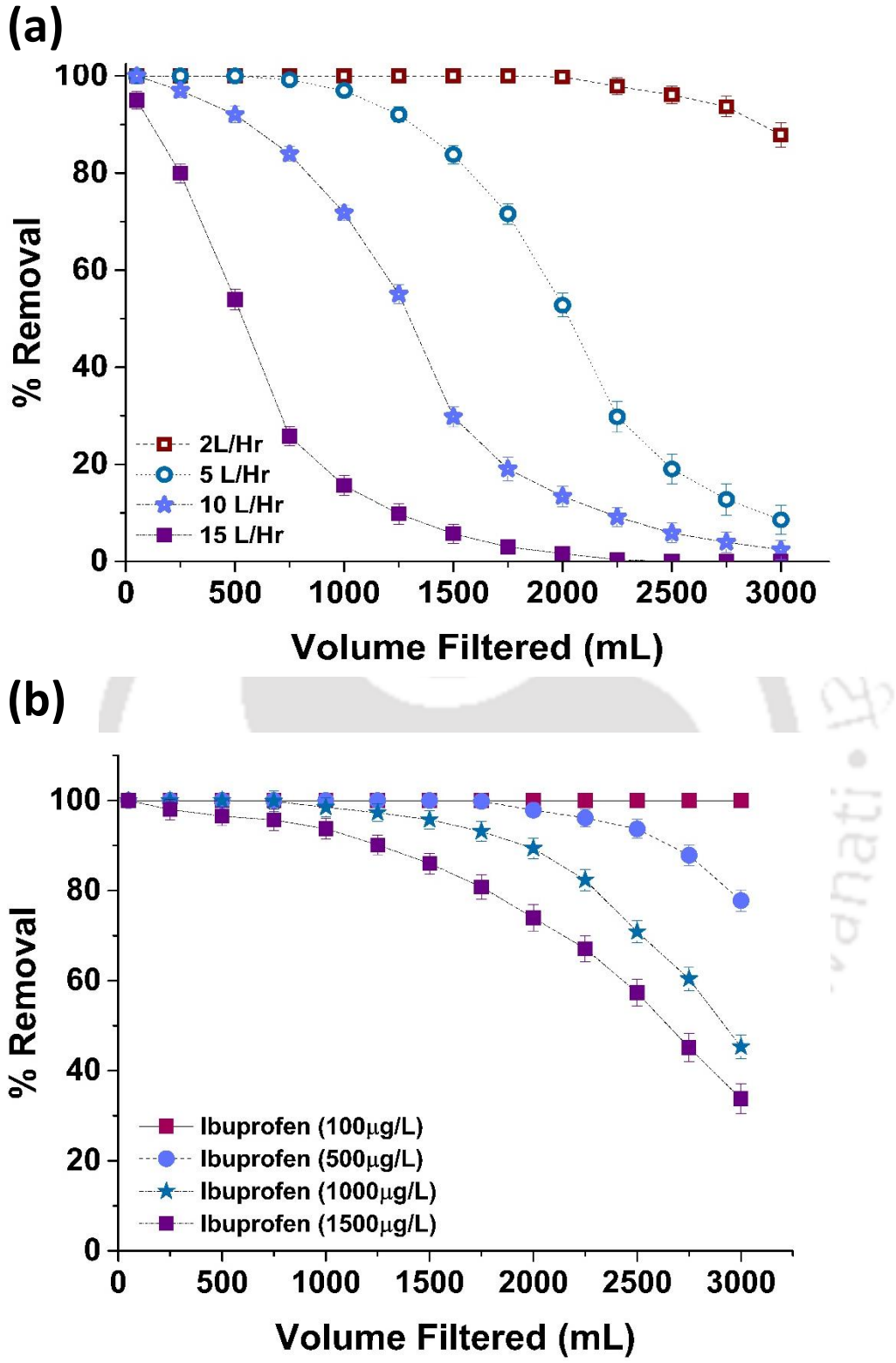

Figure 6.2. Percentage removal of Ibuprofen using sericin coated HFMF-membrane at (a) different flow rate (5, 10, 15, 20 l/h) with feed concentration of 500 µg/l (b) at different feed concentration (100, 500, 1000, 1500 µg/l) with fixed flow rate of 5 l/h.

6.4.1.2. Effect of feed concentration

Experiments were also performed at different feed concentrations (100, 500, 1000 µg/L) with ibuprofen aqueous solution at a low flow rate of 5 l/h. Complete removal was observed at a low concentration of 100 µg/l for a filtration cycle of 3 liters. While at 500 and 1000 µg/l, complete removal was noticed up to 1750 mL and 1000mL of volume filtered, respectively (see *Figure 6.2*b). An increase in feed concentration results in early saturation of binding sites on the membrane surface, and hence drug appears quickly in the permeate water. The reported concentration of analgesic drugs like ibuprofen lies well below in the range of 1-100 µg/l (see Table 3-*2*), and hence the fabricated membrane can perform very well for addressing these levels of contamination.

6.4.2. The removal efficiency of the modified HFMF membrane with a different class of drugs

A set of experiments were performed at a fixed initial feed concentration of 500 µg/l, pH 7, and room temperature (30°C) to evaluate the removal of selected drugs (Ibuprofen, Diclofenac, Amoxicillin, ciprofloxacin, Estrone, and β-estradiol) using sericin coated HFMF-membrane. During continuous filtration (5 cycles of 3-litres filtrate), the process was maintained under gravity-based flow (see filtration set up *Figure 3.9*) with constant permeate flux of 2.75 $lhr^{-1}m^{-2}$. The particle size of all the selected drugs are adequately smaller than the pore size of the sericin coated HFMF-membrane (0.20 microns) and hence cannot be physically retained by size exclusion method unless adsorption takes place on the membrane surface. The drug removal efficiency of the uncoated HFMF membrane was found to be zero. The sericin-coated HFMF membrane contains distributed amide, carboxyl, and hydroxyl functional groups on the membrane surface, facilitating charge-based interaction/salt bridge and hydrogen bonding for drug molecules. The positive log D (distribution coefficient) and log P (partition coefficient) value of selected NSAIDs (Ibuprofen, Diclofenac), Antibiotics (Amoxicillin and Ciprofloxacin) and unionized steroid drugs (Estrone, β-estradiol) at pH 7 indicates that these drugs are moderately lipophilic in nature and hence will have affinity towards protein (see Appendix A 9). *Figure 6.3* shows the retention of six different drugs using a sericin-coated membrane. Ibuprofen and Diclofenac exhibited higher removal (91.83 and 83.47%), whereas, Amoxicillin and Ciprofloxacin showed moderate removal (82.74 and 62.89%) while Estrone (47.48%) and β-estradiol (11.30%) showed lower removal efficiency with the sericin coated HFMF membrane. Although Estrone and β-estradiol

had positive log P and log D value, the sericin coated HFMF membrane exhibited comparatively low removal of these steroids relative to the NSAIDs and antibiotics.

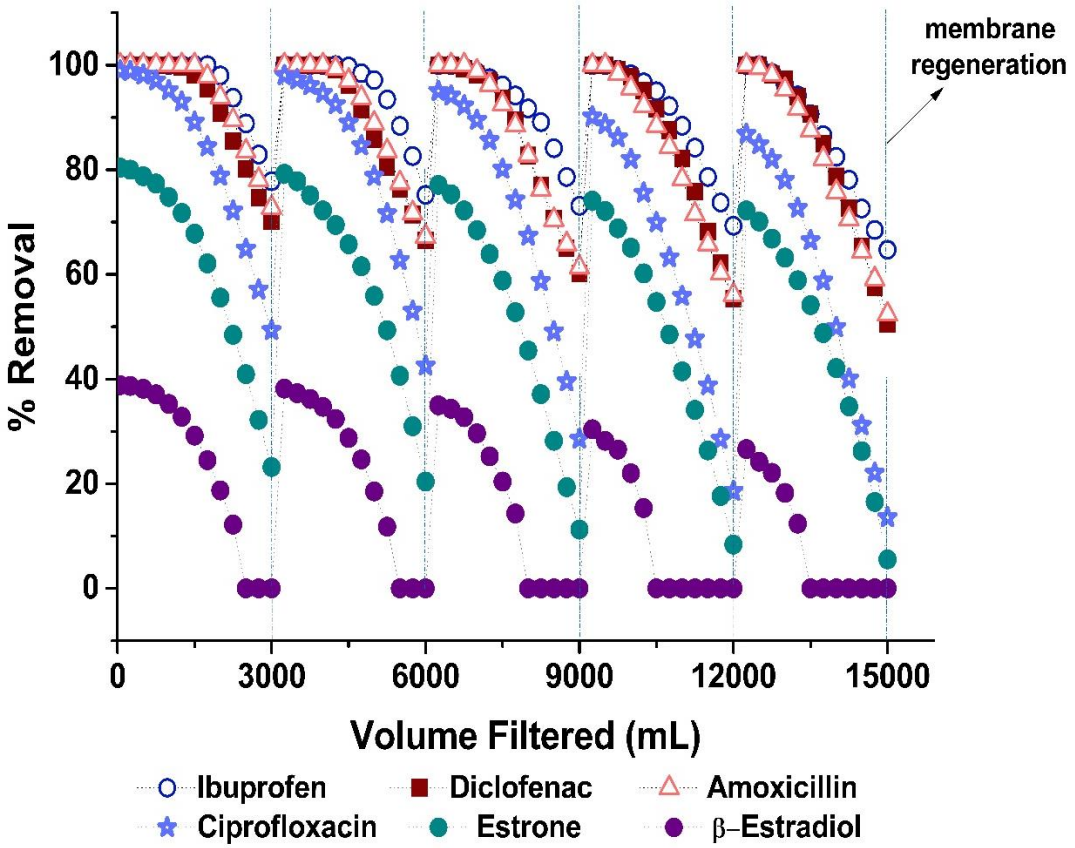

Figure 6.3. The sericin coated HFMF membrane performance for drug removal from aqueous solution at a feed concentration of 500 µg/l, pH 7, and temperature 30°C (error = ±2.65%)

This suggests that hydrophobic interaction is not the main phenomenon governing the adsorption for these drugs [295]. The contact angle analysis (*Figure 6.4*) of different drug solutions on the sericin-coated membrane reveals that the steroid drug solution (Estrone>β-estradiol) had a low contact angle than NSAIDs and antibiotics solution (Ibuprofen>Diclofenac>Amoxicillin>Ciprofloxacin). Which in turn, indicates that the charged drug particles interact directly with membrane surface via hydrogen bonding, and hence, water contact angle increased, while in case of uncharged drug particles, the water and membrane surface interaction was dominant, and hence contact-angle is found be equivalent to pure water. Zeta potential analysis also shows the respective charge on drug solution (see *Figure 6.4*). Ibuprofen and diclofenac have zeta potentials of -5.74 mV and -5.65 mV, respectively, and exist predominantly in anionic phase (≈ 99.2 and

99.8%, respectively). As they are above dissociation constant at physiological pH, they have high potential to bind with the protonated amine group of the sericin-coated layer with charge +5.72 mV. Hence, Ibuprofen and diclofenac are easily captured on the membrane surface and show high removal efficiency. Amoxicillin -2.06 mV and Ciprofloxacin 0.34 mV exist in the zwitterionic phase at neutral pH (≈7). However, they have deprotonated carboxyl end (whether anionic or zwitterion) [296] at pH seven and hence can interact with an amine group present on the membrane surface. All of these charged drugs have a carboxylic functional group to form hydrogen bonding with a protonated amine group present on the membrane surface and hence exhibit high removal efficiency. In the case of Steroid hormones, which exist predominantly in uncharged state at neutral pH, the removal efficiency decreases, particularly with β-estradiol showing very low removal. Though the chemical structure of estrone and β-estradiol are almost similar, the presence of ketone group at the C-17 position in estrone, which is an active hydrogen acceptor than hydroxyl group present in β-estradiol may result in better interaction via HB [292]. The presence of a carboxyl functional group (a strong hydrogen acceptor) in ibuprofen, diclofenac, amoxicillin, and ciprofloxacin facilitates better adsorption via hydrogen bonding with amide groups on the membrane surface, otherwise lacking in estrone and β-estradiol. The proposed HB of drug particles with membrane surface is shown in Appendix Figure A10, A11, and A12.

Drug Solution	Image	Contact-angle	Zeta Potential Charge
Ibuprofen	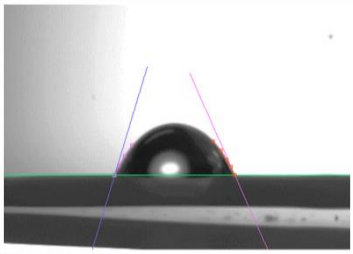	70.83-62.92	-5.74mV
Diclofenac	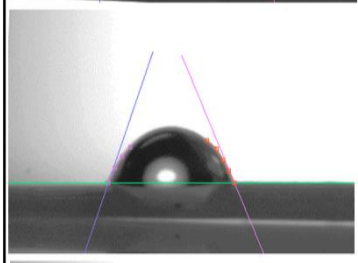	68.41-64.29	-5.65mV
Amoxicillin	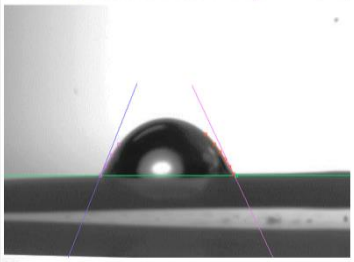	65.49-61.54	-2.06 mV
Ciprofloxacin	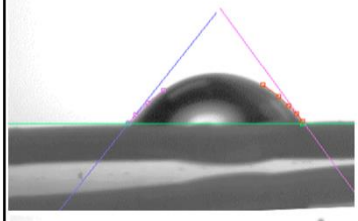	53.97-56.20	0.34 mV
Estrone	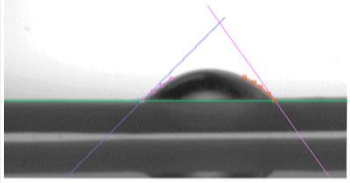	46.90-56.20	-0.06 mV
B-estradiol	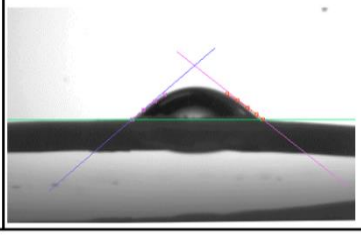	40.64-38.17	0.07 mV

Figure 6.4. Contact angle measurement on the sericin-coated membrane and zeta potential of different drug solutions in water (the contact angle of sericin coated HFMF membrane with pure water is 38°).

6.4.3. *Effect of background salt interaction on drug removal*

The influence of background salts on drug removal efficiency of the sericin-coated membrane was investigated using common salts (monovalent and divalent) found in water. Experiments were performed using three different salts: NaCl (monovalent), $CaCl_2$, and $MgSO_4$ (divalent) dissolved at 100 mg/l strength with one drug from each class (Ibuprofen, Amoxicillin, and Estrone) and compared with a standalone drug case. *Figure 6.5*a shows the effect of salts on the removal of Ibuprofen from aqueous solution. The presence of salt resulted in an earlier appearance of Ibuprofen in permeate (i.e., after 1250 ml) with the volume of solution filtered, which was 1750 ml without salt, except NaCl. The reduction in removal efficiency may have happened because of the screening effect of salt on the membrane surface, where charged ions may have accumulated around opposite charge sites on the membrane surface and thereby obstructing binding sites for drug particles.

Similar results were observed for Amoxicillin, too, where divalent salts exhibited an inhibitory effect on removal efficiency, which eventually resulted in the early appearance of Amoxicillin in permeate. Amoxicillin can form complex with divalent ions (i.e., Ca^{2+}, Mg^{2+}), and hence, its removal was found to be affected by the presence of background divalent salt (*Figure 6.5*b). Pre-binding of salt to the deprotonated carboxylic end of amoxicillin must have inhibited interaction with the amide group of the coated membrane surface.

However, the presence of divalent cations exhibited poor removal efficiency for Estrone, and almost no removal was noticed (*Figure 6.5*c). Estrone at neutral pH is un-dissociated, and only polar moieties contribute to its charge distribution within the molecule. It mostly exists as a hydrophobic but an ionizable group. Hydroxyl and carbonyl functional groups present in Estrone facilitate the formation of weak hydrogen bonding between the molecule and the membrane surface, which was further disturbed in the presence of salt. Therefore, the presence of counter-ions in the solution must have partially screened the bonding of these functional groups with the membrane surface. Sodium chloride did not show any inhibitory effect on the adsorption of drugs in all three cases.

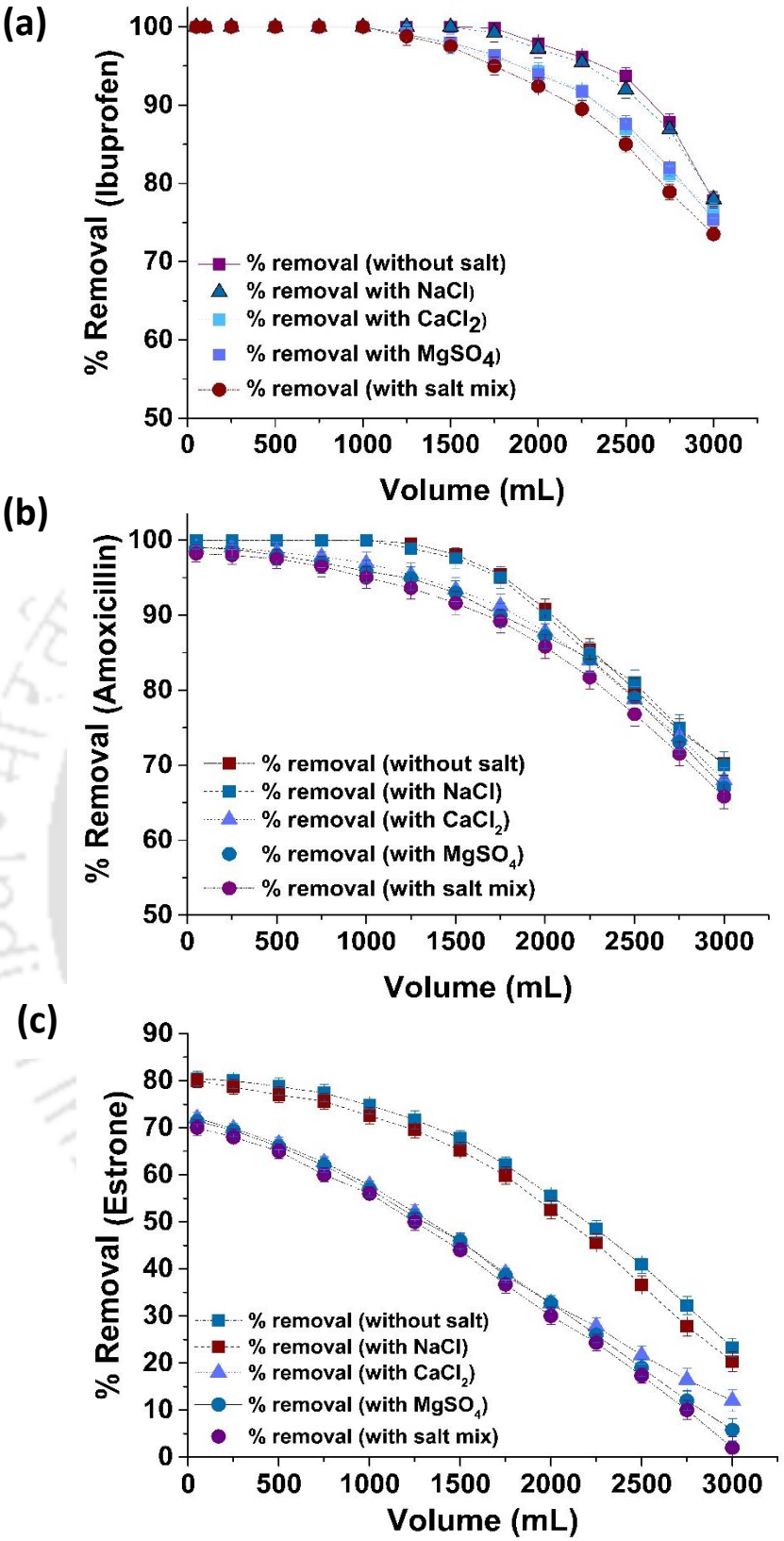

Figure 6.5. Influence of different salt (100 mg/l) on the removal of drugs by sericin coated HFMF membrane (a) Ibuprofen (500 µg/l), (b) Amoxicillin (500 µg/l) (c) Estrone (500 µg/l), operated at pH 7, under gravity flow and temperature 30°C.

6.4.4. *Effect of interaction between drugs*

The behavior of a multi-drug mixture is expected to be entirely different and complicated than in standalone condition, and its study is mandatory for further application. The removal efficiency of the sericin coated HFMF membrane for the individual drug in the presence of other drugs are studied at a concentration of 20 µg/l and 100 µg/l for each drug (*Figure 6.6*a-b). The adsorption of drugs on the membrane surface involves molecular interaction, which includes ionic interaction, dipolar interaction, ion-dipole interaction, and hydrogen bonding. In a multi-drug mixture, all the drugs have a bipolar functional group such as hydroxyl, carboxylic, and/or amine groups, which may interact with each other via hydrogen bonding. The interaction among the drugs and between drug and membrane will play a major role in multi-drug mixture removal. *Figure 6.6*b presents interesting results where, except for β-estradiol, removal of all selected five drugs is found to be very high and efficient. At higher concentrations, as expected, when multi drugs particles compete for sorption at the same site on the membrane surface, the sorption of each drug was less than that in the single-solute system. In low concentration experiments, all selected drugs were removed entirely in a 3-liter filtration cycle except β-estradiol. While at high concentration (100 µgl-1/solute), the interaction was high, and hence the relative adsorption between drugs to membrane inhibited the overall drug removal efficiency. The removal capacity follows the sequence; Ibuprofen > Diclofenac > Amoxicillin > Ciprofloxacin > Estrone > β-estradiol, showing the role of charge-based interaction and hydrogen bonding as the main mechanism behind the removal. Since the level of reported concentration for most of the antibiotics, analgesic and steroid drugs lies in the range of ~1-20 µg/l (see Table 3-*2*), the sericin-coated HFMF membrane is well equipped to address the real-time drug contamination in drinking water.

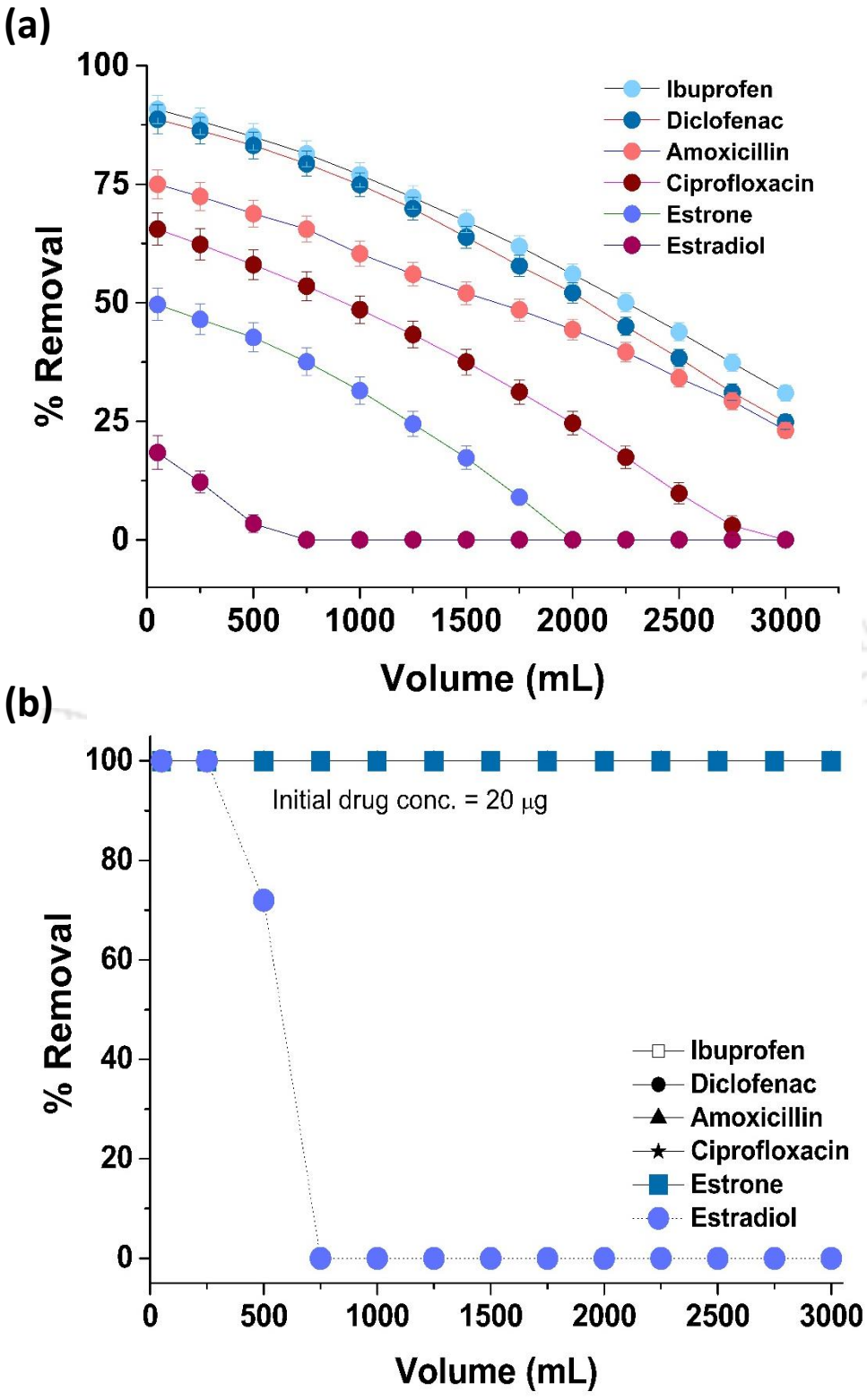

Figure 6.6. Removal efficiencies of the drug from aqueous mixed drug solution using sericin coated HFMF membrane (a) at an initial feed concentration of 100 µg/l for each drug (b) at an initial feed concentration of 20 µg/l for each drug, operated at pH 7, under gravity flow and temperature 30°C.

6.4.5. *Membrane regeneration*

For membrane regeneration, the used sericin coated membrane was washed with a different cleaning solution to test for the desorption of drugs. As aforementioned, the adsorption of drugs on the membrane surface is highly influenced by charged based interaction and is endothermic. Hence, altering the pH and temperature of the stripping solution can facilitate the desorption of drugs from the membrane surface. The used sericin-coated membrane was washed using an acidic solution (0.01N HCl; pH 3), an alkaline solution (0.01 M NaOH, pH 11), hot water (40 °C) and cold water (10 °C) to remove adsorbed drugs. Maximum drug desorption was observed when used membrane is cleaned with an alkaline solution (94.38%). Coldwater (36.71%), Hot water (23.84%) and acidic solution (7.24%) were not very efficient in the dissociation of adsorbed drugs (see *Figure 6.7*). The membrane was re-tested for its adsorption efficiency and > 90% efficiency was noticed. However, the high NaOH concentration used for stripping resulted in the denaturation of few binding sites on the sericin coated membrane. Therefore, the optimization of NaOH concentration may help to reduce the impact of sericin protein denaturation and can be taken as a future study.

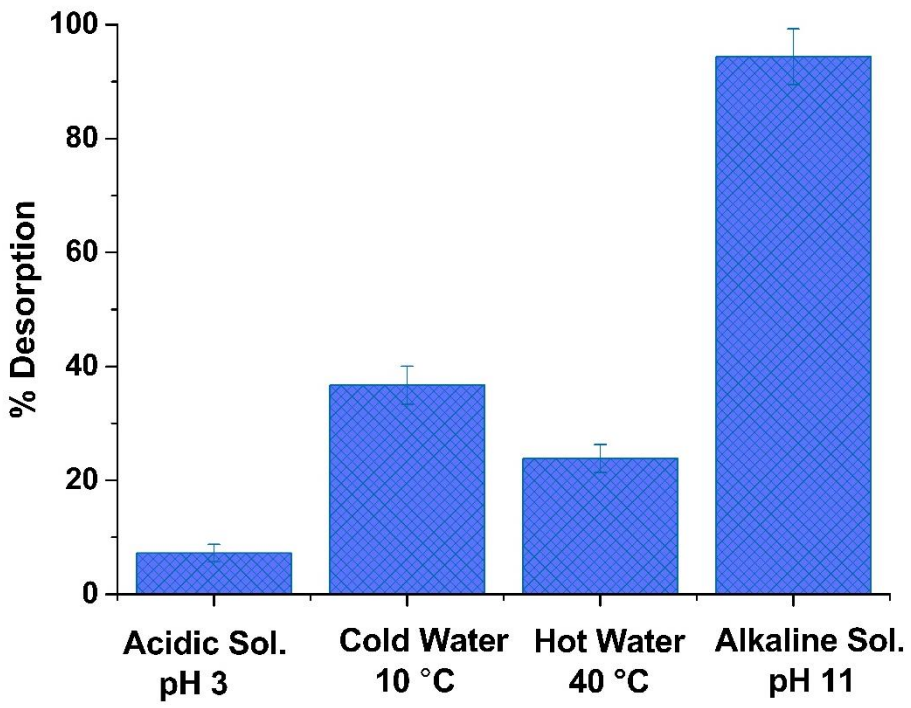

Figure 6.7. The effect of stripping solution on drug desorption efficiency from the membrane surface.

Modeling for drug adsorption

The adsorption behavior for each drug on the sericin-coated HFMF membrane was evaluated using different breakthrough curve models (i.e., Bohart-Adams, Thomas, Yoon-Nelson, and Clark model). *Figure 6.8a* shows the breakthrough curve obtained for adsorption of selected drugs on the sericin-coated HFMF membrane at a fixed initial feed concentration of 500 µg/l, temperature 30°C, and 5 l/h flow rate. The breakthrough time (C_p/C_f =0.05) and exhaust time (C_p/C_f = 0.9, time after which adsorbent can no longer remove sorbate molecules) for the different drugs are shown in *Figure 6.8a*. The evaluated parameters for breakthrough curve fitting using Thomas, Yoon-Nelson, and Clark models are presented in *Table 6-1*. The Bohart-Adams model provided the best fit with the obtained experimental data for the breakthrough curve with a high correlation coefficient and low average percentage error (see *Table 6-2*). This rectangular isotherm assumes that initially, there is no adsorbate (drug) on the adsorbent surface (sericin layer of MF membrane), while with time, the drugs occupy the membranes binding sites on the surface. Thus, it relates to monolayer adsorption on the membrane surface with the first-order reaction. The adsorption of drugs takes place via chemical bonding between the membrane surface and adsorbate. As in the present case, binding of drugs on membrane surface mainly involves intermolecular forces, i.e., hydrogen bonding between drug and amide groups present on the membrane surface. The K_{BA} value of different drugs was found in the following decreasing sequence; Ibuprofen > Diclofenac > Amoxicillin > Ciprofloxacin > Estrone > β-estradiol (*Table 6-2*). This is based on the binding affinity of each drug with the sericin-coated membrane surface, as explained in the previous section. It shows that the adsorption was more favorable in the case of NSAID (Ibuprofen and Diclofenac), followed by antibiotics, i.e., Amoxicillin and Ciprofloxacin and was comparatively least favorable in case of steroids (estrone and β-estradiol). Owing to which, the maximum adsorbed amount (q_e) decreased for least favored steroids drugs followed by antibiotics, while maximum adsorption was observed for NSAIDs. Fixed bed studies were performed at a different flow rate of 5, 10, 15, and 20 l/h for Ibuprofen as a model drug at an initial feed concentration of 500 µg/l, pH 7, and at 30°C, (other column parameters were kept fixed). *Figure 6.8*b shows the breakthrough curve for adsorption of Ibuprofen at a different flow rate. At a high flow rate, because of low residence time, the drug particles had less time for interaction, and hence breakthrough time and saturation time decreases. *Table 6-1* shows that as the flow rate is increased, the

value of K_{BA} increases, and the value of q_e, decreases. Since at high flow rate, the high rate of mass transfer and availability of drug particles were high, which leads to faster saturation, and hence, the K_{BA} value increased. While with quick saturation, the driving force decreased gradually, and hence, the q_e value was found to decrease. Whereas, at a low flow rate, the drug particles had more time to interact with the membrane surface and hence resulted in high removal of drugs (i.e., q_e). *Figure 6.8*c shows the breakthrough curve for adsorption of ibuprofen at different initial feed concentration for Ibuprofen. The breakthrough time decreased at a higher concentration as binding sites were quickly saturated. *Table 6-1* shows that as the initial feed concentration increases, the value of K_{BA} is reduced while the value of q_e increases. An increase in feed concentration leads to a greater concentration gradient, which reduces the adsorption rate coefficient. While due to more availability of drug particles on the membrane surface at higher concentration results in better uptake of drug solutes per unit mass of absorbent. Similar trend results have been reported earlier for fixed-bed adsorption of pollutants [293,294,297].

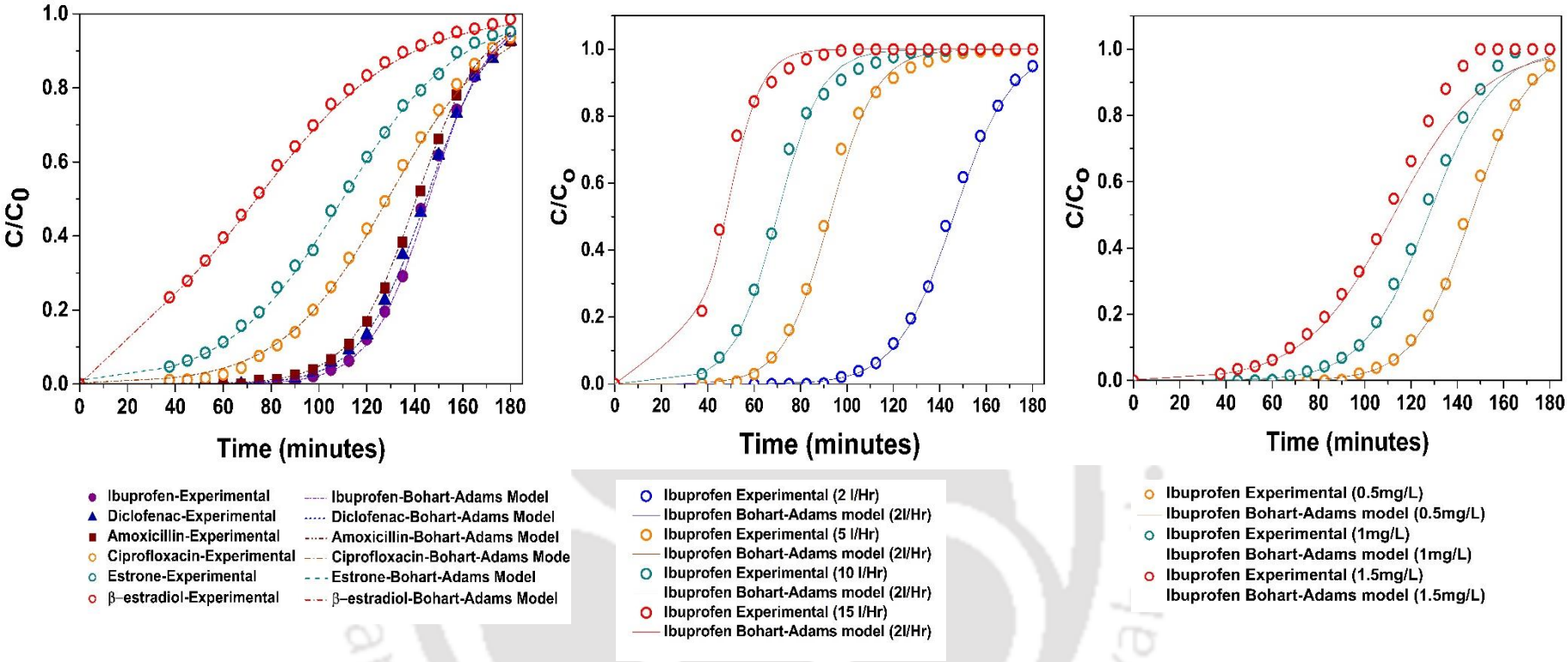

Figure 6.8. Packed bed breakthrough curve and Bohart-Adams model prediction for (a) adsorption of selected drugs at 5 l/h flow rate and 500 µg/l initial feed conc. (b) effect of flow rate (5, 10, 15, 20 l/h) on ibuprofen adsorption (c) effect of feed concentration (500, 1000, 1500 µg/l) on ibuprofen adsorption in sericin coated HFMF bundle.

Table 6-1. Model parameters for Thomas, Yoon-Nelson and Clark model under various operating conditions and using different drugs

	Parameters		Thomas model			Yoon-Nelson model			Clark Model		
Drug Name	**C_0 µg/L**	**Q (l/hr)**	**K_{Th} ($mlmg^{-1}min^{-1}$**	**qe (mg/g)**	**R^2**	**K_{YN} (1/min)**	**τ (min)**	**R^2**	**A**	**r (1/min)**	**R^2**
Ibuprofen	500	5	0.0027	0.24	0.98	0.089	145	0.93	0.080	11.39	0.97
	500	10	0.0033	0.15	0.97	0.083	96	0.95	0.078	7.22	0.96
	500	15	0.0034	0.11	0.97	0.079	72	0.96	0.076	5.12	0.96
	500	20	0.0043	0.07	0.98	0.102	45	0.95	0.099	4.33	0.96
	1000	5	0.0025	0.21	0.97	0.085	120	0.95	0.078	9.21	0.97
	1500	5	0.0021	0.18	0.98	0.060	105	0.96	0.054	5.42	0.97
Diclofenac	500	5	0.0025	0.24	0.93	0.073	142	0.92	0.067	9.34	0.96
Amoxicillin	500	5	0.0024	0.24	0.98	0.071	140	0.95	0.647	8.81	0.91
Ciprofloxacin	500	5	0.0016	0.21	0.98	0.051	125	0.90	0.046	5.59	0.94
Estrone	500	5	0.0013	0.18	0.98	0.042	106	0.93	0.039	3.96	0.93
β-estradiol	500	5	0.0011	0.12	0.96	0.035	72	0.95	0.034	2.23	0.90

Table 6-2. Bohart-Adams model parameter with respect to drugs feed flow rate and concentration

Drug Name	K_{BA} ($m^3mg^{-1}s^{-1}$)	qe (mg/g)	C_0 (µg/L)	Q (l/h)	R^2	% Error	BT_{time} (minutes)	$Exhaust_{time}$ (minutes)
Ibuprofen	0.0027	0.62	500	5	0.93	5.94	112.5	172.5
	0.0032	0.58	500	10	0.98	2.31	52.5	120
	0.0034	0.55	500	15	0.96	3.09	37.5	97.5
	0.0041	0.50	500	20	0.95	3.86	37.5	67.5
	0.0025	0.66	1000	5	0.91	7.18	60	150
	0.0020	0.69	1500	5	0.93	9.42	37.5	135
Diclofenac	0.0024	0.61	500	5	0.93	5.45	105	172.5
Amoxicillin	0.0024	0.50	500	5	0.94	5.03	105	172.5
Ciprofloxacin	0.0015	0.46	500	5	0.93	5.52	67.5	165
Estrone	0.0013	0.27	500	5	0.99	1.33	37.5	157
β-estradiol	0.0011	0.13	500	5	0.98	2.19	37.5	142

R^2=1-(SSE/SSTO) where, SSR=Regression sum of squares, SSE=Error sum of squares and SSTO=Total sum of square (i.e. SSR+SSE), Error = $\frac{(\text{Experimental value} - \text{Theoretical value})}{\text{Theoretical Value}}$

6.4.6. Membrane fouling resistance

Membrane fouling resistance to synthetic greywater solution was studied through normal filtration and backwash cycle employing uncoated, and sericin coated HFMF membrane. Fouling behavior was evaluated in terms of flux decline and changes in permeate turbidity. The single HFMF membrane was used throughout the process in each case.

6.4.6.1. Filtration of greywater

The performance of uncoated and sericin coated membrane was evaluated and compared by filtering synthetic greywater under the same initial permeate flux of 28 l/m^2h. *Figure 6.9*a shows the time-dependent normalized flux of uncoated and sericin coated membrane during 500 liters of greywater filtration in 10 cycles with a 2-minute backwash after each 50-liter cycle**.** A partial recovery of membrane flux is seen immediately after each backwashing step. As expected, calcium influences the rate of flux decline and the reversibility of fouling after backwashing. As the operation cycle is increased, flux recovery after backwashing is reduced, which indicates the formation of more cohesive

gel layers on the membrane surface, and irreversible fouling is observed. Also, the observed flux decline can be attributed to the fact that aggregates may form a cake on the membrane surface with relatively high permeability.

It was found that the sericin coated membrane had comparatively 15% less fouling than the uncoated membrane indicating the sericin coated membrane can mitigate the surface deposition of foulants (Ca^{2+} and detergent additives) and thereby improving the fouling resistance. The sericin coated membrane surface exhibited a positive surface zeta potential of 5.72 mV at pH 7 and +1.54 mV at pH 9.5. While the uncoated polypropylene membrane was neutral and had a surface zeta potential of +0.44 mV to -0.22 mV. The amine groups (NH_2) present on the sericin coated membrane surface exist in the protonated form (NH_3^+) at neutral pH when it is exposed to water [298]. However, the surface charge reduced to +1.54 mV at pH 9. This must have happened because the major amino acids (serine, glycine, aspartic acid, threonine, and alanine) [299] that contribute to sericin have pKa (carboxyl) in the range of (2-2.63); and pKb (amino) in the range of (9.15-10.43) [300]. Hence at pH 9.5, a portion of mole fraction (≈50%) of these amino acids still exist as zwitterion and hence acid form (≈25% in NH_3^+ state) while the rest exist in conjugate base (NH_2) neutral form (≈50%) [301]. Therefore, the positive charge reduced (by almost ≈73%) on the membrane surface as pH increases. The presence of positively charged amine groups on the membrane surface must have assisted in repelling divalent calcium ion (2.25mM) and deposition (zeta potential of greywater foulant particles +7.95mV) of foulants. The higher rate of flux decline indicates that comparatively sever fouling has happened with the uncoated membrane. The mitigation of membrane fouling is mainly due to the improved surface hydrophilicity, modified surface morphology. Permeate turbidity was decreased by more than 80%, and hence, better removal capacity was observed for sericin coated MF membrane, though there was not a very noticeable change in TDS after filtration. The reduced turbidity is observed mainly due to reduced pore size with sericin coating (*Figure 5.12*), and hence the sericin coated membrane was able to remove turbidity more efficiently and improve separation. *Figure 6.9*b clearly shows the advantage of the sericin coated membrane by producing more volume (around 30 liters) of treated greywater than the uncoated membrane at the same interval of time. Moreover, the rate of flux decline was also comparatively less in sericin coated membrane due to the mitigation of foulant deposition on the membrane

surface. The further detailed analysis is performed based on reversible and irreversible fouling percentage.

$$Irreversible\ fouling = \frac{J_0 - J_1}{J_0} \quad (6.2)$$

$$Reversible\ fouling = \frac{J_1 - J_2}{J_0} \quad (6.3)$$

Where J_0 is pure water flux of new membrane, J_1 is pure water flux after each backwash, and J_2 is pure water flux of the fouled membrane at the end of each cycle.

The cleaning results in *Figure 6.9*c shows that the membrane fouling was reversible and can be cleaned by a physical method. The reversible and irreversible fouling for greywater filtration was found to reduce by 30% and 83% for sericin coated membrane in comparison to the uncoated membrane. After 500 liters of the filtration cycle, the fouled membrane was subjected to chemical cleaning with 0.01M NaOH solution. Sodium hydroxide reacts with calcium chloride to form solid calcium hydroxide precipitate and soluble sodium chloride (which was quickly washed away by flushing with pure water). Flux recovery with chemical cleaning for sericin coated and the uncoated membrane was 99.5% and 97%, respectively. Sodium hydroxide was found to be very effective at cleaning of greywater fouled sericin coated PP HFMF membrane. Both physical and chemical cleaning methods provided better flux recovery with sericin coated membrane than the uncoated membrane, showing the antifouling effect of hydrophilic sericin coating on the membrane.

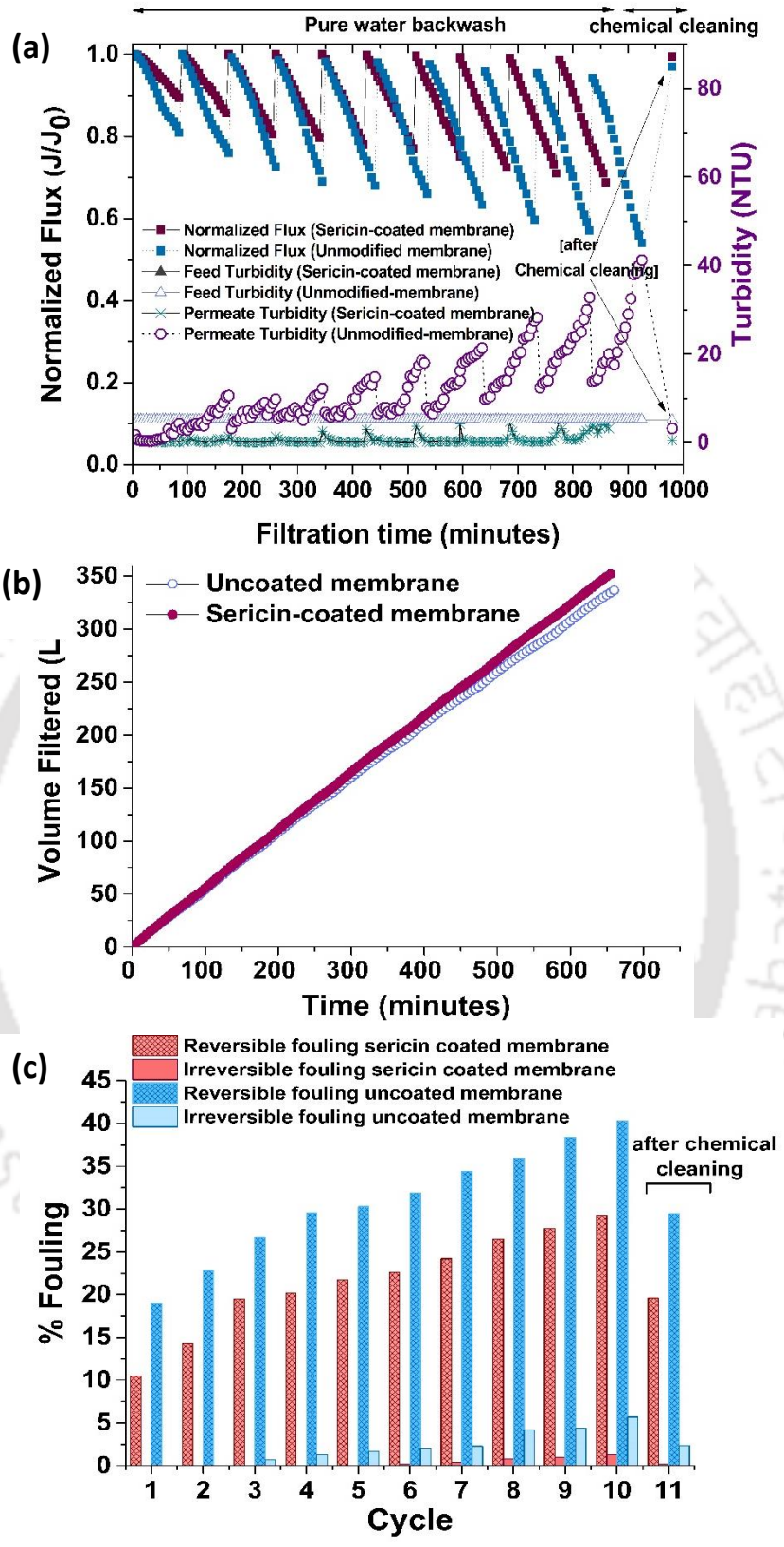

Figure 6.9. Life cycle study of sericin coated filter for greywater filtration (a) Permeate flux and turbidity (error on normalized flux is ±1.04%) (b) Volume filtered (c) Reversible and Irreversible fouling for sericin coated and uncoated HFMF membrane.

6.4.6.2. Filtration of produced water

Once the sericin coated membrane exhibited satisfactory performance with greywater, the membrane was then tested with produced water (PW) to assess its ability to address the different natures of foulants. *Figure 6.10* shows the performance of the sericin coated HFMF membrane with PW. The sericin coated membrane was found to be very effective in treating PW with respect to the uncoated membrane. The permeate water characteristics (*Table 6-3*) were well below the range specified for treated water reuse by governing authorities [302]: pH (7.0), Conductivity (<250 ppm), COD (< 43 mg/l), BOD, (< 6.8 mg/l), SS (completely removed), TDS (< 112 ppm), turbidity (< 5 NTU), and oil content (<0.044 mg/l).

Table 6-3. Characteristics of produced water after membrane treatment

Sl. No.	Parameters	Uncoated	Sericin coated
1.	Conductivity	378 µS/cm	217 µS/cm
2.	TDS	195 ppm	112 ppm
3.	Turbidity	5-26 NTU	<5 NTU
4.	COD	60-73 ppm	32-43 ppm
5.	BOD	9.3 ppm	6.8 ppm
6.	pH	7.3	7.0
7.	Oil content (HEM)	0.438 mg/l	0.044 mg/l

The fouling studies show that during 350 liters of filtration in seven cycles, the sericin coated membrane exhibited 10.5% less fouling than the uncoated membrane. The response of the sericin-coated membrane towards pure water backwash was more effective, and the flux recovery was more than the uncoated membrane. *Figure 6.10*b shows that around 17 liters of more volume was filtered with sericin coated membrane during the same interval of time. *Figure 6.10*c shows the irreversible and irreversible fouling during PW filtration. In comparison to the uncoated membrane, the irreversible and reversible fouling reduced by 66% and 21%, respectively, for the sericin coated membrane.

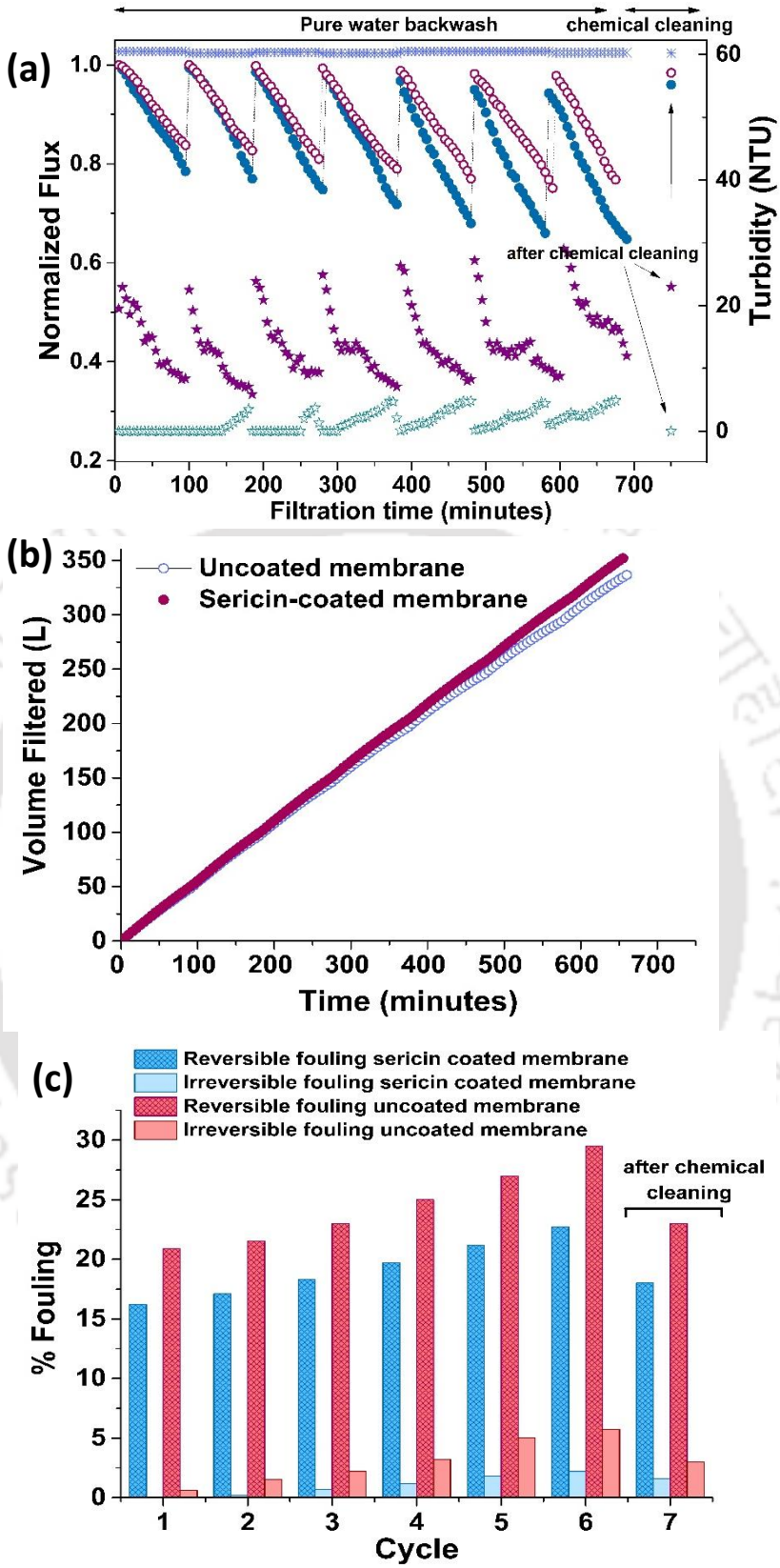

Figure 6.10. Life cycle study of sericin coated filter using produced water filtration (a) permeate flux and turbidity (error on normalized flux is ±1.40%) (b) Volume filtered (c) Reversible and Irreversible fouling for sericin coated and uncoated HFMF membrane.

After 350 liters of the filtration cycle, the membrane was cleaned with 0.1 M solution of sodium hydroxide with 96% and 98.4% flux recovery for uncoated and sericin coated membranes. The irreversible fouling in the case of produced water was more on the uncoated membrane because of the permanent deposition of foulants on the hydrophobic membrane surface. While the hygroscopic nature of the sericin coated membrane prevented deposition of oil-based foulants on the membrane and hence exhibited comparatively better flux throughout the operation.

6.5. Conclusion

In this study, the modified PP-HFMF membrane was assessed for its potential to remove drug-based micropollutants from a single and multi-component aqueous solution. It was found that the adsorption of drug particles on to active protein layer plays the main role in the removal of drugs. Complete removal was noticed at lower concentrations (100 µg/l); however, the removal efficiency reduced with an increase in drug concentration. The adsorption behavior was studied using the Bohart-Adams model to predict the dynamic behavior of the HFMF membrane module fitted in housing. The desorption study revealed that the protein layer could be regenerated for reuse of membrane using a cold alkaline solution. Membrane re-usability was tested for five cycles with six different drugs, and the membrane was found to be effective for multiple cycles. The interaction effect of background salt and mixed drug scenario was studied. The adsorption mechanism was highly influenced by charged based interaction and hydrogen bonding resulting in less removal of uncharged drugs compared to anionic drugs. In a multidrug mixture, the removal efficiency for different selected drugs follows the sequence; Ibuoprofen>Diclofenac>Amoxicillin>Ciprofloxacin>Estrone>β-estradiol. The study reveals that the sericin-coated membrane can be used for target-specific removal of drug-based micropollutants.

During fouling resistance experiments, 15% less fouling was noticed for the sericin coated membrane, and more than 90% turbidity removal was observed for the greywater purification application. While with produced water, the sericin coated membrane exhibited 10.5% less fouling, and more than 65% turbidity was removed during filtration. The pure water backwash was quite effective in mitigating reversible fouling for sericin coated membrane and hence filtered more volume of water than the uncoated membrane in the same timeframe. Flux recovery for both physical and chemical cleaning methods

shows a better result with sericin coated membrane. Hence, considering the obtained results, it is conclusive that sericin coated membrane is quite promising for mitigating membrane fouling by imparting hydrophilicity together with excellent separation efficiency for greywater purification application.

Chapter 7

Sericin-coated polymeric air filter for air purification

Parts of this Chapter are published as research articles:

- V.K. Verma, S. Subbiah, S.H. Kota, Sericin-coated polyester-based air-filter for removal of particulate matter and volatile organic compounds (BTEX) from indoor air, Chemosphere. 237 (2019). doi:10.1016/j.chemosphere.2019.124462.

7.1. Theoretical Consideration

The most often used material for air filtration includes woven/nonwoven fibers, Polyester pleated filters, nano-fibers, and fiberglass [166,303,304]. The HEPA and ULPA filters are made of thin glass fiber woven into a paper-like material that is pleated to achieve high surface area per unit volume of the filter module [305]. Due to dense packing, the HEPA filter requires a higher power blower to get sufficient airflow through the filter, and since HEPA filters are not washable and not recommended to reuse [305]. Recently hybrid fabrics like bi-component, nano-fiber, melt-blown media, etc., have been used for fabricating air-filters as they provide better strength than HEPA filters and offer high air permeability for the lowest pressure drop [306]. A bi-component polyester has multiple types of polymer with different desired characteristics, which can be further modified via surface modification. The use of polyester for fabricating air filter offers specific merits like required permeability, better particulate matter (PM) collection efficiency, low-pressure drop, cost-efficient, stiffness to get optimal pleat, and are easy to modify the surface properties [307,308]. Polyester fabric is widely used in the air-filtration process due to its maximum working temperature and very high abrasion resistance, complicated structure, and thickness [304]. Air filter cleaning and its reuse may enable low-cost green technology in the air purification sector. However, the cleaning and filter regeneration is not recommended for the HEPA filter. Because such activity may lead to permanent damage to the HEPA filter surface. The hydrophilicity has been related with antifouling character of the filter, the possibility of rendering hydrophilicity on the polyester surface may resist foulant deposition and impart easy cleaning possibility.

sericin is a hydrophilic biopolymer [108,309], and they provide the additional benefit of antimicrobial and antifouling properties [105]. Sarovart et al. (2003) [165] used sericin for the coating of nylon and polyester fiber for providing antibacterial and antifungal properties. Purwar et al. (2016) [166] used a blend of sericin/Polyvinyl alcohol (PVA)/ to make nano-fibrous mats through electrospinning technique. The antimicrobial air filtration mask worked well for filtration (i.e., filtered concentration 0.725 mg/m^3/s) of particulate matter of size ~1 micron and had antimicrobial properties. The affinity of sericin towards drug-based organic compounds phenolic groups have been established in earlier chapters, and hence it is discernible to assume they may have an affinity towards other similar aromatic compounds as well. Hence this study, a simple dip-coating method, has been used to coat sericin on a bi-component hybrid polyester mesh fabric, which can

facilitate the adsorption of volatile organic compounds together with the size-based exclusion of particulate matter.

7.2. Hypothesis

The polyester-based filter can be used in air purification application, and it can be washed with cleaning agents for regeneration. But the separation efficiency of the standalone polyester-based filter is observed to be very low. Therefore, the surface modification of filter fabric can improve removal efficiency, provide easy washing, and subsequently enhance the performance of the filter. Moreover, the presence of multi-functional groups in sericin can be harnessed to capture volatile gases like BTEX.

7.3. Result and Discussion

7.3.1. Sericin coated Air-filter Characterization

7.3.1.1.FESEM Analysis

FESEM analysis of polyester sheet before sericin coating and post-coating was analyzed to ascertain coating and study morphological changes imparted. *Figure 7.1*b and *Figure 7.1*d clearly shows the sericin deposition on coated polyester fabric. Moreover, after sericin deposition, the fiber diameter has increased (see *Figure 7.1*a-d). The average width of each fiber (denoted as "Pa" in FESEM images) before coating as shown in *Figure 7.1*a (i.e., Pa1=14.32, Pa2=14.48, Pa3=14.26, Pa4=14.38, Pa5=13.99, Pa6=13.83, Pa7=14.48, Pa8=14.17) is 14.23 microns. Which evidently increased to 15.73 microns after sericin coating as visible in *Figure 7.1*b (i.e., Pa1=15.03, Pa2=15.99, Pa3=16.15, Pa4=15.52, Pa5=16.50, Pa6=15.61, Pa7=15.46, Pa8=15.61). The FESEM morphology analysis shows warp and weft-knitting patterns in sericin coated bi-component polyester sheet. The sheet was pleated, and the dual-layer was placed in the filter module. The sericin coating on each fiber of bi-component material further assists in easy washing of deposited foulants otherwise not possible in case of HEPA filter. The HEPA-filter has a dense overlapped woven structure (see *Figure 7.1*e and *Figure 7.1*f) which assists in quick removal of PM but at the same time attracts more pollutants deposition, which cannot be cleaned easily and he HEPA filter manufacturer recommends not to clean with liquids instead replace the filter once choked.

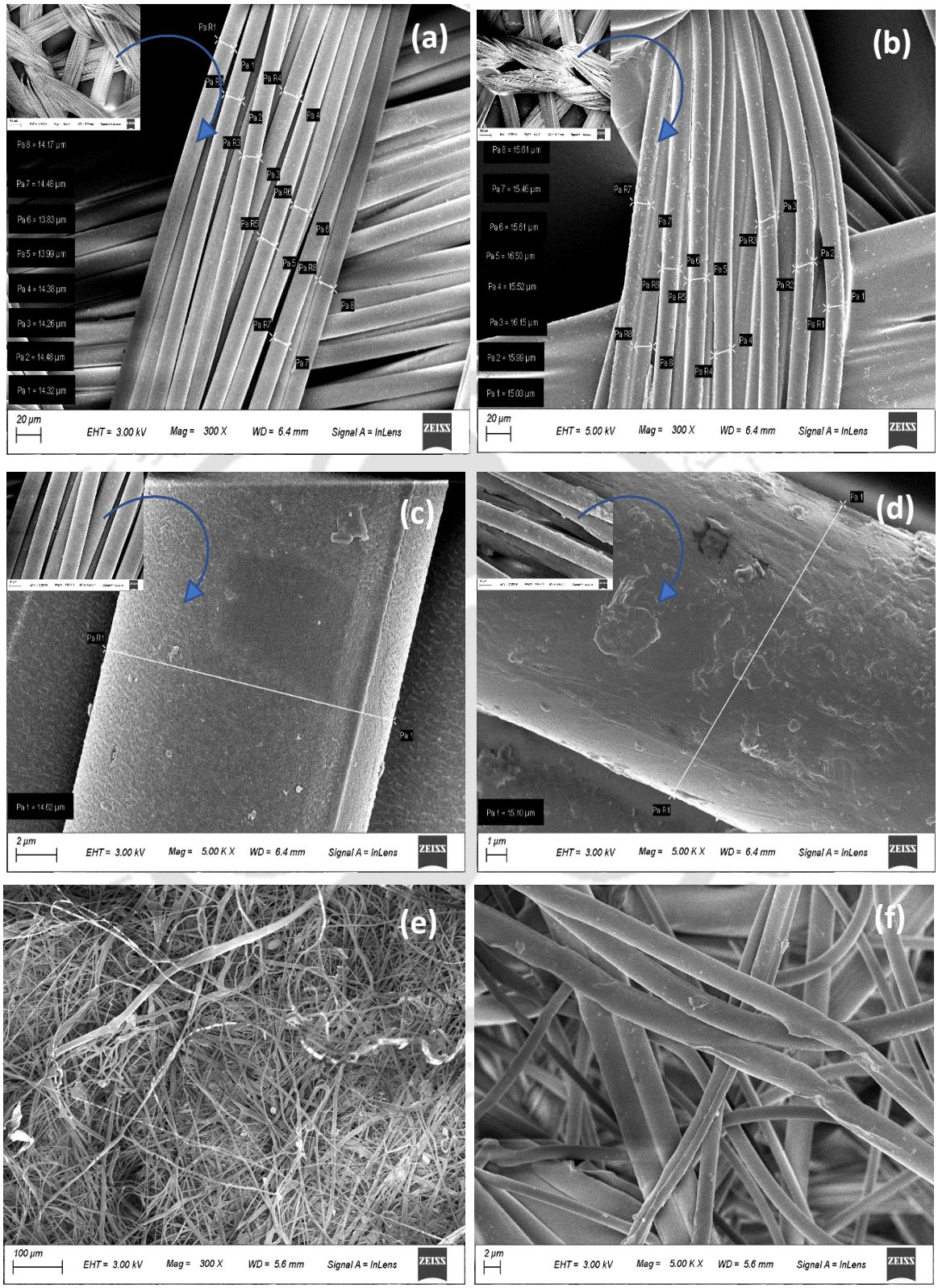

Figure 7.1. FESEM analysis of (a) uncoated polyester sheet at 300X (b) sericin-coated polyester sheet at 300X (c) uncoated polyester sheet at 5KX (d) sericin-coated polyester sheet at 5KX (e) HEPA filter at 300X (f) HEPA filter at 5KX.

7.3.1.2.FTIR Analysis

Absorption bands in the FTIR spectrum of the uncoated polyester sheet (see *Figure 7.2*c) were noticed between 3100–2800 cm^{-1} attributed to C-H stretch, at 2264 cm^{-1} (O-H and C=O stretch), at 1711 cm^{-1} to stretching band of the ester carbonyl group. The band at 1248 cm^{-1} presents C-C vibration, 1096 cm^{-1} (methylene and ester C-O bond vibration), at 850 $cm^{-1,}$ and 709 cm^{-1} to polar ester groups and aromatic ring [310,311].

Additional functional groups were noticed on the polyester sheet after sericin coating on the FTIR spectrum of the sericin-coated polyester sheet (see *Figure 7.2*b). New FTIR peaks originated at position 3614 cm^{-1}, 3680 cm^{-1} (representing amide NH stretch), at 2358 cm^{-1}, 2330 cm^{-1} (for stretching of C=N bonds), 1701 cm^{-1}, 1652 cm^{-1} (for stretching of C–N and bending of $–NH_2$ vibrations). Peaks for amide-type I, II, and III appeared at 1701, 1524, and 1237 cm^{-1} (attributing to sericin coating). Absorption peaks at 1423 cm^{-1} indicate CH_3 stretch, C-OH stretching, at 1088 cm^{-1} for CN symmetric stretching [109].

The FTIR peaks after BTEX adsorption on sericin-coated polyester sheet (see *Figure 7.2*a) appeared at 3017 cm^{-1}(aromatic CH-stretch), 2955 cm^{-1} (toluene alkyl group), 2923 cm^{-1}, 2861 cm^{-1}, 1460 cm^{-1} (ring modes), 1516 cm^{-1} (C-C stretch aromatics), 1019 cm^{-1}, 1090 cm^{-1}, (in-plane CH-bending), 874 cm^{-1}, peaks at 729 cm^{-1}, 697 cm^{-1} attribute to ring bends and CH-wag (adsorbed BTEX gases) of aromatics [312].

7.3.1.3.XRD Analysis

Figure 7.3 shows the XRD pattern of the uncoated polyester sheet and sericin-coated polyester sheet. In the uncoated polyester sheet, three diffraction peaks were observed at 17.67°, 22.78°, and 25.80°. A similar kind of diffraction pattern was noticed for polyethylene terephthalate in earlier studies involving the aminolysis of PET fabric [313]. The XRD profile of the sericin-coated polyester sheet conserved the main diffraction peaks of polyester and found to be almost similar. However, the amorphous nature of sericin reduced the intensity of the three main diffraction peaks post-coating in the polyester sheet.

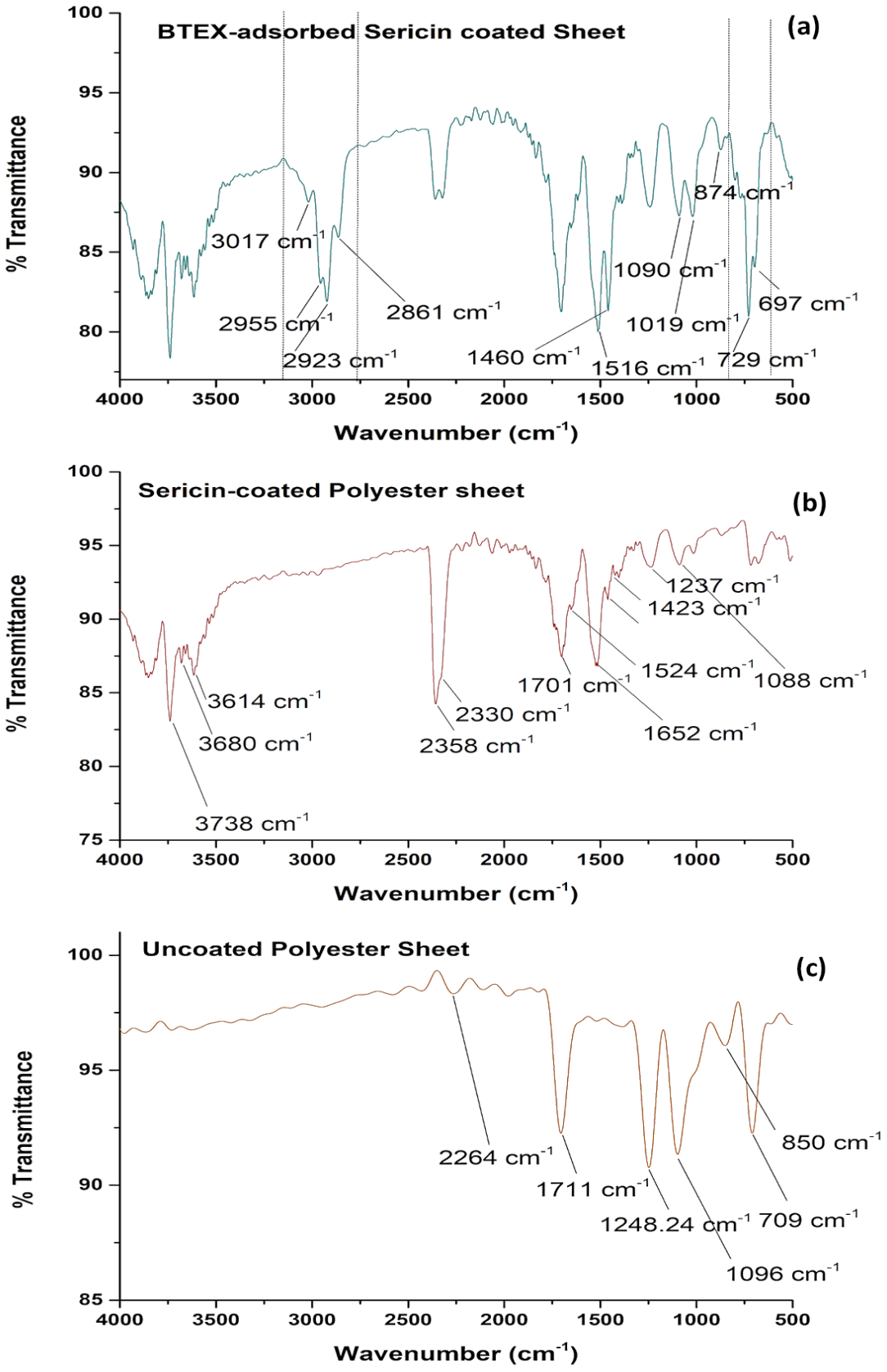

Figure 7.2. FTIR-analysis for (a) BTEX-adsorbed sericin-coated polyester sheet (b) sericin-coated polyester sheet (c) uncoated polyester sheet.

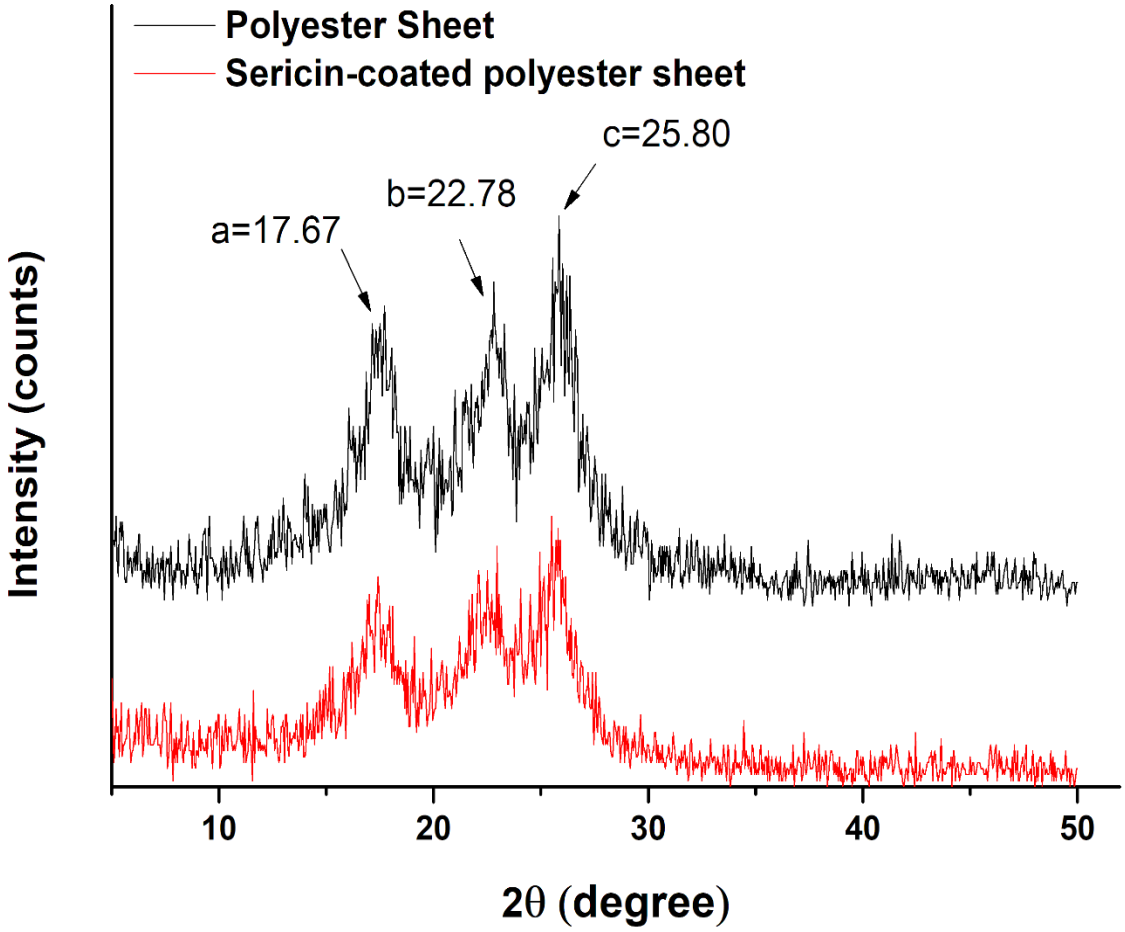

Figure 7.3. XRD-profile for uncoated polyester sheet and sericin-coated polyester sheet.

7.3.2. Air filtration using Sericin coated Air-Filter

7.3.2.1.PM removal through Sericin coated Air-Filter

The particulate matter generated using incenses stick in the closed chamber was filtered using sericin-coated air–filter. Filtration was performed at a different flow rate, and comparative analysis was performed to evaluate its performance with uncoated and HEPA filter. At a low flow rate (145 m^3/h), the filter was more efficient than at a higher flow rate (445 m^3/h). This could be due to a high-pressure drop at an increased flow rate, which leads to a decreased time of contact between PM and air-filter. Also, a high flow rate results in a turbulent condition that may cause decreases in removal efficiency. For complete removal, the sericin-coated air-filter took 26.80, 45.91, 50.88, and 61.8 minutes at 145, 300, 375, and 445 m^3/h of flow rate, respectively (see *Figure 7.4a*). *Figure 7.4b* shows the removal efficiency of sericin coated, uncoated, and HEPA filter.

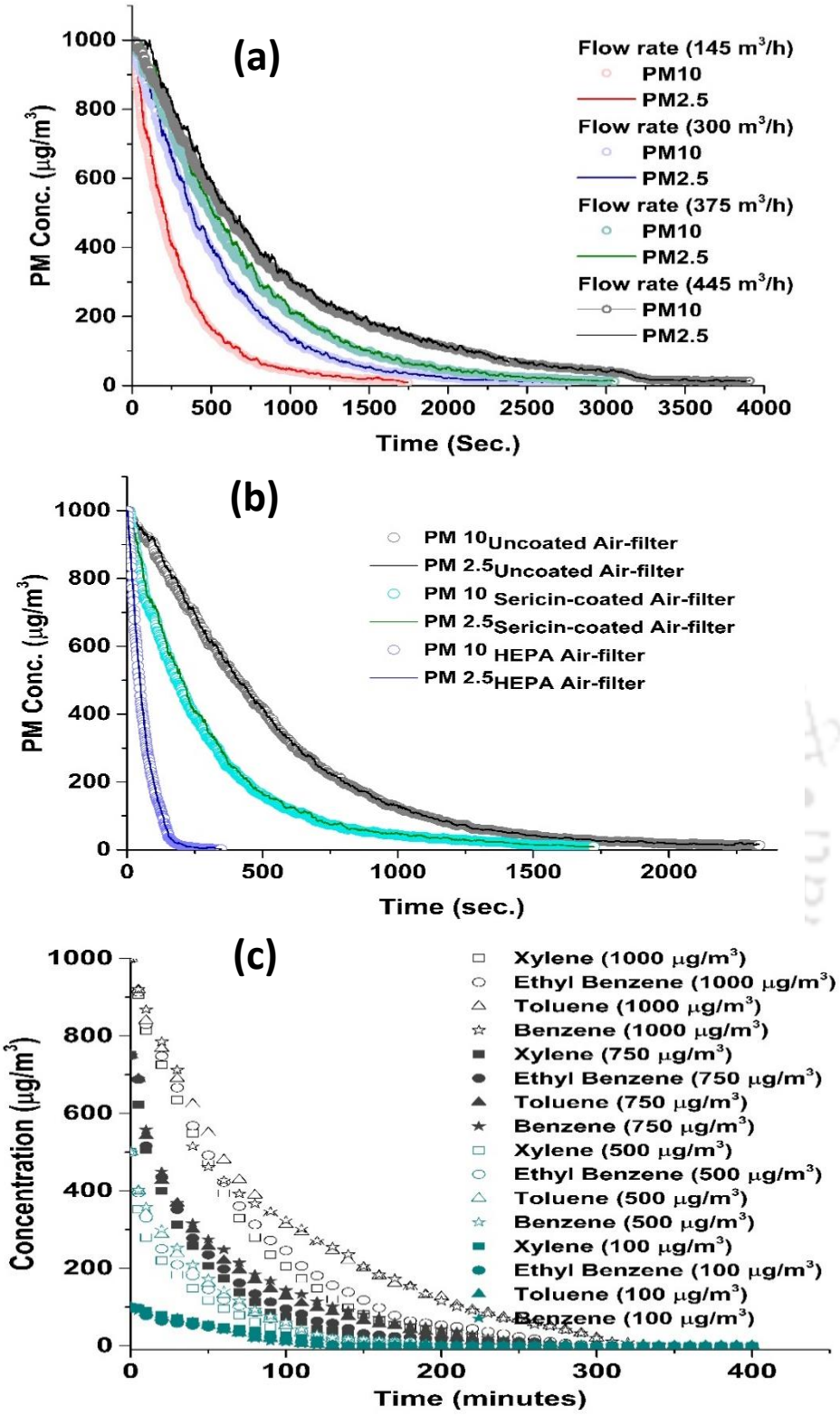

Figure 7.4. PM removal using sericin-coated air filter (a) at a different flow rate (b) comparative performance analysis of sericin-coated air-filter with uncoated and HEPA filter at a fixed flow rate of 145 m^3/h, error = ±2.8% (c) BTEX removal at a varying initial concentration (100, 500, 750 and 1000 μg/m^3) and flow rate of 145 m^3/h (error = 3.65%).

The HEPA filter was able to remove both $PM_{2.5}$ and PM_{10} in 8.5 minutes at 145 m^3/h flow rate, while sericin coated and uncoated air filter took 26.80 minutes and 37.23 minutes, respectively for complete removal. The HEPA filter is found to be highly efficient in comparison to the fabricated filter in terms of time taken for the complete removal of particulate matter.

7.3.2.2.BTEX removal through Sericin coated Air-Filter

The fabricated sericin-coated air-filter was also tested for the removal of VOCs (BTEX) generated using gasoline in the closed chamber. *Figure 7.4*c shows the time-based percentage removal of BTEX gases using fabricated air-filter. The comparative removal of BTEX follows the order Xylene> Ethyl Benzene> Toluene> Benzene (see Table 6.1a-b). It may be a result of a comparative Octanol-air partition (log K_{oa}) coefficient of BTEX gases in air (Xylene>Ethylbenzene>Toluene>Benzene) and low molecular weight, Benzene being the smallest (see appendix Table A1). The filter was found to be very effective at a lower concentration of VOCs (100-1000 µg/m^3), and complete removal was noticed up to 1000 µg/m^3 for all the selected VOCs (BTEX). The sericin-coated air-filter was regenerated after each experiment via washing with pure water, followed by exposure to heat treatment at 50 °C for 3 hours. The regenerated air-filter was reused in the same condition and was found to retain more than 99% efficiency. For comparison purposes, the performance of the HEPA filter for VOC removal is also experimentally studied, and results conclude that HEPA is not capable of removing VOC.

7.3.3. Adsorption Isotherm and kinetics

Three classic adsorption models, Langmuir, Freundlich, and Sips, using non-linear regression, were employed to evaluate adsorption of selected VOCs on sericin-coated air-filter to describe adsorption equilibrium. The Langmuir model relates to monolayer adsorption on the adsorbent surface containing a finite number of identical binding sites with the assumption of the homogeneous surface without interaction between adjacent adsorbed particles [314]. The Freundlich isotherm refers to multilayer adsorption on heterogeneous surface assuming binding depends on whether or not the adjacent sites are already occupied [315]. The Sips isotherm is a combination of both isotherms, which is used for protein-ligand interaction [316]. This model provides a better explanation with a system involving a heterogeneous surface with adsorption cooperativity. The value of n_s provides the extent of cooperativity involved in the binding interaction [316]. The non-

interacting purely independent sites exhibit a value of n_s=1. Positive cooperativity is expected when n_s>1 and when 0<n_s<1 negative cooperativity is proposed in binding. The adsorption isotherm parameters obtained for all three applied models are presented in *Table 7-1*a. All three models depicted different fittings for the adsorption data of VOCs on the membrane surface (*Figure 7.5*). The Sips model provided the best fit based on R^2 and χ^2 values for all cases. Also, the obtained Q_m is closer to experimental data with the Sips model. *Figure 7.5* shows the non-linear fits to the Sips model for the drug adsorption isotherms on the sericin coated membrane. For the Sips model, the Q_m (mg/g) values were 6.978, 5.688, 5.357 and 4.780 for Xylene, Ethyl Benzene, Toluene and Benzene, respectively. For all the cases, the value of n_s is found to be positive and lies between 1-2, implying positive cooperativity and heterogeneous adsorption. Cooperativity during adsorption arises from multi-functional groups resulting in multiple interactions. Both the sericin coated air-filter surface, as well as gasoline particle, have multi-functional groups (carboxyl, hydroxyl, amine etc.) leading to multiple interactions.

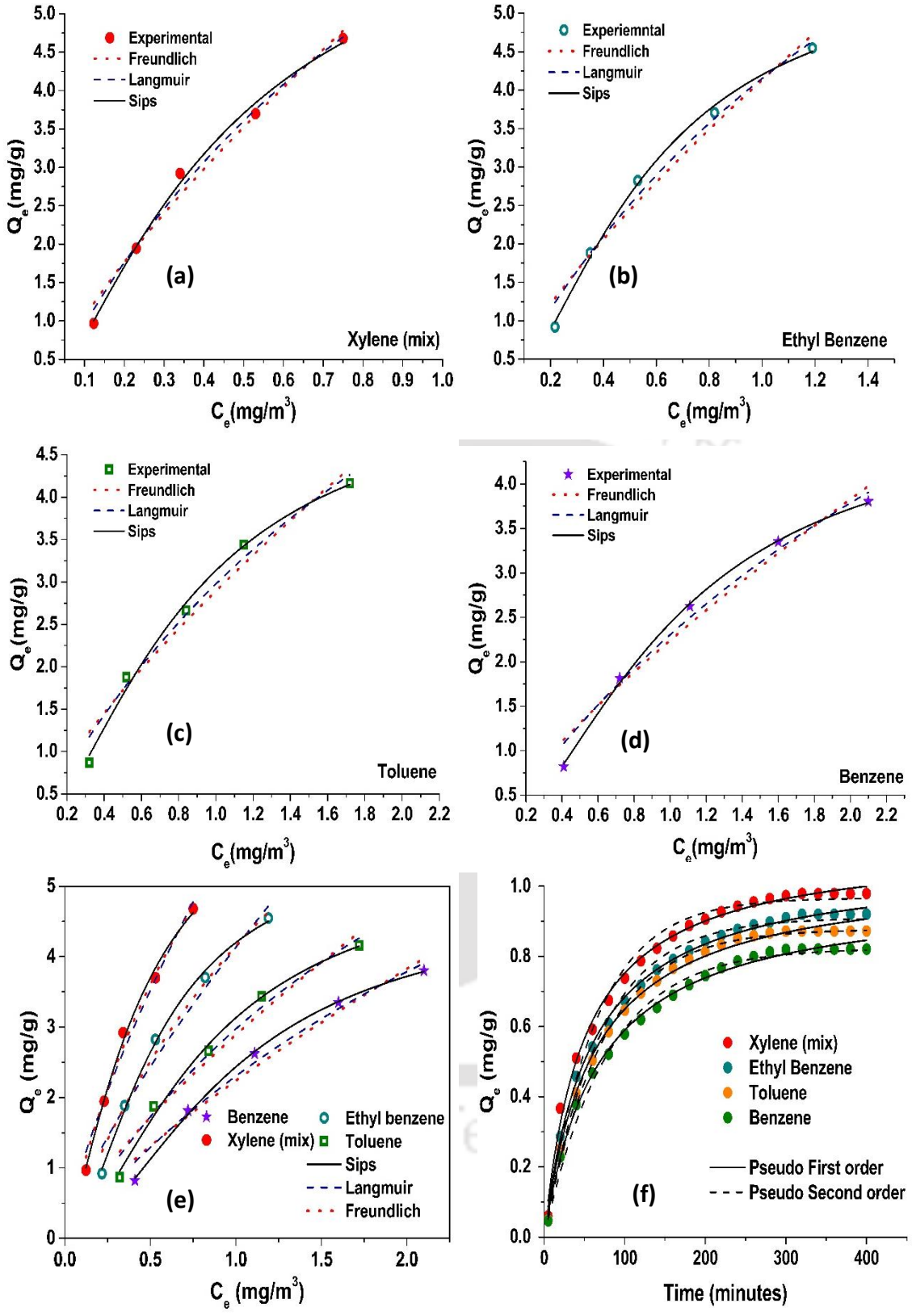

Figure 7.5. Isotherm and kinetics involved with BTEX adsorption on fabricated sericin-coated air filter (a) Xylene (b) Ethyl Benzene (c) Toluene (d) Benzene (e) combined isotherm (f) Kinetics (at initial conc. of 2 mg/m^3) involved with BTEX adsorption.

Table 7-1. (a) Results obtained from Langmuir, Freundlich and Sips model fitting to adsorption data of BTEX on sericin-coated air filter (b) Results obtained from the kinetic model fitting for BTEX adsorption on fabricated sericin-coated air filter

(a)													
Aromatic Compounds	**Langmuir Model**				**Freundlich Model**				**Sips Model**				
	Q_{max}	**K_L**	**R^2**	**χ^2**	**K_F**	**n_F**	**R^2**	**χ^2**	**Q_{max}**	**K_S**	**n_s**	**R^2**	**χ^2**
Xylene	11.921	0.867	0.987	0.026	5.930	1.330	0.974	0.0889	6.97	2.905	1.362	0.990	0.020
Ethyl Benzene	11.956	0.531	0.975	0.050	4.132	1.314	0.956	0.0529	5.68	2.823	1.702	0.995	0.010
Toluene	10.706	0.384	0.972	0.046	2.890	1.332	0.951	0.0809	5.35	1.407	1.643	0.989	0.017
Benzene	10.605	0.277	0.975	0.035	2.239	1.293	0.957	0.0608	4.78	1.038	1.755	0.998	0.002

(b)								
Aromatic Compounds	**Pseudo First Order**				**Pseudo Second Order**			
	Q_e	**K_1**	**χ^2**	**R^2**	**Q_e**	**K_2**	**$\chi 2$**	**R^2**
Xylene	0.9665	0.0157	$3.53E^{-4}$	0.992	1.123	0.0180	0.0012	0.974
Ethyl Benzene	0.9092	0.0144	$1.92E^{-4}$	0.995	1.072	0.0164	$8.07E^{-4}$	0.982
Toluene	0.8772	0.0139	$2.16E^{-4}$	0.995	1.044	0.0157	$3.45E^{-4}$	0.992
Benzene	0.8228	0.0127	$1.98E^{-4}$	0.995	0.989	0.0149	$5.04E^{-4}$	0.987

The adsorption kinetics of selected VOCs on sericin-coated air-filter were analyzed for the pseudo-first-order and second-order kinetics. The obtained data of adsorption kinetics for BTEX gases on air-filter are shown in *Figure 7.5*f, and kinetic parameters are summarized in *Table 7-1b*. *Figure 7.5f* shows non-linear fitting for the pseudo-first-order kinetic model for BTEX gases adsorbed on the air-filter surface. The pseudo-first-order model is based on the hypothesis that initially, there is no adsorbate (VOCs) on the adsorbent surface (sericin layer of air-filter), while with time, the VOCs occupy the binding sites on the air-filter surface. The adsorption rate correlates with the number of free adsorption sites in direct proportion via physio-sorption. *Figure 7.5f* shows non-linear fitting for the pseudo-second-order kinetic model for BTEX gases adsorbed on the air-filter surface. If the adsorption system follows pseudo-second-order kinetics, then the rate-limiting step is chemical adsorption involving chemical bonding between the adsorbent and adsorbate. As in the present case binding of VOCs on the filter surface mainly involves intermolecular forces, i.e., hydrophobic and electrostatic interaction and hence the experimental data provide the better fitting with a pseudo-first-order kinetic model with a high correlation coefficient (R^2=0.99) value and low chi-square values (Table 7-*1b* and Figure *7.5f*). The easy desorption of VOCs during air-filter regeneration seconds involvement of weak binding forces in adsorption. The Q_e values estimated through the pseudo-first-order model (Table 6.1b) are also closer to experimentally calculated values. These results imply that the adsorption system studied follows the pseudo-first-order kinetic model.

7.3.4. Lifetime study for Sericin coated Air-filter

Continuous removal for multiple cycles and ease of regeneration are crucial factors to assess the performance of an air filter. The sericin-coated air-filter was operated for 2160 cycles (from a 1000 μgm^{-3} level to 5 μgm^{-3} in a 6.28 m^3 chamber). *Figure 7.6* shows the performance of the fabricated air-filter for 2160 cycles with intermittent washing after every 180 cycles. Pure water was used to wash the air-filter, followed by air-drying at room temperature. The Air-filter was capable of removing the $PM_{2.5}$ and PM_{10} completely and efficiently for the tested duration. The Air-filter regained its efficiency after each wash with a <95% recovery. A very low decline in the performance of air filter was noticed in terms of time taken (increased from 26.8 to 27.30 minutes) for complete removal of PM when performed for 2160 cycles. The commercially available HEPA

filters are not washable and cannot remove VOCs, and hence generally used together with an activated carbon filter for air-filtration [317,318]. The comparative analysis shows that the HEPA filter is very effective initially and requires only 8-9 minutes for complete removal of $PM_{2.5}$ and $PM_{10,}$ but gradually after continuous use for one month and three months, the time required for a removal for PM increased to 35.06 and 47.05 minutes, respectively. The sericin-coated air filter comparatively takes longer duration for PM filtration, but the removal efficiency is consistent for a longer period, is a washable filter, and works adequately for a longer duration. Besides, the sericin-coated air-filter could provide VOC removal as well. Hence, the sericin-coated air filter may provide a better solution for the treatment of indoor air in the longer run.

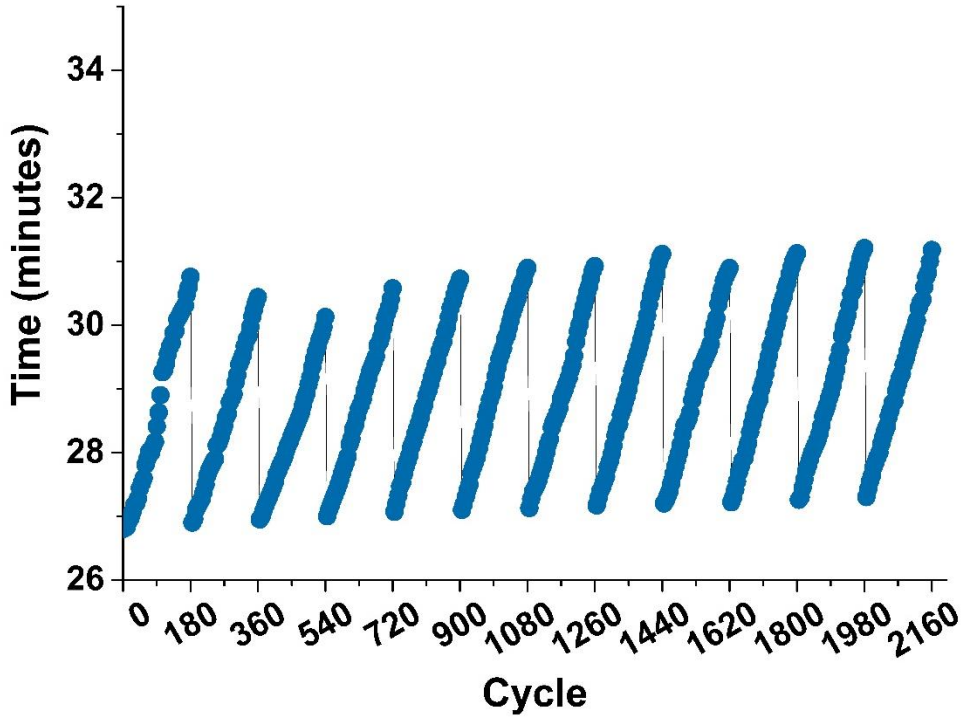

Figure 7.6. Performance of sericin-coated air-filter for 2160 cycles with intermittent washing after every 180 cycles (error = ±2.8%).

7.4. Conclusion

In this study, a sericin-coated air-filter was fabricated using a very facile and novel method. The fabricated air-filter was assessed for its capacity to remove particulate matter as well as VOCs from indoor air. Experiments were conducted in a closed chamber saturated with PM generated from incense stick and gasoline (for VOCs). The air filter

completely removed the particulate matter (PM_{10} and $PM_{2.5}$) in 27 minutes. BTEX gases were efficiently captured at lower concentrations (100-1000 ppb), while adsorption capacity gradually decreased with increasing concentration. The pseudo-first-order kinetic model and Sips adsorption isotherm provided the best fit to the adsorption data. The desorption study revealed that the protein layer could be regenerated for reuse of air-filter by washing with pure water. The sericin-coated air-filter proved was capable of removing PM with the same potency for around 2160 cycles and exhibited more than 95% recovery after each washing. The study reveals that sericin-coated air-filter can be used for efficient removal of PM as well as VOCs from indoor air.

Chapter 8

Summary and Scope for Future Work

8.1. Summary

This study involved investigations on the potential of sericin as an adsorbent and coating material for enhancement of surface properties of microfiltration (MF) polypropylene hollow fiber membrane for the removal of drug-based micropollutants in water. At the earlier stage, the adsorptive properties of sericin were identified by studying its interaction pattern with one model drug Ibuprofen, frequently found in water sources. The study was performed using an integrated adsorption-cum-membrane filtration setup. Sericin physicochemical properties relative to adsorption was studied. The study revealed sericin as non-porous material with low surface area prone to conformational change with physical stimuli like pH and temperature. Its adsorption ability was analyzed at different operating conditions (concentration, temperature, and pH). High pH and increasing temperature were found to assist in better adsorption of Ibuprofen. Ibuprofen interaction with sericin was found to be endothermic in nature but dependent on protein unfolding. Ibuprofen binding was related to the sericin transition to a random coil structure.

Once a detailed knowledge was gained on its binding and interaction patterns, the sericin was used further for membrane modification. A flow-through coating through physical and chemical adsorption was carried out as a facile surface modification technique. Physical adsorption of hydrophilic sericin followed by chemical linking and thermal fixation as a suitable way to enhance surface characteristics of the PPMF membrane has been demonstrated. The high molecular weight globular sericin protein was uniformly coated on the membrane surface. The coating materials dually impacted the membrane surface properties by enhancing its hydrophilicity and providing it with multi-functional groups for pollutant entrapment via adsorption. The obtained results from different analytical techniques revealed uniform deposition of sericin on the modified membrane surface, inside pores, and walls of the membrane. The pore size compaction post-coating resulted in decreased pure water permeability by 19.10% compared to that of the pristine membrane. The sericin coated PP-HFMF membrane exhibited increased hydrophilicity, reduced contact angle (38°), high water content (64.87%) with the presence of multi-functional groups on the membrane surface. The sericin enhanced hydrophilic membranes was then tested for its antifouling and adsorptive properties for charge-based separation of pollutants from water.

The modified PP-HFMF membrane was used to remove drug-based micropollutants from a single and multi-component system. Complete removal via adsorption of drugs on to the membrane surface was noticed for low-concentration (~20 µg) systems. The adsorption behavior was studied using different fixed bed models, with the best predictive model being the Bohart-Adams model. The model predicted the dynamic behavior of the HFMF membrane module fitted in housing with minimum error. The protein layer could be regenerated very easily with stimulation by using a cold alkaline solution. Membrane re-usability was tested for five cycles with six different drugs, and the membrane was found to be effective for multiple cycles. The interaction effect of background salt and mixed drug scenarios exhibited negligible influence. The adsorption mechanism was highly influenced by charged based interaction and hydrogen bonding resulting in less removal of uncharged drugs compared to anionic drugs. In a multidrug mixture, the removal efficiency for different selected drugs follows the sequence; Ibuoprofen>Diclofenac>Amoxicillin>Ciprofloxacin>Estrone>β-estradiol. The membrane was found to be effective for the anionic drug rather than uncharged drugs.

Subsequently, the modified membrane was tested for its antifouling properties. The fouling resistance experiments revealed 15% less fouling for sericin coated membrane with >90% turbidity removal for the greywater purification application. With the produced water, the sericin coated membrane exhibited 10.5% less fouling, and >65% turbidity was removed during the filtration process. The pure water backwash was quite effective in mitigating reversible fouling for sericin coated membrane and flux recovery was high for both physical and chemical cleaning methods.

Based on sericin's ability to interact with pollutants and its easy incorporation with other polymers, it was used to coat a polyester-based air-filter via a very facile and novel method. The bi-component polyester fabric used for air filter was dip-coated and crosslinked using glutaraldehyde followed by heat curing. The fabricated air-filter removed the particulate matter (PM_{10} and $PM_{2.5}$) in a short time of 27 minutes. Then subsequently, air-filter was also tested for its capability to remove VOC gases from indoor air. BTEX gases were efficiently captured at lower concentrations (100-1000 ppb), while adsorption capacity gradually decreased with increasing concentration. The adsorption isotherm and kinetics were studied for BTEX adsorption using classic Langmuir, Freundlich, and Sips model. The adsorption of gases followed the pseudo-

first-order kinetic model and Sips adsorption isotherm. The air-filter could be easily generated by washing with pure water. The sericin-coated air-filter proved capable of removing PM with the same potency for around 2160 cycles and exhibited more than 95% recovery after each washing. The study reveals that Sericin-coated air-filter is quite efficient in the removal of PM as well as VOCs from indoor air.

Overall, it is demonstrated that membrane modification with sericin coating is a simple and efficient way to modify the surface properties of polymeric membranes for water and air filtration application. The improved performance of the coated membrane was evident, and increased membrane life and operational performance.

8.2. Recommendation for future research

Further investigations into the use of other coating materials with adsorbing properties to address the problem of fouling alongside drug-based micropollutant removal are recommended, as well as the use of other types of membrane material (i.e., ceramic) and module configuration (such as flat sheet). Natural or synthetic non-toxic materials with high hydrophilicity and anti-fouling property which can cross-link/bind and achieve firm anchorage to the base membrane material surface will be very useful to provide a barrier adsorbing structure for organic pollutants removal while limiting the fouling effects via hydrophilicity. The examples of such materials may include natural and synthetic hydrophilic polymers like chitosan, cyclodextrin, polydopamine, etc. Also, the blending of such potent materials with the base membrane polymer material at the earlier production stage may be a good option to improve the permeate water flux, which can impart high anti-fouling properties on the membrane surface as well as pores and walls of the produced membrane.

An investigation into pore size distribution control by manipulating physical properties (pH, temperature, thermal fixation, etc.) while fabricating the adsorptive membrane can be an interesting topic for better application. Fabrication of adsorptive membrane with anti-fouling properties with flux recovery capabilities without compromising water permeability, which can show specificity towards selective removal of other organic pollutants (like heavy metals, herbicides, pesticides, etc.) will be interesting for future studies.

Further investigation on the use of sericin for coating of different membrane modules can be taken as a future study. The use of more robust characterization techniques for the modified membrane on a holistic approach rather than a representative approach is recommended. The advanced characterization techniques can specifically identify the binding amino acid groups present in sericin responsible for the removal of pollutants. Characterization methods such as; liquid chromatography-mass spectroscopy (LC-MS), Electrospray ionization mass spectroscopy (ESI-MS), matrix-assisted laser desorption/ionization mass spectroscopy (MALDI-MS), X-ray Photoelectron Spectroscopy, high-resolution Atomic Force Microscopy, Transmission Electron Microscopy in addition to the Field Emission Scanning Electron Microscopy; can provide relevant information on the surface characteristics and microstructure of the membrane. The in-depth detailed characterization may demand multi-disciplinary expertise and collaboration.

Continuous operation coated membrane to investigate the durability of the coated layer, and the effects of other dissolved pollutants on removal are also recommended. The coated membrane can also be tested with other foulants to check its applicability in other water matrices. In this study, site-based produced water and synthetic greywater water were used, which contains limited organic pollutants at a time. Although the investigation into the problems of membrane fouling related to wastewater was not within the scope of this study, future studies may include fouling mitigation in real municipal wastewater containing a cocktail of pollutants. A thorough operation optimization and membrane material functionalization are also recommended

References

[1] United Nations Environment Programme, Towards a Pollution-Free Planet Background Report, Nairobi, Kenya, 2017. https://wedocs.unep.org/bitstream/handle/20.500.11822/21800/UNEA_towardspollution_long version_Web.pdf?sequence=1&isAllowed=y.

[2] I. V. Muralikrishna, V. Manickam, Chapter One - Introduction, in: I. V Muralikrishna, V.B.T.-E.M. Manickam (Eds.), Environ. Manag. Sci. Eng. Ind., Butterworth-Heinemann, 2017: pp. 1–4. doi:10.1016/b978-0-12-811989-1.00001-4.

[3] UNESCO, The United Nations world water development report 2019: leaving no one behind, UNESCO, Paris, 2019. https://unesdoc.unesco.org/ark:/48223/pf0000367306/PDF/367306eng.pdf.multi.

[4] M.M. Mekonnen, A.Y. Hoekstra, Sustainability: Four billion people facing severe water scarcity, Sci. Adv. (2016). doi:10.1126/sciadv.1500323.

[5] WHO, Don't pollute my future! The impact of the environment on children's health, World Health Organization, 2017. https://www.who.int/ceh/publications/don-t-pollute-my-future/en/.

[6] IWMI, Water policy briefing, issue 8, Colombo, 2003. http://www.iwmi.cgiar.org/publications/briefs/water-policy-briefs/iwmi-water-policy-briefing-8/.

[7] J. V Tarazona, Pollution, Water, in: P.B.T.-E. of T. (Third E. Wexler (Ed.), Academic Press, Oxford, 2014: pp. 1024–1027. doi:https://doi.org/10.1016/B978-0-12-386454-3.00532-7.

[8] D. Earnhart, Water Pollution from Industrial Sources, in: Encycl. Energy, Nat. Resour. Environ. Econ., 2013: pp. 114–120. doi:10.1016/B978-0-12-375067-9.00091-7.

[9] S. Dwivedi, S. Mishra, R.D. Tripathi, Ganga water pollution: A potential health threat to inhabitants of Ganga basin, Environ. Int. 117 (2018) 327–338.

doi:https://doi.org/10.1016/j.envint.2018.05.015.

[10] R.P. Schwarzenbach, T. Egli, T.B. Hofstetter, U. von Gunten, B. Wehrli, Global Water Pollution and Human Health, Annu. Rev. Environ. Resour. 35 (2010) 109–136. doi:10.1146/annurev-environ-100809-125342.

[11] FAO and UN-Water, Progress on level of water stress. Global baseline for SDG 6 Indicator 6.4.2, Rome, 2018. https://www.unwater.org/publications/progress-on-level-of-water-stress-642/.

[12] S.D. Richardson, T.A. Ternes, Water Analysis: Emerging Contaminants and Current Issues, Anal. Chem. 90 (2018) 398–428. doi:10.1021/acs.analchem.7b04577.

[13] S. Sauvé, M. Desrosiers, A review of what is an emerging contaminant, Chem. Cent. J. 8 (2014) 15. doi:10.1186/1752-153X-8-15.

[14] E. Sanganyado, W. Gwenzi, Antibiotic resistance in drinking water systems: Occurrence, removal, and human health risks, Sci. Total Environ. 669 (2019) 785–797. doi:https://doi.org/10.1016/j.scitotenv.2019.03.162.

[15] C. Xi, Y. Zhang, C.F. Marrs, W. Ye, C. Simon, B. Foxman, J. Nriagu, Prevalence of Antibiotic Resistance in Drinking Water Treatment and Distribution Systems, Appl. Environ. Microbiol. 75 (2009) 5714 LP – 5718. doi:10.1128/AEM.00382-09.

[16] C. Stamm, K. Räsänen, F.J. Burdon, F. Altermatt, J. Jokela, A. Joss, M. Ackermann, R.I.L. Eggen, Chapter Four - Unravelling the Impacts of Micropollutants in Aquatic Ecosystems: Interdisciplinary Studies at the Interface of Large-Scale Ecology, in: A.J. Dumbrell, R.L. Kordas, G.B.T.-A. in E.R. Woodward (Eds.), Large-Scale Ecol. Model Syst. to Glob. Perspect., Academic Press, 2016: pp. 183–223. doi:https://doi.org/10.1016/bs.aecr.2016.07.002.

[17] A. Gogoi, P. Mazumder, V.K. Tyagi, G.G. Tushara Chaminda, A.K. An, M. Kumar, Occurrence and fate of emerging contaminants in water environment: A review, Groundw. Sustain. Dev. 6 (2018) 169–180. doi:https://doi.org/10.1016/j.gsd.2017.12.009.

[18] J.M. Philip, U.K. Aravind, C.T. Aravindakumar, Emerging contaminants in Indian environmental matrices – A review, Chemosphere. 190 (2018) 307–326. doi:https://doi.org/10.1016/j.chemosphere.2017.09.120.

[19] P.K. Mutiyar, S.K. Gupta, A.K. Mittal, Fate of pharmaceutical active compounds (PhACs) from River Yamuna, India: An ecotoxicological risk assessment approach, Ecotoxicol. Environ. Saf. 150 (2018) 297–304. doi:https://doi.org/10.1016/j.ecoenv.2017.12.041.

[20] D.J. Lapworth, N. Baran, M.E. Stuart, R.S. Ward, Emerging organic contaminants in groundwater: A review of sources, fate and occurrence, Environ. Pollut. 163 (2012) 287–303. doi:https://doi.org/10.1016/j.envpol.2011.12.034.

[21] D.G.J. Larsson, C. de Pedro, N. Paxeus, Effluent from drug manufactures contains extremely high levels of pharmaceuticals, J. Hazard. Mater. 148 (2007) 751–755. doi:10.1016/j.jhazmat.2007.07.008.

[22] J.L. Oaks, M. Gilbert, M.Z. Virani, R.T. Watson, C.U. Meteyer, B.A. Rideout, H.L. Shivaprasad, S. Ahmed, M.J. Iqbal Chaudhry, M. Arshad, S. Mahmood, A. Ali, A. Ahmed Khan, Diclofenac residues as the cause of vulture population decline in Pakistan, Nature. 427 (2004) 630–633. http://dx.doi.org/10.1038/nature02317.

[23] K. Fent, A.A. Weston, D. Caminada, Ecotoxicology of human pharmaceuticals, Aquat. Toxicol. 76 (2006) 122–159. doi:10.1016/j.aquatox.2005.09.009.

[24] J. Fick, H. Söderström, R.H. Lindberg, C. Phan, M. Tysklind, D.G.J. Larsson, Contamination of surface, ground, and drinking water from pharmaceutical production, Environ. Toxicol. Chem. 28 (2010) 2522–2527. doi:10.1897/09-073.1.

[25] K. Fent, A.A. Weston, D. Caminada, Ecotoxicology of human pharmaceuticals, Aquat. Toxicol. 76 (2006) 122–159. doi:10.1016/j.aquatox.2005.09.009.

[26] R. Thibaut, S. Schnell, C. Porte, The interference of pharmaceuticals with endogenous and xenobiotic metabolizing enzymes in carp liver: An in-vitro study, Environ. Sci. Technol. 40 (2006) 5154–5460. doi:10.1021/es0607483.

[27] H.J. De Lange, W. Noordoven, A.J. Murk, M. Lürling, E. Peeters, Behavioural responses of< i> Gammarus pulex</i>(Crustacea, Amphipoda) to low concentrations of pharmaceuticals, Aquat. Toxicol. 78 (2006) 209–216.

[28] J.L. Oaks, M. Gilbert, M.Z. Virani, R.T. Watson, C.U. Meteyer, B. a Rideout, H.L. Shivaprasad, S. Ahmed, M.J.I. Chaudhry, M. Arshad, S. Mahmood, A. Ali, A.A. Khan, Diclofenac residues as the cause of vulture population decline in Pakistan., Nature. 427 (2004) 630–633. doi:10.1038/nature02317.

[29] P. Bottoni, S. Caroli, A.B. Caracciolo, Pharmaceuticals as priority water contaminants, Toxicol. Environ. Chem. 92 (2010) 549–565. doi:10.1080/02772241003614320.

[30] J. Olsson, E. Thorin, E. Nehrenheim, A. Juszkiewicz, S. Schwede, Comparative Study–Pharmaceutical Residues in Wastewater and Sludge from a Micoralgae Plant and an Activated Sludge Process, in: 5th Int. Conf. Ind. Hazard. Waste Manangement, 27-30 Sept. 2016, Crete, Greece, 2016.

[31] J.L. Tambosi, L.Y. Yamanaka, H.J. José, R. de F.P.M. Moreira, H.F. Schröder, Recent research data on the removal of pharmaceuticals from sewage treatment plants (STP) , Química Nov. . 33 (2010) 411–420.

[32] M.-K. Kim, K.-D. Zoh, Occurrence and removals of micropollutants in water environment, Environ. Eng. Res. 21 (2016) 319–332.

[33] P.E. Stackelberg, J. Gibs, E.T. Furlong, M.T. Meyer, S.D. Zaugg, R.L. Lippincott, Efficiency of conventional drinking-water-treatment processes in removal of pharmaceuticals and other organic compounds, Sci. Total Environ. 377 (2007) 255–272. doi:https://doi.org/10.1016/j.scitotenv.2007.01.095.

[34] R. Tröger, P. Klöckner, L. Ahrens, K. Wiberg, Micropollutants in drinking water from source to tap - Method development and application of a multiresidue screening method, Sci. Total Environ. 627 (2018) 1404–1432. doi:https://doi.org/10.1016/j.scitotenv.2018.01.277.

[35] World Health Organization, Ambient air pollution: A global assessment of exposure and burden of disease, World Health Organization, Geneva,

Switzerland, 2016. https://apps.who.int/iris/bitstream/handle/10665/250141/9789241511353-eng.pdf?sequence=1.

[36] H.E. Institute, State of Global Air, Boston, MA, 2019. doi:https://www.stateofglobalair.org/sites/default/files/soga_2019_report.pdf.

[37] R. Esworthy, Air Quality: EPA's 2013 Changes to the Particulate Matter (PM) Standard, Congr. Res. Serv. (2015) 49. www.crs.gov.

[38] F. Han, S.H. Kota, Y. Wang, H. Zhang, Source apportionment of PM2.5 in Baton Rouge, Louisiana during 2009–2014, Sci. Total Environ. 586 (2017) 115–126. doi:https://doi.org/10.1016/j.scitotenv.2017.01.189.

[39] P.E. Schwarze, J. Øvrevik, M. Låg, M. Refsnes, P. Nafstad, R.B. Hetland, E. Dybing, Particulate matter properties and health effects: Consistency of epidemiological and toxicological studies, Hum. Exp. Toxicol. (2006). doi:10.1177/096032706072520.

[40] J. Löndahl, A. Massling, J. Pagels, E. Swietlicki, E. Vaclavik, S. Loft, Size-resolved respiratory-tract deposition of fine and ultrafine hydrophobic and hygroscopic aerosol particles during rest and exercise, Inhal. Toxicol. 19 (2007) 109–116.

[41] K.-H. Kim, E. Kabir, S. Kabir, A review on the human health impact of airborne particulate matter, Environ. Int. 74 (2015) 136–143. doi:https://doi.org/10.1016/j.envint.2014.10.005.

[42] NAAQS, National Ambient Air Quality Standards (NAAQS), Seventh Amendment Rules-2009, Ministry of Environment and Forests Notification (MoEF Gazette, 2009), CPCB (Central Pollution Control Board), India, 2009. http://cpcb.nic.in/air-quality-standard/.

[43] S.H. Kota, H. Guo, L. Myllyvirta, J. Hu, S.K. Sahu, R. Garaga, Q. Ying, A. Gao, S. Dahiya, Y. Wang, H. Zhang, Year-long simulation of gaseous and particulate air pollutants in India, Atmos. Environ. 180 (2018) 244–255. doi:https://doi.org/10.1016/j.atmosenv.2018.03.003.

[44] H. Guo, S.K. Sahu, S.H. Kota, H. Zhang, Characterization and health risks of criteria air pollutants in Delhi, 2017, Chemosphere. 225 (2019) 27–34. doi:https://doi.org/10.1016/j.chemosphere.2019.02.154.

[45] R. Garaga, S.K. Sahu, S.H. Kota, A Review of Air Quality Modeling Studies in India: Local and Regional Scale, Curr. Pollut. Reports. 4 (2018) 59–73. doi:10.1007/s40726-018-0081-0.

[46] M. Ezzati, Indoor Air Pollution/Developing Countries, in: H.K. (Kris) B.T.-I.E. of P.H. Heggenhougen (Ed.), Academic Press, Oxford, 2008: pp. 547–553. doi:https://doi.org/10.1016/B978-012373960-5.00296-3.

[47] A.D. Lopez, C.D. Mathers, M. Ezzati, D.T. Jamison, C.J.L. Murray, Global burden of disease and risk factors, The World Bank, 2006.

[48] Y. Yang, Z. Ruan, X. Wang, Y. Yang, T.G. Mason, H. Lin, L. Tian, Short-term and long-term exposures to fine particulate matter constituents and health: A systematic review and meta-analysis, Environ. Pollut. (2018). doi:https://doi.org/10.1016/j.envpol.2018.12.060.

[49] K.R. Smith, Fuel Combustion, Air Pollution Exposure, and Health: The Situation in Developing Countries, Annu. Rev. Energy Environ. 18 (1993) 529–566. doi:10.1146/annurev.eg.18.110193.002525.

[50] D.G. Fullerton, N. Bruce, S.B. Gordon, Indoor air pollution from biomass fuel smoke is a major health concern in the developing world, Trans. R. Soc. Trop. Med. Hyg. 102 (2008) 843–851. doi:https://doi.org/10.1016/j.trstmh.2008.05.028.

[51] J.G. Calvert, R. Atkinson, K.H. Becker, R.M. Kamens, J.H. Seinfeld, T.J. Wallington, G. Yarwood, The Mechanisms of Atmospheric Oxidation of the Aromatic Hydrocarbons, Oxford University Press, 2002.

[52] P.J. Lupo, E. Symanski, D.K. Waller, W. Chan, P.H. Langlois, M.A. Canfield, L.E. Mitchell, Maternal exposure to ambient levels of benzene and neural tube defects among offspring: Texas, 1999–2004, Environ. Health Perspect. 119 (2010) 397–402.

[53] A. Masih, A.S. Lall, A. Taneja, R. Singhvi, Inhalation exposure and related health risks of BTEX in ambient air at different microenvironments of a terai zone in north India, Atmos. Environ. 147 (2016) 55–66. doi:https://doi.org/10.1016/j.atmosenv.2016.09.067.

[54] A.J. Buczynska, A. Krata, M. Stranger, A.F.L. Godoi, V. Kontozova-Deutsch, L. Bencs, I. Naveau, E. Roekens, R. Van Grieken, Atmospheric BTEX-concentrations in an area with intensive street traffic, Atmos. Environ. 43 (2009) 311–318.

[55] L.M. McKenzie, R.Z. Witter, L.S. Newman, J.L. Adgate, Human health risk assessment of air emissions from development of unconventional natural gas resources, Sci. Total Environ. 424 (2012) 79–87.

[56] R. Bono, E. Scursatone, T. Schilirò, G. Gilli, Ambient air levels and occupational exposure to benzene, toluene, and xylenes in northwestern Italy, J. Toxicol. Environ. Heal. Part A. 66 (2003) 519–531.

[57] F.I. Khan, A. Kr. Ghoshal, Removal of Volatile Organic Compounds from polluted air, J. Loss Prev. Process Ind. 13 (2000) 527–545. doi:https://doi.org/10.1016/S0950-4230(00)00007-3.

[58] H.C. Chuang, K.F. Ho, L.Y. Lin, T.Y. Chang, G.B. Hong, C.M. Ma, I.J. Liu, K.J. Chuang, Long-term indoor air conditioner filtration and cardiovascular health: A randomized crossover intervention study, Environ. Int. 106 (2017) 91–96. doi:10.1016/j.envint.2017.06.008.

[59] R. Sawlani, R. Agnihotri, C. Sharma, P.K. Patra, A.P. Dimri, K. Ram, R.L. Verma, The severe Delhi SMOG of 2016: A case of delayed crop residue burning, coincident firecracker emissions, and atypical meteorology, Atmos. Pollut. Res. 10 (2019) 868–879. doi:10.1016/j.apr.2018.12.015.

[60] R. Singh, N.P. Hankins, Chapter 2 - Introduction to Membrane Processes for Water Treatment, in: N.P. Hankins, R.B.T.-E.M.T. for S.W.T. Singh (Eds.), Elsevier, Boston, 2016: pp. 15–52. doi:https://doi.org/10.1016/B978-0-444-63312-5.00002-4.

[61] H. Strathmann, L. Giorno, E. Drioli, Introduction to membrane science and technology, Wiley-VCH Weinheim, 2011.

[62] R. Molinari, M. Mungari, E. Drioli, A. Di Paola, V. Loddo, L. Palmisano, M. Schiavello, Study on a photocatalytic membrane reactor for water purification, Catal. Today. 55 (2000) 71–78. doi:https://doi.org/10.1016/S0920-5861(99)00227-8.

[63] R. Ordóñez, D. Hermosilla, I.S. Pío, Á. Blanco, Evaluation of MF and UF as pretreatments prior to RO applied to reclaim municipal wastewater for freshwater substitution in a paper mill: A practical experience, Chem. Eng. J. 166 (2011) 88–98. doi:https://doi.org/10.1016/j.cej.2010.10.016.

[64] M.A. Al-Ghouti, M.A. Al-Kaabi, M.Y. Ashfaq, D.A. Da'na, Produced water characteristics, treatment and reuse: A review, J. Water Process Eng. 28 (2019) 222–239. doi:https://doi.org/10.1016/j.jwpe.2019.02.001.

[65] V.M. Boddu, T. Paul, M.A. Page, C. Byl, L. Ward, J. Ruan, Gray water recycle: Effect of pretreatment technologies on low pressure reverse osmosis treatment, J. Environ. Chem. Eng. 4 (2016) 4435–4443. doi:https://doi.org/10.1016/j.jece.2016.09.031.

[66] W. Naessens, T. Maere, G. Gilabert-Oriol, V. Garcia-Molina, I. Nopens, PCA as tool for intelligent ultrafiltration for reverse osmosis seawater desalination pretreatment, Desalination. 419 (2017) 188–196. doi:https://doi.org/10.1016/j.desal.2017.06.018.

[67] M. Talaeipour, J. Nouri, A.H. Hassani, A.H. Mahvi, An investigation of desalination by nanofiltration, reverse osmosis and integrated (hybrid NF/RO) membranes employed in brackish water treatment, J. Environ. Heal. Sci. Eng. 15 (2017) 18. doi:10.1186/s40201-017-0279-x.

[68] E. Nagy, Chapter 20 - Reverse Osmosis, in: E.B.T.-B.E. of M.T.T. a M.L. (Second E. Nagy (Ed.), Elsevier, 2019: pp. 497–503. doi:https://doi.org/10.1016/B978-0-12-813722-2.00020-0.

[69] D. Attarde, M. Jain, P.K. Singh, S.K. Gupta, Energy-efficient seawater

desalination and wastewater treatment using osmotically driven membrane processes, Desalination. 413 (2017) 86–100. doi:https://doi.org/10.1016/j.desal.2017.03.010.

[70] Z.V.P. Murthy, S.K. Gupta, Sodium cyanide separation and parameter estimation for reverse osmosis thin film composite polyamide membrane, J. Memb. Sci. 154 (1999) 89–103. doi:https://doi.org/10.1016/S0376-7388(98)00280-4.

[71] C. Fonseca Couto, L.C. Lange, M.C. Santos Amaral, A critical review on membrane separation processes applied to remove pharmaceutically active compounds from water and wastewater, J. Water Process Eng. 26 (2018) 156–175. doi:https://doi.org/10.1016/j.jwpe.2018.10.010.

[72] P. Shojaee Nasirabadi, E. Saljoughi, S.M. Mousavi, Membrane processes used for removal of pharmaceuticals, hormones, endocrine disruptors and their metabolites from wastewaters: a review, Desalin. Water Treat. 57 (2016) 24146–24175. doi:10.1080/19443994.2016.1140081.

[73] K.P.M. Licona, L.R. de O. Geaquinto, J. V Nicolini, N.G. Figueiredo, S.C. Chiapetta, A.C. Habert, L. Yokoyama, Assessing potential of nanofiltration and reverse osmosis for removal of toxic pharmaceuticals from water, J. Water Process Eng. 25 (2018) 195–204. doi:https://doi.org/10.1016/j.jwpe.2018.08.002.

[74] L.L.S. Silva, C.G. Moreira, B.A. Curzio, F. V da Fonseca, Micropollutant removal from water by membrane and advanced oxidation processes—A review, J. Water Resour. Prot. 9 (2017) 411.

[75] J. Radjenovic, M. Petrovic, F. Ventura, D. Barcelo, Rejection of Pharmaceuticals in Nanofiltration and Reverse Osmosis Membrane Drinking Water Treatment, Water Res. 42 (2008) 3601–3610. doi:10.1016/j.watres.2008.05.020.

[76] N. Rosman, W.N.W. Salleh, M.A. Mohamed, J. Jaafar, A.F. Ismail, Z. Harun, Hybrid membrane filtration-advanced oxidation processes for removal of pharmaceutical residue, J. Colloid Interface Sci. 532 (2018) 236–260. doi:https://doi.org/10.1016/j.jcis.2018.07.118.

[77] K.C. Verma, A.S. Kushwaha, Demineralization of drinking water: Is it prudent?,

Med. Journal, Armed Forces India. 70 (2014) 377–379. doi:10.1016/j.mjafi.2013.11.011.

[78] M.R. Adam, S.K. Hubadillah, M.I.M. Esham, M.H.D. Othman, M.A. Rahman, A.F. Ismail, J. Jaafar, Chapter 12 - Adsorptive Membranes for Heavy Metals Removal From Water, in: A.F. Ismail, M.A. Rahman, M.H.D. Othman, T.B.T.-M.S.P. and A. Matsuura (Eds.), Handbooks Sep. Sci., Elsevier, 2019: pp. 361–400. doi:https://doi.org/10.1016/B978-0-12-812815-2.00012-0.

[79] K.C. Khulbe, T. Matsuura, Removal of heavy metals and pollutants by membrane adsorption techniques, Appl. Water Sci. 8 (2018) 19. doi:10.1007/s13201-018-0661-6.

[80] R.S. Vieira, M.M. Beppu, Dynamic and static adsorption and desorption of Hg (II) ions on chitosan membranes and spheres, Water Res. 40 (2006) 1726–1734.

[81] M.M. Nasef, A.H. Yahaya, Adsorption of some heavy metal ions from aqueous solutions on Nafion 117 membrane, Desalination. 249 (2009) 677–681.

[82] K.A.M. Said, G.G. George, N.A.M. Alipah, N.Z. Ismail, R.L. Jama'in, Effect of activated carbon in PSF-PEI-Ag symmetric membrane, MATEC Web Conf. 87 (2017). https://doi.org/10.1051/matecconf/20178703008.

[83] W. Zhu, J. Liu, M. Li, Fundamental studies of novel zwitterionic hybrid membranes: kinetic model and mechanism insights into strontium removal, Sci. World J. 2014 (2014).

[84] S. Chatterjee, S. De, Adsorptive removal of fluoride by activated alumina doped cellulose acetate phthalate (CAP) mixed matrix membrane, Sep. Purif. Technol. 125 (2014) 223–238.

[85] R.J. Gohari, W.J. Lau, T. Matsuura, A.F. Ismail, Fabrication and characterization of novel PES/Fe–Mn binary oxide UF mixed matrix membrane for adsorptive removal of As (III) from contaminated water solution, Sep. Purif. Technol. 118 (2013) 64–72.

[86] B. Li, F. Zhou, K. Huang, Y. Wang, S. Mei, Y. Zhou, T. Jing, Highly efficient

removal of lead and cadmium during wastewater irrigation using a polyethylenimine-grafted gelatin sponge, Sci. Rep. 6 (2016) 33573. https://doi.org/10.1038/srep33573.

[87] L. Li, Y. Li, C. Yang, Chemical filtration of Cr (VI) with electrospun chitosan nanofiber membranes, Carbohydr. Polym. 140 (2016) 299–307.

[88] J.H. Jhaveri, C.M. Patel, Z.V.P. Murthy, Preparation, characterization and application of GO-TiO2/PVC mixed matrix membranes for improvement in performance, J. Ind. Eng. Chem. 52 (2017) 138–146. doi:https://doi.org/10.1016/j.jiec.2017.03.035.

[89] M. Taheran, M. Naghdi, S.K. Brar, E. Knystautas, M. Verma, R.Y. Surampalli, J.R. Valero, Development of adsorptive membranes by confinement of activated biochar into electrospun nanofibers, Beilstein J. Nanotechnol. 7 (2016) 1556–1563. doi:10.3762/bjnano.7.149.

[90] J.-H. Kim, P.-K. Park, C.-H. Lee, H.-H. Kwon, Surface modification of nanofiltration membranes to improve the removal of organic micro-pollutants (EDCs and PhACs) in drinking water treatment: Graft polymerization and cross-linking followed by functional group substitution, J. Memb. Sci. 321 (2008) 190–198. doi:https://doi.org/10.1016/j.memsci.2008.04.055.

[91] M. Kamrani, A. Akbari, A. Yunessnia lehi, Chitosan-modified acrylic nanofiltration membrane for efficient removal of pharmaceutical compounds, J. Environ. Chem. Eng. 6 (2018) 583–587. doi:https://doi.org/10.1016/j.jece.2017.12.044.

[92] N. Yin, K. Wang, L. Wang, Z. Li, Amino-functionalized MOFs combining ceramic membrane ultrafiltration for Pb (II) removal, Chem. Eng. J. 306 (2016) 619–628. doi:https://doi.org/10.1016/j.cej.2016.07.064.

[93] J. de Grooth, D.M. Reurink, J. Ploegmakers, W.M. de Vos, K. Nijmeijer, Charged Micropollutant Removal With Hollow Fiber Nanofiltration Membranes Based On Polycation/Polyzwitterion/Polyanion Multilayers, ACS Appl. Mater. Interfaces. 6 (2014) 17009–17017. doi:10.1021/am504630a.

[94] D. Möckel, E. Staude, M.D. Guiver, Static protein adsorption, ultrafiltration behavior and cleanability of hydrophilized polysulfone membranes, J. Memb. Sci. 158 (1999) 63–75. doi:http://dx.doi.org/10.1016/S0376-7388(99)00028-9.

[95] M. Papageorgiou, C. Kosma, D. Lambropoulou, Seasonal occurrence, removal, mass loading and environmental risk assessment of 55 pharmaceuticals and personal care products in a municipal wastewater treatment plant in Central Greece, Sci. Total Environ. 543 (2016) 547–569. doi:https://doi.org/10.1016/j.scitotenv.2015.11.047.

[96] E.P. Favvas, F.K. Katsaros, S.K. Papageorgiou, A.A. Sapalidis, A.C. Mitropoulos, A review of the latest development of polyimide based membranes for CO2 separations, React. Funct. Polym. 120 (2017) 104–130. doi:https://doi.org/10.1016/j.reactfunctpolym.2017.09.002.

[97] S. Mu, S. Wang, S. Liang, K. Xiao, H. Fan, B. Han, C. Liu, X. Wang, X. Huang, Effect of the relative degree of foulant "hydrophobicity" on membrane fouling, J. Memb. Sci. 570–571 (2019) 1–8. doi:https://doi.org/10.1016/j.memsci.2018.10.023.

[98] K. Xiao, X. Wang, X. Huang, T.D. Waite, X. Wen, Combined effect of membrane and foulant hydrophobicity and surface charge on adsorptive fouling during microfiltration, J. Memb. Sci. 373 (2011) 140–151. doi:https://doi.org/10.1016/j.memsci.2011.02.041.

[99] W. Sun, J. Liu, H. Chu, B. Dong, Pretreatment and membrane hydrophilic modification to reduce membrane fouling, Membranes (Basel). 3 (2013) 226–241. doi:10.3390/membranes3030226.

[100] Y. Fang, Z.-K. Xu, J. Wu, E.M. V Hoek, V. V Tarabara, Surface Modification of Membranes, in: Encycl. Membr. Sci. Technol., John Wiley & Sons, Inc., 2013. doi:10.1002/9781118522318.emst061.

[101] Z. Wang, Y. Zhang, J. Zhang, L. Huang, J. Liu, Y. Li, G. Zhang, S.C. Kundu, L. Wang, Exploring natural silk protein sericin for regenerative medicine: an injectable, photoluminescent, cell-adhesive 3D hydrogel., Sci. Rep. 4 (2014)

7064. doi:10.1038/srep07064.

[102] M. Nagura, R. Ohnishi, Y. Gitoh, O. Faculty, T. Science, R. October, A. February, Structures and Physical Properties of Cross-Linked Sericin Membranes, J Insect Biotechnol Sericol. 70 (2001) 149–153. doi:10.11416/jibs2001.70.149.

[103] S.I. Voicu, R.M. Condruz, V. Mitran, A. Cimpean, F. Miculescu, C. Andronescu, M. Miculescu, V.K. Thakur, Sericin Covalent Immobilization onto Cellulose Acetate Membrane for Biomedical Applications, ACS Sustain. Chem. Eng. 4 (2016) 1765–1774. doi:10.1021/acssuschemeng.5b01756.

[104] M.A. Khosa, S.S. Shah, X. Feng, Metal sericin complexation and ultrafiltration of heavy metals from aqueous solution, Chem. Eng. J. 244 (2014) 446–456. doi:https://doi.org/10.1016/j.cej.2014.01.091.

[105] S. Yu, G. Yao, B. Dong, H. Zhu, X. Peng, J. Liu, M. Liu, C. Gao, Improving fouling resistance of thin-film composite polyamide reverse osmosis membrane by coating natural hydrophilic polymer sericin, Sep. Purif. Technol. 118 (2013) 285–293. doi:10.1016/j.seppur.2013.07.018.

[106] D. Gupta, H. Chaudhary, C. Gupta, Sericin based bioactive coating for polyester fabric, Indian J. Fibre Text. Res. 40 (2015) 70–80.

[107] J.S. Ahn, H.K. Choi, C.S. Cho, A novel mucoadhesive polymer prepared by template polymerization of acrylic acid in the presence of chitosan, Biomaterials. 22 (2001) 923–928. doi:10.1016/S0142-9612(00)00256-8.

[108] R. Rajendran, C. Balakumar, R. Sivakumar, T. Amruta, N. Devaki, Extraction and application of natural silk protein sericin from Bombyx mori as antimicrobial finish for cotton fabrics, J. Text. Inst. 103 (2012) 458–462. doi:10.1080/00405000.2011.586151.

[109] D. Gupta, A. Agrawal, A. Rangi, Extraction and characterization of silk sericin, Indian J. Fibre Text. Res. 39 (2014) 364–372. doi:http://op.niscair.res.in/index.php/IJFTR/article/view/3446.

[110] M. Muldar, Basic Principles of Membrane Technology, Springer Science & Business Media, 1997. doi:10.1007/978-94-009-1766-8.

[111] Y. Yoon, P. Westerhoff, S.A. Snyder, E.C. Wert, Nanofiltration and ultrafiltration of endocrine disrupting compounds, pharmaceuticals and personal care products, J. Memb. Sci. 270 (2006) 88–100. doi:10.1016/j.memsci.2005.06.045.

[112] D. Jermann, W. Pronk, M. Boller, A.I. Schäfer, The role of NOM fouling for the retention of estradiol and ibuprofen during ultrafiltration, J. Memb. Sci. 329 (2009) 75–84. doi:10.1016/j.memsci.2008.12.016.

[113] C. Sheng, A.G.A. Nnanna, Y. Liu, J.D. Vargo, Removal of Trace Pharmaceuticals from Water using coagulation and powdered activated carbon as pretreatment to ultrafiltration membrane system, Sci. Total Environ. 550 (2016) 1075–1083. doi:https://doi.org/10.1016/j.scitotenv.2016.01.179.

[114] C. Gadipelly, A. Pérez-González, G.D. Yadav, I. Ortiz, R. Ibáñez, V.K. Rathod, K. V. Marathe, Pharmaceutical Industry Wastewater: Review of the Technologies for Water Treatment and Reuse, Ind. Eng. Chem. Res. 53 (2014) 11571–11592. doi:10.1021/ie501210j.

[115] S.A. Snyder, S. Adham, A.M. Redding, F.S. Cannon, J. DeCarolis, J. Oppenheimer, E.C. Wert, Y. Yoon, Role of membranes and activated carbon in the removal of endocrine disruptors and pharmaceuticals, Desalination. 202 (2007) 156–181. doi:10.1016/j.desal.2005.12.052.

[116] L.C. Capozzi, F.M. Mehmood, M. Giagnorio, A. Tiraferri, M. Cerruti, M. Sangermano, Ultrafiltration Membranes Functionalized with Polydopamine with Enhanced Contaminant Removal by Adsorption, Macromol. Mater. Eng. 302 (2017) 1600481. doi:10.1002/mame.201600481.

[117] M. Nadour, F. Boukraa, A. Benaboura, Removal of Diclofenac, Paracetamol and Metronidazole using a carbon-polymeric membrane, J. Environ. Chem. Eng. 7 (2019) 103080. doi:https://doi.org/10.1016/j.jece.2019.103080.

[118] Z. Ouyang, Z. Huang, X. Tang, C. Xiong, M. Tang, Y. Lu, A dually charged

nanofiltration membrane by pH-responsive polydopamine for pharmaceuticals and personal care products removal, Sep. Purif. Technol. 211 (2019) 90–97. doi:https://doi.org/10.1016/j.seppur.2018.09.059.

[119] K. Kimura, G. Amy, J. Drewes, Y. Watanabe, Adsorption of hydrophobic compounds onto NF/RO membranes: an artifact leading to overestimation of rejection, J. Memb. Sci. 221 (2003) 89–101. doi:https://doi.org/10.1016/S0376-7388(03)00248-5.

[120] L.D. Nghiem, A.I. Sch??fer, M. Elimelech, Pharmaceutical retention mechanisms by nanofiltration membranes, Environ. Sci. Technol. 39 (2005) 7698–7705. doi:10.1021/es0507665.

[121] M. Röhricht, J. Krisam, U. Weise, U.R. Kraus, R.A. Düring, Elimination of carbamazepine, diclofenac and naproxen from treated wastewater by nanofiltration, Clean - Soil, Air, Water. 37 (2009) 638–641. doi:10.1002/clen.200900040.

[122] T. Heberer, D. Feldmann, K. Reddersen, H.-J. Altmann, T. Zimmermann, Removal of pharmaceutical residues and other persistent organics from municipal sewage and surface waters applying membrane filtration, J. Contemp. Water Res. Educ. 120 (2011) 3.

[123] V. Yangali-quintanilla, S.K. Maeng, T. Fujioka, M. Kennedy, Z. Li, G. Amy, Nanofiltration vs. reverse osmosis for the removal of emerging organic contaminants in water reuse, Desalin. Water Treat. 34 (2011) 50–56. doi:10/5004/dwt.2011.2860.

[124] W. Xiaobing, Z. Ping, The Development of Glass-Fiber Filter and the Process of the Needle-Punched Felt Made by Glass-Fiber [J], Tech. Text. 3 (2000).

[125] V. Kothari, S. Singh, Filtration behaviour of woven and nonwoven fabrics, Indian J. Fibre Text. Res. 32 (2007).

[126] G.E.R. Lamb, P. Costanza, B. Miller, Influences of Fiber Geometry on the Performance of Nonwoven Air Filters, Text. Res. J. 45 (1975) 452–463. doi:10.1177/004051757504500603.

[127] P. Kolte, U. Patil, Knitted and Non-Woven Filter Fabric, Man-Made Text. India. XLV (2017) 411–415.

[128] R. Neelakandan, V.R. Giridev, M. Murugesan, M. Madhusoothanan, Surface resistivity and shear characteristics of polyaniline coated polyester fabric, J. Ind. Text. 39 (2009) 175–186.

[129] T.E. Denny, Fibrillated polytetrafluoroethylene woven filter fabric, (1977).

[130] T. Tamura, Air filter, (1984).

[131] K. Desai, K. Kit, J. Li, P. Michael Davidson, S. Zivanovic, H. Meyer, Nanofibrous chitosan non-wovens for filtration applications, Polymer (Guildf). 50 (2009) 3661–3669. doi:https://doi.org/10.1016/j.polymer.2009.05.058.

[132] M.E. Yuksekkaya, M. Tercan, G. Dogan, An experimental investigation of nonwoven filter cloth with and without reinforcement of woven fabric, J. Text. Inst. 101 (2010) 950–957. doi:10.1080/00405000902986133.

[133] E.H. Tanabe, P.M. Barros, K.B. Rodrigues, M.L. Aguiar, Experimental investigation of deposition and removal of particles during gas filtration with various fabric filters, Sep. Purif. Technol. 80 (2011) 187–195. doi:https://doi.org/10.1016/j.seppur.2011.04.031.

[134] N.D. Gobi N, Evangelin S, Kasthuri R, Multilayer nonwoven fabrics for filtration of micron and submicron particles, J. Text. Eng. Fash. Technol. 5 (2019) 81–84. doi:10.15406/jteft.2019.05.00185.

[135] G. Liu, M. Xiao, X. Zhang, C. Gal, X. Chen, L. Liu, S. Pan, J. Wu, L. Tang, D. Clements-Croome, A review of air filtration technologies for sustainable and healthy building ventilation, Sustain. Cities Soc. 32 (2017) 375–396. doi:https://doi.org/10.1016/j.scs.2017.04.011.

[136] L. LIU, S. WANG, The development and applications of air filter [J], Filter Sep. 4 (2000).

[137] M.W. First, Hepa Filters, J. Am. Biol. Saf. Assoc. 3 (1998) 33–42. https://journals.sagepub.com/doi/pdf/10.1177/109135059800300111.

[138] J. Howard, Guidance for filtration an air-cleaning systems to protect building environments from airborne chemical, biological, or radiological attacks, Natl. Inst. Occup. Saf. Heal. 136 (2003).

[139] W. Zhang, S. Deng, Y. Wang, Z. Lin, Dust Loading performance of the PTFE HEPA Media and its comparison with the glass fibre HEPA media, Aerosol Air Qual. Res. 18 (2018) 1921–1931.

[140] N.A. George, M.G. Sutsko, D.B. McKenna, ULPA filter, (1996).

[141] W. Molter, H. Fissan, Evaluation of the internal structure data of HEPA glass fibre filter media, 55 (1995) 353–358.

[142] B.Y.H. Liu, K.L. Rubow, D.Y.H. Pui, Performance of HEPA and ULPA Filters, in: Proceedings, Annu. Tech. Meet. - Inst. Environ. Sci., 1985: pp. 25–28. https://www.scopus.com/inward/record.uri?eid=2-s2.0-0021942729&partnerID=40&md5=b69977531612df70b47d7d52c0cee7d8.

[143] H. Wang, Z.Y. Yang, J.Y. Liu, G.F. Zheng, Y.P. Liu, Research on the advantages of nanofibrous air filtration membrane, in: Key Eng. Mater., Trans Tech Publ, 2011: pp. 2016–2019.

[144] A. Podgórski, A. Bałazy, L. Gradoń, Application of nanofibers to improve the filtration efficiency of the most penetrating aerosol particles in fibrous filters, Chem. Eng. Sci. 61 (2006) 6804–6815. doi:https://doi.org/10.1016/j.ces.2006.07.022.

[145] W.W.-F. Leung, C.-H. Hung, P.-T. Yuen, Effect of face velocity, nanofiber packing density and thickness on filtration performance of filters with nanofibers coated on a substrate, Sep. Purif. Technol. 71 (2010) 30–37. doi:https://doi.org/10.1016/j.seppur.2009.10.017.

[146] D. Cho, A. Naydich, M.W. Frey, Y.L. Joo, Further improvement of air filtration efficiency of cellulose filters coated with nanofibers via inclusion of electrostatically active nanoparticles, Polymer (Guildf). 54 (2013) 2364–2372. doi:https://doi.org/10.1016/j.polymer.2013.02.034.

[147] R. Zhang, C. Liu, P.-C. Hsu, C. Zhang, N. Liu, J. Zhang, H.R. Lee, Y. Lu, Y. Qiu, S. Chu, Y. Cui, Nanofiber Air Filters with High-Temperature Stability for Efficient PM2.5 Removal from the Pollution Sources, Nano Lett. 16 (2016) 3642–3649. doi:10.1021/acs.nanolett.6b00771.

[148] X. Gao, J. Gou, L. Zhang, S. Duan, C. Li, A silk fibroin based green nano-filter for air filtration, RSC Adv. 8 (2018) 8181–8189. doi:10.1039/C7RA12879G.

[149] M. Suzuki, Activated carbon fiber: Fundamentals and applications, Carbon N. Y. 32 (1994) 577–586. doi:https://doi.org/10.1016/0008-6223(94)90075-2.

[150] P. Navarri, D. Marchal, A. Ginestet, Activated carbon fibre materials for VOC removal, Filtr. Sep. 38 (2001) 33–40. doi:https://doi.org/10.1016/S0015-1882(01)80150-6.

[151] C.H. Ao, S.C. Lee, Enhancement effect of TiO2 immobilized on activated carbon filter for the photodegradation of pollutants at typical indoor air level, Appl. Catal. B Environ. 44 (2003) 191–205. doi:https://doi.org/10.1016/S0926-3373(03)00054-7.

[152] C.H. Ao, S.C. Lee, Indoor air purification by photocatalyst TiO2 immobilized on an activated carbon filter installed in an air cleaner, Chem. Eng. Sci. 60 (2005) 103–109. doi:https://doi.org/10.1016/j.ces.2004.01.073.

[153] M.A. Sidheswaran, H. Destaillats, D.P. Sullivan, S. Cohn, W.J. Fisk, Energy efficient indoor VOC air cleaning with activated carbon fiber (ACF) filters, Build. Environ. 47 (2012) 357–367. doi:https://doi.org/10.1016/j.buildenv.2011.07.002.

[154] B. Panilaitis, G.H. Altman, J. Chen, H.J. Jin, V. Karageorgiou, D.L. Kaplan, Macrophage responses to silk, Biomaterials. 24 (2003) 3079–3085. doi:10.1016/S0142-9612(03)00158-3.

[155] T. Gamo, T. Inokuchi, H. Laufer, Polypeptides of fibroin and sericin secreted from the different sections of the silk gland in Bombyx mori, Insect Biochem. 7 (1977) 285–295. doi:10.1016/0020-1790(77)90026-9.

[156] J. Huang, R. Valluzzi, E. Bini, B. Vernaglia, D.L. Kaplan, Cloning, Expression, and Assembly of Sericin-like Protein, J. Biol. Chem. 278 (2003) 46117–46123. doi:10.1074/jbc.M307792200.

[157] T. Gamo, T. Inokuchi, H. Laufer, Polypeptides of fibroin and sericin secreted from the different sections of the silk gland in Bombyx mori, Insect Biochem. 7 (1977) 285–295. doi:10.1016/0020-1790(77)90026-9.

[158] P. Aramwit, S. Kanokpanont, W. De-Eknamkul, K. Kamei, T. Srichana, The effect of sericin with variable amino-acid content from different silk strains on the production of collagen and nitric oxide., J Biomater Sci Polym Edn. 20 (2009) 1295–1306. doi:10.1163/156856209X453006.

[159] K. K., Recent advances in sericin research, J. Sericult. Sci. Japan. 69 (1980) 457–465.

[160] H.W. Kwak, Y.S. Yang, M.K. Kim, J.Y. Lee, H. Yun, M.H. Kim, K.H. Lee, Chromium (VI) Adsorption Behavior of Silk Sericin Beads, Int. J. Ind. Entomol. 26 (2013) 47–53.

[161] X. Chen, K.F. Lam, S.F. Mak, K.L. Yeung, Precious metal recovery by selective adsorption using biosorbents, J. Hazard. Mater. 186 (2011) 902–910. doi:10.1016/j.jhazmat.2010.11.088.

[162] H. Teramoto, K. Nakajima, C. Takabayashi, Preparation of elastic silk sericin hydrogel., Biosci. Biotechnol. Biochem. 69 (2005) 845–847. doi:10.1271/bbb.69.845.

[163] H.W. Kwak, Y. Kim, N.K. Yun, K.H. Lee, Silk sericin microparticles as a biosorbent for hexavalent chromium ion, Macromol. Res. 22 (2014) 788–795. doi:10.1007/s13233-014-2122-x.

[164] X. Chen, K.F. Lam, S.F. Mak, W.K. Ching, T.N. Ng, K.L. Yeung, Assessment of sericin biosorbent for selective dye removal, Chinese J. Chem. Eng. 20 (2012) 426–432. doi:10.1016/S1004-9541(11)60149-3.

[165] S. Sarovart, B. Sudatis, P. Meesilpa, B.P. Grady, R. Magaraphan, The use of

sericin as an antioxidant and antimicrobial for polluted air treatment, Rev. Adv. Mater. Sci. 5 (2003) 193–198. doi:https://www.scopus.com/inward/record.uri?eid=2-s2.0-4944254022&partnerID=40&md5=81db7c83ea66e9316e0a0cb69ec26a91.

[166] R. Purwar, K. Sai Goutham, C.M. Srivastava, Electrospun Sericin/PVA/Clay nanofibrous mats for antimicrobial air filtration mask, Fibers Polym. 17 (2016) 1206–1216. doi:10.1007/s12221-016-6345-7.

[167] C. Wang, S. Wu, M. Jian, J. Xie, L. Xu, X. Yang, Q. Zheng, Y. Zhang, Silk nanofibers as high efficient and lightweight air filter, Nano Res. 9 (2016) 2590–2597.

[168] K. Min, S. Kim, S. Kim, Silk protein nanofibers for highly efficient, eco-friendly, optically translucent, and multifunctional air filters, Sci. Rep. 8 (2018) 9598. doi:10.1038/s41598-018-27917-w.

[169] X. Chen, K.F. Lam, S.F. Mak, K.L. Yeung, Precious metal recovery by selective adsorption using biosorbents, J. Hazard. Mater. 186 (2011) 902–910. doi:10.1016/j.jhazmat.2010.11.088.

[170] H.W. Kwak, Y.S. Yang, M.K. Kim, J.Y. Lee, H. Yun, M.H. Kim, K.H. Lee, Chromium(VI) Adsorption Behavior of Silk Sericin Beads, Int. J. Ind. Entomol. 26 (2013) 47–53. doi:10.7852/ijie.2013.26.1.047.

[171] T.L. da Silva, A.C. da Silva, M.G.A. Vieira, M.L. Gimenes, M.G.C. da Silva, Biosorption study of copper and zinc by particles produced from silk sericin ??? alginate blend: evaluation of blend proportion and thermal cross-linking process in particles production, J. Clean. Prod. 137 (2016) 1470–1478. doi:10.1016/j.jclepro.2015.05.067.

[172] V.R. Silva, F. Hamerski, T.A. Weschenfelder, M. Ribani, M.L. Gimenes, A.P. Scheer, Equilibrium, kinetic, and thermodynamic studies on the biosorption of Bordeaux S dye by sericin powder derived from cocoons of the silkworm Bombyx mori, Desalin. Water Treat. 57 (2016) 5119–5129. doi:10.1080/19443994.2014.996776.

[173] P. Koley, M. Sakurai, M. Aono, Controlled Fabrication of Silk Protein Sericin Mediated Hierarchical Hybrid Flowers and Their Excellent Adsorption Capability of Heavy Metal Ions of Pb(II), Cd(II) and Hg(II), ACS Appl. Mater. Interfaces. 8 (2016) 2380–2392. doi:10.1021/acsami.5b11533.

[174] B. Van der Bruggen, M. Mänttäri, M. Nyström, Drawbacks of applying nanofiltration and how to avoid them: A review, Sep. Purif. Technol. 63 (2008) 251–263. doi:10.1016/j.seppur.2008.05.010.

[175] N. Hilal, O.O. Ogunbiyi, N.J. Miles, R. Nigmatullin, Methods employed for control of fouling in MF and UF membranes: A comprehensive review, Sep. Sci. Technol. 40 (2005) 1957–2005. doi:10.1081/SS-200068409.

[176] E.M. Vrijenhoek, S. Hong, M. Elimelech, Influence of membrane surface properties on initial rate of colloidal fouling of reverse osmosis and nanofiltration membranes, J. Memb. Sci. 188 (2001) 115–128. doi:10.1016/S0376-7388(01)00376-3.

[177] Q. Li, Z. Xu, I. Pinnau, Fouling of reverse osmosis membranes by biopolymers in wastewater secondary effluent: Role of membrane surface properties and initial permeate flux, J. Memb. Sci. 290 (2007) 173–181. doi:10.1016/j.memsci.2006.12.027.

[178] G. Genç, O. Bayraktar, G. Basal, A research on the production of silk sericin powders by using spray drying method, Tekst. ve Konfeksiyon. 19 (2009) 273–279.

[179] R.. Patel, M.. Modasiya, Sericin: Pharmaceutical Applications, Int. J. Res. Pharm. Biomed. Sci. 2 (2011) 913–917.

[180] I. Belhaj Khalifa, N. Ladhari, M. Touay, Application of sericin to modify textile supports, J. Text. Inst. 103 (2012) 370–377. doi:10.1080/00405000.2011.580539.

[181] W. Senakoon, S. Nuchadomrong, S. Sirimungkararat, T. Senawong, P. Kitikoon, Antibacterial action of eri (samia ricini) sericin against escherichia coli and staphylococcus aureus, Asian J Food Agro-Ind. 2 (2009) S222--228. Retrieved.

[182] J. Pandiarajan, B.P. Cathrin, T. Pratheep, M. Krishnan, Defense role of the cocoon in the silk worm Bombyx mori L., Rapid Commun. Mass Spectrom. 25 (2011) 3203–3206. doi:10.1002/rcm.5213.

[183] P.N. Bhat, S. Nivedita, S. Roy, Use of sericin of Bombyx mori in the synthesis of silver nanoparticles, their characterization and application, Indian J. Fibre Text. Res. 36 (2011) 167–171.

[184] P. Aramwit, N. Bang, J. Ratanavaraporn, S. Ekgasit, Green synthesis of silk sericin-capped silver nanoparticles and their potent anti-bacterial activity, Nanoscale Res. Lett. 9 (2014) 79. doi:10.1186/1556-276X-9-79.

[185] R. Zhao, X. Li, B. Sun, Y. Zhang, D. Zhang, Z. Tang, X. Chen, C. Wang, Electrospun chitosan/sericin composite nanofibers with antibacterial property as potential wound dressings, Int. J. Biol. Macromol. 68 (2014) 92–97. doi:10.1016/j.ijbiomac.2014.04.029.

[186] M. Joshi, M.L. Gulrajani, M. Bar, Novel cross-linked sericin films: Characterization and properties, J. Appl. Polym. Sci. 132 (2015). doi:10.1002/app.41400.

[187] B. Kasprzyk-Hordern, Pharmacologically active compounds in the environment and their chirality., Chem. Soc. Rev. 39 (2010) 4466–4503. doi:10.1039/c000408c.

[188] Y. Wang, C. Shen, L. Li, H. Li, M. Zhang, Electrocatalytic degradation of ibuprofen in aqueous solution by a cobalt-doped modified lead dioxide electrode: influencing factors and energy demand, RSC Adv. 6 (2016) 30598–30610.

[189] A. Leach, Chemical database of bioactive molecules with drug-like properties (ChEMBL), Eur. Mol. Biol. Lab. (2019). https://www.ebi.ac.uk/chembl/ (accessed September 8, 2019).

[190] P.K. Mutiyar, A.K. Mittal, Occurrences and fate of an antibiotic amoxicillin in extended aeration-based sewage treatment plant in Delhi, India: a case study of emerging pollutant, Desalin. Water Treat. 51 (2013) 6158–6164. doi:10.1080/19443994.2013.770199.

[191] V. Diwan, A.J. Tamhankar, R.K. Khandal, S. Sen, M. Aggarwal, Y. Marothi, R. V Iyer, K. Sundblad-Tonderski, C. Stålsby- Lundborg, Antibiotics and antibiotic-resistant bacteria in waters associated with a hospital in Ujjain, India, BMC Public Health. 10 (2010) 414. doi:10.1186/1471-2458-10-414.

[192] B. Subedi, K. Balakrishna, R.K. Sinha, N. Yamashita, V.G. Balasubramanian, K. Kannan, Mass loading and removal of pharmaceuticals and personal care products, including psychoactive and illicit drugs and artificial sweeteners, in five sewage treatment plants in India, J. Environ. Chem. Eng. 3 (2015) 2882–2891. doi:https://doi.org/10.1016/j.jece.2015.09.031.

[193] B. Subedi, K. Balakrishna, D.I. Joshua, K. Kannan, Mass loading and removal of pharmaceuticals and personal care products including psychoactives, antihypertensives, and antibiotics in two sewage treatment plants in southern India, Chemosphere. 167 (2017) 429–437. doi:https://doi.org/10.1016/j.chemosphere.2016.10.026.

[194] G. Archana, R. Dhodapkar, A. Kumar, Offline solid-phase extraction for preconcentration of pharmaceuticals and personal care products in environmental water and their simultaneous determination using the reversed phase high-performance liquid chromatography method, Environ. Monit. Assess. 188 (2016) 512. doi:10.1007/s10661-016-5510-1.

[195] K.P. Singh, P. Rai, A.K. Singh, P. Verma, S. Gupta, Occurrence of pharmaceuticals in urban wastewater of north Indian cities and risk assessment, Environ. Monit. Assess. 186 (2014) 6663–6682. doi:10.1007/s10661-014-3881-8.

[196] T. Anumol, A. Vijayanandan, M. Park, L. Philip, S.A. Snyder, Occurrence and fate of emerging trace organic chemicals in wastewater plants in Chennai, India, Environ. Int. 92–93 (2016) 33–42. doi:https://doi.org/10.1016/j.envint.2016.03.022.

[197] S. Mohapatra, C.-H. Huang, S. Mukherji, L.P. Padhye, Occurrence and fate of pharmaceuticals in WWTPs in India and comparison with a similar study in the United States, Chemosphere. 159 (2016) 526–535.

doi:https://doi.org/10.1016/j.chemosphere.2016.06.047.

[198] A.C. Johnson, M.D. Jürgens, N. Nakada, S. Hanamoto, A.C. Singer, H. Tanaka, Linking changes in antibiotic effluent concentrations to flow, removal and consumption in four different UK sewage treatment plants over four years, Environ. Pollut. 220 (2017) 919–926. doi:https://doi.org/10.1016/j.envpol.2016.10.077.

[199] F.O. Agunbiade, B. Moodley, Pharmaceuticals as emerging organic contaminants in Umgeni River water system, KwaZulu-Natal, South Africa, Environ. Monit. Assess. 186 (2014) 7273–7291. doi:10.1007/s10661-014-3926-z.

[200] T.A. Ternes, M. Bonerz, N. Herrmann, B. Teiser, H.R. Andersen, Irrigation of treated wastewater in Braunschweig, Germany: An option to remove pharmaceuticals and musk fragrances, Chemosphere. 66 (2007) 894–904. doi:https://doi.org/10.1016/j.chemosphere.2006.06.035.

[201] T. Venkatesh, S. Senthilmurugan, Grey water treatment and simultaneous surfactant recovery using UF and RO process, Sep. Sci. Technol. 52 (2017) 2262–2273. doi:10.1080/01496395.2016.1273244.

[202] S.K. Behera, S.Y. Oh, H.S. Park, Sorptive removal of ibuprofen from water using selected soil minerals and activated carbon, Int. J. Environ. Sci. Technol. 9 (2012) 85–94. doi:10.1007/s13762-011-0020-8.

[203] G. Capar, Separation of silkworm proteins in cocoon cooking wastewaters via nanofiltration: Effect of solution pH on enrichment of sericin, J. Memb. Sci. 389 (2012) 509–521. doi:10.1016/j.memsci.2011.11.021.

[204] H.-C. Mahler, W. Friess, U. Grauschopf, S. Kiese, Protein aggregation: Pathways, induction factors and analysis, J. Pharm. Sci. 98 (2009) 2909–2934. doi:https://doi.org/10.1002/jps.21566.

[205] Z. Wang, Y. Zhang, J. Zhang, L. Huang, J. Liu, Y. Li, G. Zhang, S.C. Kundu, L. Wang, Exploring natural silk protein sericin for regenerative medicine: an injectable, photoluminescent, cell-adhesive 3D hydrogel., Sci. Rep. 4 (2014)

7064. doi:10.1038/srep07064.

[206] X. Du, Y. Li, Y.-L. Xia, S.-M. Ai, J. Liang, P. Sang, X.-L. Ji, S.-Q. Liu, Insights into Protein-Ligand Interactions: Mechanisms, Models, and Methods., Int. J. Mol. Sci. 17 (2016) 144. doi:10.3390/ijms17020144.

[207] M.S. Jahan, M.J. Islam, R. Begum, R. Kayesh, A. Rahman, A Study of Method Development, Validation, and Forced Degradation for Simultaneous Quantification of Paracetamol and Ibuprofen in Pharmaceutical Dosage Form by RP-HPLC Method, Anal. Chem. Insights. 9 (2014) 75–81. doi:10.4137/ACI.S18651.

[208] B. Yilmaz, A. Asci, S.S. Palabiyik, HPLC Method for Determination of Diclofenac in Human Plasma and Its Application to a Pharmacokinetic Study in Turkey, J. Chromatogr. Sci. 49 (2011) 422–427. doi:10.1093/chrsci/49.6.422.

[209] L.R.P. De Abreu, R.A.M. Ortiz, S.C. de Castro, J. Pedrazzoli, HPLC determination of amoxicillin comparative bioavailability in healthy volunteers after a single dose administration., J. Pharm. Pharm. Sci. (2003).

[210] J. Vella, F. Busuttil, N.S. Bartolo, C. Sammut, V. Ferrito, A. Serracino-Inglott, L.M. Azzopardi, G. LaFerla, A simple HPLC–UV method for the determination of ciprofloxacin in human plasma, J. Chromatogr. B. 989 (2015) 80–85. doi:https://doi.org/10.1016/j.jchromb.2015.01.006.

[211] W. Mnif, I. Zidi, A.I.H. Hassine, E. Gomez, A. Bartegi, B. Roig, P. Balaguer, Monitoring Endocrine Disrupter Compounds in the Tunisian Hamdoun River using In Vitro Bioassays, Soil Sediment Contam. An Int. J. 21 (2012) 815–830. doi:10.1080/15320383.2012.691575.

[212] A.H. Pelofsky, Propylene-Sulfuric Acid Reaction, Ind. Eng. Chem. Prod. Res. Dev. 11 (1972) 187–191. doi:10.1021/i360042a012.

[213] M. Ahsani, R. Yegani, Study on the fouling behavior of silica nanocomposite modified polypropylene membrane in purification of collagen protein, Chem. Eng. Res. Des. 102 (2015) 261–273. doi:10.1016/J.CHERD.2015.06.035.

[214] H.C. Thomas, Heterogeneous Ion Exchange in a Flowing System, J. Am. Chem. Soc. 66 (1944) 1664–1666. doi:10.1021/ja01238a017.

[215] Y.H.E.E. YOON, J.H. NELSON, Application of Gas Adsorption Kinetics I. A Theoretical Model for Respirator Cartridge Service Life, Am. Ind. Hyg. Assoc. J. 45 (1984) 509–516. doi:10.1080/15298668491400197.

[216] R.M. Clark, Evaluating the cost and performance of field-scale granular activated carbon systems, Environ. Sci. Technol. 21 (1987) 573–580. doi:10.1021/es00160a008.

[217] K.H. Chu, Fixed bed sorption: Setting the record straight on the Bohart–Adams and Thomas models, J. Hazard. Mater. 177 (2010) 1006–1012. doi:https://doi.org/10.1016/j.jhazmat.2010.01.019.

[218] G.S. Bohart, E.Q. Adams, Some aspects of the behavior of charcoal with respect to chlorine, J. Am. Chem. Soc. 42 (1920) 523–544. doi:10.1021/ja01448a018.

[219] I. Langmuir, The adsorption of gases on plane surfaces of glass, mica and platinum., J. Am. Chem. Soc. 40 (1918) 1361–1403.

[220] H.M.F. Freundlich, Over the adsorption in solution, J. Phys. Chem. 57 (1906) 1100–1107.

[221] R. Sips, Combined form of Langmuir and Freundlich equations, J. Chem. Phys. 16 (1948) 490–495.

[222] V.K. Gupta, I. Ali, T.A. Saleh, A. Nayak, S. Agarwal, Chemical treatment technologies for waste-water recycling-an overview, RSC Adv. 2 (2012) 6380–6388. doi:10.1039/C2RA20340E.

[223] K. Kimura, S. Toshima, G. Amy, Y. Watanabe, Rejection of neutral endocrine disrupting compounds (EDCs) and pharmaceutical active compounds (PhACs) by RO membranes, J. Memb. Sci. 245 (2004) 71–78. doi:10.1016/j.memsci.2004.07.018.

[224] I. Vergili, Application of nanofiltration for the removal of carbamazepine, diclofenac and ibuprofen from drinking water sources, J. Environ. Manage. 127

(2013) 177–187. doi:10.1016/j.jenvman.2013.04.036.

[225] J. Radjenović, M. Petrović, F. Ventura, D. Barceló, Rejection of pharmaceuticals in nanofiltration and reverse osmosis membrane drinking water treatment, Water Res. 42 (2008) 3601–3610. doi:10.1016/j.watres.2008.05.020.

[226] V.K. Gupta, T.A. Saleh, Sorption of pollutants by porous carbon, carbon nanotubes and fullerene- An overview, Environ. Sci. Pollut. Res. 20 (2013) 2828–2843. doi:10.1007/s11356-013-1524-1.

[227] K. Tiek Wong, Y. Yoon, M. Jang, Enhanced recyclable magnetized palm shell waste-based powdered activated carbon for the removal of ibuprofen: Insights for kinetics and mechanisms, PLoS One. 10 (2015) e0141013. doi:10.1371/journal.pone.0141013.

[228] P. Westerhoff, Y. Yoon, S. Snyder, E. Wert, Fate of endocrine-disruptor, pharmaceutical, and personal care product chemicals during simulated drinking water treatment processes, Environ. Sci. Technol. 39 (2005) 6649–6663. doi:10.1021/es0484799.

[229] T.M.S. Attia, X.L. Hu, Y. Da Qiang, Synthesized magnetic nanoparticles coated zeolite for the adsorption of pharmaceutical compounds from aqueous solution using batch and column studies, Chemosphere. 93 (2013) 2076–2085. doi:10.1016/j.chemosphere.2013.07.046.

[230] T.X. Bui, H. Choi, Adsorptive removal of selected pharmaceuticals by mesoporous silica SBA-15, J. Hazard. Mater. 168 (2009) 602–608. doi:10.1016/j.jhazmat.2009.02.072.

[231] Y. Liu, Y. Guo, Y. Zhu, D. An, W. Gao, Z. Wang, Y. Ma, Z. Wang, A sustainable route for the preparation of activated carbon and silica from rice husk ash, J. Hazard. Mater. 186 (2010) 1314–1319. doi:10.1016/j.jhazmat.2010.12.007.

[232] H. Li, W. Shi, W. Wang, H. Zhu, The extraction of sericin protein from silk reeling wastewater by hollow fiber nanofiltration membrane integrated process, Sep. Purif. Technol. 146 (2015) 342–350. doi:10.1016/j.seppur.2015.04.004.

[233] C. Fabiani, M. Pizzichini, M. Spadoni, G. Zeddita, Treatment of waste water from silk degumming processes for protein recovery and water reuse, Desalination. 105 (1996) 1–9. doi:10.1016/0011-9164(96)00050-1.

[234] H. Li, W. Shi, W. Wang, H. Zhu, The extraction of sericin protein from silk reeling wastewater by hollow fiber nanofiltration membrane integrated process, Sep. Purif. Technol. 146 (2015) 342–350. doi:10.1016/j.seppur.2015.04.004.

[235] X. Chen, K.F. Lam, S.F. Mak, W.K. Ching, T.N. Ng, K.L. Yeung, Assessment of sericin biosorbent for selective dye removal, Chinese J. Chem. Eng. 20 (2012) 426–432. doi:10.1016/S1004-9541(11)60149-3.

[236] S.M. Edington, Environmental Biotechnology, in: A. Kumar (Ed.), Bioscience, Daya Books, New Delhi, 1994: pp. 420-.

[237] D.P. Grover, J.L. Zhou, P.E. Frickers, J.W. Readman, Improved removal of estrogenic and pharmaceutical compounds in sewage effluent by full scale granular activated carbon: Impact on receiving river water, J. Hazard. Mater. 185 (2011) 1005–1011. doi:http://dx.doi.org/10.1016/j.jhazmat.2010.10.005.

[238] A. Rossner, S.A. Snyder, D.R.U. Knappe, Removal of emerging contaminants of concern by alternative adsorbents, Water Res. 43 (2009) 3787–3796. doi:http://dx.doi.org/10.1016/j.watres.2009.06.009.

[239] X. Li, L. Li, M. Zheng, G. Fu, J.S. Lar, Anaerobic co-digestion of cattle manure with corn stover pretreated by sodium hydroxide for efficient biogas production, Energy & Fuels. 23 (2009) 4635–4639.

[240] J. Heo, L. Joseph, Y. Yoon, Y.-G. Park, N. Her, J. Sohn, S.-H. Yoon, Removal of micropollutants and NOM in carbon nanotube-UF membrane system from seawater, Water Sci. Technol. 63 (2011) 2737–2744.

[241] Y.-L. Zhang, J. Zhang, C.-M. Dai, X.-F. Zhou, S.-G. Liu, Sorption of carbamazepine from water by magnetic molecularly imprinted polymers based on chitosan-Fe_3O_4, Carbohydr. Polym. 97 (2013) 809–816. doi:10.1016/j.carbpol.2013.05.072.

[242] A. Alsbaiee, B.J. Smith, L. Xiao, Y. Ling, D.E. Helbling, W.R. Dichtel, Rapid removal of organic micropollutants from water by a porous β-cyclodextrin polymer, Nature. 529 (2016) 190–194. http://dx.doi.org/10.1038/nature16185.

[243] H.M. Ötker, I. Akmehmet-Balcıoğlu, Adsorption and degradation of enrofloxacin, a veterinary antibiotic on natural zeolite, J. Hazard. Mater. 122 (2005) 251–258. doi:http://dx.doi.org/10.1016/j.jhazmat.2005.03.005.

[244] Z. Bekçi, Y. Seki, M.K. Yurdakoç, Equilibrium studies for trimethoprim adsorption on montmorillonite KSF, J. Hazard. Mater. 133 (2006) 233–242. doi:http://dx.doi.org/10.1016/j.jhazmat.2005.10.029.

[245] E.K. Putra, R. Pranowo, J. Sunarso, N. Indraswati, S. Ismadji, Performance of activated carbon and bentonite for adsorption of amoxicillin from wastewater: Mechanisms, isotherms and kinetics, Water Res. 43 (2009) 2419–2430. doi:http://dx.doi.org/10.1016/j.watres.2009.02.039.

[246] Y.-H. Kim, B. Lee, K.-H. Choo, S.-J. Choi, Selective adsorption of bisphenol A by organic–inorganic hybrid mesoporous silicas, Microporous Mesoporous Mater. 138 (2011) 184–190. doi:http://dx.doi.org/10.1016/j.micromeso.2010.09.007.

[247] M. Acharya, S. Mishra, R.N. Sahoo, S. Mallick, Infrared spectroscopy for analysis of co-processed ibuprofen and magnesium trisilicate at milling and freeze drying, Acta Chim. Slov. 64 (2017) 45–54.

[248] M.L. Vueba, M.E. Pina, L.A.E. Batista De Carvalho, Conformational stability of ibuprofen: Assessed by DFT calculations and optical vibrational spectroscopy, J. Pharm. Sci. 97 (2008) 845–859. doi:10.1002/jps.21007.

[249] H. Teramoto, M. Miyazawa, Molecular orientation behavior of silk sericin film as revealed by ATR infrared spectroscopy, Biomacromolecules. 6 (2005) 2049–2057. doi:10.1021/bm0500547.

[250] M. Jackson, H.H. Mantsch, Protein secondary structure from FT-IR spectroscopy: correlation with dihedral angles from three-dimensional Ramachandran plots, Can. J. Chem. 69 (1991) 1639–1642. doi:10.1139/v91-240.

[251] H. Zhang, L. Deng, M. Yang, S. Min, L. Yang, L. Zhu, Enhancing effect of glycerol on the tensile properties of bombyx mori cocoon sericin films, Int. J. Mol. Sci. 12 (2011) 3170–3181. doi:10.3390/ijms12053170.

[252] D.M. Byler, H. Susi, Examination of the secondary structure of proteins by deconvolved FTIR spectra, Biopolymers. 25 (1986) 469–487. doi:10.1002/bip.360250307.

[253] W.K. Surewicz, H.H. Mantsch, D. Chapman, Determination of protein secondary structure by Fourier transform infrared spectroscopy: A critical assessment, Biochemistry. 32 (1993) 389–394. doi:10.1021/bi00053a001.

[254] H. Teramoto, A. Kakazu, T. Asakura, Native structure and degradation pattern of silk sericin studied by 13C NMR spectroscopy, Macromolecules. 39 (2006) 6–8. doi:10.1021/ma0521147.

[255] R. Dash, S.K. Ghosh, D.L. Kaplan, S.C. Kundu, Purification and biochemical characterization of a 70??kDa sericin from tropical tasar silkworm, Antheraea mylitta, Comp. Biochem. Physiol. - B Biochem. Mol. Biol. 147 (2007) 129–134. doi:10.1016/j.cbpb.2007.01.009.

[256] J.R. Lakowicz, Principles of fluorescence spectroscopy, Springer Science & Business Media, 2006. doi:10.1007/978-0-387-46312-4.

[257] X. Yu, Y. Yang, L. Shiyu, Q. Yao, L. Heting, L. Xiaofang, Y. Pinggui, The fluorescence spectroscopic study on the interaction between imidazo[2,1-b]thiazole analogues and bovine serum albumin, Spectrochim. Acta - Part A Mol. Biomol. Spectrosc. 83 (2011) 322–328. doi:10.1016/j.saa.2011.08.038.

[258] G. Mandal, M. Bardhan, T. Ganguly, Interaction of bovine serum albumin and albumin-gold nanoconjugates with l-aspartic acid. A spectroscopic approach, Colloids Surfaces B Biointerfaces. 81 (2010) 178–184. doi:10.1016/j.colsurfb.2010.07.002.

[259] R. Perozzo, G. Folkers, L. Scapozza, Thermodynamics of Protein–Ligand Interactions: History, Presence, and Future Aspects, J. Recept. Signal Transduct. 24 (2004) 1–52. doi:10.1081/RRS-120037896.

[260] E. Dudognon, F. Danède, M. Descamps, N.T. Correia, Evidence for a new crystalline phase of racemic Ibuprofen, Pharm. Res. 25 (2008) 2853–2858. doi:10.1007/s11095-008-9655-7.

[261] L.-S. Wan, Z.-M. Liu, Z.-K. Xu, Surface engineering of macroporous polypropylene membranes, Soft Matter. 5 (2009) 1775–1785.

[262] M. Ulbricht, Advanced functional polymer membranes, Polymer (Guildf). 47 (2006) 2217–2262. doi:10.1016/j.polymer.2006.01.084.

[263] L.Y. Ng, A.W. Mohammad, C.P. Leo, N. Hilal, Polymeric membranes incorporated with metal/metal oxide nanoparticles: A comprehensive review, Desalination. 308 (2013) 15–33. doi:https://doi.org/10.1016/j.desal.2010.11.033.

[264] T.-C. Chung, Hydrophilic polypropylene membranes, (1998).

[265] N.F. Himma, A.K. Wardani, I.G. Wenten, Preparation of Superhydrophobic Polypropylene Membrane Using Dip-Coating Method: The Effects of Solution and Process Parameters, Polym. Plast. Technol. Eng. 56 (2017) 184–194. doi:10.1080/03602559.2016.1185666.

[266] D.A. and A.K. Wardani, Modification and Applications of Hydrophilic Polypropylene Membrane, IOP Conf. Ser. Mater. Sci. Eng. 214 (2017) 12014. doi:10.1088/1757-899X/214/1/012014.

[267] A. Mukhopadhyay, 7 - Composite nonwovens in filters: theory, in: D. Das, B.B.T.-C.N.-W.M. Pourdeyhimi (Eds.), Woodhead Publishing, 2014: pp. 120–163. doi:https://doi.org/10.1533/9780857097750.120.

[268] J.A. Nilson, F.A. DiGiano, Influence of NOM composition on nanofiltration, J. / Am. Water Work. Assoc. 88 (1996) 53–66. doi:10.1002/j.1551-8833.1996.tb06555.x.

[269] Y. Lv, X. Yu, S.-T. Tu, J. Yan, E. Dahlquist, Wetting of polypropylene hollow fiber membrane contactors, J. Memb. Sci. 362 (2010) 444–452. doi:https://doi.org/10.1016/j.memsci.2010.06.067.

[270] Y.-F. Zhao, L.-P. Zhu, Z. Yi, B.-K. Zhu, Y.-Y. Xu, Improving the hydrophilicity

and fouling-resistance of polysulfone ultrafiltration membranes via surface zwitterionicalization mediated by polysulfone-based triblock copolymer additive, J. Memb. Sci. 440 (2013) 40–47. doi:https://doi.org/10.1016/j.memsci.2013.03.064.

[271] C.-H. Zhang, F. Yang, W.-J. Wang, B. Chen, Preparation and characterization of hydrophilic modification of polypropylene non-woven fabric by dip-coating PVA (polyvinyl alcohol), Sep. Purif. Technol. 61 (2008) 276–286. doi:https://doi.org/10.1016/j.seppur.2007.10.019.

[272] H.-Y. Yu, L.-Q. Liu, Z.-Q. Tang, M.-G. Yan, J.-S. Gu, X.-W. Wei, Surface modification of polypropylene microporous membrane to improve its antifouling characteristics in an SMBR: Air plasma treatment, J. Memb. Sci. 311 (2008) 216–224. doi:https://doi.org/10.1016/j.memsci.2007.12.016.

[273] J. Han, W. Qiu, J. Hu, W. Gao, Chemisorption of estrone in nylon microfiltration membranes: Adsorption mechanism and potential use for estrone removal from water, Water Res. 46 (2012) 873–881. doi:https://doi.org/10.1016/j.watres.2011.11.066.

[274] B. Bhadra, I. Ahmed, S. Kim, S. Jhung, Adsorptive removal of ibuprofen and diclofenac from water using metal-organic framework-derived porous carbon, Chem. Eng. J. 314 (2017) 50–58. doi:10.1016/j.cej.2016.12.127.

[275] P.W. Seo, B.N. Bhadra, I. Ahmed, N.A. Khan, S.H. Jhung, Adsorptive Removal of Pharmaceuticals and Personal Care Products from Water with Functionalized Metal-organic Frameworks: Remarkable Adsorbents with Hydrogen-bonding Abilities, Sci. Rep. 6 (2016) 34462. https://doi.org/10.1038/srep34462.

[276] K.A. Landry, P. Sun, C.-H. Huang, T.H. Boyer, Ion-exchange selectivity of diclofenac, ibuprofen, ketoprofen, and naproxen in ureolyzed human urine, Water Res. 68 (2015) 510–521. doi:https://doi.org/10.1016/j.watres.2014.09.056.

[277] X. Peng, F. Hu, F.L.-Y. Lam, Y. Wang, Z. Liu, H. Dai, Adsorption behavior and mechanisms of ciprofloxacin from aqueous solution by ordered mesoporous carbon and bamboo-based carbon, J. Colloid Interface Sci. 460 (2015) 349–360.

doi:https://doi.org/10.1016/j.jcis.2015.08.050.

[278] M. Wiśniewska, G. Fijałkowska, K. Szewczuk-Karpisz, T. Urban, A. Nosal-Wiercińska, G. Wójcik, Comparison of adsorption affinity of anionic and cationic polyacrylamides for montmorillonite surface in the presence of chromium(VI) ions, Adsorption. 25 (2019) 41–50. doi:10.1007/s10450-018-9990-x.

[279] J. Ma, M. Yang, F. Yu, J. Zheng, Water-enhanced Removal of Ciprofloxacin from Water by Porous Graphene Hydrogel, Sci. Rep. 5 (2015) 13578. https://doi.org/10.1038/srep13578.

[280] V.K. Verma, S. Subbiah, Prospects of Silk Sericin as an Adsorbent for Removal of Ibuprofen from Aqueous Solution, Ind. Eng. Chem. Res. 56 (2017) 10142–10154. doi:10.1021/acs.iecr.7b01827.

[281] Y.N. Jo, B.-D. Park, I.C. Um, Effect of storage and drying temperature on the gelation behavior and structural characteristics of sericin, Int. J. Biol. Macromol. 81 (2015) 936–941. doi:https://doi.org/10.1016/j.ijbiomac.2015.09.016.

[282] H. Teramoto, A. Kakazu, K. Yamauchi, T. Asakura, Role of Hydroxyl Side Chains in Bombyx mori Silk Sericin in Stabilizing Its Solid Structure, Macromolecules. 40 (2007) 1562–1569. doi:10.1021/ma062604e.

[283] K. Kodama, The preparation and physico-chemical properties of sericin, Biochem. J. 20 (1926) 1208–1222. doi:10.1042/bj0201208.

[284] L. Ricq, S. Narçon, J.-C. Reggiani, J. Pagetti, Streaming potential and protein transmission ultrafiltration of single proteins and proteins in mixture: β-lactoglobulin and lysozyme, J. Memb. Sci. 156 (1999) 81–96. doi:https://doi.org/10.1016/S0376-7388(98)00341-X.

[285] C. Longo, M. Savaris, M. Zeni, R.N. Brandalise, A.M.C. Grisa, Degradation study of polypropylene (PP) and bioriented polypropylene (BOPP) in the environment, Mater. Res. 14 (2011) 442–448. doi:10.1590/S1516-14392011005000080.

[286] C.L. de Carvalho, A.F. Silveira, D. dos S. Rosa, A study of the controlled degradation of polypropylene containing pro-oxidant agents, Springerplus. 2 (2013) 623. doi:10.1186/2193-1801-2-623.

[287] E. Andreassen, Infrared and Raman spectroscopy of polypropylene BT - Polypropylene: An A-Z reference, in: J. Karger-Kocsis (Ed.), Springer Netherlands, Dordrecht, 1999: pp. 320–328. doi:10.1007/978-94-011-4421-6_46.

[288] S. Babić, A.J.M. Horvat, D. Mutavdžić Pavlović, M. Kaštelan-Macan, Determination of pKa values of active pharmaceutical ingredients, TrAC Trends Anal. Chem. 26 (2007) 1043–1061. doi:https://doi.org/10.1016/j.trac.2007.09.004.

[289] H. Mansouri, R.J. Carmona, A. Gomis-Berenguer, S. Souissi-Najar, A. Ouederni, C.O. Ania, Competitive adsorption of ibuprofen and amoxicillin mixtures from aqueous solution on activated carbons, J. Colloid Interface Sci. 449 (2015) 252–260. doi:https://doi.org/10.1016/j.jcis.2014.12.020.

[290] H. Cheng, D. Song, H. Liu, J. Qu, Permanganate oxidation of diclofenac: The pH-dependent reaction kinetics and a ring-opening mechanism, Chemosphere. 136 (2015) 297–304. doi:https://doi.org/10.1016/j.chemosphere.2014.11.062.

[291] R. Chadha, N. Kashid, D.V.S. Jain, Kinetic studies of the degradation of an aminopenicillin antibiotic (amoxicillin trihydrate) in aqueous solution using heat conduction microcalorimetry, J. Pharm. Pharmacol. 55 (2003) 1495–1503. doi:10.1211/0022357022179.

[292] P.A. Neale, B.I. Escher, A.I. Schäfer, pH dependence of steroid hormone—organic matter interactions at environmental concentrations, Sci. Total Environ. 407 (2009) 1164–1173. doi:https://doi.org/10.1016/j.scitotenv.2008.09.035.

[293] H. Demey-Cedeño, M. Ruiz, J.A. Barron-Zambrano, A.M. Sastre, Boron removal from aqueous solutions using alginate gel beads in fixed-bed systems, J. Chem. Technol. Biotechnol. 89 (2014) 934–940. doi:10.1002/jctb.4361.

[294] Q. Li, X. Tang, Y. Sun, Y. Wang, Y. Long, J. Jiang, H. Xu, Removal of Rhodamine B from wastewater by modified Volvariella volvacea: batch and

column study, RSC Adv. 5 (2015) 25337–25347.

[295] M. Lázníček, A. Lázníčková, The effect of lipophilicity on the protein binding and blood cell uptake of some acidic drugs, J. Pharm. Biomed. Anal. 13 (1995) 823–828. doi:https://doi.org/10.1016/0731-7085(95)01504-E.

[296] R. Maecker, New method for determination of beta-lactam antibiotics by means of diffuse reflectance spectroscopy using polyurethane foam as sorbent, University of Duisburg-Essen, Ecuador, South America, 2005. https://duepublico2.uni-due.de/servlets/MCRFileNodeServlet/duepublico_derivate_00005682/Diss_Rodriguez.pdf.

[297] M.A. Mahmoud, Kinetics studies of uranium sorption by powdered corn cob in batch and fixed bed system, J. Adv. Res. 7 (2016) 79–87. doi:https://doi.org/10.1016/j.jare.2015.02.004.

[298] S.H. Pine, J. Hendrickson, D.J. Cram, G.S. Hammono, Organic Chemistry McGraw-Hill, 5th ed., 1987.

[299] J.T.B. Shaw, S.G. Smith, Amino-acids of Silk Sericin, Nature. 168 (1951) 745. doi:10.1038/168745a0.

[300] N. V Bhagavan, Chapter 2 - Amino Acids, in: N.V.B.T.-M.B. (Fourth E. Bhagwan (Ed.), Academic Press, San Diego, 2002: pp. 17–33. doi:https://doi.org/10.1016/B978-012095440-7/50004-4.

[301] N. V Bhagavan, C.-E. Ha, Chapter 2 - Water, Acids, Bases, and Buffers, in: N. V Bhagavan, C.-E.B.T.-E. of M.B. Ha (Eds.), Academic Press, San Diego, 2011: pp. 9–17. doi:https://doi.org/10.1016/B978-0-12-095461-2.00002-3.

[302] A. Echchelh, T. Hess, R. Sakrabani, Reusing oil and gas produced water for irrigation of food crops in drylands, Agric. Water Manag. 206 (2018) 124–134. doi:https://doi.org/10.1016/j.agwat.2018.05.006.

[303] C. Kanaoka, Fine particle filtration technology using fiber as dust collection medium, KONA Powder Part. J. 36 (2019) 88–113.

[304] I. Zerin, E. Datta, A Review Article on Applications of Filter Cloth, Int. J. Cloth. Sci. 5 (2018) 1–6.

[305] R.W. Fox, Air cleaners: A review, J. Allergy Clin. Immunol. 94 (1994) 413–416. doi:10.1053/ai.1994.v94.a56025.

[306] A. Mukhopadhyay, 8 - Composite nonwovens in filters: applications, in: D. Das, B.B.T.-C.N.-W.M. Pourdeyhimi (Eds.), Woodhead Publishing, 2014: pp. 164–210. doi:https://doi.org/10.1533/9780857097750.164.

[307] H. Xiao, X. Li, L. Liu, Y. Liu, D. Zhao, Development of Environmental Protection Air Filter Media, (n.d.).

[308] X.J. Xiaoling Yu, Factors Influencing Design of Fiber Filter Products, J. Filtr. Sep. 15 (2005) 36–38.

[309] W. Senakoon, S. Nuchadomrong, S. Sirimungkararat, T. Senawong, P. Kitikoon, Antibacterial action of eri (samia ricini) sericin against escherichia coli and staphylococcus aureus, Asian J Food Agro-Ind. 2 (2009) S222-228. Retrieved from www.ajofai.info.

[310] H. Szczepanowska, W. Wilson, Permanency of Reprographic Images on Polyester Film, J. Am. Inst. Conserv. 39 (2000) 371–390. doi:10.1179/019713600806113185.

[311] A.P. dos S. Pereira, M.H.P. da Silva, É.P. Lima Júnior, A. dos S. Paula, F.J. Tommasini, Processing and Characterization of PET Composites Reinforced With Geopolymer Concrete Waste, Mater. Res. 20 (2017) 411–420. doi:10.1590/1980-5373-mr-2017-0734.

[312] B.C. Smith, Distinguishing Structural Isomers: Mono-and Disubstituted Benzene Rings, Spectroscopy. 31 (2016) 36–39.

[313] J. Zhou, M. Li, L. Zhong, F. Zhang, G. Zhang, Aminolysis of polyethylene terephthalate fabric by a method involving the gradual concentration of dilute ethylenediamine, Colloids Surfaces A Physicochem. Eng. Asp. 513 (2017) 146–152. doi:https://doi.org/10.1016/j.colsurfa.2016.11.016.

[314] S. Sohn, D. Kim, Modification of Langmuir isotherm in solution systems—definition and utilization of concentration dependent factor, Chemosphere. 58 (2005) 115–123. doi:https://doi.org/10.1016/j.chemosphere.2004.08.091.

[315] P. Nanta, K. Kasemwong, W. Skolpap, Isotherm and kinetic modeling on superparamagnetic nanoparticles adsorption of polysaccharide, J. Environ. Chem. Eng. 6 (2018) 794–802. doi:https://doi.org/10.1016/j.jece.2017.12.063.

[316] S. Sharma, G.P. Agarwal, Interactions of Proteins with Immobilized Metal Ions: A Comparative Analysis Using Various Isotherm Models, Anal. Biochem. 288 (2001) 126–140. doi:https://doi.org/10.1006/abio.2000.4894.

[317] B. Guieysse, C. Hort, V. Platel, R. Munoz, M. Ondarts, S. Revah, Biological treatment of indoor air for VOC removal: Potential and challenges, Biotechnol. Adv. 26 (2008) 398–410. doi:https://doi.org/10.1016/j.biotechadv.2008.03.005.

[318] L. Fang, C. Norris, K. Johnson, X. Cui, J. Sun, Y. Teng, E. Tian, W. Xu, Z. Li, J. Mo, J.J. Schauer, M. Black, M. Bergin, J. Zhang, Y. Zhang, Toxic volatile organic compounds in 20 homes in Shanghai: Concentrations, inhalation health risks, and the impacts of household air cleaning, Build. Environ. 157 (2019) 309–318. doi:10.1016/j.buildenv.2019.04.047.

[319] Pubchem, PubChem substance and compound databases, Pubchem.Ncbi.Nlm.Nih.Gov. (2019). https://www.ncbi.nlm.nih.gov/pccompound/[Accessed 26 march 2019].

[320] D.P.H. Hsieh, T.E. McKone, F. Chiao, R.C. Currie, L. Kleinschmidt, Final Draft Report: Intermedia transfer factors for contaminants found at hazardous waste sites, Prep. Off. Sci. Aff. Dep. Toxic Subst. Control. Calif. Environ. Prot. Agency. (1994).

[321] M.M. Renfew, NIOSH Pocket guide to chemical hazards (US Department of Health and Human Services-National Institute for Occupational Safety and Health), (1991).

[322] S. Ly-Verdú, F.A. Esteve-Turrillas, A. Pastor, M. de la Guardia, Determination of volatile organic compounds in contaminated air using semipermeable

membrane devices, Talanta. 80 (2010) 2041–2048. doi:https://doi.org/10.1016/j.talanta.2009.11.001.

[323] I.-Y. Eom, Estimation of partition coefficients of benzene, toluene, ethylbenzene, and p-xylene by consecutive extraction with solid phase microextraction, Bull. Korean Chem. Soc. 32 (2011) 1463–1464.

[324] J.L. Schnoor, Environmental modeling: fate and transport of pollutants in water, air, and soil., John Wiley and Sons, 1996.

[325] F. Edition, Guidelines for drinking-water quality, WHO Chron. 38 (2011) 104–108.

[326] F. Leusch, M. Bartkow, A short primer on benzene, toluene, ethylbenzene and xylenes (BTEX) in the environment and in hydraulic fracturing fluids, Smart Water Res Cent. 189 (2010) 1–8.

Appendix:

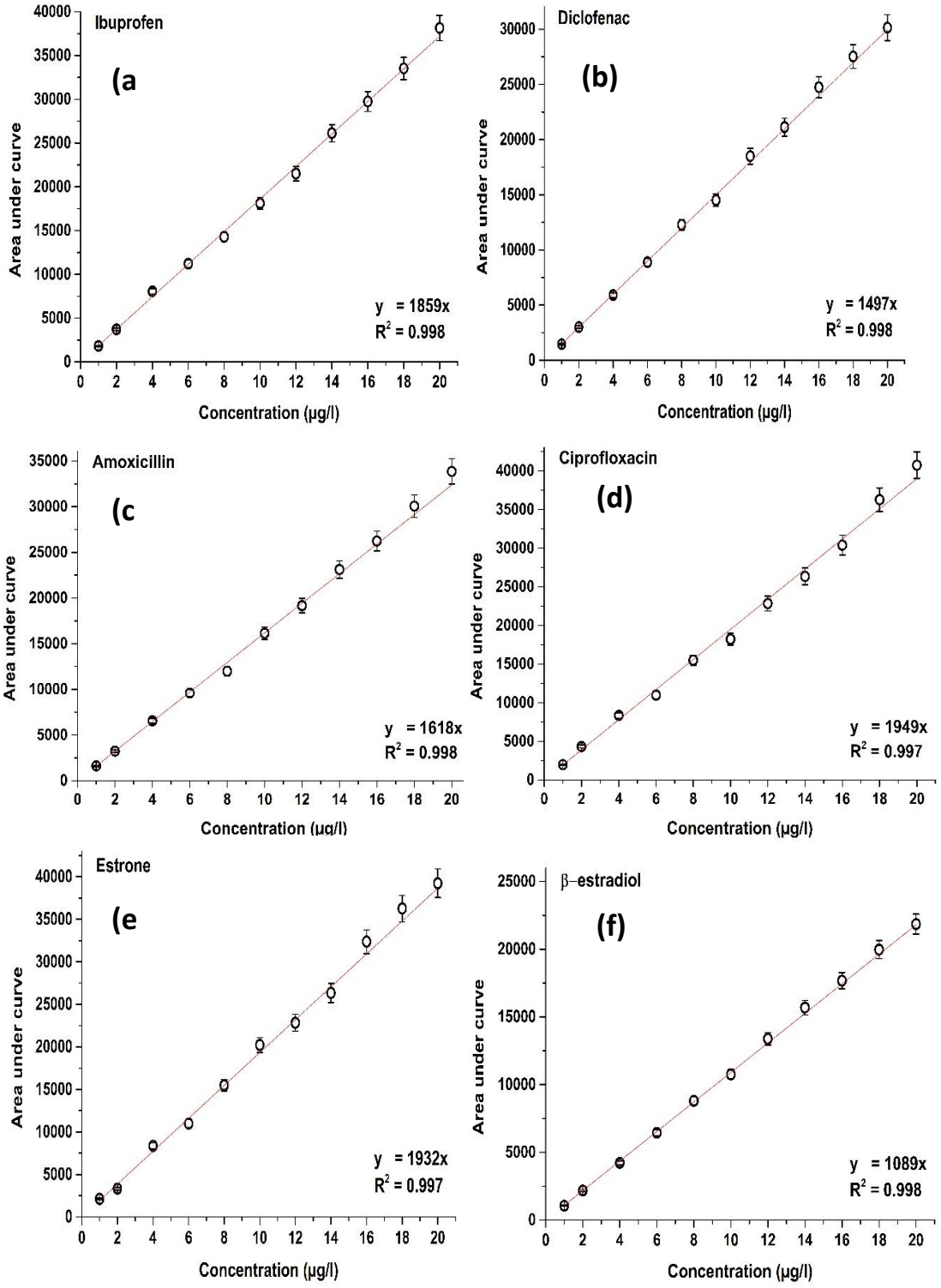

Figure A. 1 Calibration plot for (a) Ibuprofen (b) Diclofenac (c) Amoxicillin (d) Ciprofloxacin (e) Estrone and (f) β-estradiol.

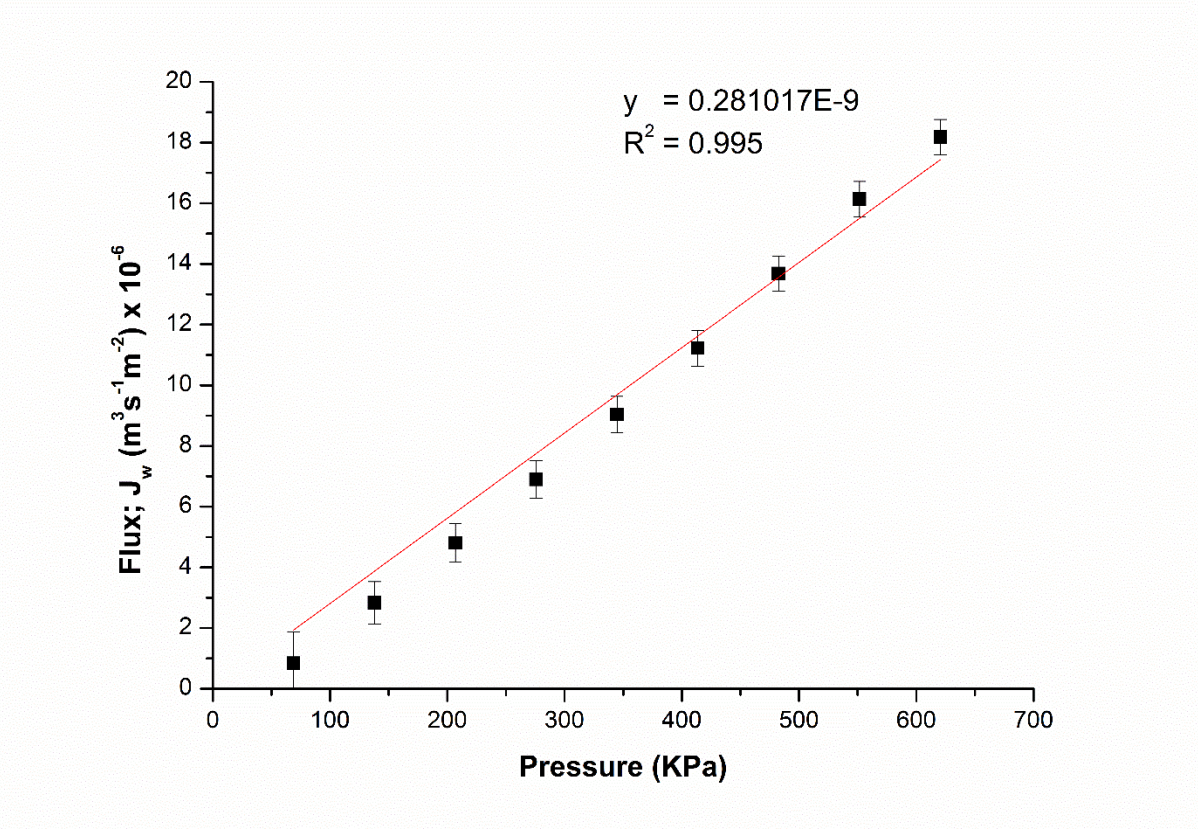

Figure A 2. Pure water flux (Jw) for RO-sheet membrane (ΔP; 10-90 psi).

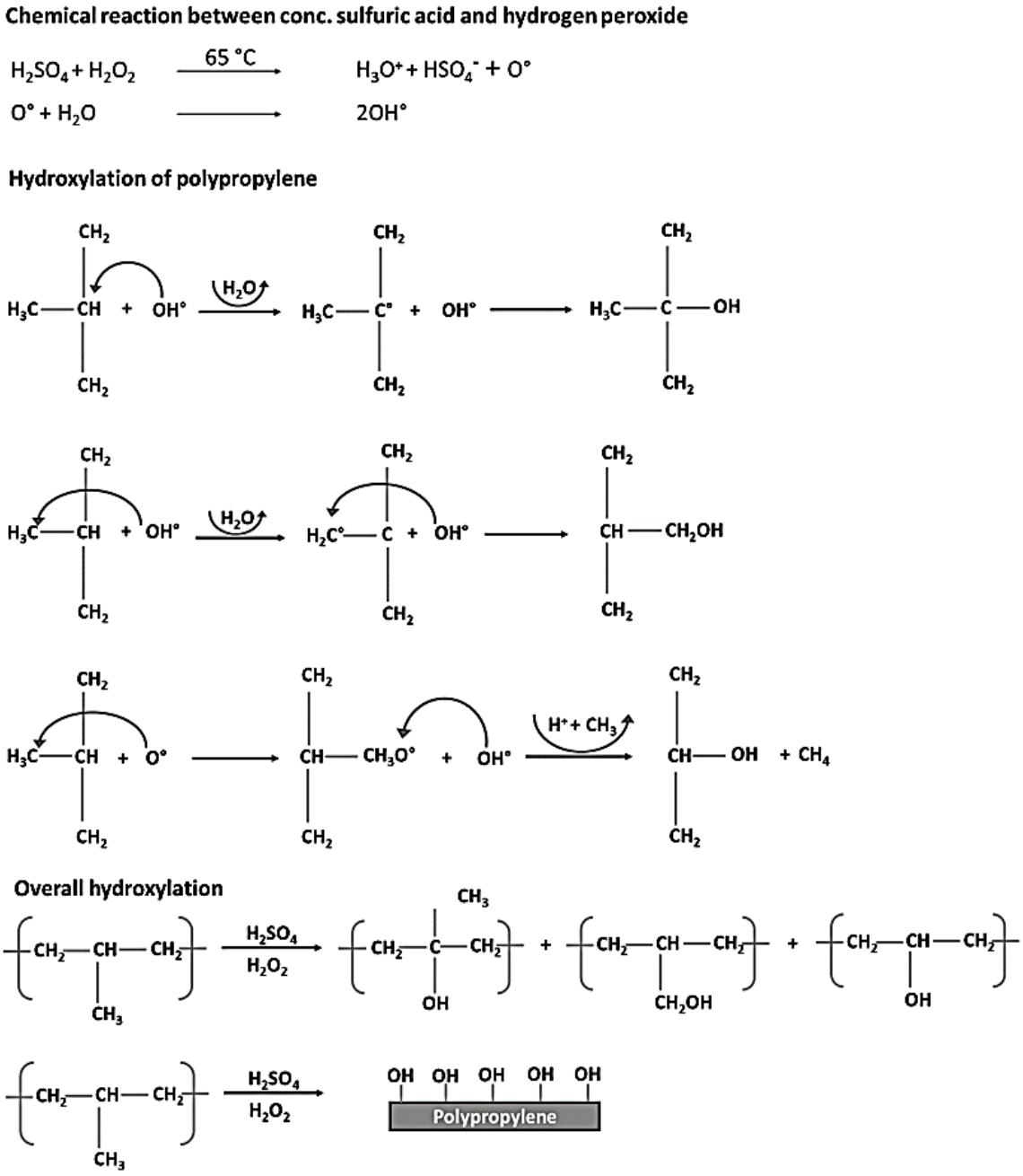

Figure A 3. Proposed schematic illustration of polypropylene hydroxylation reaction.

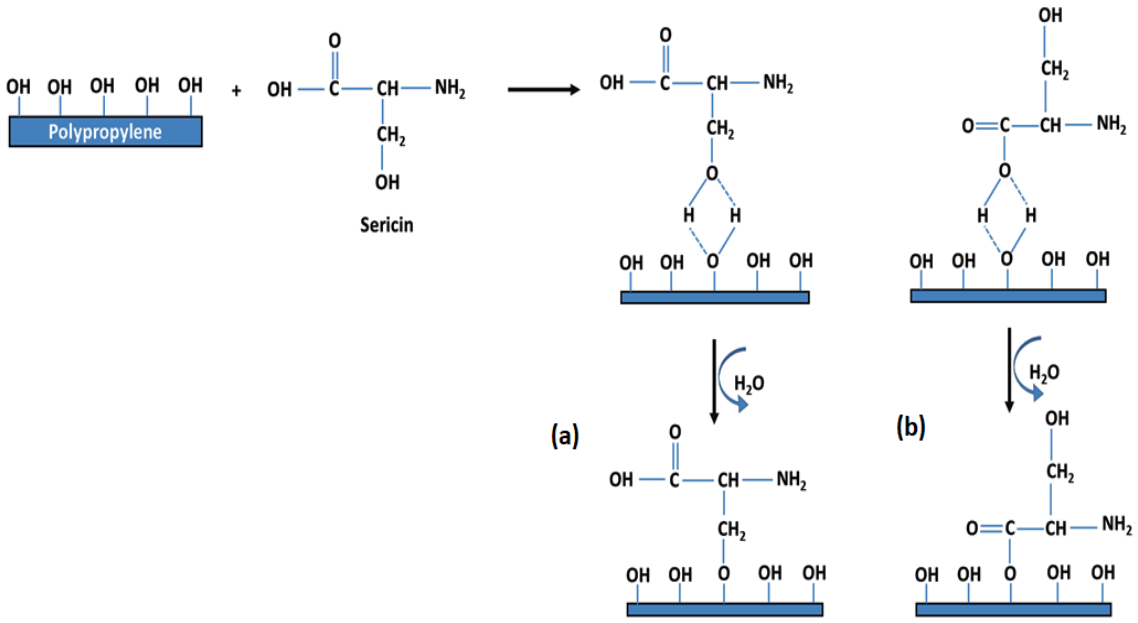

Figure A 4. Sericin binding to hydroxylated PP fibre surface of HFMF membrane via hydrogen bonding using two possible hydroxyl ends.

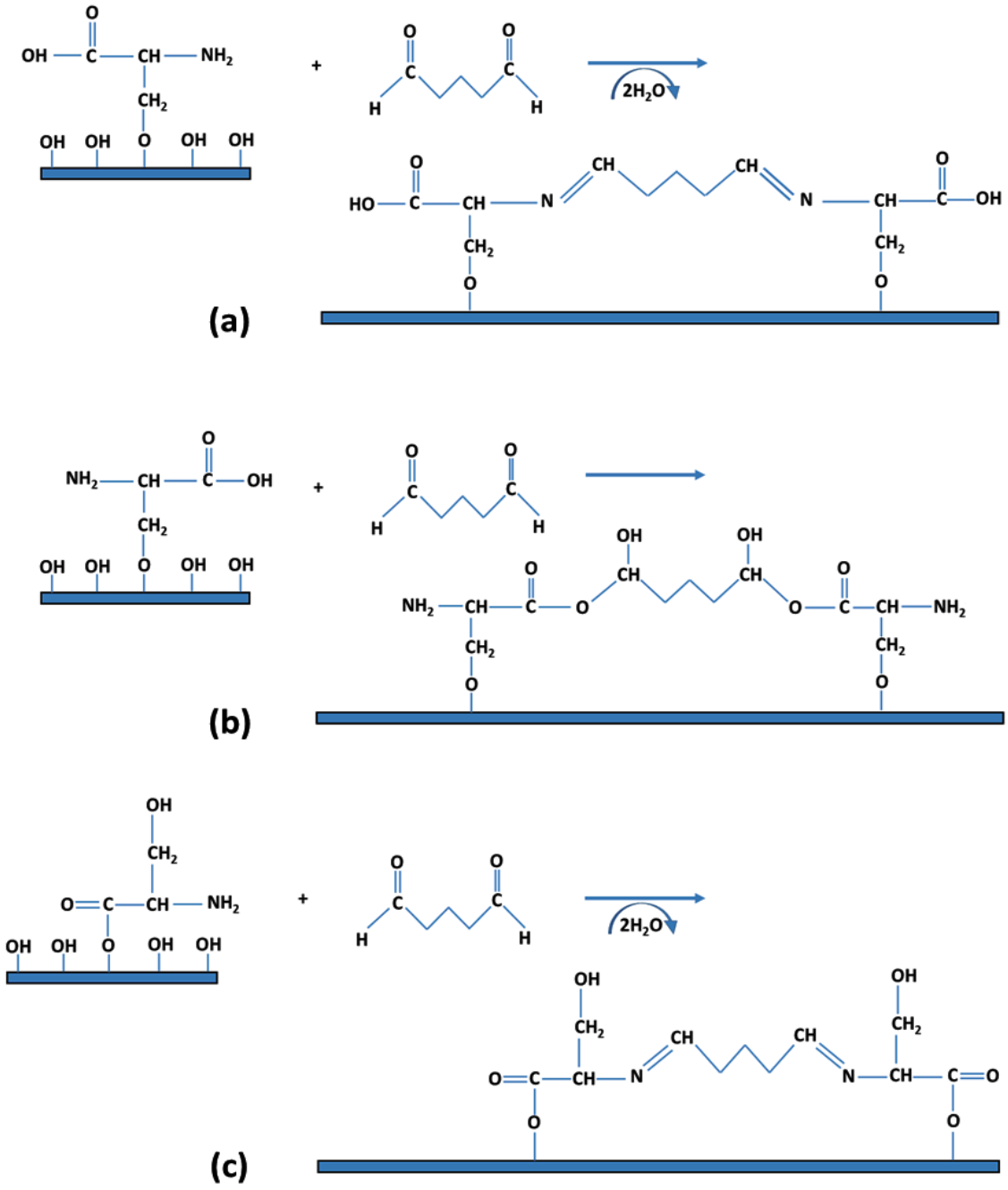

Figure A 5. Sericin cross-linking via glutaraldehyde using amine (structure a and c) and hydroxyl end (structure b).

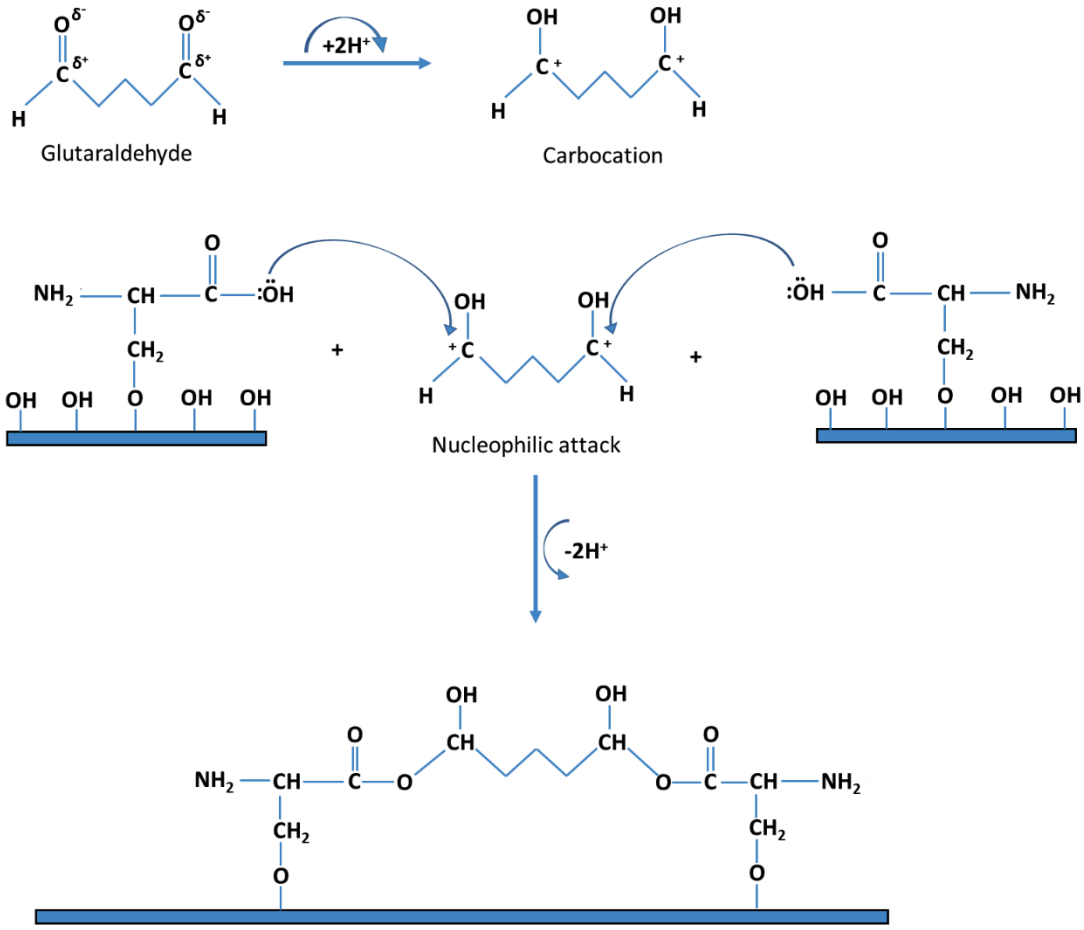

Figure A 6. Detail mechanism for the cross-linking reaction of sericin by glutaraldehyde via hemiacetal formation.

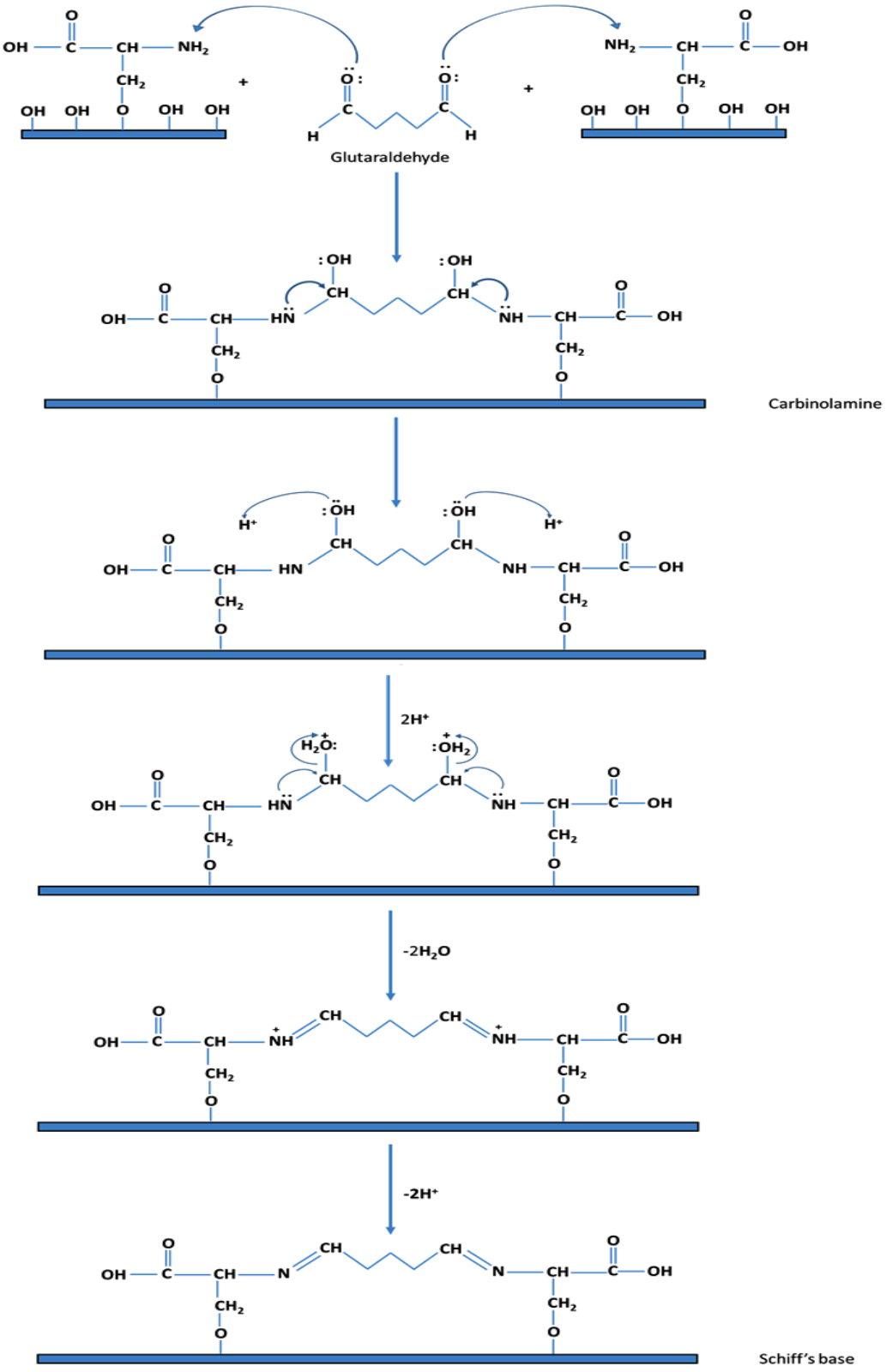

Figure A 7. Detail mechanism for the cross-linking reaction of sericin by glutaraldehyde via Schiff base formation.

The sericin rejection profile at different initial feed concentration of sericin show that the HFMF membrane exhibited ~13%, ~15% and ~20% rejection at 10 g/l, 20 g/l, and 30 g/l of sericin initial feed concentration, respectively. The rejection of sericin by HFMF membrane slightly increases (4-5%) with time during recirculation, and it reaches an asymptotic value (due to deposition of sericin layer and concentration polarization near membrane surface).

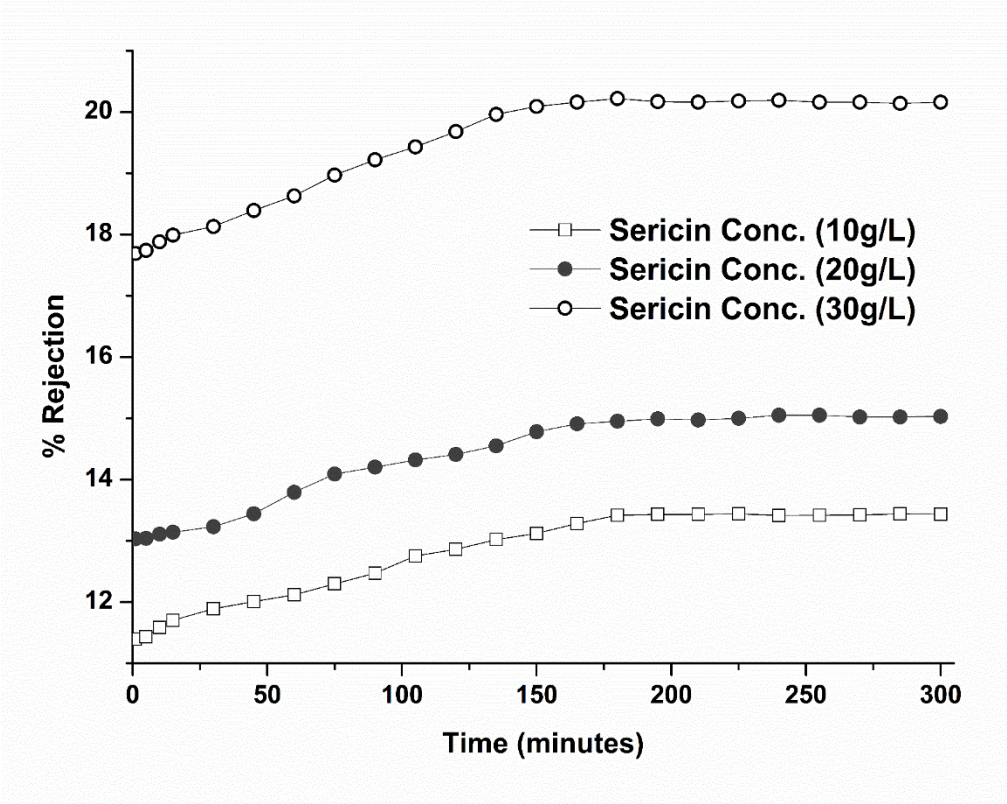

Figure A 8. Rejection profile at different sericin feed concentration using sericin coated HFMF membrane.

Drugs	Un-charged (neutral species)	Anionic (negatively charged species)	Zwitterionic species
Ibuprofen (pKa=4.91) (log D=1.40) (log P=3.5)[a]	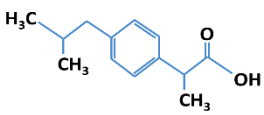	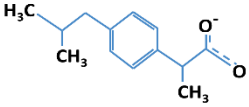	-
Diclofenac (pKa=4.15) (log D=1.70) (log P=4.55)[a]	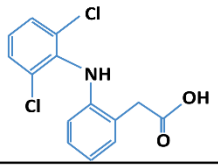	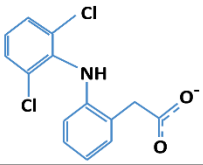	-
	Cationic (positively charged species)	**Anionic (negatively charged species)**	**Zwitterionic species**
Amoxicillin (pKa_1=2.63) (pKa_2=7.16) (pKa_3=9.55) (log D=0.49) (log P=0.88)[a]	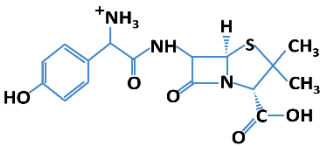	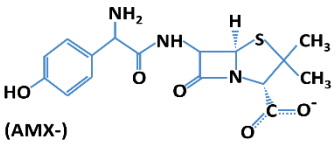 (AMX-) 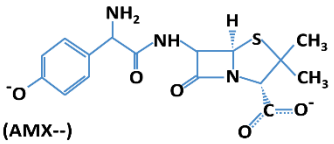 (AMX--)	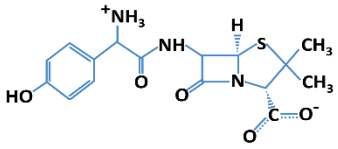
Ciprofloxacin (pKa_1=6.09) (pKa_2=8.74) (log D=0.65) (log P=1.62)[a]	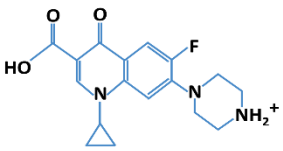	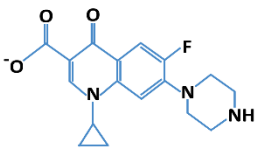	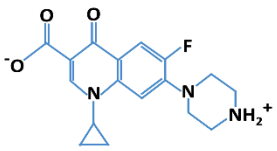
Estrone (pKa=10.40) (log D=3.62) (log P=3.62)[a]	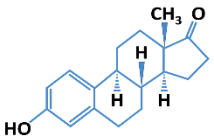	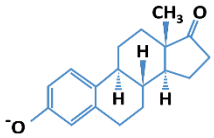	
β-estradiol (pKa=10.71) (log D=4.15) (log P=4.14)[a]	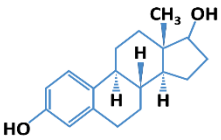	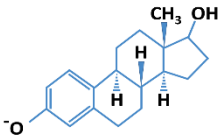	

Figure A9. Molecular structure and physiochemical properties (pKa, log P and log D values) of selected drugs in this study; a[189].

Table A 1. Analysis of air quality in major Indian cities* – (from 1-Jan 2018 to 31 Dec 2018)

Major Cities	Monitoring Stations	PM10 ($\mu g/m^3$)	PM2.5 ($\mu g/m^3$)	Benzene ($\mu g/m^3$)	Toluene ($\mu g/m^3$)	Ethyl benzene ($\mu g/m^3$)	Xylene ($\mu g/m^3$)
New Delhi	Alipur, Delhi - DPCC	347.56	229.42	5.28	49.41	-	2.72
	Anand Vihar, Delhi - DPCC	349.90	162.24	11.12	40.62	-	29.44
	Ashok Vihar, Delhi - DPCC	264.26	120.23	5.40	35.77	-	22.86
	Aya Nagar, Delhi - IMD	187.81	94.85	-	-	-	-
	Bawana, Delhi - DPCC	262..39	118.47	1.13	104.85		15450
	Burari Crossing, Delhi - IMD	222.57	131.47	-	-	-	-
	CRRI Mathura Road, Delhi - IMD	253.98	124.34	-	-	1.22	-
	DTU, Delhi - CPCB	266.30	129.15	5.988	72.19	7.53	-
	Dr. Karni Singh Shooting Range, Delhi - DPCC	200.99	73.83	2.60	19.48	-	13.02
	Dwarka-Sector 8, Delhi - DPCC	292.61	107.91	2.89	24.80		22.58
	East Arjun Nagar	-	-	5.62	106.38	-	-
	IGI Airport (T3), Delhi - IMD	193.6	85.15	-	-	-	-
	IHBAS, Dilshad Garden, Delhi - CPCB	-	104.84	-	-	-	-
	ITO, Delhi - CPCB	196.58	119.19	1.14	6.75	1.38	-
	Jahangirpuri, Delhi - DPCC	303.13	144.94	3.14	20.48	-	12.82
	Jawaharlal Nehru Stadium, Delhi - DPCC	235.83	105.54	3.04	31.60	-	17.03
	Lodhi Road, Delhi - IMD	198.16	90.15	0.14	0.59		0.90
	Major Dhyan Chand National Stadium, Delhi - DPCC	238.35	102.38	3.37	24.46	-	14.22
	Mandir Marg, Delhi - DPCC	202.33	110.16	4.16	18.19	-	6.05
	Mundka, Delhi - DPCC	313.91	144.74	6.22	109.55	-	121.31
	NSIT Dwarka, Delhi - CPCB	-	118.63	3.43	8.91	1.72	-
	Najafgarh, Delhi - DPCC	198.71	87.204	1.53	13.55	-	2.14
	Narela, Delhi - DPCC	259.22	121.16	2.84	44.23	-	6.39
	Nehru Nagar, Delhi - DPCC	234.57	122.57	3.15	25.05	-	26.81

	North Campus, DU, Delhi - IMD	242.72	111	0.72	1.27	-	0.37
	Okhla Phase-2, Delhi - DPCC	251.11	104.61	3.67	28.94	-	15.83
	Patparganj, Delhi - DPCC	211.55	100.78	0.98	-	6.11	160.63
	Punjabi Bagh, Delhi - DPCC	246.73	131.42	4.56	-	37.03	21.30
	Pusa, Delhi - DPCC	169.47	82.76	0.09	-	0.58	1.40
	Pusa, Delhi - IMD	247.56	124.2	11.09	-	23.97	4.70
	R K Puram, Delhi - DPCC	248.4	124.84	11.09	23.97	-	4.70
	Rohini, Delhi - DPCC	291.6	128.53	3.59	32.39	-	4782.8
	Shadipur, Delhi - CPCB	-	113.52	4.59	16.39	3.46	-
	Sirifort, Delhi - CPCB	269.23	105.24	7.54	46.11	7.90	-
	Sonia Vihar, Delhi - DPCC	242.32	117.17	3.51	61.71	-	25.64
	Sri Aurobindo Marg, Delhi - DPCC	168.51	93.88	5.27	62.35	-	1836.1
	Vivek Vihar, Delhi - DPCC	253.11	110.37	2.61	24.53	-	7.48
	Wazirpur, Delhi - DPCC	317.55	137.48	4.50	60.18	-	196.02
	BTM Layout, Bengaluru - CPCB	-	34.08	0.55	0.99	0.24	-
	BWSSB Kadabesanahalli, Bengaluru - CPCB	-	26.38	0.62	1.55	0.28	-
	Bapuji Nagar, Bengaluru - KSPCB	82.66	38.70	0.10	0.59	-	-
	City Railway Station, Bengaluru - KSPCB	81.04	-	-	-	-	-
Bengaluru	Hebbal, Bengaluru - KSPCB	51.84	24.27	0.33	2.21	-	-
	Hombegowda Nagar, Bengaluru - KSPCB	59.41	26.74	0.27	4.01	-	-
	Jayanagar 5th Block, Bengaluru - KSPCB	81.20	38.10	0.73	6.18	-	-
	Peenya, Bengaluru - CPCB	-	28.84	-	-	-	-
	Sanegurava Halli, Bengaluru - KSPCB	58.15	-	-	-	-	-
	Silk Board, Bengaluru - KSPCB	101.89	37.45	1.34	4.66	-	-
Mumbai	Bandra Mumbai-MPCB	62.22	24.50	0.76	0.10	1.37	0.056
Navi Mumbai	Airoli, Navi Mumbai - MPCB	91.28	-	-	-	-	-
	Rabindra Bharati University, Kolkata - WBPCB	17.18	29.41		-	337.73	200.58
Kolkata	Victoria, Kolkata - WBPCB	4.53	8.91	3.18	-	85.01	51.86

Howrah	Ghusuri, Howrah - WBPCB	6.17	9.20	1.60	-	133.60	59.60
	Padmapukur, Howrah - WBPCB	7.71	23.78	7.15	-	129.28	72.08
Chennai	Alandur Bus Depot, Chennai - CPCB	-	61.02	0.61	0.63	0.93	-
	Manali, Chennai - CPCB	-	61.40	-	-	-	-
	Velachery Res. Area, Chennai - CPCB		39.80	0.41	3.53	0.34	-
Hyderabad	Bollaram Industrial Area, Hyderabad - TSPCB	102.30	45.47	0.25	4.84	-	0.20
	Central University, Hyderabad - TSPCB	91.07	38.25	4.92	13.00	-	5.05
	ICRISAT Patancheru, Hyderabad - TSPCB	93.16	39.74	0.052	0.66	-	0.14
	IDA Pashamylaram, Hyderabad - TSPCB	93.53	41.75	3.94	40.20	-	12.85
	Sanathnagar, Hyderabad - TSPCB	-	47.28	0.97	11.90	-	0.83
	Zoo Park, Hyderabad - TSPCB	100.67	48.50	1.91	17.25	-	2.71
Pune	Karve Road, Pune - MPCB	39.43	22.18	0.29	0.11	-	42.81
Ahmedabad	Maninagar, Ahmedabad - GPCB	-	160.84	8.11	37.56	1.15	6.01
Lucknow	Central School, Lucknow - CPCB	-	61.41	0.23	1.54	29.30	-
	Lalbagh, Lucknow - CPCB	-	84.14	0.629	1.21	0.72	-
	Nishant Ganj, Lucknow - UPPCB	-	110.74	0.99	1.16	-	14.55
	Talkatora District Industries Center, Lucknow - CPCB		139.80				

*Data taken from Central Pollution Control Board, India (https://app.cpcbccr.com/ccr/#/caaqm-dashboard-all/caaqm-landing)

Table A 2. Physiochemical properties of BTEX gases

Parameters	Benzene	Toluene	Ethylbenzene	Xylene	References
Molecular Formula	C_6H_6	$C_6H_5CH_3$	$C_6H_5CH_2\ CH_3$	$C_6H_4(CH_3)_2$	[319], [320]
Molecular weight (gm mole^{-1})	78.11	92.14	106.17	106.16	
Density (gm ml^{-1})	0.8765	0.8669	0.8670	0.8685	
Polarity	Non-polar	Non-polar	Non-polar	Non-polar	
Solubility (mg L^{-1})	1780	500	150	150	
Boiling Point (°C)	80.1	110.8	136.2	140.6	
Vapour Pressure (Pa)	12672.2	3769.3	1276.7	1074.0	
Partition coefficient*					
[a]log K_{oc}	1.99	2.25	2.94	3.15	[321]
[b]log K_{oa}	2.78	3.31	3.74	3.82	[322]
[c]log K_{ow}	2.13	2.69	2.84	3.15	[323]
[d]K_h	0.221	0.325	0.422	0.357	[324]
Water-air	4.35	3.76	3.02	3.61	[320]
Soil-air	47.7	150.8	315.7	332.6	
Suspended particles-air	473.5	1591.86	4699.6	5586.4	
Vegetation-air	6.0	12.4	23.2	27.4	

Acceptable limits					
Water (ppb)	10	700	300	500	[325]
Air (ppb)	3	100	NA	200	[326]
Half-Life (h)					
Water	267.6	312.0	156.0	420.0	[325]
Air	141.8	57.1	47.0	23.3	[326]

[a]Octanol-carbon partition coefficient (K_{oc}), [b]Octanol-air partition coefficient (K_{oa}), [c]Octanol-water partition coefficient (K_{ow}), [d]Dimensionless Henry's law constant (K_h)

List of publications and conference proceedings

Publications

- V.K. Verma, S. Subbiah, Prospects of Silk sericin as an Adsorbent for Removal of Ibuprofen from Aqueous Solution, Ind. Eng. Chem. Res. 56 (2017) 10142–10154. doi:10.1021/acs.iecr.7b01827.

- V.K. Verma, S. Subbiah, Fouling resistant sericin coated polymeric microfiltration membrane, J. Chem. Technol. Biotechnol. (2019) jctb.6169. doi:10.1002/jctb.6169.
- V.K. Verma, S. Subbiah, Sericin coated polymeric microfiltration membrane for removal of drug-based micropollutants, J. Chem. Technol. Biotechnol. (2019) jctb.6168. doi:10.1002/jctb.6168.
- V.K. Verma, S. Subbiah, S.H. Kota, Sericin-coated polyester-based air-filter for removal of particulate matter and volatile organic compounds (BTEX) from indoor air, Chemosphere. 237 (2019) 124462. doi:10.1016/j.chemosphere.2019.124462.

Patents

- Vishal Kumar Verma, Senthilmurugan S., S K Sankar, Sericin coated membrane and use thereof, Indian patent application no 201821013079 filed on 2018-04-05

- Vishal Kumar Verma, Senthilmurugan S., S K Sankar, System and method for producing Sericin coated membranes Indian Patent application no 201922013927, published on 03-01-2020

Conferences

- Removal of micropollutants using modified MF-membrane. SEEC-2018, IISC Bengaluru